

Characterisation of proteinaceous  
toxins isolated from *Pyrenophora*  
*teres* f. *teres*

by

Ismail Ahmed Ismail

A thesis submitted for the degree of Doctor of Philosophy

at

The University of Adelaide

Faculty of Science

School of Agriculture, Food and Wine

Waite Campus

Adelaide, South Australia

2013

## Table of contents

Table of contents.....	II
List of Tables.....	XIV
Abstract.....	XVI
Declaration .....	XX
Acknowledgment .....	XXI
Abbreviation .....	XXII
Chapter 1 General introduction .....	1
1.1 Fungal phytotoxins .....	1
1.2 Necrotrophic phytotoxins and disease development .....	3
1.3 Net blotch disease in barley .....	5
1.4 <i>Ptt</i> -barley interaction.....	7
1.4.1 Infection process.....	7
1.4.2 <i>P. teres</i> toxins .....	8
1.4.2.1 HNSTs .....	9
1.4.2.2 Proteinaceous HSTs.....	10
1.5 Virulence and proteinaceous HSTs.....	12
1.6 The mode of action of necrotrophic effectors (HSTs) .....	13
1.7 Identification of necrotrophic fungal toxins might contribute to the development of resistant barley .....	15
1.8 The objectives of this study.....	18
Chapter 2 Fungal growth and virulence of <i>Pyrenophora teres</i> f. <i>teres</i> on barley .....	20
2.1 Introduction .....	20
2.2 Materials and methods.....	22
2.2.1 Plant growth.....	22
2.2.2 Fungal isolation and culturing .....	22
2.2.3 Virulence testing of <i>Ptt</i> isolates.....	23
2.2.4 <i>In vitro</i> and <i>in planta</i> conidial germination assays.....	24
2.2.5 Determination of fungal growth <i>in planta</i> .....	27
2.2.6 Optimisation of proteinaceous toxin production and extraction ....	27

2.2.6.1	Effect of media type and incubation conditions on protein production.....	28
2.2.6.2	Protein extraction from <i>Ptt</i> culture filtrate .....	29
2.2.6.2.1	Ultrafiltration purification (UFP) .....	30
2.2.6.2.2	Ammonium sulfate precipitation (ASP).....	31
2.2.6.2.3	TCA protein extraction.....	31
2.2.6.3	PAGE.....	32
2.2.6.3.1	Coomassie Brilliant Blue staining (CBB R250).....	32
2.2.6.3.2	Silver staining.....	33
2.2.6.4	Evaluation of UFP and ASP extraction methods .....	34
2.2.6.5	Proteinaceous toxin bioassay for six isolates of <i>Ptt</i> .....	34
2.2.7	Statistical analysis .....	35
<b>2.3</b>	<b>Results.....</b>	<b>35</b>
2.3.1	Virulence of <i>Ptt</i> isolates .....	35
2.3.2	Germination and fungal growth are correlated with virulence.....	39
2.3.2.1	Germination <i>in vitro</i> and <i>in planta</i> .....	39
2.3.2.2	Fungal hyphal growth <i>in planta</i> .....	40
2.3.3	Effect of media on protein production.....	45
2.3.4	Optimisation of protein production conditions.....	46
2.3.5	Evaluation of UFP and ASP extraction methods .....	49
2.3.6	Bioassay of total protein extracted from culture filtrates of six <i>Ptt</i> isolates .....	49
<b>2.4</b>	<b>Discussion .....</b>	<b>52</b>
<b>Chapter 3</b>	<b>Identification of individual candidate proteinaceous toxins from <i>Pyrenophora teres f. teres</i>.....</b>	<b>58</b>
<b>3.1</b>	<b>Introduction .....</b>	<b>58</b>
<b>3.2</b>	<b>Material and methods .....</b>	<b>60</b>
3.2.1	Plant growth.....	60
3.2.2	Fungal isolation and toxin production.....	60
3.2.3	Proteinaceous toxin fractionation and bioassays .....	60
3.2.3.1	Bioassay of protein fractions from two isolates with different virulence .....	61
3.2.3.2	Bioassay of protein fractions and sub-fractions on barley cultivars of different susceptibility.....	62
3.2.4	Investigation of <i>Ptt</i> toxins in intercellular washing fluids (ICWFs) and cell components in infected plants.....	62
3.2.4.1	Plant inoculation.....	63

3.2.4.2	Protein extraction from ICWFs .....	63
3.2.4.3	Protein extraction from cell components.....	64
3.2.5	Visualisation of proteins and candidate toxin identification .....	66
3.2.5.1	PAGE.....	66
3.2.5.2	2DGE.....	66
3.2.5.3	Candidate proteinaceous toxin identification .....	67
<b>3.3</b>	<b>Results.....</b>	<b>69</b>
3.3.1	Identification of potential toxins .....	69
3.3.1.1	From fractions of culture filtrate proteins from two isolates with different virulence .....	69
3.3.1.2	From fractions and sub-fractions of culture filtrate proteins that induce symptoms differentially on barley cultivars of different susceptibility.....	75
3.3.1.3	Comparing active and less active protein fractions .....	86
3.3.2	Identification of virulence-related candidate proteins (VRCPs) ....	88
3.3.3	Characterisation of ICWFs and cell components from infected plants.....	91
<b>3.4</b>	<b>Discussion .....</b>	<b>99</b>
<b>Chapter 4</b>	<b>Isolation, characterisation and cloning of cDNA encoding for virulence-related candidate proteins (VRCPs) from <i>Pyrenophora teres f. teres (Ptt)</i> .....</b>	<b>108</b>
<b>4.1</b>	<b>Introduction .....</b>	<b>108</b>
<b>4.2</b>	<b>Materials and methods.....</b>	<b>111</b>
4.2.1	Isolation of the full length of cDNA for virulence-related candidate gene transcripts (VRCGs).....	111
4.2.1.1	Culturing the isolate .....	111
4.2.1.2	Primer design.....	111
4.2.1.3	RNA extraction, quantification and DNase treatment.....	112
4.2.1.4	Isolation of the full length of VRCGs .....	113
4.2.1.5	cDNA extraction from agarose gel and confirmation of sequences .....	114
4.2.2	Bioinformatics analysis .....	114
4.2.2.1	Conserved domains analyses for VRCPs .....	114
4.2.2.2	Alignment of individual VRCPs .....	115
4.2.2.3	Phylogenetic analysis .....	117
4.2.2.4	Secondary structure and three dimensional modelling of VRCPs	117
4.2.3	Semi-quantitative RT-PCR.....	118

4.2.3.1	<i>In vitro</i> .....	118
4.2.3.2	<i>In planta</i> .....	119
<b>4.3</b>	<b>Results</b> .....	<b>120</b>
4.3.1	Isolation of the full length of cDNA for virulence-related candidate gene transcripts (VRCGs).....	120
4.3.2	Conserved domains and phylogenetic analyses for VRCPs .....	120
4.3.2.1	PttXyn11A .....	120
4.3.2.2	PttCHFP1 .....	130
4.3.2.3	PttGPI-CFEM .....	136
4.3.2.4	PttSP1 .....	140
4.3.3	Semi-quantitative RT-PCR.....	144
4.3.3.1	<i>In vitro</i> .....	144
4.3.3.2	<i>In planta</i> .....	145
<b>4.4</b>	<b>Discussion</b> .....	<b>146</b>
<b>Chapter 5</b>	<b>Heterologous expression and bioassays of virulence-related candidate proteins (VRCPs)</b> .....	<b>152</b>
<b>5.1</b>	<b>Introduction</b> .....	<b>152</b>
<b>5.2</b>	<b>Material and methods</b> .....	<b>153</b>
5.2.1	Cloning of cDNA of VRCGs .....	153
5.2.2	Heterologous expression of candidate proteins .....	155
5.2.2.1	Ligation of PCR amplicons in pDEST17 vector .....	155
5.2.2.2	Expression of recombinant protein.....	156
5.2.2.3	Purification of heterologously expressed proteins .....	156
5.2.2.3.1	Purification under denaturing conditions .....	157
5.2.2.3.2	Purification under native conditions.....	157
5.2.2.4	Visualisation and LC-eSI-IT MS identification of expressed recombinant proteins .....	158
5.2.2.5	The effect of recombinant protein on the viability of <i>E. coli</i> .....	158
5.2.3	Bioassay of heterologously expressed proteins .....	159
5.2.4	Activity of xylanase in six isolates of <i>Ptt in vitro</i> .....	160
5.2.5	Statistical analysis and photography .....	162
<b>5.3</b>	<b>Results</b> .....	<b>162</b>
5.3.1	Heterologous expression of VRCPs .....	162
5.3.1.1	PttGPI-CFEM .....	162
5.3.1.2	PttXyn11A.....	163
5.3.1.3	PttCHFP1 .....	168
5.3.1.4	PttSP1 .....	172

5.3.2	Bioassay for candidate proteins.....	176
5.3.2.1	Biological activity of recombinant proteins on barley cultivars ..	176
5.3.2.2	Biological activity of recombinant proteins on cv. Sloop .....	183
5.3.3	Biological activity of commercial xylanase .....	186
5.3.4	Xylanase activity in isolates of <i>Ptt</i> with different virulence .....	187
<b>5.4</b>	<b>Discussion .....</b>	<b>188</b>
<b>Chapter 6</b>	<b>Expression of virulence-related candidate genes (VRCG) during the interaction between barley and isolates of <i>P. teres f. teres</i> with different virulence .....</b>	<b>194</b>
<b>6.1</b>	<b>Introduction .....</b>	<b>194</b>
<b>6.2</b>	<b>Material and methods .....</b>	<b>197</b>
6.2.1	Quantification of expression of VRCGs in six isolates of <i>Ptt</i> .....	197
6.2.1.1	Primer design for RT-qPCR .....	197
6.2.1.2	Plant inoculation and <i>in planta</i> cDNA synthesis.....	199
6.2.1.3	Optimisation of RT-qPCR for VRCGs gene expression.....	199
6.2.1.3.1	VRCGs expression using Comparative C <sub>T</sub> ( $\Delta\Delta C_T$ ).....	200
6.2.1.3.2	qPCR for genomic DNA for six isolates of <i>Ptt</i> at 192 hpi .....	201
6.2.1.3.3	VRCGs expression using absolute quantification .....	201
6.2.1.3.3.1	Primer efficiency .....	201
6.2.1.3.3.2	Standard curve optimisation .....	202
6.2.1.3.3.3	Optimisation of final cDNA and primer concentration for <i>in planta</i> analysis .....	203
6.2.1.3.4	Absolute quantification of VRCGs expression using the optimal cDNA and primer concentrations .....	203
6.2.2	Statistical analysis and photography .....	204
<b>6.3</b>	<b>Results.....</b>	<b>204</b>
6.3.1	Virulence of <i>Ptt</i> isolates .....	204
6.3.2	Optimisation of quantitative RT-PCR for VRCGs.....	206
6.3.2.1	VRCGs expression using Comparative C <sub>T</sub> ( $\Delta\Delta C_T$ ).....	206
6.3.2.2	qPCR for genomic DNA for six isolates at 192 hpi .....	207
6.3.2.3	VRCGs expression using absolute quantification .....	208
6.3.2.3.1	Primer efficiency and standard curves .....	208
6.3.2.3.2	Optimisation of cDNA concentration <i>in planta</i> .....	209
6.3.2.3.2.1	Absolute quantification of VRCGs during the interaction .....	210
<b>6.4</b>	<b>Discussion .....</b>	<b>216</b>
<b>Chapter 7</b>	<b>General discussion .....</b>	<b>222</b>

<b>7.1</b>	<b>Virulence needs both toxin production and fungal growth ....</b>	<b>223</b>
7.1.1	Xylanase contributes to <i>Ptt</i> virulence.....	224
7.1.2	PttCHFP1 might contribute to <i>Ptt</i> virulence .....	227
7.1.3	Contribution of other proteinaceous toxins to <i>Ptt</i> virulence .....	228
7.1.4	Proposed infection process of barley by <i>Ptt</i> .....	229
<b>7.2</b>	<b>Conclusion and future directions .....</b>	<b>232</b>
	<b>References.. .....</b>	<b>234</b>
	<b>Appendix 1 .....</b>	<b>257</b>
	<b>Appendix 2 .....</b>	<b>259</b>
	<b>Appendix 3 .....</b>	<b>266</b>
	<b>Appendix 4 .....</b>	<b>269</b>
	<b>Appendix 5 .....</b>	<b>278</b>

## List of Figures

Figure 1.1. Net blotch disease in barley, spot form net blotch (A) and net form net blotch (B).....	6
Figure 2.1. Specially designed Petri dish inoculation system used in this study to allow easy visualisation of <i>Ptt</i> growth on barley. ....	26
Figure 2.2. Representative images depicting differences in the virulence of the six <i>Ptt</i> isolates on barley cv. Sloop 6 days post inoculation.....	36
Figure 2.3. Representative images depicting differences in the virulence of the six <i>Ptt</i> isolates on barley cv. Sloop 17 days post inoculation.....	37
Figure 2.4. Representative images for fungal development of two isolates of <i>Ptt</i> after 11 days post inoculation <i>in planta</i> . ....	38
Figure 2.5. Percentage of conidia germinated for six isolates of <i>Ptt</i> after 24 h <i>in vitro</i> or <i>in planta</i> in barley cv. Sloop.....	40
Figure 2.6. Representative images for fungal development of six isolates of <i>Ptt</i> <i>in planta</i> .....	41
Figure 2.7. Differences in the hyphal length between six isolates of <i>Ptt</i> at 24 hours post inoculation (hpi) <i>in planta</i> in barley cv. Sloop. ....	43

Figure 2.8. Fungal development of six isolates of <i>Ptt</i> after 24 hours post inoculation (hpi) <i>in planta</i> . .....	44
Figure 2.9. Optimisation of toxin production in two isolates of <i>Ptt</i> (32/98, more virulent) and 08/08f (less virulent) using two types of media. ....	45
Figure 2.10. Optimisation of protein production in 32/98 and 152/09 (more virulent isolates) grown for 12 days (d) on two types of media. ....	47
Figure 2.11. Concentration of protein in the filtrates of two virulent isolates (32/98 and 152/09). .....	48
Figure 2.12. PAGE for total protein extracted from the filtrates of 32/98 and 152/09 grown for 23 days in two types of media. ....	48
Figure 2.13. Effect toxin extraction methods on the bioassay of toxins on barley cv. Sloop. ....	49
Figure 2.14. Bioassay test for proteinaceous toxins extracted from filtrates of the six isolates of <i>Ptt</i> . ....	51
Figure 3.1. Bioassays of 5 fractions (F1 to F5) from the culture filtrates of the more virulent isolate (32/98) and less virulent isolate (08/08f) after 5 days post injection. ....	70
Figure 3.2. Protein comparison on PAGE between protein fractions (F2 to F5) of the culture filtrates of the more (32/98) and less (08/08f) virulent isolates. ....	72
Figure 3.3. Bioassay of 10 protein fractions (F1 to F10) from filtrates of the more virulent isolate (32/98) on three barley cultivars 5 days post injection. ....	77
Figure 3.4. Bioassay of 6 protein sub-fractions (SF4/1 to SF4/6) of more virulent isolate (32/98) on three barley cultivars after 5 days post injection. ....	78
Figure 3.5. Separation of protein fractions (F3 to F10), protein sub-fractions (4/1-4/6) and crude toxin (32T) for more virulence isolate 32/98 on PAGE. ....	80



Figure 3.6. 2DGE comparison of protein profiles of fraction 4 (A) and fraction 6 (B) from 32/98 isolate. ....	87
Figure 3.7. Identification of proteins extracted from culture filtrates from the more virulent isolate 32/98 (A) and the least virulent isolate 08/08f (B) using 2-D gel electrophoresis.....	89
Figure 3.8. PAGE for proteins extracted after 6 and 9 day post inoculation (dpi) from uninfected leaves (C) and leaves infected with 32/98 isolate (32) of <i>Ptt</i> . ....	92
Figure 3.9. Separation of proteins extracted from 32/98 crude toxin (32T), fraction 4 (F4), sub-fraction 4/2 (SF4/2) and intercellular washing fluids (ICWFs) using PAGE.....	92
Figure 3.10. 2DGE comparison of protein profiles of ICWFs from infected and uninfected plants.....	97
Figure 4.1. The full length of <i>PttXyn11A</i> cDNA and PttXyn11A protein (JX900133) (A). ....	121
Figure 4.2. Multiple alignment and phylogenetic analysis of PttXyn11A and proteins containing Glycosyl hydrolases family 11 domain. ....	124
Figure 4.3. Alignment of PttXyn11A of <i>Ptt</i> with TrXyn11A, <i>Trichoderma reesei</i> and BcXyn11A, <i>B. cinerea</i> (Brito <i>et al.</i> , 2006). ....	126
Figure 4.4. Secondary and three dimensional structure of PttXyn11A of <i>Ptt</i> . .	129
Figure 4.5. The full length of <i>PttCHFPI</i> cDNA and PttCHFPI protein (JX900134).....	131
Figure 4.6. Phylogenetic tree of selected members of cysteine hydrolase superfamily. ....	132
Figure 4.7. Multiple alignment of PttCHFPI and selected members of isochorismatase family proteins. ....	134
Figure 4.8. The predicted three dimensional structure of PttCHFPI of <i>Ptt</i> (A) and <i>P. aeruginosa</i> 1NF8 protein (B). ....	135
Figure 4.9. The full length of <i>PttGPI-CFEM</i> cDNA and PttGPI-CFEM protein (A).....	137

Figure 4.10. Multiple alignment of PttGPI-CFEM and fungal proteins showing the eight cysteine-containing CFEM domain (A). .....	138
Figure 4.11. The predicted three dimensional structure of PttGPI-CFEM of <i>Ptt</i> . .....	139
Figure 4.12. The full length of <i>PttSP1</i> cDNA and PttSP1 protein (A). .....	141
Figure 4.13. Multiple alignment of PttSP1 and bacterial proteins showing lipid attachment site. ....	142
Figure 4.14. Secondary and three dimensional structure of PttSP1. ....	143
Figure 4.15. The predicted three dimensional structure of PttSP1 of <i>Ptt</i> . ....	144
Figure 4.16. Differences in the expression level of VRCGs for six isolates ( <i>in vitro</i> ) growing for 10 days in FCM. ....	145
Figure 4.17. Differences in the expression level of VRCGs for six isolates <i>in planta</i> at 192 hours post inoculation. ....	146
Figure 5.1. Denaturing purification of PttGPI-CFEM heterologously expressed in <i>E. coli</i> . ....	163
Figure 5.2. Optimisation of heterologous expression of PttXyn11A in <i>E. coli</i> with different temperatures. ....	165
Figure 5.3. Optimisation of heterologous expression of PttXyn11A in <i>E. coli</i> with different incubation time and L-arabinose concentration. ....	166
Figure 5.4. Heterologous expression of PttXyn11A in <i>E. coli</i> . ....	167
Figure 5.5. The effect of overexpression of PttXyn11A on the viability of <i>E. coli</i> . ....	168
Figure 5.6. Optimisation of heterologous expression of PttCHFP1 in <i>E. coli</i> with different incubation conditions and L-arabinose concentration. ....	169
Figure 5.7. Heterologous expression and denaturing purification of PttCHFP1 in <i>E. coli</i> . ....	170
Figure 5.8. Heterologous expression and native purification of PttCHFP1 in <i>E. coli</i> . ....	170

Figure 5.9. The effect of overexpression of PttCHFP1 on the viability of <i>E. coli</i> . .....	171
Figure 5.10. Optimisation of heterologous expression of PttSP1 in <i>E. coli</i> with different incubation conditions and L-arabinose concentration. ..	173
Figure 5.11. Heterologous expression and denaturing purification of PttSP1 in <i>E. coli</i> .....	174
Figure 5.12. Heterologous expression and native purification of PttSP1 in <i>E.</i> <i>coli</i> . .....	175
Figure 5.13. The effect of overexpression of PttSP1 on the viability of <i>E.coli</i> . .....	176
Figure 5.14. Bioassay of heterologously expressed PttXyn11A (X), PttCHFP1 (C) and PttSP1 (S) (expressed in <i>E. coli</i> ) unwashed protein. ....	179
Figure 5.15. Bioassay of heterologously expressed PttXyn11A (X), PttCHFP1 (C) and PttSP1 (S) (expressed in <i>E. coli</i> ) washed protein. ....	180
Figure 5.16. Bioassay of heterologously expressed PttXyn11A (X), PttCHFP1 (C) and PttSP1 (S) (expressed in <i>E. coli</i> ) on three cultivars. ....	181
Figure 5.17. Bioassay of heterologously expressed PttXyn11A (X), PttCHFP1 (C) and PttSP1 (S) (expressed in <i>E. coli</i> ), clear lysate on three cultivars. ....	182
Figure 5.18. Effect of protein concentration on the bioassay of heterologously expressed PttCHFP1 (expressed in <i>E. coli</i> ) on cv. Sloop.....	184
Figure 5.19. Bioassay of heterologously expressed PttSP1 (expressed in <i>E. coli</i> ) on cv. Sloop. ....	185
Figure 5.20. Bioassay of commercial xylanase on cv. Sloop. ....	186
Figure 5.21. Activity of xylanase (X) in the culture filtrate of six isolates of <i>Ptt</i> grown at FCM for 10 and 15 days. ....	188
Figure 6.1. Virulence of six isolates at different time on barley cv. Sloop, starting from 40 hours post inoculation (hpi) until 192 hpi.....	205
Figure 6.2. Virulence score of six isolates at different time on barley cv. Sloop, from 64 hours post inoculation (hpi) until 192 hpi.....	206

Figure 6.3. Fluorescent value of qPCR of <i>PttGAPDH</i> for six isolates at 192 hours post inoculation (hpi).....	208
Figure 6.4. The expression of VRCGs during the interaction of <i>Ptt</i> isolates and barley. ....	215
Figure 7.1. Simplified schematic showing the proposed scenario for <i>Ptt</i> infection process.....	231
Figure A1.1. Tekauz’s scale (Tekauz, 1985); the scale describes the reaction of barley to <i>P. teres</i> f. <i>teres</i> and illustrates these reaction using numbers from 1 to 10. ....	257
Figure A2.1. RT-PCR cycle number optimisation for VRCGs <i>PttSP1</i> , <i>PttXyn11A</i> , <i>PttCHFP1</i> , <i>PttGPI-CFEM</i> and <i>PttGAPDH</i> . ....	259
Figure A2.2. Multiple alignment of PttCHFP1and CSHase family proteins. .	260
Figure A2.3. The evolutionary history of PttCHFP1 and its homologues from CSHase family.....	261
Figure A2.4. Multiple alignment of PttCHFP1and Nicotinamidase family proteins. ....	262
Figure A2.5.The evolutionary history of PttCHFP1 and its homologues from Nicotinamidase family.....	263
Figure A2.6. Secondary structure of PttGPI-CFEM and 4 selected members of CFEM family.....	264
Figure A2.7. Graphical summary of PttSP1 BLAST in UniProtKB databases. ....	265
Figure A3.1. Native extraction of heterologous expression of PttXyn11A from <i>E. coli</i> with different temperatures. ....	266
Figure A3.2. Denaturing extraction of heterologous expression of PttXyn11A in new transformant of <i>E. coli</i> . ....	267

Figure A3.3. Optimisation of heterologous expression of <i>PttCHF1</i> in <i>E. coli</i> with different incubation conditions and L-arabinose concentration. ....	267
Figure A3.4. Optimisation of heterologous expression of <i>PttSP1</i> in <i>E. coli</i> with different incubation conditions and L-arabinose concentration. ..	268
Figure A4.1. RT-PCR products (partial product) for four VRCGs isolated from 32/98 mycelium grown for 10 day on FCM. ....	269
Figure A4.2. Sequence confirmation and alignment of qRT-PCR primers products with the full length of corresponding genes. ....	273
Figure A4.3. Expression of VRCGs at 40 and 192 hours post inoculation (hpi) using comparative CT ( $\Delta\Delta C_T$ ) method. ....	274
Figure A4.4. Amplification efficiency for VRCGs at different primer concentrations. ....	274
Figure A4.5. Standard curves for VRCGs with low concentration of cDNA. ....	275
Figure A4.6. Optimising of standard curve for VRCGs at lower cDNA concentration. ....	275
Figure A4.7. Standard curve for VRCGs with high concentration of cDNA. ....	276
Figure A4.8. Optimising standard curve for VRCGs at higher cDNA concentration. ....	276
Figure A4.9. The expression of VRCGs ( <i>PttSP1</i> , <i>PttXyn11A</i> , <i>PttCHF1</i> , <i>PttGPI-CFEM</i> and <i>PttGAPDH</i> ) in (pg) at 40, 64, 120 and 144 hours post inoculation (hpi) in six isolates of <i>Ptt</i> in three experiments. ....	277

## List of Tables

Table 2.1. Origin and isolation year of <i>Pyrenophora teres</i> f. <i>teres</i> isolates used in this study and the host barley cultivar from which they were isolated.....	23
Table 2.2. Media and their components used for toxin production optimisation. ....	29
Table 3.1. Protein identification of the active fractions from more (32/98) and less (08/08f) virulent isolates.....	74
Table 3.2. Protein concentrations in fractions and sub-fractions of culture filtrates from the 32/98 isolate.....	75
Table 3.3. Protein identification of the active fractions and sub-fractions from the culture filtrate of a more virulent isolate (32/98). ....	82
Table 3.4. Protein identification of whole fraction 4 and 4/4 from filtrates of a more virulent isolate (32/98). ....	84
Table 3.5. Protein identification of differentially expressed two-dimensional gel electrophoresis (2DGE) protein spots (Figure 3.7). ....	90
Table 3.6. Protein identification of ICWFs from barley leaves infected with <i>Ptt</i> isolate 32/98 after 9 dpi. ....	93
Table 3.7. Protein identification of 2DGE comparison of ICWFs from infected and uninfected leaves after 9 dpi (Figure 3.10). ....	98
Table 3.8. The most dominant proteins as identified in the biologically active protein profiles and their accession number, source, family and proposed function. ....	104
Table 4.1. List of primers used in full length isolation and semi-quantitative RT-PCR to amplify the cDNA of the VRCGs <i>PttXyn11A</i> , <i>PttCHFPI</i> , <i>PttSP1</i> , <i>PttGPI-CFEM</i> and <i>PttGAPDH</i> . ....	112
Table 4.2. Selected proteins of GH11 family and their accession numbers and organisms which were used in multiple alignments with <i>PttXyn11A</i> (JX900133). ....	115

Table 4.3. Cysteine hydrolase families used in the alignments and phylogenetic analysis. ....	116
Table 6.1. List of primers used in RT-qPCR to amplify the partial length of cDNA of VRCGs <i>PttSPI</i> , <i>PttXyn11A</i> , <i>PttCHFPI</i> , <i>PttGPI-CFEM</i> and <i>PttGAPDH</i> . ....	198
Table A1.1. A numerical scale to assess development of <i>P. teres</i> during its growth upon barley using light microscopy (Lightfoot and Able, 2010). ....	258

## **Abstract**

*Pyrenophora teres f. teres* (*Ptt*) causes net form net blotch disease (NFNB), an important disease of barley in Australia and worldwide. This fungus uses proteinaceous toxins to cause necrosis and different isolates of *Ptt* differ in their ability to cause symptoms on different cultivars of barley. However, little is known about the roles of pathogen growth and individual toxins in symptom development. This project therefore aimed to determine whether there is a relationship between toxin production, fungal growth and virulence in NFNB.

Conidial germination, extent of fungal growth and culture filtrate toxicity were compared for six South Australian *Ptt* isolates with different virulence on the barley cultivar ‘Sloop’. In addition, *Ptt* toxin production was optimised before identification and selection of virulence-related candidate proteins (VRCPs) for further characterisation. The biological activity of recombinant VRCPs on susceptible and resistant cultivars and VRCPs gene expression during the interaction of Sloop with each isolate were also compared.

In general, the more virulent isolates had higher rates of conidial germination (both *in vitro* and *in planta*) and fungal development *in planta*, represented by longer hyphae and more appressoria, compared with less virulent isolates. Similarly, *PttGAPDH* and its transcript were more abundant during the interaction of barley with more virulent isolates.



A proteomics approach was used to identify proteins unique to the more virulent isolate, proteins from bioactive fractions on either susceptible (Sloop) or resistant cultivars (CI9214 and Beecher) and proteins from the intercellular washing fluids (ICWFs) of infected barley. These analyses revealed that *Ptt* produced proteins between 37 and 150 kDa that have biological activity.

Liquid Chromatography-Electrospray Ionisation Ion-Trap Mass Spectrometry (LC-eSI-IT MS), of individual biologically active proteins was used to identify peptides which matched to 17 proteins that belong to three groups of fungal proteins including virulence-related proteins; fungal growth and development proteins; and those with unknown function (hypothetical proteins). However, *Ptt* toxins were not detected in the ICWF protein profiles suggesting that *Ptt* toxins were either in trace amounts or might be internalised into the cell.

The four VRCPs selected, were identified as hypothetical proteins with unknown function in the *Ptt* database. Further bioinformatic analysis characterised these VRCPs as an isochorismatase (PttCHFP1), an endo-1, 4- $\beta$ -xylanase A (PttXyn11A), a glycoposphatidylinositol (GPI)-anchored common in fungal extracellular membrane (CFEM) domain-containing protein (PttGPI-CFEM) and an unknown proteinaceous secreted (but conserved) hypothetical protein (PttSP1). These VRCPs were heterologously expressed and characterised using gene expression studies.

PttXyn11A had strong homology with the well characterised endoxylanases, TrXyn11A from *Trichoderma reesei* and BcXyn11A from *Botrytis cinerea*, known to contribute to virulence. A necrosis-inducing region on the surface of the enzyme was also identified in PttXyn11A, suggesting a potential role in necrosis induction. The culture filtrates for more virulent isolates had significantly greater xylanase activity than those from less virulent isolates. Even though heterologously expressed *PttXyn11A* was toxic to *Escherichia coli*, xylanase activity was detectable at very low levels and was not enough to cause symptoms in the bioassay. In addition, semi-quantitative reverse transcriptase polymerase chain reaction (RT-PCR) and RT-quantitative PCR (RT-qPCR) analysis demonstrated that *PttXyn11A* was expressed more abundantly by the more virulent isolates compared with the other isolates in culture and during the plant-pathogen interaction. Together, these results suggest that *PttXyn11A* plays a role in virulence, either through its ability to degrade the plant cell wall to assist fungal growth or through its necrosis-inducing ability.

PttCHFP1 showed homology to an isochorismatase, an enzyme that has been proposed to have a role in plant defence via inhibition of salicylic acid production. PttSP1 showed homology to a membrane lipoprotein proposed to have a role in fungal development. Bioassay of recombinant *PttCHFP1* and *PttSP1* induced chlorosis symptoms in the susceptible barley cultivar (Sloop). The cysteine-rich CFEM domain identified in PttGPI-CFEM has been

suggested to have an important role in hyphal attachment and fungal networking. However, *E. coli* was not able to express this gene probably due to its attachment to the plasma membrane and/or cell wall. Analysis of the gene expression profiles for *PttCHFPI*, *PttGPI-CFEM* and *PttSPI* showed no significant differences between isolates *in vitro* and *in planta* suggesting that all isolates regulated the expression of these genes to the essential level possibly required for pathogenesis.

This is the first study to identify the relationship between fungal growth and proteinaceous toxin production, characterise individual proteinaceous toxins in the mixture of *Ptt* culture filtrate and investigate the expression profiles of genes encoding VRCPs during the *Ptt*-barley interaction. This study therefore provides a better understanding of the *Ptt*-barley interaction by identifying the potential toxins which might lead to identify the toxin targets and ultimately support the breeding of resistant cultivars of barley.

## **Declaration**

I declare that the work presented in this thesis contains no material which has been accepted for the award of any other degree or diploma in any university or other tertiary institution to Ismail Ahmed Ismail, and to the best of my knowledge and belief, this thesis does not contain any material previously published or written by another person, except where due reference has been made in the text.

I give consent to this copy of my thesis, when deposited in the University Library, being made available for loan and photocopying, subject to the provisions of the Copyright Act 1968.

The author acknowledges that copyright of the published works contained within this thesis (as listed in the Appendix 5) resides with the copyright holder (s) of those works. I also give permission for the digital version of my thesis to be made available on the web, via the University's digital research repository, the Library catalogue, and also through web search engines, unless permission has been granted by the University to restrict access for a period of time.

Ismail Ahmed Ismail

/ /

## **Acknowledgment**

I would like to thank the Ministry of Higher Education and Scientific Research of Iraq for providing me this PhD scholarship. My sincere thanks to my principal supervisor Associate Professor Amanda J. Able for the support, help, encouragement, patience, guidance and for believing in me. I am also grateful for my co-supervisor Dr. Dale Godfrey for her assistance, advices and support in my research.

Thanks to the Grains Research and Development Corporation for their support of this research and for providing a travel scholarship to attend the 4th Asian Conference on Plant Pathology and the 18th Biennial Australasian Plant Pathology Conference in Darwin. My thanks to Dr. Hugh Wallwork for providing *Pyrenophora teres* f. *teres* isolates and Mark Butt for his assistance in plant and fungal preparations.

I also would like to thank Dr William Bovill and Dr Kelvin Khoo for their help, Darren Wong, Wan Mohd Aizat Wan Kamaruddin, Duc Thong Le and all Able Lab members for their warm and beneficial discussion.

I am appreciative for the Iraqi Cultural Affair in Australia, the International Student Centre in Adelaide, especially Ms Jane Copeland, and the School of Agriculture, Food and Wine for their continuous support.

Finally, my special thanks to my beautiful wife Entesar for her incredible patience and love, my lovely three kids, Durar, Yousif and Ibrahim. Many thanks to my mother for her prayer, asking my lord to recuperate her, my brothers and sister for their sacrifices and support.

## Abbreviation

<u>Abbreviation</u>	<u>Full term</u>
×	Times
°C	Degree Celsius
2DGE	Two-Dimensional Gel Electrophoresis
3′	Three prime
5′	Five prime
ASP	Ammonium sulfate precipitation
BLAST	Basic Local Alignment Search Tool
BLM	Barley leaf medium
bp	Base pair
BSA	Bovine serum albumin
cDNA	Complementary DNA
CHAPS	3-[(3- cholamidopropyl) dimethylammonio]-1-propanesulfonate
cm	Centimeter
cv	Cultivar
DNA	Deoxyribonucleic acid
DNase	Deoxyribonuclease
dpi	Day post inoculation
DTT	Dithiothreitol
EDTA	Ethylene diamine tetraacetic acid
EST	Expressed sequence tag

FCM	Fries culture medium
FCM-noTE	FCM with no trace elements
<i>g</i>	<i>g</i> -force
<i>g</i>	Gram
<i>h</i>	Hour
<i>hpi</i>	Hour post inoculation
HNST	Host non-selective toxin
HST	Host specific toxin
ICWF	Intercellular washing fluid
IEF	Isoelectric focusing
IPTG	Isopropylthiogalactosidase
Kb	Kilobase
kDa	Kilodaltons
L	Liter
LB	Luria Bertani
LC-eSI-ITMS	Liquid Chromatography-Electrospray Ionisation Ion-Trap Mass Spectrometry
LMWC	Low molecular weight compound
LSD	Least significant difference
M	Molar
mA	Milliampere
MES	2-(N-morpholino) ethanesulfonic acid
mg	Milligram

min	Minute
mL	Millilitre
ML/min	Millilitre per minute
mM	Milimolar
mm	Millimeter
mRNA	Messenger ribonucleic acid
MS	Mass spectrophotometry
MW	Molecular weight
NCBI	National Center for Biotechnology Information
ng	Nanogram
Ni-NTA	Nikle-nitrilotriacetic acid
nm	Nanometers
OD	Optical density
ORF	Open reading frame
P	Probability
PAGE	Polyacrylamide Gel Electrophoresis
PCD	Programmed cell death
PCR	Polymerase chain reaction
PDA	Potato dextrose agar
PFCM	Phosphate buffered FCM
pH	Potential of Hydrogen
<i>pI</i>	Isoelectric point
PR-Protein	Pathogenesis related-protein



PS	Photosystem
QTL	Quantitative trait loci
r	Correlation coefficient
RNA	Ribonucleic acid
RNase	Ribonuclease
ROS	Reactive oxygen species
rpm	Revolutions per minute
RQ	Relative quantification
RT-PCR	Reverse transcriptase PCR
SDS	Sodium dodecyl sulphate
SDW	Sterile distilled water
sec	Second
SNW	Sterile nanopure water
TAE buffer	Tris-acetate EDTA buffer
TCA	Trichloroacetic acid
TE buffer	Tris EDTA buffer
Tm	Melting temperature
Tris	Tris (hydroxymethyl) amino methane
U	Unit
UFP	Ultrafiltration purification
UV	Ultra violet
V	Voltage
v/v	Volume for volume
Vhr	Volt hours
w/v	Weight for volume
µg	Micrograms
µg/mL	Micrograms per millilitre
µL	Micro litre
µM	Micromolar
µm	Micrometer

## **Chapter 1    General introduction**

### **1.1    Fungal phytotoxins**

Many microorganisms (such as bacteria and fungi) produce low molecular weight secondary metabolites which are toxic to plants (Möbius and Hertweck, 2009). These phytotoxins may be classified by their structure and may include spirocyclic lactams, sesquiterpenoids, sesterterpenoids, perylenequinones, isocoumarins, polyketides, tetramic acids, diketopiperazines and peptides (Berestetskiy, 2008; Turkkan and Dolar, 2008; Walton, 1996). However, the main classification system used is based on selectivity by the toxin rather than on their chemical properties or structural characteristics (Berestetskiy, 2008; Stergiopoulos *et al.*, 2013). Hence, toxins are usually classified as either Host Selective Toxins (HSTs) or Host Non-Selective Toxins (HNSTs) (Ballio, 1991; Friesen *et al.*, 2008a; Möbius and Hertweck, 2009; Sarpeleh *et al.*, 2007; Stergiopoulos *et al.*, 2013; Turkkan and Dolar, 2008; Walton, 1996). HSTs are metabolites produced by plant pathogenic isolates of certain fungal species. These metabolites induce toxicity in specific genotypes of the host and promote particular symptoms. The ability to produce these toxins determines the pathogenicity and host specificity for the pathogens, while plant susceptibility depends upon the presence of the toxin target (Stergiopoulos *et al.*, 2013). In addition, HSTs are mostly ribosome-produced peptides (Friesen *et al.*, 2008a; 2008b). In contrast, HNSTs affect a wide range of plant species and contribute to the virulence of the pathogen (the degree of damage to the host by parasite) but not to the pathogenicity (the qualitative capacity of a parasite to infect and

cause disease on a host) (Friesen *et al.*, 2008a; Markham and Hille, 2001; Stergiopoulos *et al.*, 2013; Walton, 1996; Wolpert *et al.*, 2002). The broad effect of HNSTs is achieved by affecting the most common physiological processes in plants including energy production (for example, tentoxin produced by *Alternaria* spp. affects the chloroplast electron transport chain); lipid biosynthesis (for example, cyperin produced by *Ascochyta cypericola* affects protoporphyrinogen oxidase, a key enzyme in porphyrin synthesis); actin polymerisation (cytochalasins produced by many fungal species); and production of reactive oxygen species (ROS) (for example, cercosporins produced by *Cercospora* spp. affects lipid peroxidation of cell membranes, electrolyte leakage and eventually cause cell death) (Berestetskiy, 2008; Dayan *et al.*, 2008; You *et al.*, 2008).

The virulence and pathogenicity of pathogens, especially necrotrophic fungi, are heavily dependent upon the secretion of these phytotoxins which allows the release of nutrients to facilitate colonisation of host tissues (Berestetskiy, 2008; Wolpert *et al.*, 2002). For example, *Cochliobolus* spp., *Mycosphaerella zae-maydis*, *Leptosphaeria maculans*, *Periconia circinata*, *Stemphylium vesicarium*, *Pyrenophora tritici-repentis* and *Stagonospora nodorum* are known to produce a range of structurally diverse HSTs that act as virulence factors (Amaike *et al.*, 2008; Ciuffetti *et al.*, 2010; Ellwood *et al.*, 2010; Liu *et al.*, 2009; Stergiopoulos *et al.*, 2013; Walton, 1996; 2006) and affecting the extent of symptoms (Stergiopoulos *et al.*, 2013).

## 1.2 Necrotrophic phytotoxins and disease development

Three modes of nutrition are used by pathogens during infection of host plants: biotrophic, necrotrophic and hemi-biotrophic. A biotrophic fungus lives within the living cell by establishing a long term relationship, rather than killing the plant cell (Gan *et al.*, 2010; Stergiopoulos and de Wit, 2009). A hemi-biotrophic fungus spends the first part of its life as a biotroph and the rest as a necrotroph (Horbach *et al.*, 2011; Koeck *et al.*, 2011) but a clear distinction between biotrophs and hemi-biotrophs can be difficult (Stergiopoulos *et al.*, 2013). A necrotrophic fungus uses toxins to kill plant cells which then provide nutrition for fungal growth (Able, 2003; Friesen *et al.*, 2008a; Howlett, 2006; Möbius and Hertweck, 2009; Tan *et al.*, 2010). Phytotoxins produced by necrotrophic fungi have several roles in disease development. The majority of HSTs induce programmed cell death (Howlett, 2006; Jonathan and Jacques, 2001). For example, victorin (produced by *C. victoriae*); PC-toxin (produced by *Periconia circinata*); SV-toxins I and II (produced by *S. vesicarium*), PtrToxA and PtrToxB (produced by *P. tritici-repentis*); and SnToxA (produced by *S. nodorum*) trigger responses to programmed cell death (Friesen *et al.*, 2007; Manning *et al.*, 2007; Navarre and Wolpert, 1999; Stergiopoulos *et al.*, 2013). Phytotoxins, which function as cell wall enzymes, also provide the fungus with access to the host during the penetration stage (Beliën *et al.*, 2006; Jaroszuk-Scisel and Kurek, 2012). Some toxins cause diffusion of low molecular weight nutrients (amino acids and sugar) outside plant cells, so the fungal mycelium can easily absorb these materials from the apoplast (Jonathan and Jacques,

2001; Walton, 1996). Toxins may also have an impact on membrane integrity, inhibit root growth, or cause general necrosis, chlorosis and deactivation of defence processes (El-Bebany *et al.*, 2010; Friis *et al.*, 1991; Knogge, 1996; Walton, 1996; Yoder, 1980). Some toxins prevent the expression of plant defence genes, for example, HC-toxin which is produced by *C. carbonum*, inhibits histone deacetylase leading to the induction of symptoms on susceptible plants (Takken and Joosten, 2000; Walton, 1996). The isochorismatase enzyme produced by *Verticillium dahliae* has also been proposed to inhibit plant defence responses (El-Bebany *et al.*, 2010) because of its ability to affect salicylic acid production (Wildermuth *et al.*, 2001).

The biological activity of many fungal toxins depends on several factors such as light, temperature and the maturity of the plant host. Toxins produced by *Cercospora* spp. on most hosts, *Botrytis cinerea* on *Phaseolus vulgaris*, *Ramularia collo-cygni* on *Arabidopsis* and *Pyrenophora teres* on barley have been shown to only be active in the presence of light (Colmenares *et al.*, 2002; Daub and Ehrenshaft, 2000; Miethbauer *et al.*, 2003; 2009; Sarpeleh *et al.*, 2008). The light dependency suggests a role for particular organelles such as the chloroplast (Manning and Ciuffetti, 2005; Manning *et al.*, 2008; Sarpeleh *et al.*, 2009). For example, tentoxin which is produced by *Alternaria alternata* induces chlorosis in seedlings and targets energy transfer during light-driven photophosphorylation in chloroplasts by binding to chloroplast coupling factor 1 (Avni *et al.*, 1992). However, some *Alternaria* toxins are light-independent (Berestetskiy, 2008). Light-independent toxins are more likely to affect some

physiological processes such as electrolyte leakage (Dayan *et al.*, 2000; Strange, 2007). Hence, the measurement of electrolyte leakage from plant tissues is a popular method of determining toxicity of compounds (Strange, 2007). Furthermore, temperature affects the activity of metabolism which is necessary for toxin-dependent symptom induction. Temperatures above 32°C were found to inhibit the activity of helminthosporoside (produced by *Helminthosporium sacchari*) in sugarcane tissues (Byther and Steiner, 1975). Proteinaceous toxins isolated from *P. teres* do not induce symptoms on barley leaves at 4°C (Sarpeleh *et al.*, 2008). Low temperature may, therefore, cause a decline in metabolism, inactivation of the proteinaceous toxins or loss of enzyme activity (Kwon *et al.*, 1998; Lehtinen, 1993). For example, Ptr ToxA (a HST produced by *P. tritici* f. *repentis*) has also been shown to require an active host metabolism for symptom induction (Kwon *et al.*, 1998).

### **1.3 Net blotch disease in barley**

Net blotch disease is one of the main barley diseases in Australia and worldwide (Wallwork, 2000; Xi *et al.*, 2008). This disease has two forms, spot form net blotch (SFNB) and net form net blotch (NFNB) caused by *P. teres* f. *maculata* (*Ptm*) and *P. teres* f. *teres* (*Ptt*) respectively (Figure 1.1) (Liu *et al.*, 2011; Mathre, 1997). Each form is responsible for particular symptoms. In SFNB, symptoms appear as dark brown spots surrounded by a chlorotic halo, while in NFNB, irregular dark-brown lines are present in reticulated patterns (McLean *et al.*, 2009). Currently, in South Australia, the net blotch form is

more important economically than the spot form (Hugh Wallwork, SARDI, personal communication) and worldwide (Liu *et al.*, 2011; Wallwork, 2000; Xi *et al.*, 2008) causing yield reductions of up to 44% (Jayasena *et al.*, 2002; 2007; Murray and Brennan, 2010). The potential for total loss is greatest if susceptible cultivars are grown and optimal disease conditions are met (Murray and Brennan, 2010). More recently, in southern Australia resistant cultivars have shown susceptibility to the NFNB pathogen. Therefore, understanding the basis for virulence is key to future disease control strategies because the evolution of virulence may determine the emergence and re-emergence of pathogens leading to host resistance being broken down and subsequent host range expansion (Sacristan and Garcia-Arenal, 2008).



**Figure 1.1. Net blotch disease in barley, spot form net blotch (A) and net form net blotch (B).**

#### **1.4 *Ptt*-barley interaction**

Interaction between necrotrophic pathogens and host plants is facilitated by two main factors; the physiological growth of the fungus and secretion of phytotoxins (Tan *et al.*, 2010). However, how much each factor contributes to the infection and how they are associated with each other is still not clear in the *Ptt*-barley interaction.

##### **1.4.1 Infection process**

The infection of *P. teres* starts after the conidia lands on the leaf, with suitable temperature and water availability, conidia starts to germinate in a few hours (Vandenberg and Rossnagel, 1990), and then hyphae grow to varying lengths from the germ tubes (Lightfoot and Able, 2010; Vancaesele and Grumbles, 1979). Within 24 h, a swollen club-shaped appressorial structure forms (Amaike *et al.*, 2008; Lightfoot and Able, 2010; Mathre, 1997; Vancaesele and Grumbles, 1979). The formation of these appressoria, however, appears to require signal transduction agents such as the mitogen-activated protein kinase (MAPK) PTK1 (Ruiz-Roldán *et al.*, 2001). Disruption of this gene reduced the ability of the fungus to produce appressoria *in vitro* and *in planta* and consequently the fungus lost its ability to infect the plant. Penetration occurs via the lower epidermal cell wall into the mesophyll tissue (Dushnicky *et al.*, 1996; Lightfoot and Able, 2010). Resistant cultivars may form papillae or papillae-like deposits in an attempt to stop the entry of the fungus (Keon and Hargreaves, 1983; Lyngs Jørgensen *et al.*, 1998). After the successful



penetration, hyphae forms primary and secondary intracellular vesicles within the epidermal cell and then hyphae starts to grow into the mesophyll tissue when necrosis starts to appear (Keon and Hargreaves, 1983). During this process several fungal secondary metabolites may be produced to facilitate conidial adhesion, conidial germination, appressorial formation, germ tube penetration and necrosis induction. Although the growth of *Ptt* and *Ptm* have been comprehensively compared (Lightfoot and Able, 2010), limited information is available about the differences in the growth of *Ptt* isolates with different virulence during the infection process on barley.

#### **1.4.2 *P. teres* toxins**

The relationship between *P. teres* toxins and induction of net blotch disease symptoms in barley has been the focus of recent research (Able, 2003; 2009; Sarpeleh *et al.*, 2007; 2008; Weiergang *et al.*, 2002). Two types of phytotoxins are produced by *P. teres*: low molecular weight compounds (Sarpeleh *et al.*, 2007; Weiergang *et al.*, 2002) and proteinaceous toxins (Sarpeleh *et al.*, 2009; 2007). The low molecular weight compounds appeared to be responsible for chlorosis and affected a wide range of hosts (HNSTs), whereas proteinaceous toxins caused necrosis only on barley (HSTs) and symptoms appeared to be more extensive in the susceptible cultivars. However, individual proteinaceous toxins produced by *P. teres* need to be characterised further, especially their individual contributions to the development of net blotch disease symptoms.

#### 1.4.2.1 HNSTs

Several LMWCs excreted by *P. teres* are considered as non-selective toxins (Friis *et al.*, 1991; Smedegård, 1977; Weiergang *et al.*, 2002). LMWCs from *P. teres* are marasmine derivatives (Gäumann and Jaag, 1946) and include four toxins: Toxin A [L,L-N-(2-amino-2-carboxyethyl) aspartic acid], Toxin B [1-(2-amino-2-carboxyethyl)-6-carboxy-3-carboxymethyl-2-piperazinone], Toxin C [N-[2-(2-amino-2-carboxy ethyl-amino)-2-carboxyethyl]], and aspergillomarasmine B and its derivatives (ninhydrin-positive compounds S-1 and S-2) (Friis *et al.*, 1991; Sarpeleh *et al.*, 2009; Weiergang *et al.*, 2002). Sarpeleh *et al.* (2007) demonstrated that LMWCs contribute to the general chlorosis and water soaking symptoms induced in susceptible barley. The symptoms induced by the *P. teres* LMWCs are generally the same as those induced by the pathogen (Sarpeleh *et al.*, 2007), but do not include the brown necrosis normally associated with net blotch disease. In contrast, Weiergang *et al.* (2002) compared the biological activity of toxin A, B and C and found that toxin C was the most active toxin, which caused distinct necrosis, followed by A and then B, which caused mainly chlorosis. The activity of aspergillomarasmine B was light-dependent suggesting it is targeting the metabolites of the light-dependent organelles such as the chloroplast (Sarpeleh *et al.*, 2009). Localisation of toxin may help to understand the process of interaction between toxins and their targets (Nimchuk *et al.*, 2003). However, the role of each LMWC is not clear yet in terms of characterisation of particular targets for individual toxins.

#### 1.4.2.2 Proteinaceous HSTs

Micro-organisms of many plant pathogenic genera are known to produce HSTs including *Cochliobolus* spp., *Alternaria* spp. and *Pyrenophora* spp (Friesen *et al.*, 2008a; Stergiopoulos *et al.*, 2013). These HSTs interact with specific targets in their hosts to produce symptoms (Friesen *et al.*, 2008a). Proteinaceous toxins have also been isolated from culture filtrates of both forms of *P. teres*, and have been shown to induce necrosis in susceptible cultivars of barley, but not in resistant barley genotypes or in other plant species (Sarpeleh *et al.*, 2007; 2008). This selectivity suggests individual proteins may be HSTs and therefore have a specific target. This is yet to be determined for the *P. teres* HSTs, but may prove to involve a similar mechanism to that seen in the interaction between PtrToxA toxin produced by *P. tritici* f. *repentis* and wheat (Manning and Ciuffetti, 2005; 2008; Manning *et al.*, 2007; Sarma *et al.*, 2005). Furthermore, susceptible barley seedlings are only sensitive to the proteinaceous *P. teres* toxins in the presence of light and higher temperatures, indicating the potential involvement of the chloroplast and the requirement for active metabolism in the interaction (Sarpeleh *et al.*, 2008). In wheat, PtrToxA targets ToxA-binding protein 1 (Tox-ABP1) which is present in both chloroplast membranes and chloroplast stroma (Manning and Ciuffetti, 2005; Manning *et al.*, 2007).

Sarpeleh (2007) and Wong (2010) have compared the biological activity of the culture filtrates of *Ptt* and *Ptm* and they found that both filtrates caused

necrosis similar to that induced by both forms. However, no information is available about the differences between culture filtrates of *Ptt* isolates with different virulence. Host-specific necrosis appeared to be associated with proteins of a particular molecular weight (between 20 and 100 kDa), suggesting this protein fraction may contain HSTs (Sarpeleh *et al.*, 2007; 2008). Sarpeleh (2007) identified several of the proteinaceous toxins in this fraction. They appeared to show homology to ABC transporters, ceratoplatanin and exo- $\beta$ -1, 3 glucanase in genome databases of other fungal species. Interestingly, ABC transporters have been shown to be necessary for toxin transport (Amnuaykanjanasin and Daub, 2009); ceratoplatanins might induce necrosis in plants by eliciting the production of phytoalexins and plant cell death (Boddi *et al.*, 2004; Comparini *et al.*, 2009); and exoglucanases may contribute to host cell wall degradation (Tamano *et al.*, 2007). However, due to the lack of a *P. teres* database at the time of those studies, no information is available about these proteins and other individual toxins in terms of their characteristics, functions and contribution to the infection of barley. Therefore, further characterisation of the individual proteins within the HST-fraction is required. In addition, comparison between culture filtrates of *Ptt* isolates with different virulence might provide information about the differences in their protein profiles.

Each proteinaceous HST may interact with an individual target (plant protein) that could be localised to particular organelles. Extraction of this toxin from intercellular washing fluids and/or different components of the plant cell

from leaves either infected with *Ptt* or treated with each individual fungal protein will help to localise each toxin in the plant tissue. Characterisation of the individual *in planta* targets of the HSTs will also allow a greater understanding of why the susceptible cultivars are sensitive to the toxin. For example, the quantitative trait loci (QTLs) responsible for sensitivity could be determined as has been done for Stagonospora leaf blotch in wheat caused by *S. nodorum* (Liu *et al.*, 2004b). This would allow the candidate gene responsible for sensitivity for toxins to be identified. The gene responsible for sensitivity to the SnTox1 produced by *S. nodorum* in wheat has been designated *Snn1* (Liu *et al.*, 2004a). Alternatively, as has been done for PtrToxA, plant proteins that directly bind to the toxin may be identified (Manning *et al.*, 2007). Whether the proteins from *Ptt* interact with chloroplastic or other plant proteins remains to be determined.

### **1.5 Virulence and proteinaceous HSTs**

The virulence and/or pathogenicity of necrotrophic fungi are dependent upon small toxic peptides (Oliver and Solomon, 2010; Tan *et al.*, 2010) which act as effectors, inducing host necrosis or chlorosis in a specific manner (Friesen *et al.*, 2008a; Friesen *et al.*, 2008b). These molecules usually cause tissue death in the susceptible plants that possess dominant sensitivity genes leading to successive pathogen colonisation (Koeck *et al.*, 2011; Tan *et al.*, 2010).

Necrotrophic effectors are a diverse group of small proteinaceous or secondary metabolite molecules, that can induce cell death in the host plant

(Tan *et al.*, 2010). Several effectors have been identified including victorin from *C. victoriae*; AAL-toxin from *A. alternata* (Walton, 1996; Wolpert *et al.*, 2002); PtrToxA and PtrToxB from *P. tritici-repentis* (Ballance *et al.*, 1989; Tomas *et al.*, 1990; Tuori *et al.*, 1995); SnToxA, SnTox1, SnTox2, SnTox3, SnTox4 from *S. nodorum* (Friesen and Faris, 2010); Abr-toxin from *A. brassicae* (Parada *et al.*, 2008) and several small cysteine-rich proteins designated as necrosis-inducing peptide (NIP)1, NIP2 and NIP3 from *R. commune* (Fiegen and Knogge, 2002; Rohe *et al.*, 1995; Wevelsiep *et al.*, 1991; Wevelsiep *et al.*, 1993). The corresponding genes have been assigned for most of these effectors and appear necessary for virulence and/or pathogenicity (Ciuffetti *et al.*, 1997; Friesen *et al.*, 2006; Manning and Ciuffetti, 2005). For example, the transformation of the *PtrToxA* gene to a non-pathogenic *P. tritici-repentis* isolate rendered it pathogenic on PtrToxA-sensitive wheat lines (Ciuffetti *et al.*, 1997). However, individual proteinaceous HSTs/effectors from the *Ptt* fungus have not been identified yet.

### **1.6 The mode of action of necrotrophic effectors (HSTs)**

Given that proteinaceous HSTs are biologically active only against a particular plant species (Wolpert *et al.*, 2002), the mode of action of these effectors are generally diverse accordingly. However, not all pathogen species produce these toxins and not all genotypes of the host are sensitive to the toxins. Generally, in necrotrophic fungi the interaction between the pathogen and its host is controlled by the inverse gene-for-gene model (Friesen *et al.*, 2007; Oliver and

Solomon, 2010), meaning that both toxin production by pathogen and toxin sensitivity by the host are required for disease development (Wolpert *et al.*, 2002). In addition, the presence of a HST target allele in a specific plant genotype confers susceptibility to the pathogen rather than resistance (Oliver and Solomon, 2010).

The mode of action of proteinaceous HSTs is likely involved in the production of ROS, inhibition of calmodulin, blocking of polymerization and elongation of actin and likely inhibition of photosynthesis (Ciuffetti *et al.*, 2010; Friesen and Faris, 2010). Toxins may also induce defence responses in the host (such as pathogenesis-related proteins) (Bent and Mackey, 2007; Osbourn, 2001; Pazzagli *et al.*, 1999), when the HSTs are recognised by the plants as microbe/pathogen-associated molecular patterns (MAMPs/PAMPs) (Comparini *et al.*, 2009).

Analysis of PtrToxA protein revealed that an arginyl-glycyl-aspartic (RGD) motif presents at the surface of the PtrToxA protein (Zhang *et al.*, 1997). This motif is necessary for PtrToxA internalisation (Manning and Ciuffetti, 2005; Manning *et al.*, 2008) and for the interaction with ToxABP1 (Manning *et al.*, 2007; Sarma *et al.*, 2005). This interaction induces changes in photosystem (PS) I and PSII which might lead to light dependent accumulation of ROS in the chloroplast (Manning *et al.*, 2009). However, the development of PtrToxA-induced programmed cell death (PCD) did not completely abolished by the silencing of *ToxABP1* gene (Ciuffetti *et al.*, 2010).

Localisation, identification of toxins and their corresponding targets *in planta* and the characterisation of defence responses to the HSTs will therefore help to identify the potential resistance mechanism(s) which could be involved.

### **1.7 Identification of necrotrophic fungal toxins might contribute to the development of resistant barley**

Given that proteinaceous HSTs interact with specific plant targets, identifying these targets will allow resistance development. Resistant barley cultivars are the most cost-effective way to control *P. teres* (McLean *et al.*, 2009). However, looking for probable mechanisms of resistance to toxins can be very challenging, especially if there is more than one mechanism working together. Generally, there are two types of toxin resistance: non-specific and specific (Karlovsky, 1999; Kiraly *et al.*, 2007). Plants exhibiting non-specific resistance are resistant to all of the races of a given pathogenic species (Thordal-Christensen, 2003). Specific resistance might be divided into two categories; innate resistance such as lack of toxin receptors (insensitivity to toxins) and acquired resistance. For example, detoxification of deoxynivalenol (DON, vomitoxin), produced by *Fusarium graminearum* in resistant wheat (Miller and Arnison, 1986) and inactivation of HC-toxin, produced by *C. carbonum* race 1 on maize, by HC-toxin reductase (HCTR) (Karlovsky, 1999; Meeley *et al.*, 1992; Meeley and Walton, 1991; Wolpert *et al.*, 2002).

In addition, plant pathogenesis-related (PR) proteins can be induced by many factors including fungal toxins (Datta and Muthukrishnan, 1999; Reiss



and Bryngelsson, 1996). There are several roles that have been implied for PR proteins including: prevention of virus diffusion, restriction of fungal invasion and antimicrobial activity (Santén *et al.*, 2005; Valueva and Mosolov, 2004; Van Loon *et al.*, 1994). PR proteins have been isolated from intercellular washing fluids (ICWFs) in barley after inoculation with *P. teres* toxins (Sarpeleh, 2007). Characterisation of these PR proteins has shown they are peroxidases,  $\beta$ -1,3-glucanases (PR-1) and chitinases (Reiss and Bryngelsson, 1996; Sarpeleh, 2007). Santén *et al.* (2005) also detected that PR-1 was in the chloroplast in chlorotic and necrotic tissue during the *P. teres*-barley interaction suggesting that defence responses are induced by the toxins.

Virulence of necrotrophic and hemi-biotrophic pathogens depends on the variation of the sensitivity to toxins in plants (Walters *et al.*, 2007). Sensitivity to toxins requires specific interaction of an individual genotype of host with a particular pathotype of pathogen (Lamari and Bernier, 1989). A correlation has been reported between sensitivity to toxins and susceptibility to the fungus (Weiergang *et al.*, 2002). This correlation is controlled by the same dominant gene, for example, wheat cultivars which are sensitive to *P. tritici-repentis* because they contain the *Tsn1* gene (Anderson *et al.*, 1999; Faris *et al.*, 1996) also show sensitivity to PtrToxA produced by *P. tritici* f. *repentis* (Lamari and Bernier, 1989; Lu *et al.*, 2006). However, this type of correlation has not been established with a NFNB resistant cultivar of barley yet. Furthermore, insensitivity to toxins is promising as a potential tool in plant breeding to produce resistant plants. Weiergang *et al.* (2002) suggested that the

LMWCs, toxin A and toxin C, produced by both forms of *P. teres* could be used for selection of barley lines resistant to net blotch disease due to their observation that the reaction to these toxins was correlated with infection by the fungus. However, toxin A and C are HNST toxins affecting a wide range of plants (Berestetskiy, 2008; Sarpeleh *et al.*, 2009; Walton, 1996; Wolpert *et al.*, 2002). Selection of resistant lines could therefore be difficult given these toxins are unlikely to be targeting specific proteins. Nevertheless, significant correlations between HST insensitivity and disease resistance were observed when sensitivity to PtrToxA (produced by both *S. nodorum* and *P. tritici* f. *repentis*) was evaluated in 172 accessions of wild emmer wheat (Chu *et al.*, 2008). Evaluation of sensitivity of barley genotypes to *Ptt* HSTs could therefore allow identification of new sources of resistance.

Given that necrotrophic fungi use a large array of cell wall degrading enzymes for pathogenicity (Hammond-Kosack and Rudd, 2008), lignification is an effective means to avoid these enzymes. Accumulation of lignin and lignin-like material has been observed during the infection of wheat by *P. tritici* f. *repentis* and it has been suggested to confine the growth of the fungus (Dushnicky *et al.*, 1998). More recently PtrToxA has been shown to induce the expression of a number of genes involved in lignification including chalcone synthase (CHS), cinnamoyl-CoA reductase and phenylalanine ammonia lyase (PAL) (Adhikari *et al.*, 2009). These enzymes are involved in the phenylpropanoid pathway (Hahlbrock and Scheel, 1989) and are also involved in phytoalexin accumulation in other plant-pathogen interactions (Adhikari *et*

*al.*, 2009). The difference between cell wall structure in different genotypes might affect their response to virulence factors (which are mostly cell wall degrading enzymes). However, the ability of *Ptt* to produce cell wall degrading enzymes needs to be established in the *Ptt*-barley interaction.

### **1.8 The objectives of this study**

*Ptt* interacts with barley using different strategies including physiological fungal growth and toxin production. However, the differences in the fungal growth of *Ptt* isolates with different virulence during the interaction with susceptible barley cultivar needs to be established. In addition, the role of toxin mixtures and individual toxins in the virulence of *Ptt* isolates is unknown. Thus, the aims of this study were:

1. To examine the fungal growth of *Ptt* isolates with different levels of virulence by comparing their growth patterns on a susceptible barley cultivar, an attempt to understand the differences in the interaction between these isolates (chapter 2).
2. To investigate the potential correlation between the virulence and toxin production by associating the virulence of isolates and the bioassay of their toxins (chapter 2).
3. *Ptt* produces a mixture of proteinaceous toxins which appear to be HSTs and have crucial roles in NFNB, therefore, this aim was identifying the most common and biologically active toxin in this

mixture by separating the toxin mixture into several fractions and sub-fractions and bioassaying these toxins (chapter 3).

4. To characterise virulence-related candidate proteins (VRCs) and predict their potential pathogenesis role using bioinformatics analysis. In addition, the presence of the transcripts of these candidate proteins *in vitro* and *in planta* was also investigated using semi-quantitative RT-PCR (chapter 4).
5. To heterologously express these VRCs using an *Escherichia coli* system and then bioassay the recombinant proteins, an attempt to clarify the role of each candidate protein and establish its contribution to symptom development (chapter 5).
6. Investigation of individual VRCs contribution during the *Ptt*-barley interaction *in planta* through analysing the expression profile of gene transcripts which encode these proteins using reverse-transcription quantitative PCR (RT-qPCR). These analyses might find a correlation between the occurrence of infection events, during a designated timecourse, and the expression profile of these genes (chapter 6).

## **Chapter 2 Fungal growth and virulence of *Pyrenophora teres* f. *teres* on barley**

### **2.1 Introduction**

There is wide variation in the virulence of *Pyrenophora teres* f. *teres* (*Ptt*) populations on barley and therefore the extent of symptoms seen in net form net blotch disease (NFNB) (Afanasenko *et al.*, 2007b; Peever and Milgroom, 1994; Rau *et al.*, 2003). *Ptt* is also pathogenic on other species. Of the 43 graminaceous species that Brown *et al.* (1993) assessed, 28 were susceptible to at least one of the six *Ptt* isolates tested. The mechanisms underlying these differences in virulence between isolates have been the focus of much research (Brown *et al.*, 1993; Jalli, 2011; Robinson and Jalli, 1996). Several researchers have reported that the timing and extent of conidial germination and penetration of the plant surface by the germ tube is critical for successful infection, and ultimately virulence (Dushnicky *et al.*, 1996; Kokkelink *et al.*, 2011). When virulent and avirulent isolates were crossed, the resultant progeny only shared 92% similarity to the parents (Jalli, 2011) suggesting that sexual recombination can change virulence and that *Ptt* isolates are highly variable. In addition, the virulence of the progeny was not correlated with their morphology (such as growth rate on agar, spore production, spore width, spore length and numbers of septa per conidium) (Jalli, 2011).

Afanasenko *et al.* (2007a) reported that avirulence in *Ptt* is determined by one or two genes based on segregation analysis of ascospore-derived progeny from two crosses of isolates from different origin. Given the current understanding of plant-pathogen interactions, these genes probably encode for

cultivar-specific toxins known as effectors (Friesen *et al.*, 2008a). However, virulence of the pathogen might also be promoted by the production of other enzymes and toxins during the interaction with the host (Bent and Mackey, 2007). Sarpeleh *et al.* (2008) previously identified the involvement of proteinaceous toxins in NFNB disease development. These toxins probably act as virulence factors because they induce symptoms only on barley and more intensely on susceptible than resistant cultivars (Friesen *et al.*, 2008a; Kamoun, 2007; Sarpeleh *et al.*, 2007; Sarpeleh *et al.*, 2008).

Although some research has investigated *P. teres* growth *in planta* (Keon and Hargreaves, 1983; Lightfoot and Able, 2010; Vancaesele and Grumbles, 1979), the timing of different growth stages for *Ptt* isolates of different virulence has not been directly compared at a cellular level *in planta*. In addition, whether the virulence of NFNB isolates and the growth of these isolates on the same cultivar are associated is not clear.

Several studies have analysed toxin production in *P. teres* (Campbell *et al.*, 2003; Friis *et al.*, 1991; Sarpeleh *et al.*, 2009; 2007; 2008; Weiergang *et al.*, 2002). Even though proteinaceous toxins from one isolate of *Ptt* have been shown to induce NFNB-like symptoms (2007; Sarpeleh *et al.*, 2008), whether toxins from different isolates also induce symptoms and their relationship with virulence has not been established. Furthermore, minimal optimisation of the production of these toxins in culture filtrates has occurred (Sarpeleh, 2007). Thus, the objectives of the research presented in this chapter were to investigate the relationship between the virulence of *Ptt* isolates, their growth on a

susceptible cultivar and the symptoms caused by proteins extracted from the filtrates of these isolates. To help meet this goal, the production and extraction of proteinaceous toxins from culture filtrates was optimised.

## **2.2 Materials and methods**

### **2.2.1 Plant growth**

Seeds from the barley (*Hordeum vulgare* L.) cultivar Sloop, identified previously as susceptible (Gupta *et al.*, 2003), were grown in sterilised soil (University of California Davis mix) (Baker 1957) in a growth room at the Plant Research Centre, Waite Campus, the University of Adelaide at 21°C under a cycle of 16 h light and 8 h dark. Plants were used at Zadoks' growth stage 14 (fourth leaf more than half visible) (Zadoks *et al.*, 1974) for virulence testing and bioassay of proteins extracted from culture filtrates.

### **2.2.2 Fungal isolation and culturing**

Six isolates from *Ptt* were provided, as freeze-dried samples on barley leaves, by the South Australian Research and Development Institute (SARDI) (Table 2.1). Small pieces from the freeze-dried leaves were placed onto 3.9% Potato Dextrose Agar (PDA; Difco™, Becton, Dickinson and Company, Sparks, MD USA) and grown for 7 days at 21°C. To prepare a single spore isolate for plant inoculation and toxin production, a 5 mm disc was transferred into 1.6% water agar plates containing sterilised barley leaves and incubated at 21°C under a cycle of 12 h near-ultraviolet light and 12 h dark for conidial formation (Deadman and Cooke, 1985). A single conidium was picked using a glass

needle made from a Pasteur pipette (Choi *et al.*, 1999; Goh, 1999) and placed onto 3.9% PDA plates before growing for 7 days at 21°C. Inocula was prepared by transferring five discs onto 1.6% water agar with sterilised barley leaves placed on the surface and then grown for two weeks at 21°C under a cycle of 12 h near-ultraviolet light and 12 h dark. Conidia were harvested by adding 5 mL sterilised nanopure water (SNW) to each plate and then agitating using a sterilised camel hair brush (size 1). The conidial suspension was then filtered through two layers of sterilised cheesecloth to remove the mycelium (Cao *et al.*, 2009). Conidial concentration was measured using a haemocytometer (Ment *et al.*, 2010) and adjusted to the required concentration by adding SNW.

**Table 2.1. Origin and isolation year of *Pyrenophora teres f. teres* isolates used in this study and the host barley cultivar from which they were isolated.**

Isolate Code	Host Barley Cultivar	Location	Year
8/08f	Keel	Port Pirie, South Australia.	2008
122/09	Fleet	Ungarra, South Australia.	2009
55/07	Keel	Pinery, South Australia.	2007
123/09	Navigator	Crystal Brook, South Australia.	2009
32/98	Skiff	Mallala, South Australia.	1998
152/09	Fairview	Bordertown, South Australia.	2009

### **2.2.3 Virulence testing of *Ptt* isolates**

In each of two separate experiments and for each of the six isolates of *Ptt*, four individual plants of barley cv. Sloop grown as per section 2.2.1 were inoculated with  $5 \times 10^5$  conidia per mL in 0.1% (v/v) Tween-20 (Lightfoot and Able, 2010;



Sarpeleh *et al.*, 2007) using a sprayer until run off. Plants were scored 6 days post inoculation (dpi) using a numerical scale (1-10) adapted from Tekauz (1985). The scale describes the reactions of barley to *Ptt* (Appendix, Figure A1.1), which were monitored daily until 17 dpi and leaf sections were visualised using a dissecting microscope [Olympus CK40-F200 (Olympus Optical Co Ltd, Japan)]. Images were captured for representative leaves using a CanoScan 5600F scanner (Canon, Japan).

#### **2.2.4 *In vitro* and *in planta* conidial germination assays**

To establish the potential difference between the *in vitro* and *in planta* germination percentage of conidia, conidia from six isolates was used in an agar-coated slide system with 0.1% trypan blue in lactophenol (Fernando *et al.*, 2000; Huang *et al.*, 2001). Water agar was prepared by adding 1.5% agar to SNW before being autoclaved for 20 min at 121°C. Hot molten water agar (0.5 mL) was placed on slides previously wiped over with ethanol and spread using a hot glass (L-shaped) spreader. After the agar was set, 30µL ( $1 \times 10^4$  conidia per mL) was placed on the top of the agar and spread using the spreader. Slides were then transferred into Petri dishes (90 mm diameter) with two layers of moistened Whatman<sup>®</sup> filter paper (Whatman International, Maidstone, England) taped to the inside of the lid. Cultures were incubated at 21°C for 24 h in the dark. Conidia were stained using 0.1% trypan blue in lactophenol (Fernando *et al.*, 2000; Huang *et al.*, 2001) and examined using light microscopy. Five slides were used for each isolate and whether germination had

occurred or not was counted for 100 conidia per slide as per Fernando *et al.* (2000). Each conidium was considered germinated when its germ tube was longer than half the length of the conidium.

The *in planta* germination percentage of the six isolates of *Ptt* in barley cv. Sloop was determined using a specially designed system that provided high humidity and darkness for optimal conidia germination during the first 24 hours post inoculation (hpi) and allowed identification of the inoculated area for easy microscopic examination. Petri dishes were modified by cutting away the bottom edge of Petri dishes from two sides (in a U shape) to ensure the leaf could be fit without damaging (Figure 2.1). The appropriate amount of sterilised cotton was placed on the bottom and moistened with SNW to maintain humidity. The lids of Petri dishes were covered with white paper (0.3 mm thickness) for the first 24 hpi. These plates were supported with small inverted pots (Figure 2.1). Approximately 5 cm in the middle of the adaxial leaf surface was inoculated with  $1 \times 10^4$  conidia in a total volume of 200  $\mu$ L. Five leaves (from plants grown as per section 3.2.1) in each of three individual experiments were inoculated for each isolate and labeled with a marker pen around the 5 cm inoculation area. Samples were taken 24 hpi by cutting the labeled leaves (5 cm long) and leaf sections were prepared for microscopic visualisation using a light microscope (Olympus CK40-F200) as per Able (2003) and Lightfoot and Able (2010). Leaves were cleared in a solution of LGE (16.7% lactic acid, 16.7% glycerol and 66.7% ethanol) for 1 h at 70°C before being stained in 0.5x lactophenol blue (25% phenol, 25% lactic acid,

25% glycerol and 0.025 g aniline blue per 100 mL) for 10 min at room temperature. Leaves were cleared again using LGE for 1 h at 70°C and vacuum infiltrated in LGE for 20 min. Stained leaves were mounted in glycerol on the slides and sealed with nail polish and examined under a dissecting microscope. Whether germination had occurred or not was assessed for 10 conidia per section. Digital images were captured using an Olympus camera (Olympus UC50, Olympus Soft Imaging Solutions GMBH, Münster).

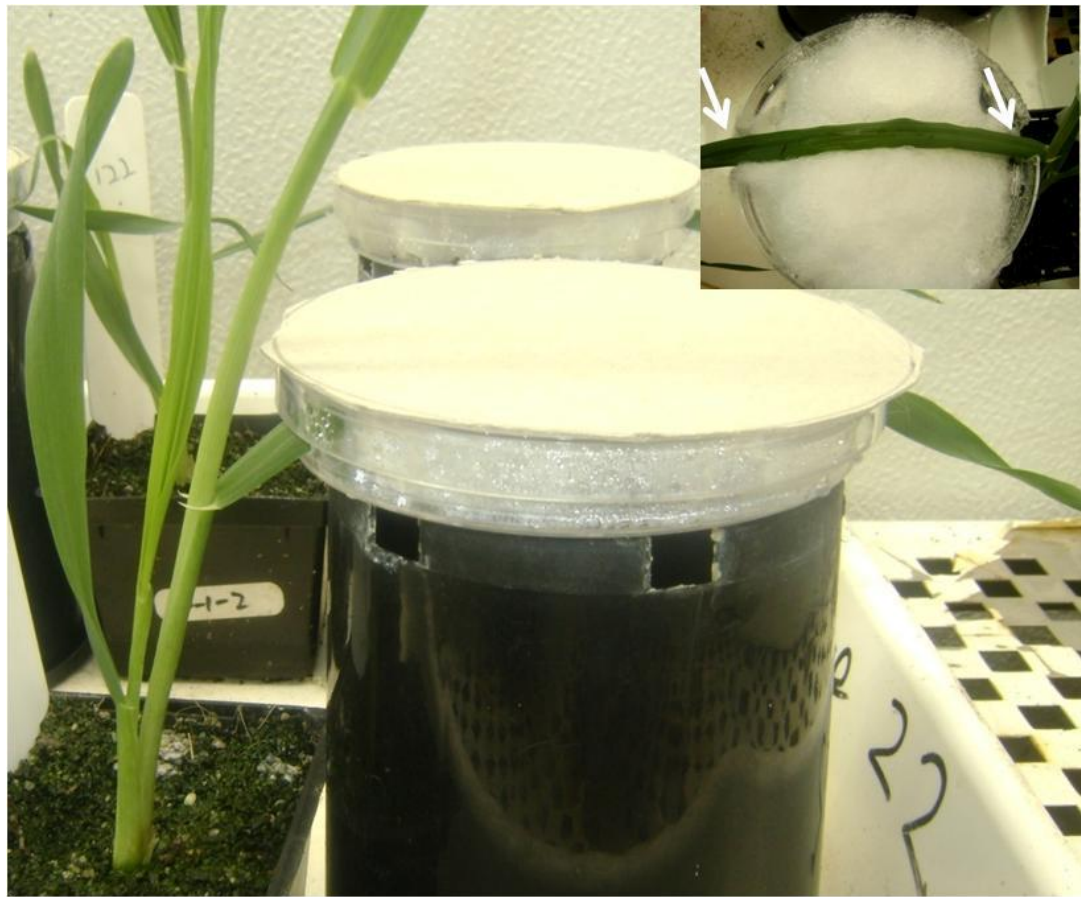


**Figure 2.1. Specially designed Petri dish inoculation system used in this study to allow easy visualisation of *Ptt* growth on barley.** The edges of the bottom part of the Petri dishes were cut in both sides (in a U shape, white arrows) to allow the leaves to lie through the Petri dish on wet cotton wool. The lids of the Petri dishes were covered with white cardboard paper. The system provides darkness and humidity to encourage growth of *Ptt* on barley and limits the inoculation area to a known site.

### **2.2.5 Determination of fungal growth *in planta***

Using the plants from the *in planta* germination experiment, five leaves for each isolate at 24, 40, 64 and 98 hpi were prepared and visualised and images captured as per section 2.2.4. Pilot experiments showed that differences in fungal growth were only distinguishable between isolates at 24 hpi (Figure 2.6). Analysis Fine software (Olympus Soft Imaging Solutions FireWire Camera V2.127, GMBH, Münster) was therefore used to analyse images at 24 hpi by measuring the hyphae growing from 10 conidia for each leaf section (a total of 50 conidia per isolate) and the growth rate was estimated using a numerical scale as per Lightfoot and Able (2010). The numerical scale scores the development of *Ptt* fungus during the interaction *in planta* using parameters such as length of hyphae in relation to cells, branching, hyphae thickness and evidence of symptoms using a scale of 0-10 (Appendix, Table A1.1).

### **2.2.6 Optimisation of proteinaceous toxin production and extraction**

Growing *Ptt* in Fries culture medium (FCM) (Barrault *et al.*, 1982) that contained all nutrients often yielded low quantities of proteinaceous toxins (data not shown) and consequently the downstream application for these toxins was limited. Therefore, optimisation of toxin production was conducted using different types of media and incubation conditions. In addition, protein extraction methods were optimised to maximise protein yields.

### **2.2.6.1 Effect of media type and incubation conditions on protein production**

Two isolates (08/08f and 32/98, Table 2.1), identified as less and more virulent, respectively, during the virulence testing (section 2.2.3), were grown in two types of media [Barley leaf medium (BLM) and FCM] to compare toxin production, in an initial experiment. BLM was used to imitate the usual source of nutrients for the fungus, as an attempt to encourage *Ptt* to produce the same toxins as during natural infection. BLM was used at two concentrations of leaves (50% and 25% w/v) or 25% w/v with 3% glucose in SNW (Table 2.2). BLM was prepared by chopping barley leaves, from 40 day old plants, into small pieces before combining with the desired amount of nanopure water and boiling for 50 min. The resultant solution was passed through cheesecloth and collected in a 1 L flask before being autoclaved for 20 min at 121°C. FCM was prepared as per Table 2.2 and autoclaved as described previously (Barrault *et al.*, 1982; Friis *et al.*, 1991; Liu *et al.*, 2004b; Sarpeleh *et al.*, 2007). Five discs (5 mm diameter) from 7 day old colonies of 32/98 and 8/08f isolates were transferred to 250 mL flasks containing 75 mL of these media before the flasks were kept at room temperature (RT) (23-25°C) in the dark for 23 days (Sarpeleh *et al.*, 2007) when protein was extracted from fungal filtrate and compared.

**Table 2.2. Media and their components used for toxin production optimisation.**

<b>Media type</b>	<b>Components/ Recipe</b>	<b>Reference</b>
<b>Barley leaf medium (BLM)</b>	50% barley leaves w/v in nanopure water. 25% barley leaves w/v in nanopure water. 25% barley leaves w/v and 3% glucose w/v in nanopure water.	
<b>Fries Culture Medium (FCM)</b>	KH <sub>2</sub> PO <sub>4</sub> , 1 g; MgSO <sub>4</sub> .7H <sub>2</sub> O, 0.5 g; NaCl, 0.1 g; CaCl <sub>2</sub> , 0.13 g; MnSO <sub>4</sub> .4H <sub>2</sub> O, 1 mg; boric acid, 1 mg; CuSO <sub>4</sub> , 0.1 mg; ZnSO <sub>4</sub> , 0.1 mg; FeSO <sub>4</sub> , 20 mg; NO <sub>3</sub> NH <sub>4</sub> , 1 g; ammonium tartrate, 5 g and glucose, 30 g; in 1 L nanopure water.	(Barrault <i>et al.</i> , 1982; Friis <i>et al.</i> , 1991; Sarpeleh <i>et al.</i> , 2007)
<b>FCM without trace elements (FCM-noTE)</b>	K <sub>2</sub> HPO <sub>4</sub> (dibasic), 1.3 g; KH <sub>2</sub> PO <sub>4</sub> (monobasic), 2.6 g; MgSO <sub>4</sub> .7H <sub>2</sub> O, 0.5 g; NO <sub>3</sub> NH <sub>4</sub> , 1 g; ammonium tartrate, 5 g; sucrose, 30 g and yeast extract, 1 g; in 1 L of nanopure water.	(Liu <i>et al.</i> , 2004a)

Because fungal growth and toxin production was better in FCM when compared with any of the BLM conditions, the incubation conditions in FCM were also optimised to improve toxin production. Two types of FCM were used to evaluate toxin production in two more virulent isolates, 32/98 and 152/09: FCM and modified FCM, without trace elements (FCM-noTE), prepared as per Table 2.2. Media were inoculated and incubated as above and flasks were covered with aluminum foil to provide darkness. Three types of conditions (no shaking, the first 2 days shaking and 23 days shaking) were used for incubation at RT. Shaking treatments were placed on a TASP-OSI orbital shaker (Thermoline, Northgate, Queensland, Australia) at 80 rpm. Images were captured for colonies after 12 days of incubation and protein was extracted from fungal filtrate after 23 days and compared.

#### **2.2.6.2 Protein extraction from *Ptt* culture filtrate**

Given that *Ptt* releases small amounts of toxin into filtrates, three protein extraction methods were trialled: ultrafiltration purification (UFP) and

ammonium sulfate precipitation, where extracts were to be used in toxin bioassay; and trichloroacetic acid (TCA) precipitation when extracts were to be analysed using polyacrylamide gel electrophoresis (PAGE).

#### **2.2.6.2.1 Ultrafiltration purification (UFP)**

Toxins were extracted, from 23 day old cultures as per Sarpeleh *et al.* (2007; 2008) using UFP. Mycelium was removed from the filtrates before passing through Whatman No. 1 filter paper followed by a 0.45 µm Millipore filter (Minisart High-Flow syringe filter, Sartorius Stedim Biotech, Germany). Filtrates were then passed through a YM-10 Amicon centriplus filter (Millipore Corporation Billerica, MA, USA), using centrifugation at 5000 *g* for 12 min at 4°C. Retentates were collected and washed twice using SNW and the same filter (YM-10). Samples were concentrated by speed-vacuuming (SpeedVac SVC100, Selby Scientific Instruments, UK) when required. Protein was quantified using the Bradford protein assay (Bradford, 1976) using a Bio-Rad protein kit (Bio-Rad, USA) and bovine serum albumin as a standard to allow prediction of the protein concentration in samples from a standard curve using Genstat Eleventh Edition (2008 Lawes Agricultural Trust, VSN International Ltd). Extracted protein was stored at -80°C until required.

#### **2.2.6.2.2 Ammonium sulfate precipitation (ASP)**

Protein was extracted using the ASP method as per Strelkov *et al.* (1999) with some modification. *Ptt* filtrate was obtained as per section 2.2.6.2.1 except that the filtrate was not passed through the YM-10 filter but was mixed with ammonium sulfate until saturation (70 to 75% w/v). The saturated solution was kept at 4°C overnight before centrifugation at 8000 *g* for 20 min at 4°C. The pellet was resuspended in SNW and centrifuged at 10000 *g* for 20 min at 4°C. The previous step was repeated to recover more protein. The concentration of protein was predicted as per section 2.2.6.2.1 and stored at -80°C until required.

#### **2.2.6.2.3 TCA protein extraction**

TCA-Acetone was used to precipitate and extract small amounts of protein where proteins were to be run on a denaturing PAGE gel. For visualisation, protein was extracted as per 2.2.6.2.1 and precipitated in a mixture of 0.07% 2-mercaptoethanol (2ME) and 10% TCA in cold acetone (Damerval *et al.*, 1986; Méchin *et al.*, 2007; Vincent *et al.*, 2009). One volume of protein was added into nine volumes of the cold TCA-2 ME-acetone solution and the solution incubated for 1 h at 4°C before centrifugation at 3000 *g* for 5 min. The pellets were collected and washed three times by centrifugation at 3000 *g* with 90% acetone for 15 min. Protein pellets were resuspended in SNW and the concentration of protein was measured as per section 2.2.6.2.1.



### **2.2.6.3 PAGE**

PAGE was used to investigate the difference between the protein profiles of filtrates for *Ptt* cultures grown under different conditions. The desired amount of protein was mixed with 1  $\mu\text{L}$  of NuPAGE<sup>®</sup> reducing agent (10 x) and 2.5  $\mu\text{L}$  of NuPAGE<sup>®</sup> LDS (lithium dodecyl sulfate) sample buffer (4 x) (Invitrogen, Life Technology, USA). The mixture was heated at 70°C for 10 min and then loaded either onto a NuPAGE<sup>®</sup> Novex<sup>®</sup> precast 4-12% Bis-Tris [Bis (2-hydroxyethyl) iminotris (hydroxymethyl) methane] Midi Gel with a well-loading capacity of 45  $\mu\text{L}$  or a NuPAGE<sup>®</sup> Novex<sup>®</sup> precast Bis-Tris Mini Gel with a well-loading capacity of 10  $\mu\text{L}$  (Invitrogen) depending upon the concentration of the protein extraction. Precision Plus Protein<sup>®</sup> Standard (Bio-Rad) was used as a marker ladder. Electrophoresis was performed for two technical replicates using an Electrophoresis Power Supply EPS 301 (Amersham Pharmacia Biotech, Sweden) with 1X MES [2-(N-morpholino) ethansulfonic acid] running buffer at 200 V, 200 mA for 40 min.

#### **2.2.6.3.1 Coomassie Brilliant Blue staining (CBB R250)**

The gel was removed from the cassette and stained in 100 mL of each solution in a series with shaking at 59 rpm using a TASP-OSI orbital shaker, all solutions were made up using nanopure water. Gels were fixed in a solution of 10% (v/v) methanol, 10% (v/v) glacial acetic acid and 40% (v/v) ethanol for 1 h, then placed in sensitisation solution [1% (v/v) glacial acetic acid and 10% (w/v) ammonium sulfate] for 2 h before being moved to a staining solution [1%

(v/v) glacial acetic acid, 45% (v/v) ethanol and 0.125% (w/v) Coomassie Brilliant Blue R 250 (CBB R250) (Sigma- Aldrich)] and stained overnight. Gels were then destained in destain solution I [5% (v/v) glacial acetic acid and 40% (v/v) ethanol] for 1 h. The gel was transferred to destain solution II [3% (v/v) glacial acetic acid and 30% (v/v) ethanol] and destained until the background was clear (Wang *et al.*, 2007). Gels were imaged as per section 2.2.3 and the gel was stored in preservation solution [5% (v/v) glacial acetic acid].

#### **2.2.6.3.2 Silver staining**

Upon completion of CBB R250 staining, if required, gels were stained using the eriochrome black T (EBT) silver staining protocol (Jin *et al.*, 2006; Khoo *et al.*, 2012). Gels were fixed twice in 100 mL of a solution containing 30% (v/v) ethanol and 10% (v/v) acetic acid solution 20 min before sensitising in 100 mL of staining solution [0.006% w/v EBT (Sigma–Aldrich, USA), 30% v/v ethanol] for 2 min, and then destaining in 200 mL of 30% ethanol solution for 2 min, and washing twice in 200 mL of nanopure water for 2 min (all at 59 rpm). Gels were then saturated in 100 mL of 0.25% (w/v) silver nitrate containing 0.037% (w/v) formaldehyde for 5 min, washed twice in 200 mL of water for 20 sec, and immersed in 100 mL of developing solution [2% (w/v) potassium carbonate, 0.04% (w/v) sodium hydroxide, 0.007% (w/v) formaldehyde, 0.002% (w/v) sodium thiosulfate] to develop the image (all steps were done at 59 rpm). The gel was then immersed in 100 mL of fixing solution to stop the

development. Gels were imaged as per section 2.2.3 and the silver-stained gel stored in a preservation solution as per section 2.2.6.3.1.

#### **2.2.6.4 Evaluation of UFP and ASP extraction methods**

UFP and ASP were compared for their protein yield from culture filtrate and the effect of protein extraction method on the toxin bioassay to be used in further experiments. Protein was extracted from 32/98 filtrate (identified as a more virulent isolate) (Figure 2.2) using UFP as per section 2.2.6.2.1 and ASP as per section 2.2.6.2.2. Five  $\mu\text{g}$  of total protein was injected at the middle of the leaf in a total volume of 200  $\mu\text{L}$  for each leaf using a Hagborg device (Sarpeleh *et al.*, 2007) at Zadoks' growth stage 14 (fourth leaf more than half visible) (Zadoks *et al.*, 1974). Three leaves were used and SNW was injected as a control, plants were grown as per section 2.2.1 and symptoms were monitored every 24 h for up to 11 days. Injected leaves were collected at 11 days post injection and images captured as per section 2.2.3.

#### **2.2.6.5 Proteinaceous toxin bioassay for six isolates of *Ptt***

A pilot experiment showed that UFP protected the activity of proteinaceous toxins compared with ASP (Figure 2.13), therefore the UFP method was used for all further bioassay experiments. To evaluate the toxicity of extracted protein mixtures from the six isolates, 5  $\mu\text{g}$  was injected into four attached leaves of cv. Sloop as per section 2.2.6.4 and plants grown as per section 2.2.1. Symptoms were monitored every 24 h for up to 8 days and images captured as per section 2.2.3.

### **2.2.7 Statistical analysis**

GenStat was used to analyse data using either One-way or Two- way analysis of variance (ANOVA). The least significant difference (LSD) at  $P<0.05$  was used to determine significant differences between means of three replicates and correlation was calculated when it required.

## **2.3 Results**

### **2.3.1 Virulence of *Ptt* isolates**

The virulence of six *Ptt* isolates on barley cv. Sloop varied from low to high (Figure 2.2). Symptoms initially appeared as small brown necrotic lesions surrounded by chlorosis but then developed to dark net lesions covering the whole leaf in the more virulent isolates by 6 dpi. Using the Tekauz disease scale (0-10 scores) (Tekauz, 1985), the virulence of 8/08f and 122/09 was significantly lower ( $P<0.001$ ,  $LSD=1.0$ ) (1.25 and 3.1 respectively) than the other isolates 55/07, 123/09, 32/98 and 152/09 (scores of 8, 8.3, 9.75 and 10 respectively). The reaction types in barley in response to the 8/08f and 122/09 isolates were small pin-point lesions even after 17 dpi confirming their lower virulence. Leaves of plants inoculated with the most virulent isolates, 32/98 and 152/09, had died and sheaths, auricles and ligules were also infected after 17 dpi (Figure 2.3). Conidia and conidiophores were observed to form more quickly in the more virulent isolates (by 11 dpi) whereas they were not visible in the less virulent isolates (Figure 2.4).



**Figure 2.2. Representative images depicting differences in the virulence of the six *Ptt* isolates on barley cv. Sloop 6 days post inoculation.** Plants were inoculated at Zadoks' Stage 14. SNW; sterilised nanopure water, six isolates from least (left) to most (right) virulent.



**Figure 2.3. Representative images depicting differences in the virulence of the six *Ptt* isolates on barley cv. Sloop 17 days post inoculation.** Plants were inoculated at Zadoks' Stage 14. SNW; sterilised nanopure water, six isolates from least (left) to most (right) virulent.

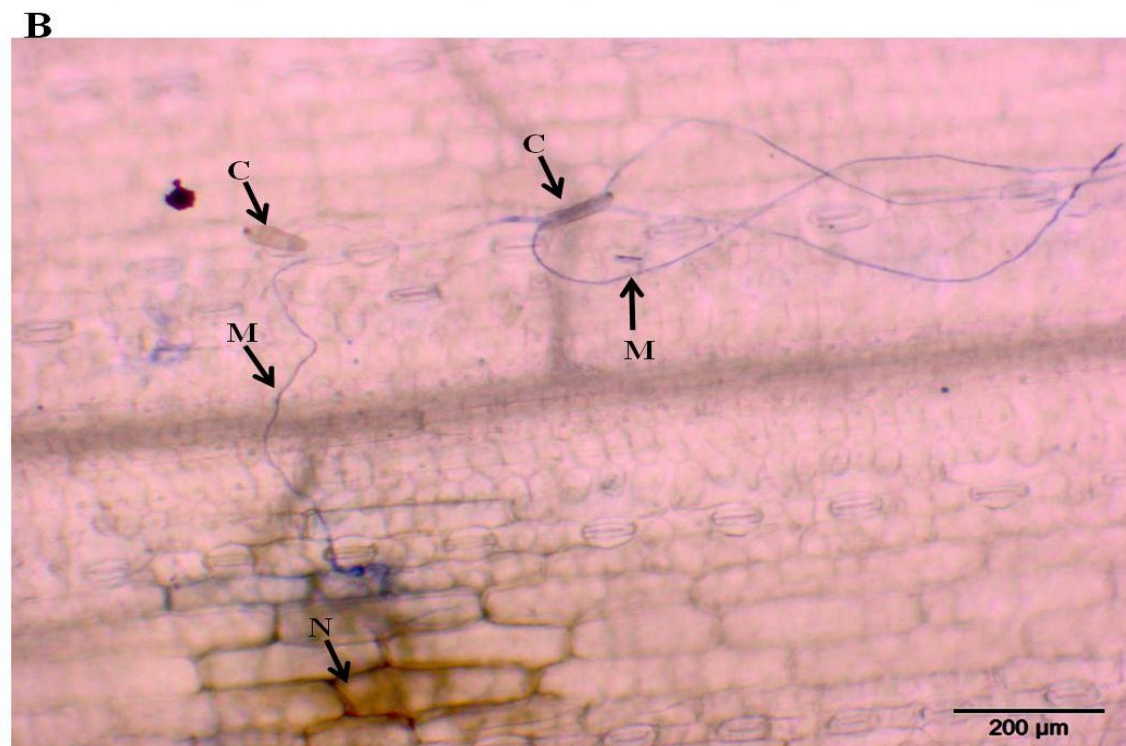
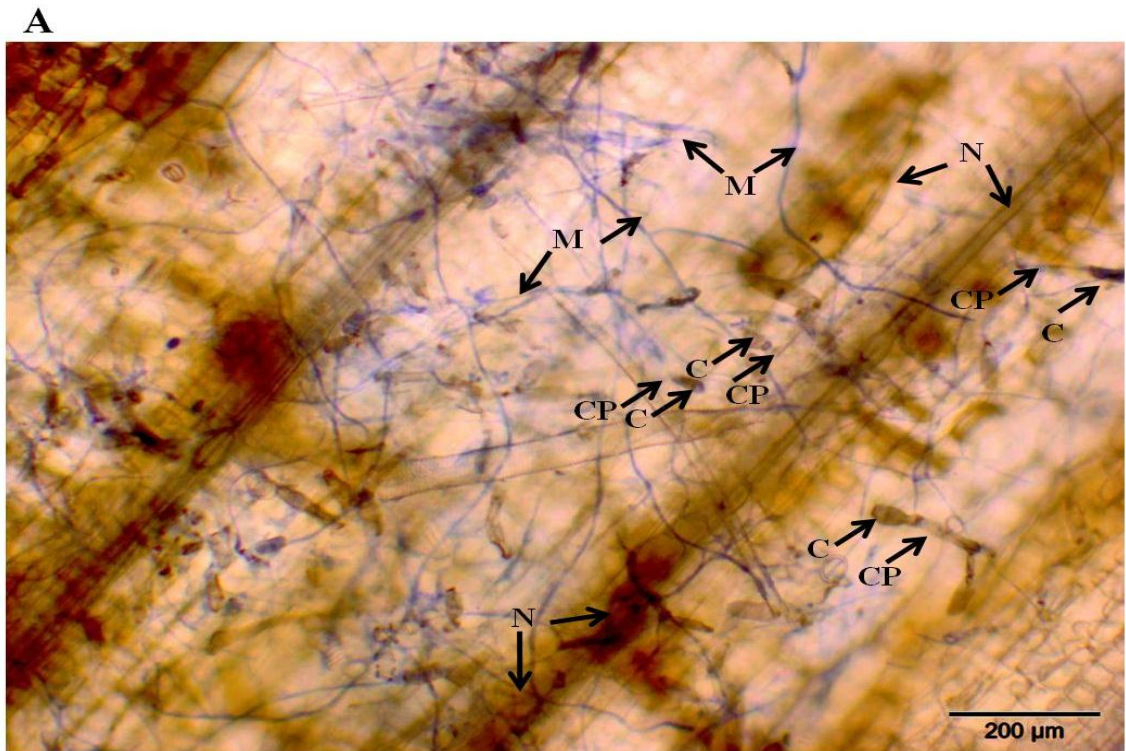


**Figure 2.4. Representative images for fungal development of two isolates of *Ptt* after 11 days post inoculation *in planta*.** Infection of plant tissue by a more virulent isolate (32/98) (A) and less virulent isolate (08/08f) are shown. M, mycelium; N, necrosis; C, conidia and CP, conidiophores and scale bars (200  $\mu$ m) are shown.

### **2.3.2 Germination and fungal growth are correlated with virulence**

To determine whether the growth of the fungus might relate to virulence, germination of conidia, *in vitro* and *in planta*, and fungal hyphal growth *in planta* were examined for the six *Ptt* isolates.

#### **2.3.2.1 Germination *in vitro* and *in planta***

At 24 hpi, the germination percentage of conidia on agar-coated slides was significantly greater for the more virulent isolates (32/98, 152/09, 55/07 and 123/09) than the less virulent isolates (8/08f and 122/09) (Figure 2.5;  $P < 0.001$ ,  $LSD = 6.7$ ). *In vitro* germination 24 hpi for 8/08f was also significantly lower than that observed for 122/09.

Germination of conidia *in planta* was significantly lower than *in vitro* for all isolates except 08/08f. Germination of conidia of the more virulent isolate 32/98 *in planta* was significantly greater than that observed for the other isolates ( $P < 0.001$ ,  $LSD = 12.5$ ). However, the *in planta* germination of conidia from isolates 123/09 and 152/09 was not significantly different from that observed for the less virulent isolates 08/08f and 122/09.



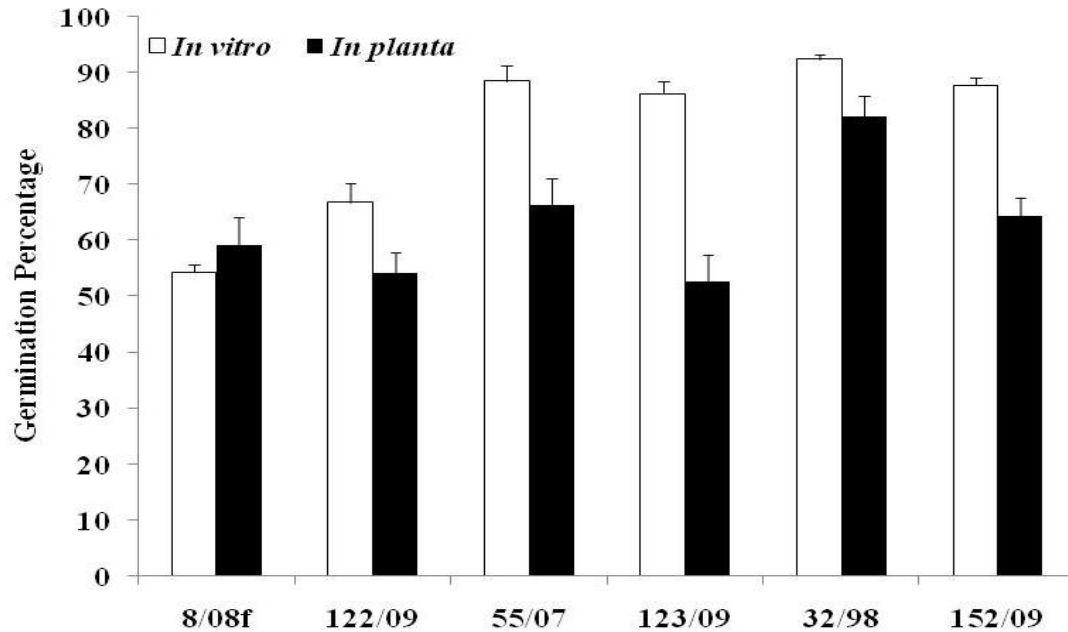


**Figure 2.5. Percentage of conidia germinated for six isolates of *Ptt* after 24 h *in vitro* or *in planta* in barley cv. Sloop.** Data is representative of three individual experiments. *In vitro* germination was counted on agar-coated slides; means of five replicates (slides) with standard error bars are shown with 100 conidia counted per slide. For *in planta* germination, the means of five replicates (leaves) are shown with 10 conidia counted per leaf.

### 2.3.2.2 Fungal hyphal growth *in planta*

The nature of fungal development of the six *Ptt* isolates *in planta* was examined at 24, 40, 64 and 98 hpi (Figure 2.6) in a pilot experiment. Microscopic examination for these isolates at different timepoints showed that at 24 hpi, germination had occurred with substantial hyphal growth in 55/07, 123/09, 32/98 and 152/09 but minimal hyphal growth in 08/08f and 122/09. By 40 hpi, hyphae had thickened but did not appear longer for 32/98 and 152/09. However, no differences in growth were obvious for 08/08f, 122/09, 55/07 and 123/09 at 40 hpi. By 64 hpi, the hyphae often grew into the mesophyll making it difficult to measure. Therefore, fungal growth was evaluated by measurement at 24 hpi.

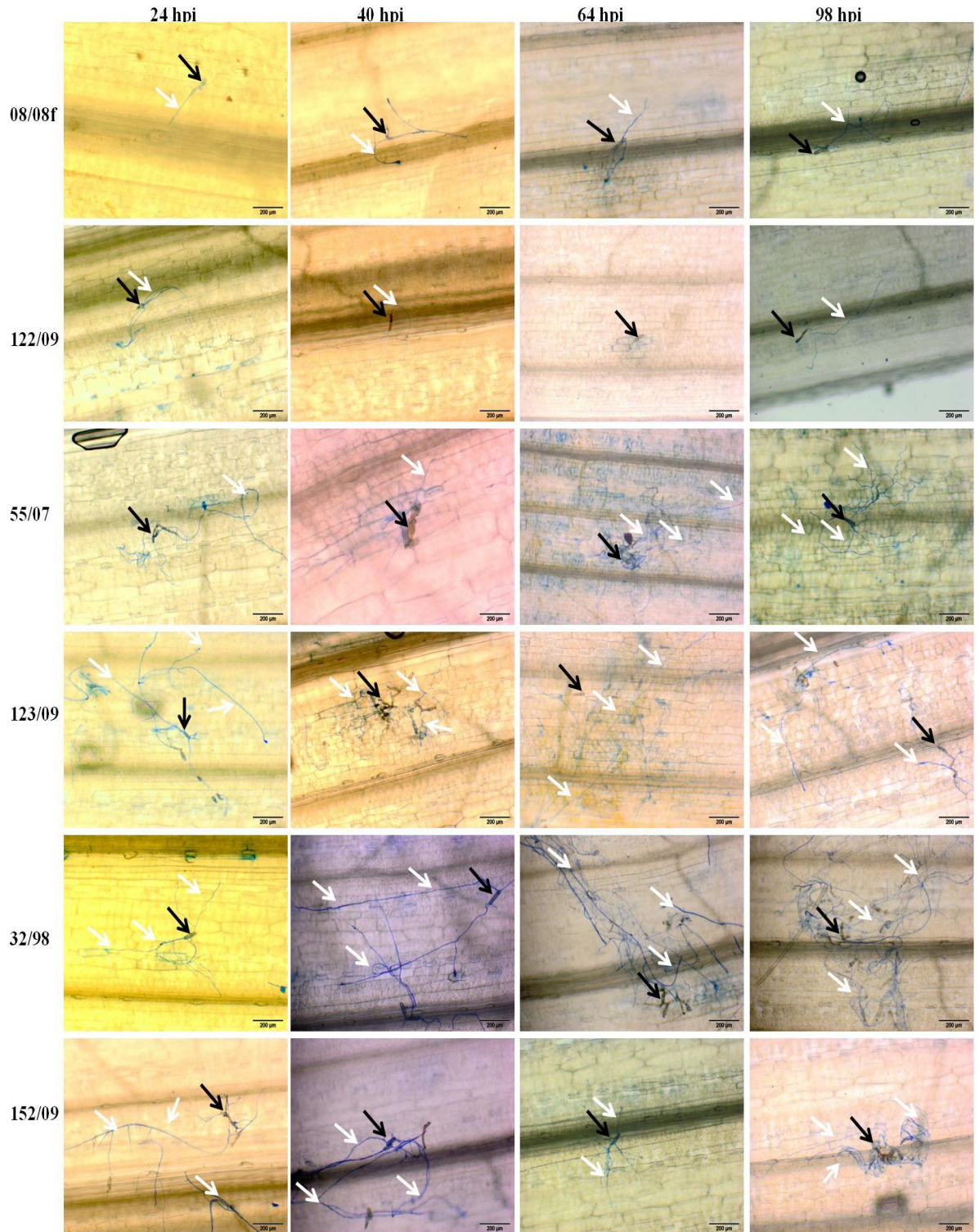


**Figure 2.6. Representative images for fungal development of six isolates of *Ptt* in planta.** Six isolates from least virulent (top left side) to the most virulent isolates (bottom left side), 4 timepoints 24, 40, 64, 98 hour post inoculation (hpi) shown at the top. Black arrows indicate conidia, white arrows indicate mycelium and scale bars (200 μm) are shown.

Hyphal length of the more virulent isolate 32/98 at 24 hpi was significantly greater than that for all other isolates ( $P<0.001$ ,  $LSD=328$ ) (Figure 2.7). The hyphal lengths of isolates 08/08f, 55/07, 123/09 and 152/09 were not significantly different from each other but were significantly greater than the length of hyphae for isolate 122/09. At 24 hpi, the fungal development score (Figure 2.8A) followed the same trend as observed for hyphal length ( $r=0.72$ ), with a significantly greater score reported for the more virulent isolate 32/98 compared with all other isolates (Figure 2.8A;  $P<0.001$ ,  $LSD=0.67$ ). By 24 hpi, hyphae of the 32/98 isolate have already branched and many appressoria have formed (Figure 2.6 and Figure 2.8B). The fungal development score for isolates 08/08f, 55/07, 123/09 and 152/09 were not significantly different from each other. The fungal development score for isolate 122/09 was only significantly lower than the score for 123/09. For the less virulent isolates 08/08f and 122/09, the amount of branching for hyphae was less than the more virulent isolates and a limited number of appressoria were observed (Figure 2.6 and Figure 2.8C). Mycelium of less virulent isolates often appeared to have not attached to the leaf (Figure 2.6).

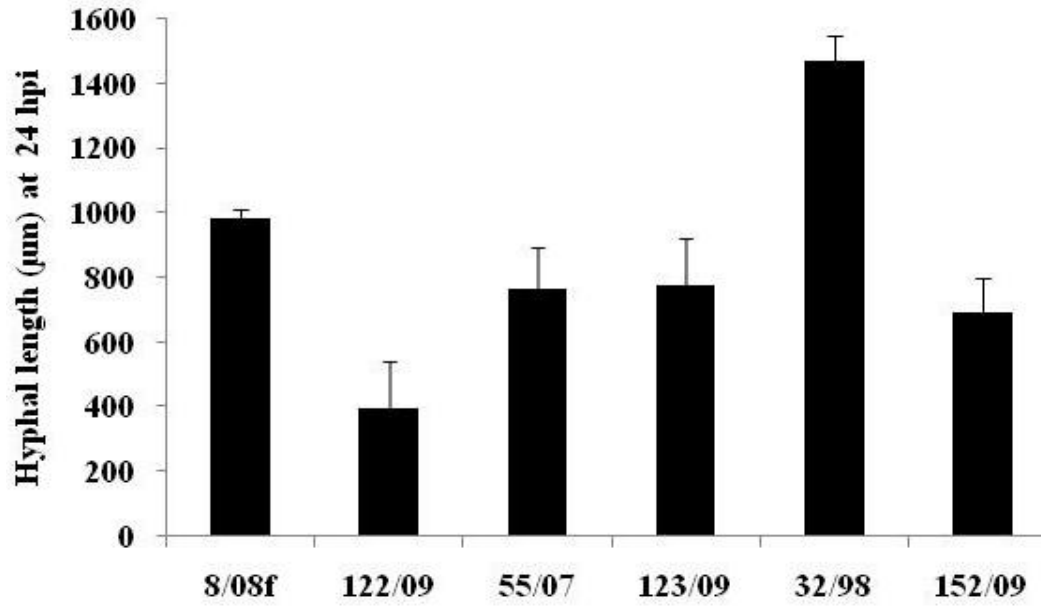


**Figure 2.7. Differences in the hyphal length between six isolates of *Ptt* at 24 hours post inoculation (hpi) *in planta* in barley cv. Sloop.** Five replicates (leaves) were used and 10 germinated conidia were assessed per leaf and the experiment repeated three times.

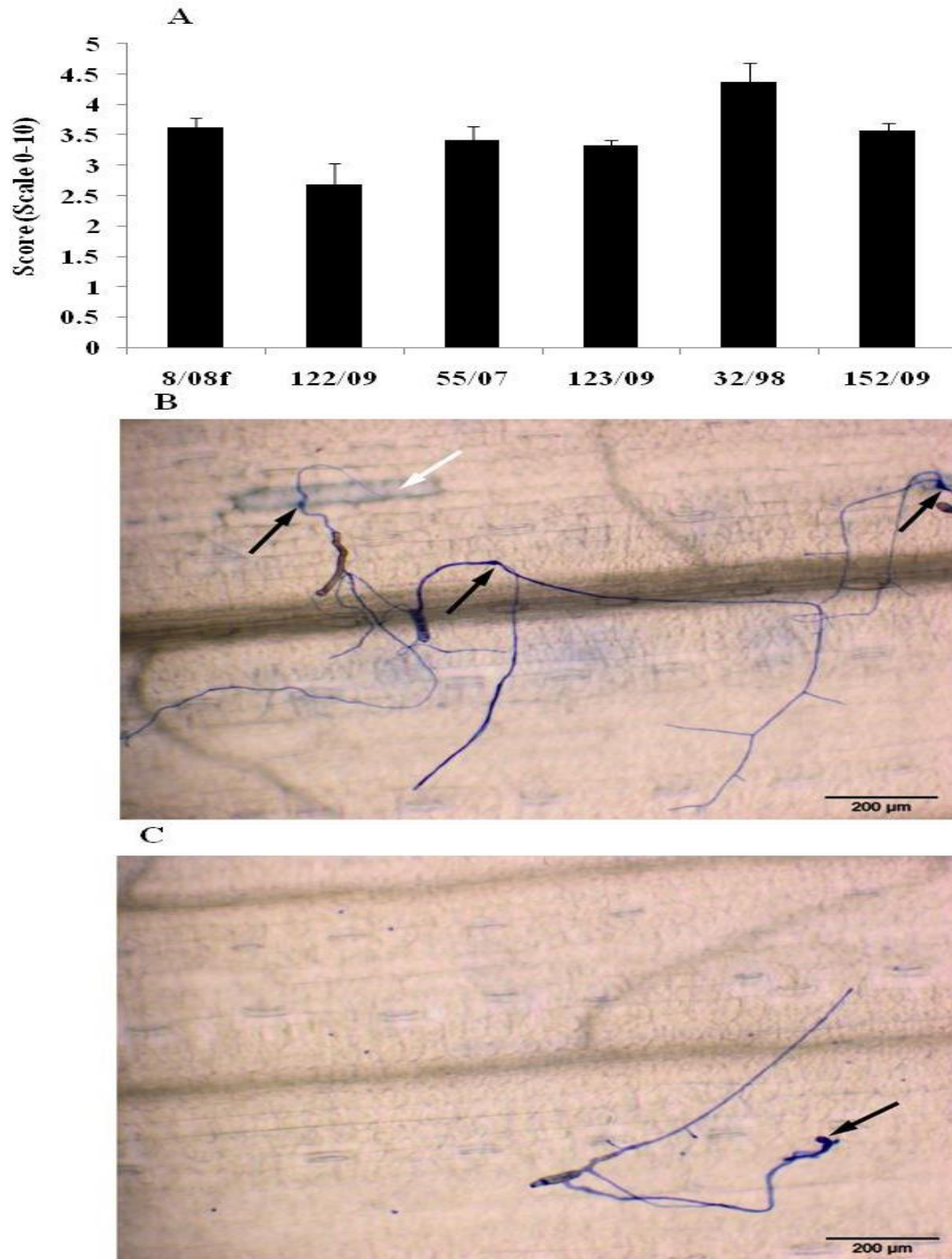


**Figure 2.8. Fungal development of six isolates of *Ptt* after 24 hours post inoculation (hpi) in *planta*.** Fungal development scores using a scale of 0-10 where 0 = Conidia are visible but have not germinated and 10 = Stromata appear mature with conidiophores and chlorosis and necrosis clearly evident (Lightfoot and Able, 2010) (A). Representative images of 50 replicates for the more virulent isolate (32/98) (B), and the least virulent isolate (08/08f) (C) are shown. Black arrows indicate appressoria. White arrow indicates necrotic lesion and scale bars (200  $\mu$ m) are shown.

### 2.3.3 Effect of media on protein production

Fungal cultures growing in BLM produced more protein than those growing in FCM (data not shown). However, PAGE analysis showed that culturing *Ptt* isolates in FCM produced distinct bands compared with BLM (Figure 2.9). In addition, the profile of two isolates appeared relatively similar. Protein extracted from fungi grown in BLM formed multiple bands that smeared on the gel but these bands also appeared in controls (BLM without fungus). Therefore, BLM was discarded due to likely contamination with plant proteins and FCM was used in toxin production.

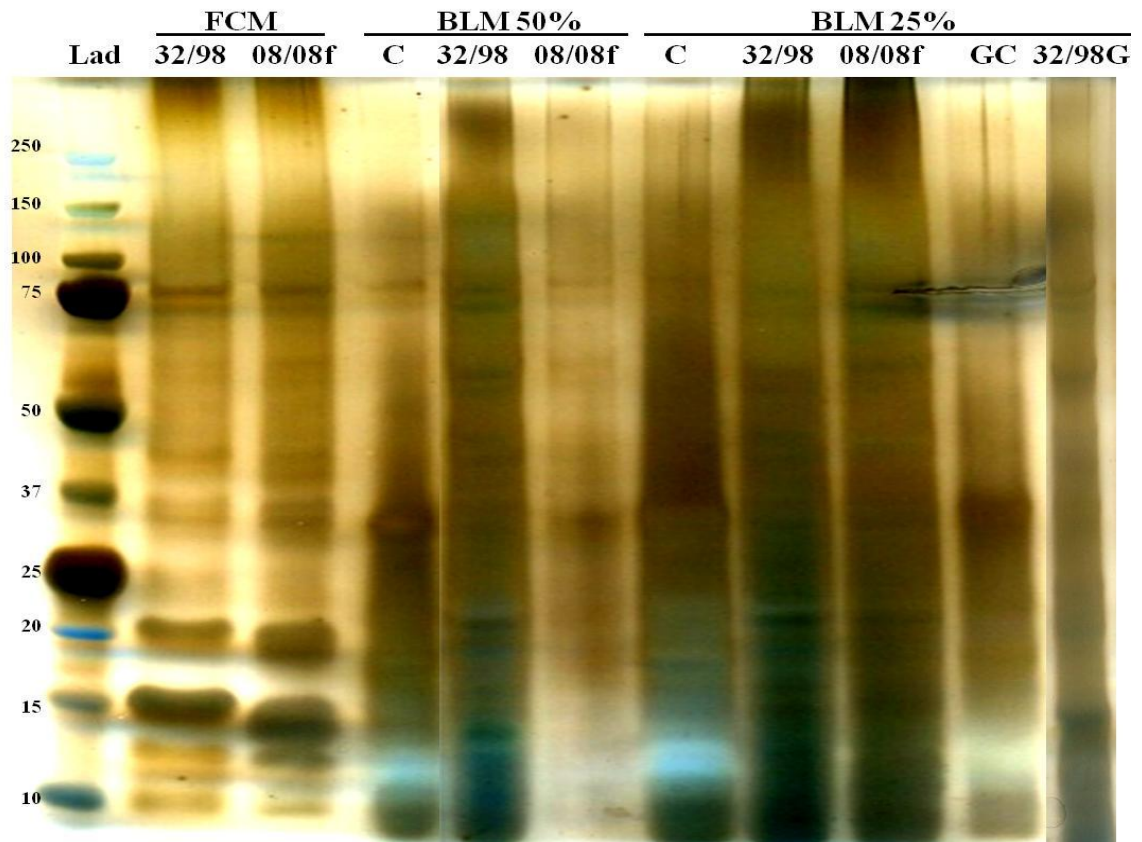


**Figure 2.9. Optimisation of toxin production in two isolates of *Ptt* (32/98, more virulent) and 08/08f (less virulent) using two types of media.** FCM, Fries Culture Medium; 50% and 25% BLM, barley leaves medium; 25% BLM with G, glucose; C, control media (without fungus) for 50% BLM, 25% BLM and 25% BLM with G. Representative silver stained polyacrylamide gel of two technical replicates, 15  $\mu$ L was loaded for each sample and Precision Plus Protein Standard (Lad) was used as marker ladder.

### **2.3.4 Optimisation of protein production conditions**

Combinations of two types of media (FCM and FCM-noTE), two virulent isolates (32/98 and 152/09) and shaking conditions (no shaking, shaking for 2 days and for 23 days), were used to optimise toxin production (Figure 2.10). By 12 days, both isolates grew to a greater extent in FCM-noTE and no shaking producing a consistent colony shape (Figure 2.10B), compared with those in FCM (Figure 2.10A). When the cultures in FCM were kept at 80 rpm for two days then removed from the shaker and incubated for 12 days, the colonies had sunk for both isolates (Figure 2.10C) while the same cultures grew on the surface of the FCM-noTE (Figure 2.10D). Regardless of isolate, FCM-noTE cultures shaking at 80 rpm for 12 days formed more gelatinous filtrates (Figure 2.10F). Colonies on FCM were darker in colour than FCM-noTE in both isolates (Figure 2.10E). Total protein concentration of filtrates suggested that 32/98 produced larger amounts compared with 152/09 (Figure 2.11,  $P < 0.05$ ,  $LSD = 136$ ). The FCM-noTE cultures produced greater amounts of protein in both isolates. PAGE analysis showed almost the same protein pattern in both isolates (32/98 and 152/09). However, a greater amount of protein, as indicated by more dense bands, was produced when cultures were grown in FCM-noTE (Figure 2.12). In addition, shaking for 23 days produced more highly concentrated protein, especially for the 32/98 isolate, (Figure 2.11) but because the filtrates were too viscous causing filter clogging to the UFP unit, very little protein was able to be extracted. Therefore, FCM-noTE without shaking was used for all further protein production.

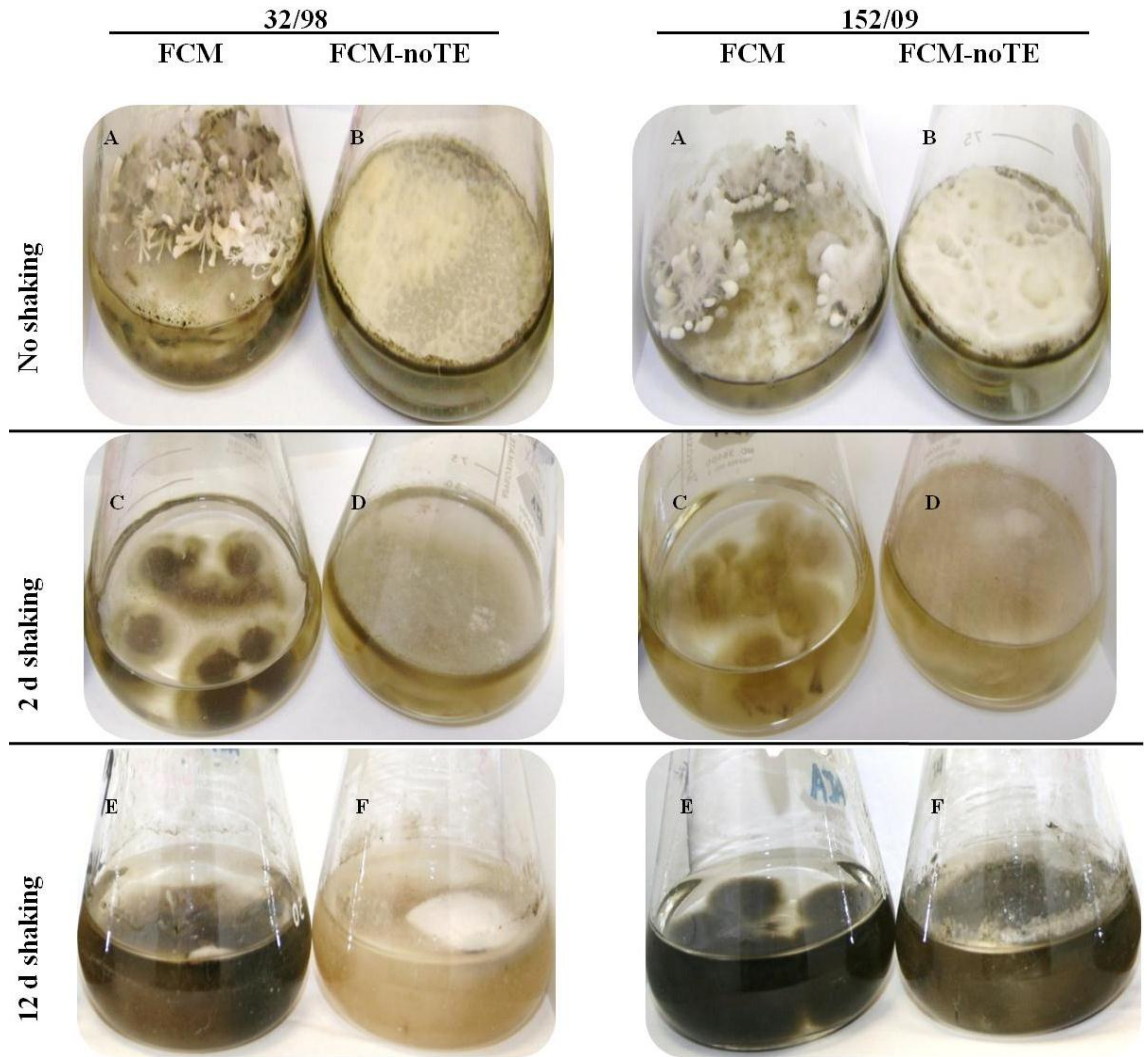


**Figure 2.10. Optimisation of protein production in 32/98 and 152/09 (more virulent isolates) grown for 12 days (d) on two types of media. (A, C, E) FCM, Fries Culture Medium with trace elements; (B, D, F) FCM-noTE, FCM without trace elements. Different shaking conditions are shown for each isolate and media type. Image shows representative colonies for three biological replicates.**



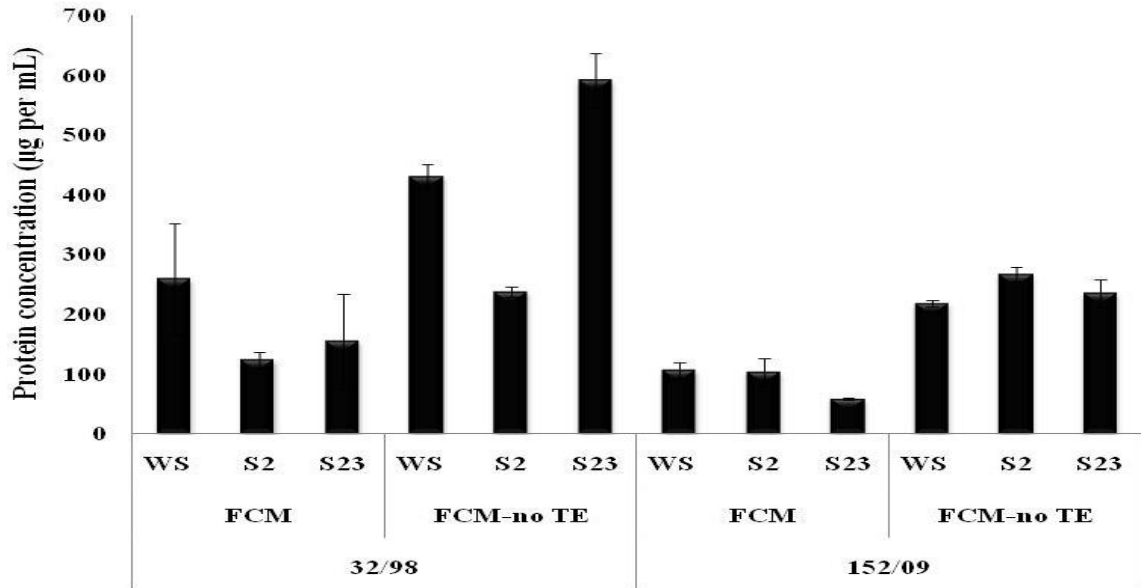


**Figure 2.11. Concentration of protein in the filtrates of two virulent isolates (32/98 and 152/09).** Cultures were either grown in FCM (Fries Culture Medium) or FCM-noTE (FCM without trace elements) and under one shaking condition (no shaking, shaking for two days or for 23 days). Protein concentration was measured after 23 days, three biological replicates were used for each treatment.

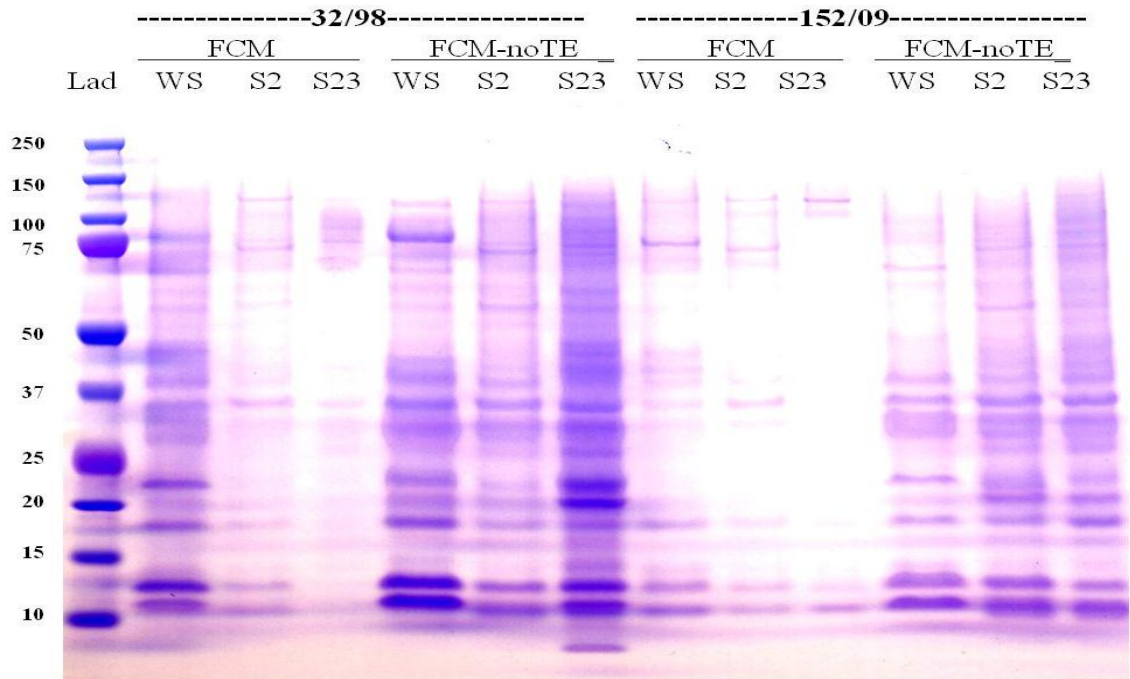


**Figure 2.12. PAGE for total protein extracted from the filtrates of 32/98 and 152/09 grown for 23 days in two types of media.** Colonies were either grown in Fries Culture Medium (FCM) or FCM without trace elements (FCM-noTE) without shaking (WS), at 80 rpm for 2 days (S2) or for 23 days (S23). 11.5 µL of each treatment filtrate was loaded and Precision Plus Protein Standard (Lad) was used as a marker ladder. Representative gel for two biological replicates.

### 2.3.5 Evaluation of UFP and ASP extraction methods

Two protein extraction methods, UFP and ASP, were evaluated with regards to protein yield and protein biological activity. Although, the yield of protein was higher in the ASP method (data not shown), the UFP method preserved the activity of the proteins compared with ASP (Figure 2.13). Therefore, UFP was used to extract proteins that were used for bioassays.



**Figure 2.13. Effect toxin extraction methods on the bioassay of toxins on barley cv. Sloop.** Five  $\mu\text{g}$  of total protein was injected in a total volume of 200  $\mu\text{L}$  for each leaf using a Hagborg device, SNW, sterilised nanopure water; protein extracted using UFP, ultrafiltration purification using Amicon YM-10 and ASP ammonium sulfate precipitation. Representative image for three replicates at 11 days post injection.

### 2.3.6 Bioassay of total protein extracted from culture filtrates of six *Ptt* isolates

To determine how much of the proteinaceous extraction from culture might contribute to symptom development (and virulence), proteinaceous toxins were extracted from the culture filtrates of the six isolates, which were varied in

virulence (Figure 2.2), and injected into barley cv. Sloop leaves. Regardless of isolate, necrosis was induced to the same extent in barley leaves by proteinaceous toxins extracted from their culture filtrates (Figure 2.14). Small necrotic lesions surrounding the area injected with the proteinaceous toxin mixture first appeared on leaves after 4 days and then spread vertically along the leaf vein covering the whole leaf by 8 days after injection.



**Figure 2.14. Bioassay test for proteinaceous toxins extracted from filtrates of the six isolates of *Ptt*.** Leaves were injected with 5  $\mu\text{g}$  of native protein from each isolate using a Hagborg device and the image taken 8 days post injection. The image is representative of three replicates. SNW; sterilised nanopure water.

## 2.4 Discussion

Given that there were great differences in the virulence between *Ptt* isolates on barley cv. Sloop (Figure 2.2), these differences were further investigated to highlight and understand the mechanisms underlying the pathogenic process. Previous researchers have suggested that virulence is based on the ability of the isolate to establish itself by colonising the tissue and secreting pathogenic proteins (Solomon and Rathjen, 2010; Tan *et al.*, 2010). The research presented herein provides support with the general observation that fungal growth might contribute to the infection process and proteins from culture filtrates cause symptoms similar to NFNB. The more virulent isolate (32/98), had higher rates of conidial germination (both *in vitro* and *in planta*) and fungal development *in planta* as evidenced by longer hyphae and the formation of more appressoria. Even though the hyphal length and fungal development *in planta* were similar for 8/08f, 55/07, 123/09 and 152/09, their virulence was different, suggesting that their reliance on the amount of toxin produced and/or the extent of fungal growth may differ. Alternatively, other mechanisms such as type of toxin and the timing of toxin production during the interaction may explain the differences observed.

Although other studies have characterised differences in virulence of *Ptt* on barley (Brown *et al.*, 1993; Serenius *et al.*, 2007), their differences have only been attributed to the difference in genetic background between isolates (Liu *et al.*, 2012; Rau *et al.*, 2003; 2007; Serenius *et al.*, 2005; Weiland *et al.*, 1999). Serenius *et al.* (2007) found that genetic differentiation was high between *Ptt*

isolates originating from Northern Europe, North America, Russia and Australia. The difference in virulence observed in this study probably also reflects the high genetic diversity of these South Australian isolates (Lehmensiek *et al.*, 2010) which were isolated from different geographic locations and at different times (Table 2.1).

Although the higher rate of conidial germination and fungal development *in planta* provides an obvious correlation with the higher virulence observed for isolate 32/98, the hyphal length and fungal development score for the more virulent isolates 55/07, 123/09 and 152/09 did not significantly differ from those for the least virulent isolate (08/08f). Previous studies of *P. teres* have shown that hyphae grow to varying lengths from the germ tubes (Lightfoot and Able, 2010; Vancaesele and Grumbles, 1979) that arise quickly from conidia once they land on the leaf (Vancaesele and Grumbles, 1979). A swollen club-shaped appressorial structure forms within 24 h (Amaike *et al.*, 2008; Lightfoot and Able, 2010; Mathre, 1997; Vancaesele and Grumbles, 1979) and then penetration via the lower epidermal cell wall into the mesophyll tissue may occur (Dushnicky *et al.*, 1996; Lightfoot and Able, 2010). A higher number of germinated conidia would therefore result in a greater chance of attachment and therefore likely penetration attempts. Indeed, the rate of conidial germination and subsequent germ tube growth and penetration has been shown to be important for successful infection of bean plants by *Botrytis cinerea* (Kokkelink *et al.* 2011). The more extensive symptoms formed on barley leaves during infection by the net form of *P. teres*

(*Ptt*) when compared with the spot form (*P. teres* f. *maculata*) were also associated with greater growth and penetration by *Ptt* (Lightfoot and Able, 2010). Although the most virulent isolate (152/09) did not have longer hyphae on the surface of the leaf (when compared with the least virulent isolates), it did form more appressoria suggesting that it may have been growing more extensively throughout the mesophyll. Furthermore, the least virulent isolate (08/08f) still had extensive hyphal growth but failed to attach to the surface of the leaf (Figure 2.6 and Figure 2.8C) suggesting that appressorial development and attachment are as equally important as the rate of conidial germination and hyphal growth.

To study the ability of proteins from culture filtrates of isolates of varying virulence to cause NFNB symptoms, their production and extraction needed to be optimised. Colonies grew more abundantly in FCM-noTE and ultimately produced more protein, compared with FCM, therefore FCM-noTE was used for proteinaceous toxin production. Media with different ingredients might affect the ability of *Ptt* to produce toxins. Sarpeleh (2007) found that *Ptt* produced more proteinaceous metabolites in FCM than phosphate-buffered FCM (PFCM). In addition, FCM (with trace elements) contains  $\text{CuSO}_4$  which has fungicidal activity (Hatvani *et al.*, 2004) and might negatively affect *Ptt* growth. Moreover, FCM-noTE contained a yeast extract (a mixture of amino acids, peptides, water soluble vitamins and carbohydrates) which might provide additional nutrients to the fungus promoting toxin production. FCM was first described by Luke and Wheeler (1955) to contain the same ingredients

mentioned in Table 2.2 except that it contained sucrose instead of glucose. This media had since been modified by Friis *et al.* (1991) by replacing glucose instead of sucrose. Although Friis *et al.* (1991) found this replacement had increased toxin production by *Ptt*, the author only analysed the low molecular weight aperyllomarasmines. Sarpeleh *et al.* (2007; 2008) then successfully used FCM for proteinaceous toxin production. In addition, FCM-noTE is routinely used to produce toxins from *Stagonospora nodorum* (Liu *et al.*, 2004a) and *P. tritici-repentis* (Manning *et al.*, 2009; Manning *et al.*, 2008; Tomas and Bockus, 1987; Tuori *et al.*, 1995). Furthermore, colonies grown on FCM had sunk compared with FCM-noTE, suggesting that the fungus grew rapidly on FCM-noTE covering the media surface more quickly and preventing colonies from sinking. Colonies in FCM also had a darker colour suggesting the fungus was unviable. Although 32/98 produced large amounts of protein when the culture was shaking for 23 days, the filtrate was gelatinous and produced less volume of retentate reducing the final amount of extracted protein. Therefore, all further experiments used FCM-noTE for proteinaceous toxin production.

Given that symptoms were induced in barley leaves by the culture filtrates from all isolates regardless of their virulence, all isolates seem likely to have the genetic ability to express toxins necessary to cause disease. The differences in virulence between isolates may therefore reflect the requirement for a certain amount of the toxins to be delivered into the plant tissues through effective fungal growth (Dushnicky *et al.*, 1998; Lamari and Bernier, 1989). Results also confirmed that the more virulent isolates developed effective



growth patterns such as more conidial germination and fungal growth (Figure 2.5, Figure 2.6, Figure 2.7 and Figure 2.8 A, B). In addition, using the Hagborg device to deliver toxins does not necessarily entirely reflect the nature of the *Ptt*-barley interaction (Sarpeleh *et al.*, 2007). Even though 5 µg of total protein induced symptoms, much lower levels are usually necessary to induce symptoms. For example, Kim and Strelkov (2007) demonstrated that as little as 33 pg of ToxB from *P. tritici-repentis* produced chlorosis in wheat leaves. However, this study is the first to explore the relationship between growth *in planta* and toxin production with virulence of *P. teres f. teres* on barley. Timing and amount of toxin production as well as the nature of the toxins produced during the interaction might also play a role in virulence and fungal growth. The more virulent isolates may have established themselves faster by producing certain types of toxin necessary for attachment, appressorial formation, cell wall penetration and host cell death induction (Amaike *et al.*, 2008; Kwon *et al.*, 1998; Manning *et al.*, 2009; Rasmussen *et al.*, 2004; Solomon and Rathjen, 2010; Tan *et al.*, 2010). The less virulent isolates might have taken a longer time to produce these toxins delaying the infection process, as has been suggested in the interaction between *Magnaporthe oryzae* and rice when endoxylanase mutants invade more slowly providing the host cells more time to prepare effective defence by strengthening their cell wall (Nguyen *et al.*, 2011). Given that hydrolysis enzymes and pressure generated by the appressoria are known to degrade the cuticle and cell wall (Keon and Hargreaves, 1983; Lyngs Jørgensen *et al.*, 1998; Vancaesele and Grumbles, 1979), whether any of the

proteins from *Ptt* culture filtrates have this activity needs to be established to determine whether in fact they may contribute to the infection process. After the fungus has established itself within plant tissues, the toxins probably play a fundamental role in necrosis induction (Sarpeleh *et al.*, 2007; 2008) as evidenced by the disruption of mesophyll cells near intercellular hyphae and subsequent cell death (Keon and Hargreaves, 1983).

In conclusion, the research presented in this chapter demonstrated that virulence of *Ptt* was associated with fungal growth and that proteinaceous toxins from all filtrates of *Ptt* isolates can cause NFNB symptoms. Therefore, identification of the individual proteinaceous toxins in the *Ptt* filtrate and how they might behave during the interaction of the host with isolates of different virulence is necessary.

## **Chapter 3 Identification of individual candidate proteinaceous toxins from *Pyrenophora teres f. teres***

### **3.1 Introduction**

The interaction between pathogenic fungi and the host plant is determined by the production of molecules from both fungus and plant (Tan *et al.*, 2010). *Pyrenophora teres f. teres* (*Ptt*) spends most of its lifecycle acting as a necrotroph (Able, 2003; Lightfoot and Able, 2010; Liu *et al.*, 2011). Necrotrophic fungi are well characterised as using large quantities of cell wall-degrading enzymes to cause diseases (Hammond-Kosack and Rudd, 2008) but they may also use effectors to colonise the susceptible host (Liu *et al.*, 2011; Tan *et al.*, 2010). Several necrotrophic fungi have been reported to use proteinaceous toxins for pathogenesis including *Rhynchosporium commune* (Wevelsiep *et al.*, 1993), *Alternaria brassicae* (Parada *et al.*, 2008), *Stagonospora nodorum* (Liu *et al.*, 2009), *P. tritici-repentis* (*Ptr*) (Friesen *et al.*, 2006), *Ptt* and *P. teres f. maculata* (Sarpeleh *et al.*, 2007; 2008). Production of a cultivar-specific toxin (also known as an effector) appears necessary for virulence of a number of Ascomycetes that infect cereals (Beattie *et al.*, 2007; Betts *et al.*, 2011; Kwon *et al.*, 1998; Rau *et al.*, 2007). These include *Ptr* ToxA and *Ptr* ToxB (produced by *Ptr*) and *SnToxA* (produced by *S. nodorum*) which are required for virulence on certain cultivars of wheat (Friesen *et al.*, 2006; Kwon *et al.*, 1998; Liu *et al.*, 2009) and the NIP1 effector protein secreted by the barley pathogen *R. commune* (Fiegen and Knogge, 2002; Schurch *et al.*, 2004). Some toxins probably also play a more significant role than others in disease development (Friesen *et al.*, 2008b). However, much less is known

regarding the molecular basis of virulence (Sacristan and Garcia-Arenal, 2008), particularly the identification of individual proteinaceous toxins that may contribute to the virulence of *Ptt*.

Many studies have established that toxin bioassay using host leaves was a successful tool to investigate the biological activity of either a mixture of toxins or an individual toxin (Campbell *et al.*, 2003; Ciuffetti *et al.*, 2010; Friesen *et al.*, 2008a; 2007; 2008b; Manning and Ciuffetti, 2005; Sarpeleh *et al.*, 2009; 2007; 2008; Weiergang *et al.*, 2002). Most of these studies have infiltrated the toxin/s using a mechanical device such as the Hagborg device used in chapter 2 (Hagborg, 1970). Campbell *et al.* (2003) found that the relative toxicity of filtrates derived from several isolates of *Pyrenophora semeniperda* was highly correlated with the virulence of these isolates. However, previous research (chapter 2) found that *Ptt* isolates were capable of producing a mixture of biologically active toxins *in vitro* (Figure 2.14) even though they were varied in their virulence (Figure 2.2). Thus, the objectives of this research were to identify the individual toxins in the filtrate (*in vitro*) of *Ptt* isolates using several approaches: size separation of proteins in culture filtrates of *Ptt* isolates and determination of the biological activity of the differently sized protein fractions; and identifying proteins differentially expressed between a more virulent and less virulent isolate *in vitro*. The differences between intercellular washing fluids (ICWF) of infected and uninfected plants were also examined.

## **3.2 Material and methods**

### **3.2.1 Plant growth**

Seeds from three barley (*Hordeum vulgare* L.) cultivars, identified previously as susceptible (Sloop) and resistant (CI9214 and Beecher) (Wallwork, personal communication; Gupta *et al.*, 2003), were grown as per section 2.2.1 for use in bioassays.

### **3.2.2 Fungal isolation and toxin production**

Six isolates of *Ptt* (Table 2.1) were isolated as per section 2.2.2 and cultures for the production of proteinaceous toxins were grown as per section 2.2.6.1 using FCM without trace elements and no shaking, toxins were extracted as per 2.2.6.2.1.

### **3.2.3 Proteinaceous toxin fractionation and bioassays**

The crude filtrate from cultured *Ptt* contains many proteins (Figure 2.12) and therefore fractionation was conducted to separate proteins and determine which fractions were toxic to the plant. Toxins were separated from two isolates (08/08f and 32/98, previously identified as less and more virulent respectively, Figure 2.2) using an ion exchange chromatography column made from Sephadex™ G-50 (GE Healthcare UK Limited, Buckinghamshire, UK). The Sephadex gel was prepared by mixing 8 g Sephadex G-50 with 80 mL running buffer (100 mM sodium chloride, 10 mM sodium acetate pH 4.8 and SNW), before placing into a hot water bath at 70°C for 3 h. The supernatant was discarded and new buffer was added to make 75% solution which was degassed

using a vacuum for 15 min. The solution (90 mL) was poured in one pour into a glass column (120 × 1 cm) and then moved to 4°C. The column was equilibrated with three beds (270 mL) of the running buffer at a flow rate of 0.33 mL/min. Protein samples (protein concentration 1551µg per mL) were loaded (2.5 mL) and 8 mL protein fractions were collected. Protein fractions were concentrated, washed with SNW using the UFP method and the concentration of protein measured as per section 2.2.6.2.1 and stored at -80°C until required. Biologically active protein fractions were sub-fractionated using a shorter column (20 × 0.8 cm) and the same procedure as above except that the volume of the Sephadex was 6 mL. Six protein sub-fractions were collected (of 1.5, 1, 0.5, 0.5, 1.5 and 1.5 mL respectively). Protein fractions were concentrated and washed with SNW using the UFP method as per section 2.2.6.2.1 and stored at -80°C until required for the bioassay.

### **3.2.3.1 Bioassay of protein fractions from two isolates with different virulence**

Bioassay experiments were conducted to investigate the toxicity of the protein fractions extracted from the filtrates of the two isolates, 08/08f and 32/98. Five µg of total protein in a total volume of 200 µL of five fractions were injected as per section 2.2.6.4. Symptoms were monitored and compared every 24 h up to 10 days post injection. Three individual plants of cv. Sloop in two individual experiments were used and representative leaves were imaged as per section 2.2.3.

### **3.2.3.2 Bioassay of protein fractions and sub-fractions on barley cultivars of different susceptibility**

To evaluate the susceptibility/sensitivity of three barley cultivars (Sloop, CI9214 and Beecher) to proteinaceous toxins, and fractionations, and to identify whether any of them contribute to the host specificity, previously described (Sarpeleh *et al.*, 2007), ten protein fractions and six sub-fractions of 32/98 filtrate were tested. Ten  $\mu\text{g}$  of total protein in a total volume of 200  $\mu\text{L}$  from fractions (4 to 7) were injected as per section 2.2.6.4, the same volume (200  $\mu\text{L}$ ) was injected from crude fractions with less than 1  $\mu\text{g}$  protein per mL. Symptoms were monitored every 24 h up to 10 days post injection. After collecting the results of bioassay of the fractions, six sub-fractions were separated from the most biologically active protein fraction (fraction 4) and 10  $\mu\text{g}$  of protein from some of the sub-fractions (2 to 5) were injected. The total volume of the injected solution was 200  $\mu\text{L}$  and the same volume was injected for these sub-fractions with less than 1  $\mu\text{g}$  protein per mL (4/1, 4/5 and 4/6) and symptoms were monitored as described above. Three individual plants in each of three individual experiments (9 replicates) were used in the bioassays of individual fractions and sub-fractions and images of the representative leaves were captured 5 days after injection as per section 2.2.3.

### **3.2.4 Investigation of *Ptt* toxins in intercellular washing fluids (ICWFs) and cell components in infected plants**

Since *Ptt* appears to use proteinaceous toxins to cause symptoms in susceptible plants (Figure 2.14) (Sarpeleh *et al.*, 2007), comparisons were made between protein profiles of ICWFs and cell components of infected and uninfected

plants. Proteomic analysis was used to compare these profiles in an attempt to identify the presence of *Ptt* toxins in these profiles.

#### **3.2.4.1 Plant inoculation**

Four individual plants (grown as per section 2.2.1) of barley cv. Sloop were inoculated with 32/98 (previously identified as a more virulent isolate, Figure 2.2) as per section 2.2.3. Leaves from infected and uninfected plants were harvested at 6 dpi and 9 dpi, the ICWFs and cell components were isolated and protein was extracted.

#### **3.2.4.2 Protein extraction from ICWFs**

Protein extraction was conducted in dim green light (wavelength, 492 – 577 nm) at 4°C to prevent light-induced changes in chloroplast ultrastructure upon infiltration with Tris [Tris (hydroxymethyl)aminomethane] buffer (Mittelheuser and Van Steveninck, 1972). Leaves from infected and uninfected plants were cut into 5 cm long pieces and arranged in bundles and rolled with plastic strips (8 × 50 cm). Bundles were introduced, with the cut end first, into tubes containing 150 mM Tris HCl and then vacuumed for 20-30 min (leaves turned to dark green color indicating efficient and uniform infiltration) (Rohringer *et al.*, 1983). Leaves were washed twice with SNW, and then dried between double layers of paper towel. Leaves were arranged transversely in strips (8 × 100 cm) with the cut ends pointed in the same direction. The strips were rolled around plastic tubes (1.5 × 7 cm) with sufficient pressure on the leaves without



damaging the leaves. Bundles of rolled leaves were introduced into specially designed centrifuge tubes, where each tube was equipped with a removable perforated plastic stage separating the bundle of rolled-up leaves from the bottom of the tube to allow for easy collection of ICWFs. Tubes were centrifuged at 800 g for 15 min (Rohringer *et al.*, 1983; Sarpeleh, 2007) and the filtrates were collected and passed through a 0.22 µm filter to remove plant material. ICWFs were collected in 1 mL tubes and protein was extracted as per section 2.2.6.2.3 and concentration of protein measured as per section 2.2.6.2.1 and stored at -80°C until required.

#### **3.2.4.3 Protein extraction from cell components**

After ICWFs extraction, the same leaves were used to extract proteins from mitochondria and chloroplast in dim green light at 4°C. Leaves [20% (w/v)] were mixed for 10 s at half speed in a blender with 100 mL ice cold grinding buffer [medium A; 50 mM HEPES-KOH [4-(2-Hydroxyethyl) piperazine-ethane sulfonic acid-potassium hydroxide] (pH 8.0), 330 mM sorbitol, 2 mM EDTA-Na<sub>2</sub> (disodium ethylenediaminetetraacetic acid) (pH 8.0), 5 mM ascorbic acid, 5 mM cysteine] (Wijk *et al.*, 2007). The homogenate was filtered through a Miracloth (Calbiochem, La Jolla, CA) (Eubel *et al.*, 2007) before being centrifuged at 1000 g for 10 min. The supernatant (Supernatant A) (containing mitochondria) was collected and kept at 4°C until required. The pellet (containing chloroplasts) was collected and suspended in medium B [50 mM HEPES-KOH (pH 8.0), 330 mM sorbitol, 2 mM EDTA-Na<sub>2</sub> (pH 8.0)]

(Wijk *et al.*, 2007). Pellet suspension was loaded into the sucrose gradient; three layers of sucrose concentration prepared by adding 20%, 45% and 60% sucrose in Honda medium (2.5% Ficol 400, 5% dextran T500, 0.25 M sucrose, 0.025 M Tris at pH 7.8, 1 mM magnesium acetate and 4 mM 2-mercaptoethanol) which was pre-prepared as per Francki *et al* (1965) (the sucrose gradient kept for 1 h at 4°C to set). The sucrose gradient loaded with pellet suspension was centrifuged at 16000 rpm for 60 min. The first and second bands in the sucrose gradient (chloroplast) were resuspended in 200 µL of buffer E [125 mM Tris-HCl (pH 8.8), 1% SDS (sodium dodecyl sulfate) (w/v), 10% glycerol (v/v) and 50 mM Na<sub>2</sub>S<sub>2</sub>O<sub>5</sub>] (Wijk *et al.*, 2007) before passing through a 0.22 µm filter to remove cell debris. Soluble protein was precipitated using TCA as per section 2.2.6.2.3 and quantified as per section 2.2.6.2.1 and stored at -80°C until required. Mitochondrial protein was extracted by centrifuging supernatant A at 6000 g for 17 min and the pellet containing mitochondria dissolved in 1 mL phenol for extraction using a phenol/ chloroform precipitation method as per Hajek *et al* (2004). After complete dissolving of the pellet, protein was mixed with 0.5 mL chloroform and shaken for 10 min before being precipitated by centrifugation at 13000 g for 92 min at 4°C. The interphase was transferred into a new tube and washed once with phenol/chloroform (1:1) and twice with pure chloroform to remove remaining phenol. After each washing step, proteins were precipitated by centrifugation (13000 g, 30 min, 4 °C). The pellet was resuspended in a buffer containing; 0.3 M mannitol, 10 mM KH<sub>2</sub>PO<sub>4</sub> (pH 7.2), 2 mM glycine in SNW

(Day *et al.*, 1985). Protein concentration was measured as per section 2.2.6.2.1 and extractions stored at -80°C until required.

### **3.2.5 Visualisation of proteins and candidate toxin identification**

Protein profiles were visualised and compared using Polyacrylamide Gel Electrophoresis (PAGE) and/or Two-Dimensional Gel Electrophoresis (2DGE).

#### **3.2.5.1 PAGE**

PAGE was used to identify the molecular weight (MW) of protein in the fractions, sub-fractions and ICWFs as per section 2.2.6.3. Gels were stained using Coomassie Brilliant Blue staining as per section 2.2.6.3.1, and silver staining as per section 2.2.6.3.2. In some cases, protein profiles were compared and differential bands analysed as per section 3.2.5.3.

#### **3.2.5.2 2DGE**

A 2DGE proteomics approach was used to identify differentially expressed proteins between: the culture filtrates of one of the least virulent isolates (08/08f) and one of the more virulent isolates (32/98); ICWFs of infected and uninfected plants, fraction 4 (active fraction) and fraction 6 (less activity). Isoelectric focusing (IEF) was used to separate proteins based on isoelectric point (*pI*) using a Ettan IPGphor (Pharmacia Biotech Inc, CA, USA) as previously described (Cao *et al.*, 2008; Khoo *et al.*, 2012; Vincent *et al.*, 2009). The first dimension separation was conducted using 11 cm IPG ReadyStrips pH 3-10 (Bio-Rad) at 22°C. Protein was precipitated using 10% TCA as per section 2.2.6.2.3 and pellets resuspended in 200 µL of solution R [7 M urea, 2 M

thiourea, 2% 3-[(3-cholamidopropyl) dimethylammonio]-1-propanesulfonate (CHAPS; w/v), 1% dithiothreitol (DTT), 0.5% of Pharmalyte™ pH 3-10 (Amersham Pharmacia Biotech A8 Uppsala, Sweden)] in SNW (Méchin *et al.*, 2007). The concentration of protein was measured as per section 2.2.6.2.1. Protein (97 µg, 87 µg and 100 µg for the culture filtrates, ICWFs and fractions respectively) was mixed with 0.0002% of Bromophenol blue and loaded into an Ettan IPGphor strip holder (Amersham Biosciences). The strips were passively rehydrated for 30 min before separation using 50 V for 12 h (linear), 250 V for 2 h (linear), 4000 V for 4 h (linear) and 8000 V for 45000 Vhr (rapid). IPG strips were equilibrated according to Görg *et al.* (1988) and Khoo *et al.* (2012). After equilibration, the second dimension was conducted using the Bio-Rad Criterion XT 10% Bis-Tris IPG +1 well 11 cm 1 mm gels (BioRad) and separated according to the manufacturer's protocol. At least three replicates were used and representative gels were imaged as per section 2.2.3. Gels were stained as per sections 2.2.6.3.1 and 2.2.6.3.2 and the gels were stored as per section 2.2.6.3.1. The protein profiles were compared manually and the unique spots were then selected and analysed using Liquid Chromatography-Electrospray Ionisation Ion-Trap Mass Spectrometry (LC-eSI-IT MS).

### **3.2.5.3 Candidate proteinaceous toxin identification**

Analysis of proteins was performed at Adelaide Proteomics Centre (The University of Adelaide) using LC-eSI-IT MS. Bands and spots were excised from the gel manually and washed in 50 mM ammonium bicarbonate. Samples

were then destained with 50 mM ammonium bicarbonate in 30% acetonitrile and digested with 100 ng of sequencing grade modified trypsin (Promega) in 5 mM ammonium bicarbonate and 10% acetonitrile (ACN). Peptides were extracted with 1% formic acid (FA) in water, 1% FA in 50% ACN and 100% ACN. The volumes of the resulting peptide extracts were reduced by speedi-vacuuming to approximately 1  $\mu$ L. Vacuum concentrated samples were resuspended with 0.1% FA in 2% ACN. LC-eSI-IT MS was performed using an online 1100 series HPLC system (Agilent Technologies, USA) and HCT Ultra 3D-Ion-Trap mass spectrometer (Bruker Daltonics, USA). The LC system was interfaced to the MS using an Agilent Technologies Chip Cube operating with a ProtID-Chip-150 (II), which integrates the enrichment column (Zorbax 300SB-C18, 4 mm, 40 nL), analytical column (Zorbax 300 SB-C18, 150 mm x 75  $\mu$ m) and nanospray emitter. Five  $\mu$ L of sample was loaded on the enrichment column at a flow rate of 4  $\mu$ L per min in mobile phase A (0.1% FA in 2% v/v ACN) and resolved with 1-30% gradient of mobile phase B (0.1% FA in 98% w/v ACN) over 32 min at 300 nL per min. Ionisable species ( $300 < m/z < 3,000$ ) were trapped and the two most intense ions eluting at the time were fragmented by collision-induced dissociation. Active exclusion was used to exclude a precursor ion for 30 sec following the acquisition of two spectra. MS and MS/MS spectra were subjected to peak detection and de-convolution using DataAnalysis (Version 3.4, Bruker Daltonics). Compound lists were exported into BioTools (Version 3.1, Bruker Daltonics) and then submitted to Mascot (Version 2.2). Protein identifications were made on the basis of having at least

two matching unique peptides with individual ion scores above the specified threshold (Kopetz *et al.*, 2012). The sequence of these peptides were analysed using BLASTp, search was initially conducted using *Ptr* database and then when *P. teres* genome annotation became available the search was done again to find equivalent proteins using NCBI BLAST search tool (<http://blast.ncbi.nlm.nih.gov/Blast.cgi?PAGE=Proteins>, accessed October 2010). The selection criteria of 100% query coverage and the lowest E-value were used. Whether an N-terminal signal peptide sequence was present predicted by SignalP ([http:// www.cbs.dtu.dk/services/SignalP/](http://www.cbs.dtu.dk/services/SignalP/)) (Bendtsen *et al.*, 2004). Domains and motifs for identified proteins were analysed using NCBI conserved domains (<http://www.ncbi.nlm.nih.gov/Structure/cdd/cddsrv.cgi>, accessed March 2012).

### **3.3 Results**

#### **3.3.1 Identification of potential toxins**

##### **3.3.1.1 From fractions of culture filtrate proteins from two isolates with different virulence**

Given that the protein extracted from culture filtrates induced symptoms regardless of the virulence of isolates (Figure 2.14), crude protein from culture filtrates of 32/98 and 08/08f (more and less virulent isolates respectively) was used to investigate the potential differences and similarities in their protein profiles. Five fractions were separated from each filtrate using ion exchange chromatography. Fraction 4 and 5 from culture filtrates of both isolates induced necrosis on cv. Sloop, while only fraction 3 from the 08/08f isolate induced

symptoms (Figure 3.1). Fraction 4 from the filtrate of the 08/08f isolate induced the most extensive necrosis on leaves with symptoms appearing distant from the injected area.



**Figure 3.1. Bioassays of 5 fractions (F1 to F5) from the culture filtrates of the more virulent isolate (32/98) and less virulent isolate (08/08f) after 5 days post injection.** Five  $\mu\text{g}$  total protein fraction in a total volume of 200  $\mu\text{L}$  was injected in cv. Sloop (susceptible). Fraction 4 and 5 induced necrosis in both isolates, fraction 3 in 08/08f isolate induced symptoms. Red rectangles indicate necrosis, representative image for three plants in two individual experiments.

Four protein fractions from the culture filtrates of 32/98 (more virulent) and 8/08f (less virulent) were loaded on PAGE (Figure 3.2). Several bands from 15 to 150 kDa were present in the active protein fractions. Proteins in fraction 4 in both isolates have almost the same protein profile, however the more virulent isolate (32/98) produced a larger quantity of protein as evidenced by the density of the bands at each size. In addition, fraction 5 in the less virulent isolate (08/08f) contained more protein compared with fraction 5 from the filtrate of the more virulent isolate. Bands 1 to 6 (Figure 3.2) from both isolates were selected as they were around the biologically active MW size as detected by (Sarpeleh *et al.*, 2007; 2008). In addition, no bands were detected in other fractions, therefore these bands were analysed further using LC-eSI-IT MS (Table 3.1).



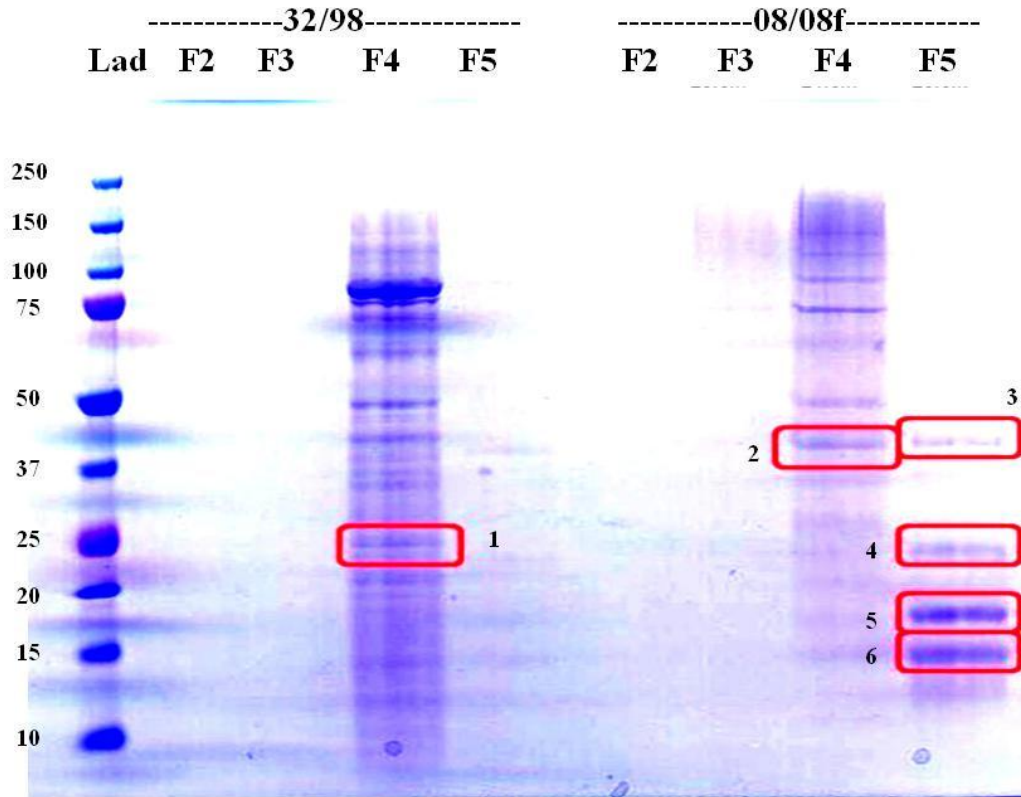


**Figure 3.2. Protein comparison on PAGE between protein fractions (F2 to F5) of the culture filtrates of the more (32/98) and less (08/08f) virulent isolates.** The maximum amount of total protein was loaded in a total of 43  $\mu$ L; 3.15  $\mu$ g and 1.11  $\mu$ g for F4 and F5 respectively for both isolates, and an unknown  $\mu$ g (less than 1  $\mu$ g per mL) for the rest of the fractions, Precision Plus Protein Standard (Lad) was used as marker ladder. Gels were stained with CBB R250. Six highlighted bands (1 to 6) were selected from the biologically active protein fractions and sequenced using LC-eSI-IT MS (Table 3.1). Representative image for two technical replicates.

LC-eSI-IT MS analysis revealed that the 25 kDa protein in fraction 4 from the culture filtrate of the 32/98 isolate (band 1, Figure 3.2) mainly contained peptides that matched to proteins annotated as endo-1, 4- $\beta$ -xylanase I precursor (XP\_001939205) and 6-phosphogluconolactonase (XP\_001938663) (Table 3.1) in *Ptr*. The 37 kDa protein in filtrates from the less virulent 08/08f isolate (band 2) contained peptides that matched to a protein annotated as glucan 1, 3- $\beta$ -glucosidase precursor (XP\_001931233) in *Ptr*. An annotated

glycophosphatidylinositol (GPI)-anchored cell wall  $\beta$ -1, 3-endoglucanase (EglC) from *Ptr* was matched to the peptide sequences identified in band 3 (approximately 37 kDa). Peptides from bands 4 and 6 matched proteins annotated as conserved hypothetical proteins in *Ptr*. However, all proteins in bands 1 to 6 matched to proteins annotated as conserved hypothetical proteins in *Ptt* (Table 3.1). All identified proteins from *Ptt* had an N-terminal signal peptide sequence predicted by SignalP (<http://www.cbs.dtu.dk/services/SignalP/>), suggesting that these proteins are secreted.

**Table 3.1. Protein identification of the active fractions from more (32/98) and less (08/08f) virulent isolates.** LC-eSI-IT MS and MASCOT was used for searches, bands present in the proteinaceous toxin mixture of the more and less virulent isolates were selected and analysed after PAGE (Figure 3.2). Two accession numbers for each protein represent the most similarity to two proteins from *Pyrenophora teres-repentis* (*Ptr*) and *Pyrenophora teres* f. *teres* (*Ptt*) databases. The *Ptr* database was used to identify these proteins then a BLAST search identified *Ptt* proteins (as *Ptt* database was not available at the identification time).

Isolate	Fraction and bands (as per Figure 3.2)	Protein identified	Accession	Identified peptides	Observed/theoretical MW (kDa)	IonScore (Identity / homology threshold) <sup>a)</sup>	E value <sup>a)</sup>	% Coverage <sup>b)</sup>	Secreted <sup>c)</sup>
32/98 more virulent	4 band 1	Endo-1,4-β-xylanase I precursor, <i>Ptr</i>	XP_001939205	R.NPLVEYYVVENFGTYDPSSQAQNK.G	25/24.3	89/39	1e <sup>-16</sup>	11%	S
		Hypothetical protein, <i>Ptt</i>	XP_003304940						
	4 band 2	6-phosphogluconolactonase, <i>Ptr</i>	XP_001938663	1. R.IGAAGRPNEDGLSAVVWEN.	25/41	1. 73/40	2e <sup>-11</sup>	12%	S
		Hypothetical protein, <i>Ptt</i>	XP_003303444	2. K.LPLNGGQPMQTIK.Y					
			3. K.LPSWLTYDNAGK.G						
8/08f Less virulent	4 band 2	Glucan 1,3-β-glucosidase precursor, <i>Ptr</i>	XP_001931233	1. K.AAETAWGAMTADR.K	37/32.4	1. 7/40	3e <sup>-19</sup>	14%	S
		Hypothetical protein, <i>Ptt</i>	XP_003301778	2. K.TQQDYMDDFQAIK.A					
				3. K.VVLGIWPDVEDSFNK.D					
	5/ band 3	Conserved hypothetical protein, <i>Ptr</i>	XP_001933504	1. K.AGGTGTYTDP LTFASAPGEFTK.C	37/19.8	1. 54/40	2e <sup>-14</sup>	19%	S
		Hypothetical protein, <i>Ptt</i>	XP_003296828	2. R.QPSANLPVDSTK.L					
		GPI-anchored cell wall β-1,3-endoglucanase EglC, <i>Ptr</i>	XP_001934358	1. R.FTDLVVGISVGS EDLYR.V	37/34.5	1. 44/40	7e <sup>-09</sup>	13%	S
Hypothetical protein, <i>Ptt</i>	XP_003300299	2. K.QLPGTNGWTSAR.L							
		3. K.QQVDFEYEFNAAK.Q							
5/ band 4	Conserved hypothetical protein, <i>Ptr</i>	XP_001933504	1. K.AGGTGTYTDP LTFASAPGEFTK.C	25/19.8	1. 59/40	4e <sup>-37</sup>	19%	S	
	Hypothetical protein, <i>Ptt</i>	XP_003296828	2. K.CEVIYDPYTR.K						
			3. R.GFKAGGTGTYTDPLTFASAPGEFTK.C						
			4. R.QPSANLPVDSTK.L						
			5. R.QPSANLPVDSTK.L						
			6. R.QPSANLPVDSTKLYVK.G						
			7. R.TQTIVRQPSANLPVDSTK.L						
			8. R.TSHVYQSYNIGDYC.						
5/ band 6	Conserved hypothetical protein, <i>Ptr</i>	XP_001933504	1. K.AGGTGTYTDP LTFASAPGEFTK.C	15/19.8	1. 1.54/40	2e <sup>-14</sup>	19%	S	
	Hypothetical protein, <i>Ptt</i>	XP_003296828	2. R.QPSANLPVDSTK.L						

a) The ion scores for each of the matched peptides and the cut off score for being considered as having extensive homology are shown.

b) The percent coverage of the matched protein by the LC-eSI-IT MS derived *de novo* peptide sequences.

c) Signal peptide sequence predicted by SignalP ([http:// www.cbs.dtu.dk/services/SignalP/](http://www.cbs.dtu.dk/services/SignalP/)).

### 3.3.1.2 From fractions and sub-fractions of culture filtrate proteins that induce symptoms differentially on barley cultivars of different susceptibility

Considering that there was no difference in the symptom induction between the filtrates of the least and the more virulent isolate (Figure 2.14 and Figure 3.1), filtrate from 32/98 isolate was used for the bioassay of fractions and sub-fractions. The concentration of ten protein fractions from 32/98 filtrate was determined using Bradford protein bioassay (Table 3.2A). The protein concentration was greatest in fractions 4 to 8, but was undetectable in fractions 1, 2, 3, 9 and 10 (less than 1 µg per mL). Six protein sub-fractions were separated from the protein fraction 4 (containing biologically active proteins). The majority of protein in fraction 4 was concentrated in sub-fraction 2 to 4 and sub-fractions 1, 5 and 6 were less than 1 µg per mL (Table 3.2B).

**Table 3.2. Protein concentrations in fractions and sub-fractions of culture filtrates from the 32/98 isolate.**

<b>(A) Fractions</b>	<b>Protein concentration (µg per mL)</b>
1	Less than 1 µg per mL
2	Less than 1 µg per mL
3	Less than 1 µg per mL
4	572
5	424
6	471
7	361
8	113
9	Less than 1 µg per mL
10	Less than 1 µg per mL
<b>(B) Sub-fractions</b>	<b>Protein concentration (µg per mL)</b>
4/1	Less than 1 µg per mL
4/2	111
4/3	103
4/4	122
4/5	Less than 1 µg per mL
4/6	Less than 1 µg per mL

Ten crude protein fractions (from 32/98 isolate) were used for bioassay and protein in fractions 4, 5, 6, 9 and 10 induced necrosis in the susceptible cultivar (cv. Sloop), while most protein fractions caused some chlorosis in the resistant cultivars (CI9214 and Beecher) (Figure 3.3). However, protein fraction 3 was biologically active on cv. CI9214 but not in cv. Sloop and cv. Beecher. Although, the protein concentration in protein fractions 9 and 10 was less than 1  $\mu\text{g}$  per mL, necrosis was induced in these fractions especially on cv. Sloop. In addition, these fractions contained proteins with various protein sizes between 10 and 150 kDa (Figure 3.5A).

Because fraction 4 induced extensive necrosis in the susceptible cultivar (Sloop) (Figure 3.3), it was subfractionated. Six protein sub-fractions (of fraction 4) were tested against three cultivars. The bioassay of these sub-fractions revealed that sub-fractions 4/2 and 4/3 had greater activity on cv. Sloop than on CI9214 and Beecher (Figure 3.4) while sub-fraction 4/4 only induced necrosis in cv. Sloop.

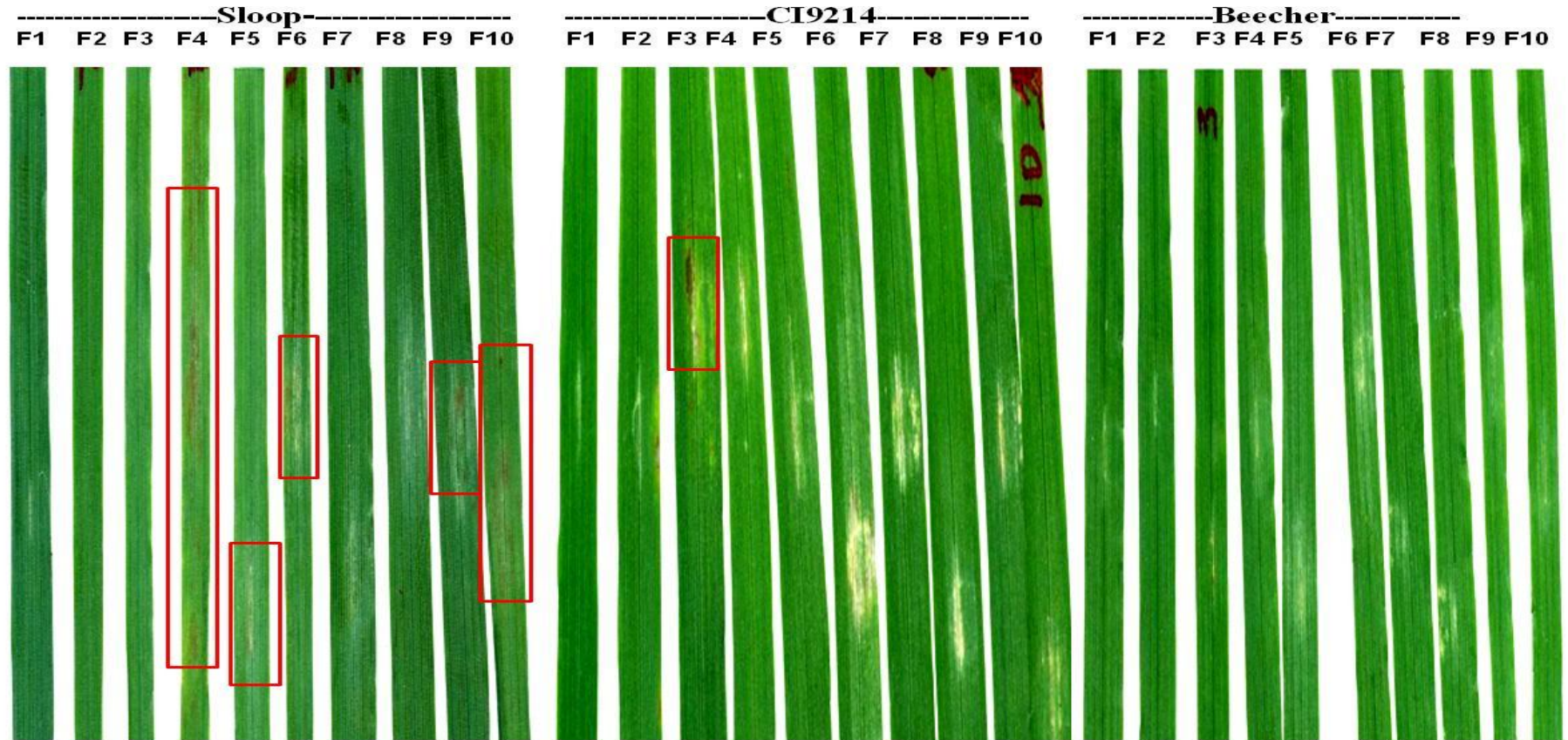


**Figure 3.3. Bioassay of 10 protein fractions (F1 to F10) from filtrates of the more virulent isolate (32/98) on three barley cultivars 5 days post injection.** Ten  $\mu\text{g}$  of total protein of F4 to F8 was injected in total volume of 200  $\mu\text{L}$  for each leaf using the Hagborg device in three different cultivars; Sloop (susceptible), CI9214 and Beecher (resistant cultivars), 200  $\mu\text{L}$  of total protein was injected for F1, F2, F3, F9 and F10 due to low protein yields. Red rectangles indicate necrosis, representative images for three plants in each of three individual experiments.



**Figure 3.4. Bioassay of 6 protein sub-fractions (SF4/1 to SF4/6) of more virulent isolate (32/98) on three barley cultivars after 5 days post injection.** Ten  $\mu\text{g}$  of total protein from SF4/2, SF4/3 and SF4/4 was injected in total volume of 200  $\mu\text{L}$  for each leaf using Hagborg device in three different cultivars; Sloop (susceptible), CI9214 (resistant) and Beecher (resistant), 200  $\mu\text{L}$  of total protein was injected for SF4/1, SF4/5 and SF4/6. Red rectangles indicate necrosis, representative images for four leaves in each of three individual experiments.

Given that protein fractions and sub-fractions have different biological activity (Figure 3.3 and Figure 3.4), PAGE was used to visualise the differences in the protein profiles (Figure 3.5). Protein in fraction 4 shared similarity with protein in fractions 3, 5 and 10 at 37 to 100 kDa, but proteins in fraction 4 were more concentrated as evidenced by greater band density (Figure 3.5A). Fraction 5 contained a mixture of proteins related with symptoms and with a high MW( above 37 kDa) that were also present in fraction 4 and 10 (biologically active fractions). Fraction 5 also contained some low MW proteins (below 37 kDa) not related with symptoms and also found in fractions 6, 7 and 8 (biologically inactive fractions). Sub-fractions 4/2, 4/3, 4/4 and 4/5 also contained similar proteins with mostly similar MW to fraction 4 and each other (Figure 3.5B). This similarity was expected because all the proteins were obtained from the same fraction. Therefore, biological activity most likely related to the proteins which have a MW between 37 to 150 kDa, as evidenced by the protein fraction bioassays (Figure 3.3 and Figure 3.4).



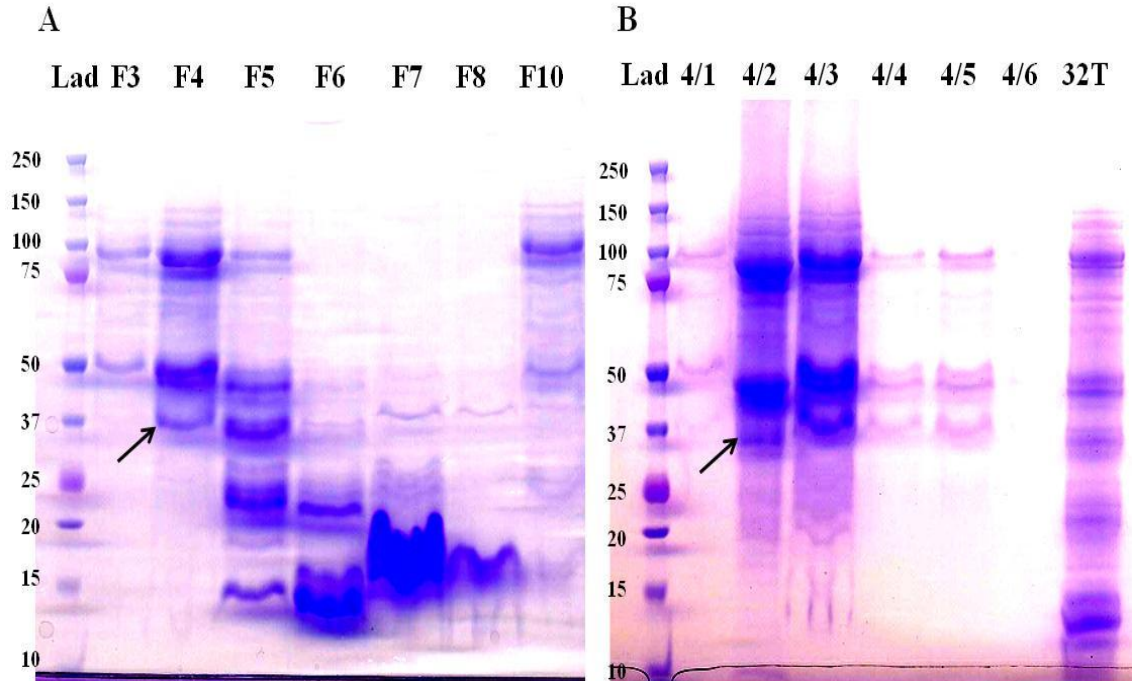


**Figure 3.5. Separation of protein fractions (F3 to F10), protein sub-fractions (4/1-4/6) and crude toxin (32T) for more virulence isolate 32/98 on PAGE.** The maximum amount of total protein was loaded; 2.27 µg for F3, 15 µg for F4. F5, F 6 and SF4/2, 10 µg for F7, 3 µg for SF4/3 and less than 1 µg per mL for F8, F10, SF4/1, SF4/4, SF4/5 and SF4/6, Precision Plus Protein Standard (Lad) was used as marker ladder. Gels were stained with CBB R250, arrows indicate band at 37 kDa was sequenced from both protein fractions and sub-fractions (Table 3.3). Representative image for two technical replicates.

Given that there were potential effectors in sub-fraction 4/4 because it only had biological activity on susceptible cultivar Sloop and not CI9214 or Beecher (Figure 3.4), proteins from the 37 kDa band in fraction 4 and sub-fraction 4/2 (Figure 3.5) were analysed using LC-eSI-IT MS (Table 3.3) as well as the total protein from the same fraction 4 and sub-fraction 4/4 (Table 3.4). The whole of fraction 4 and sub-fraction 4/4 were analysed because fractions 5, 6, 10 and sub-fractions 4/2 and 4/3, which also caused symptoms, had mostly similar profiles. However, fraction 7 and 8 were not analysed as they did not induce symptoms. Analysis revealed that there were three dominant proteins present in the 37 kDa band in both fraction 4 and sub-fraction 4/2 (Table 3.3). These bands contained peptides that

matched to proteins annotated in *Ptr* as; glucan 1, 3- $\beta$ -glucosidase precursor (XP\_001931233), conserved hypothetical protein (XP\_001936940) and endo-1, 4- $\beta$ -xylanase precursor (XP\_001939862). All these proteins were annotated as hypothetical conserved proteins in *Ptt*. LC-eSI-IT MS analysis for the total protein in fraction 4 revealed eight different proteins matched to identified peptides (Table 3.4). These proteins have been annotated in *Ptr* as carboxypeptidase S1(XP\_001932743 and XP\_001936980), isochorismatase (XP\_001932705, sometimes referred as an isochorismatase hydrolase), repressible acid phosphatase (XP\_001937694), GPI-anchored CFEM (common in fungal extracellular membrane) domain-containing protein (XP\_001931262) and two conserved hypothetical proteins (XP\_001936940 and XP\_001938421). All of these proteins were annotated as conserved hypothetical proteins in *Ptt* (Table 3.4). However, a GPI-anchored CFEM domain-containing protein (XP\_001931262) was the only protein that matched to identified peptides when the total sub-fraction 4/4 was characterised (Table 3.4).

**Table 3.3. Protein identification of the active fractions and sub-fractions from the culture filtrate of a more virulent isolate (32/98).** LC-eSI-IT MS and MASCOT was used for searches, bands present in the proteinaceous toxin mixture were selected and analysed after PAGE (Figure 3.5). Two accession numbers for each protein represent the most similarity to two proteins from *Pyrenophora teres-repentis* (*Ptr*) and *Pyrenophora teres* f. *teres* (*Ptt*) databases. The *Ptr* database was used to identify these proteins then a BLAST search identified *Ptt* proteins (as *Ptt* database was not available at the identification time).

Fraction (Figure 3.5)	Protein identified	Accession	Identified peptides	Observed/ theoretical MW (kDa)	IonScore (Identity / homology threshold) <sup>a)</sup>	E value <sup>a)</sup>	% Coverage <sup>b)</sup>	Secreted <sup>c)</sup>
4	Glucan 1,3-β-glucosidase precursor, <i>Ptr</i> Hypothetical protein, <i>Ptt</i>	XP_001931233	1. R.GYAASDCGMASLILPAAK.Q	37/32.5	1. 37(54/46)	6e <sup>-38</sup>	34%	S
		XP_003301778	2. K.AAETAAGAMTADR.K		2. 64(55/43)			
		3. K.VYLDDMYQAITHIEK.V	3. 48(54/25)					
		4. K.TQQDYMDDFQAIK.A	4. 64(56/37)					
		5. K.AAETAAGAMTADR.K	5. 45(55/40)					
		6. K.VYLDDMYQAITHIEK.V	6. 70(55/36)					
		7. K.TQQDYMDDFQAIK.A	7. 71(55/36)					
		8. K.DVADQYADTIYAVTVGSETLYR.G	8. 118(54/38)					
		9. K.VVLGIWPDVEDSFNKDLK.A	9. 21(54/30)					
		10. K.VVLGIWPDVEDSFNK.D	10. 76(54/42)					
		11. K.AAETAAGAMTADR.K	11. 56(55/-)					
		12. K.AIKDVADQYADTIYAVTVGSETLYR.G	12. 93(53/33)					
	Conserved hypothetical protein, <i>Ptr</i> Hypothetical protein, <i>Ptt</i>	XP_001936940	1. K.GAADYGTNTFFASFPDSCDAYR.A	37/34.4	1. 50(54/26)	1e <sup>-14</sup>	13%	S
		XP_003301557	2. R.AGIEFPFLDLLGDGSTSFR.W		2. 126(55/42)			
	Endo-1,4-β-xylanase precursor, <i>Ptr</i> Hypothetical protein, <i>Ptt</i>	XP_001939862	1. R.SSVFYNVLGEDFVR.I	37/35.7	1. 83(55/50)	4e <sup>-22</sup>	8%	S
		XP_003305312	2. R.YINDYNLDNANYAK.T		2. 81(55/34)			
Sub-fraction 4/2	Glucan 1,3-β-glucosidase precursor, <i>Ptr</i> Hypothetical protein, <i>Ptt</i>	XP_001931233	1. K.AAETAAGAMTADR.K	37/32.5	1. 83(55/46)	8e <sup>-39</sup>	36%	S
		XP_003301778	2. K.VYLDDMYQAITHIEK.V		2. 69(55/35)			
			3. K.TQQDYMDDFQAIK.A		3. 80(56/37)			
			4. K.AAETAAGAMTADR.K		4. 63(55/40)			
			5. K.VYLDDMYQAITHIEK.V		5. 66(55/42)			
			6. K.TQQDYMDDFQAIK.A		6. 66(55/36)			
			7. K.DVADQYADTIYAVTVGSETLYR.G		7. 113(54/41)			
			8. R.GYAASDCGMASLILPAAK.Q		8. 15(55/28)			
			9. K.VVLGIWPDVEDSFNKDLK.A		9. 21(54/25)			
			10. K.VVLGIWPDVEDSFNK.D		10. 76(53/40)			
			11. K.AAETAAGAMTADR.K		11. 51(55/48)			
			12. R.GTMGFALGTK.M		12. 32(55/43)			

**Table 3.3. continued**

Fraction (Figure 3.5)	Protein identified	Accession	Identified peptides	Observed/ theoretical MW (kDa)	IonScore (Identity / homology threshold) <sup>a)</sup>	E value <sup>a)</sup>	% Coverage <sup>b)</sup>	Secreted <sup>c)</sup>
<b>Sub-fraction 4/2</b>	Conserved hypothetical protein, <i>Ptr</i>	XP_001936940	1. R.WVPSMLMSADNAIALK.G	37/34.4	1. 36(54/38)	2e <sup>-31</sup>	18%	S
	Hypothetical protein, <i>Ptt</i>	XP_003301557	2. K.GAADYGTNTFFASFDPSCDAYR.A		2. 99(54/32)			
			3. R.AGIEFPFLDLLGDGSTSFR.W		3. 136(54/45)			
			4. R.WVPSMLMSADNAIALK.G		4. 25(55/34)			
<b>Sub-fraction 4/2</b>	Endo-1,4-β-xylanase precursor, <i>Ptr</i>	XP_001939862	1. R.SSVFYNLVGEDFVR.I	37/35.7	1. 104(54/50)	4e <sup>-22</sup>	8%	S
	Hypothetical protein, <i>Ptt</i>	XP_003305312	2. R.YINDYNLDNANYAK.T		2. 109(55/37)			

**a)** The ion scores for each of the matched peptides and the cut off score for being considered as having extensive homology are shown in the brackets.

**b)** The percent coverage of the matched protein by the LC-eSI-IT MS derived *de novo* peptide sequences.

**c)** Signal peptide sequence predicted by SignalP ([http:// www.cbs.dtu.dk/services/SignalP/](http://www.cbs.dtu.dk/services/SignalP/)).

**Table 3.4. Protein identification of whole fraction 4 and 4/4 from filtrates of a more virulent isolate (32/98).** LC-eSI-IT MS and MASCOT was used for searches. Two accession numbers for each protein represent the most similarity to two proteins from *Pyrenophora teres-repentis* (*Ptr*) and *Pyrenophora teres f. teres* (*Ptt*) databases. The *Ptr* database was used to identify these proteins then a BLAST search identified *Ptt* proteins (as *Ptt* database was not available at the identification time).

Fractions	Protein identified	Accession	Identified peptides	theoretical MW (kDa)	IonScore (Identity / homology threshold) <sup>a)</sup>	E value <sup>a)</sup>	% Coverage <sup>b)</sup>	Secreted <sup>c)</sup>
Fraction 4	Carboxypeptidase S1, <i>Ptr</i>	XP_001932743	1. K.QAGHFSFIR.I	64.1	1. 34(58/38)	1e <sup>-09</sup>	17%	S
	Hypothetical protein, <i>Ptt</i>	XP_003304436	2. R.YKEVPAGICELDPSVK.S		2. 58(57/51)			
			3. R.IYESGHEVPFYQPLASLEMFER.A		3. 50(51/45)			
			4. K.TLQGFMGAFQYSR.N		4. 46(57/48)			
	Isochorismatase, <i>Ptr</i>	XP_001932705	1. R.SMVAPTTKPVTIPMTGSR.R	33	1. 24(57/33)	2e <sup>-19</sup>	35%	S
	Hypothetical protein, <i>Ptt</i>	XP_003303790	2. K.MIDAFR.R		2. 25(56/31)			
			3. K.TSPTNSFGSDMGKLDGTELGK.M		3. 17(53/25)			
			4. R.SMVAPTTKPVTIPMTGSR.R		4. 32(56/35)			
			5. R.RAVIEPSR.S		5. 42(57/53)			
			6. R.NGMPVLWTFWGLDGKDLR.D		6. 25(56/38)			
			7. R.KAVEPTLK.M		7. 35(57/51)			
			8. R.SALIIDMQNFFLHPELTPSAEGGR.K		8. 103(55/37)			
			9. R.SMVAPTTKPVTIPMTGSR.R		9. 48(57/38)			
	Repressible acid phosphatase, <i>Ptr</i>	XP_001937694	1. R.ASYLIR.H	49.9	1. 19(57/31)	7e <sup>-14</sup>	14%	S
	Hypothetical protein, <i>Ptt</i>	XP_003299031	2. K.QSSYQEIYTKPIER.L		2. 61(56/32)			
		3. K.ILPFLSNFVIEK.M	3. 50(57/36)					
		4. K.LGVDVR.M	4. 43(59/43)					
		5. R.VLVNRDTQQLSCTDGPGQSCSK.S	5. 34(50/18)					
Conserved hypothetical protein, <i>Ptr</i>	XP_001936940	1. R.LNTAFIENNYLPCENFRGYGSG.	34.5	1. 54(53/28)	3e <sup>-07</sup>	18%	S	
Hypothetical protein, <i>Ptt</i>	XP_003301557	2. R.QLIPSNKILEHAYR.H		2. 15(57/23)				
		3. R.AKILPFKEDQYWQGVCGIR.L		3. 41(55/29)				
		4. K.ILPFKEDQYWQGVCGIR.L		4. 65(56/43)				
GPI anchored CFEM domain containing protein, <i>Ptr</i>	XP_001931262	1. K.ACNPSDQAAAISAVESTCK.A	19.3	1. 68(56/45)	9e <sup>-05</sup>	16%	S	
Hypothetical protein, <i>Ptt</i>	XP_003295367	2. K.GGQLLSQVQPCVEK.A		2. 69(57/-)				
					1e <sup>-04</sup>			

**Table 3.4. continued**

Fractions	Protein identified	Accession	Identified peptides	theoretical MW (kDa)	IonScore (Identity / homology threshold) <sup>a)</sup>	E value <sup>a)</sup>	% Coverage <sup>b)</sup>	Secreted <sup>c)</sup>
<b>Fraction 4</b>	Carboxypeptidase S1, <i>Ptr</i>	XP_001936980	1. R.IYEAGHEVPYYQPVASLEHFRR.V	61.5	1. 14(56/26)	2e <sup>-06</sup>	11%	S
	Hypothetical protein, <i>Ptt</i>	XP_003306500	2. R.SLVEEPYYAFGGRGVYDIR.H		2. 28(56/36)			
			3. R.SLVEEPYYAFGGR.G		3. 34(57/41)			
			4. K.QSDRTTEDGYLTCSSATNLCR.S		4. 48(48/37)			
	Hypothetical protein, <i>Ptt</i>	XP_003297706	1. R.RGCYYGFDLIIPDAEGGTGSAR.A	19.1	1. 25(53/31)	4e <sup>-13</sup>	20%	S
			2. K.LIQGSNVQVAAR.L		2. 93(57/-)			
	Conserved hypothetical protein, <i>Ptr</i>	XP_001938421	1. K.STDLTTVGTLLTTTATGGK.F	21.6	1. 27(56/26)	9e <sup>-05</sup>	17%	S
	Hypothetical protein, <i>Ptt</i>	XP_003297758	2. K.TYTITYSPADDTPTTFILR.Q		2. 79(55/39)			
						3e <sup>-05</sup>		
<b>Sub-fraction 4/4</b>	GPI anchored CFEM domain containing protein, <i>Ptr</i>	XP_001931262	1. K.ACNPSDQAAAISAVESTCK.A	19.3	1. 68(56/45)	9e <sup>-5</sup>	16%	S
	Hypothetical protein, <i>Ptt</i>	XP_003295367	2. K.GGQLLSQVQCVEK.A		2. 69(57/-)			
						1e <sup>-4</sup>		

a) The ion scores for each of the matched peptides and the cut off score for being considered as having extensive homology are shown in the brackets.

b) The percent coverage of the matched protein by the LC-eSI-IT MS derived de novo peptide sequences.

c) Signal peptide sequence predicted by SignalP ([http:// www.cbs.dtu.dk/services/SignalP/](http://www.cbs.dtu.dk/services/SignalP/)).

### **3.3.1.3 Comparing active and less active protein fractions**

Proteins from fraction 4 (biologically active) were compared with proteins in fraction 6 (less biological activity) using 2DGE analysis (Figure 3.6). This comparison was conducted to identify any differences between their protein profiles that might explain their differences in activity. These fractions had completely different protein profiles, with the proteins in fraction 4 having higher MW (37 to 150 kDa) and a protein *pI* between pH 4.5 to 8, while the MW of fraction 6 proteins was between 10 to 150 kDa with a more variable *pI* (pH 3 to 9). Fraction 6 contained small size proteins that probably came after fraction 4 through the Sephadex (G-50) column because they take a longer time to migrate as a result of penetration into the pores of the Sephadex beads (according to the manufacturer). In addition, protein at 37 kDa size appeared in the fraction 6 2DGE which shared similarity to protein in fraction 4, however these proteins were more dense in fraction 4. Moreover, protein in fraction 4 showed greater biological activity compared to proteins in fraction 6 (Figure 3.3), thus indicating that the activity of the protein fraction might be related to the concentration of this particular proteins which presented at 37 kDa. Because many protein spots were different in both profiles, no spot was analysed further.

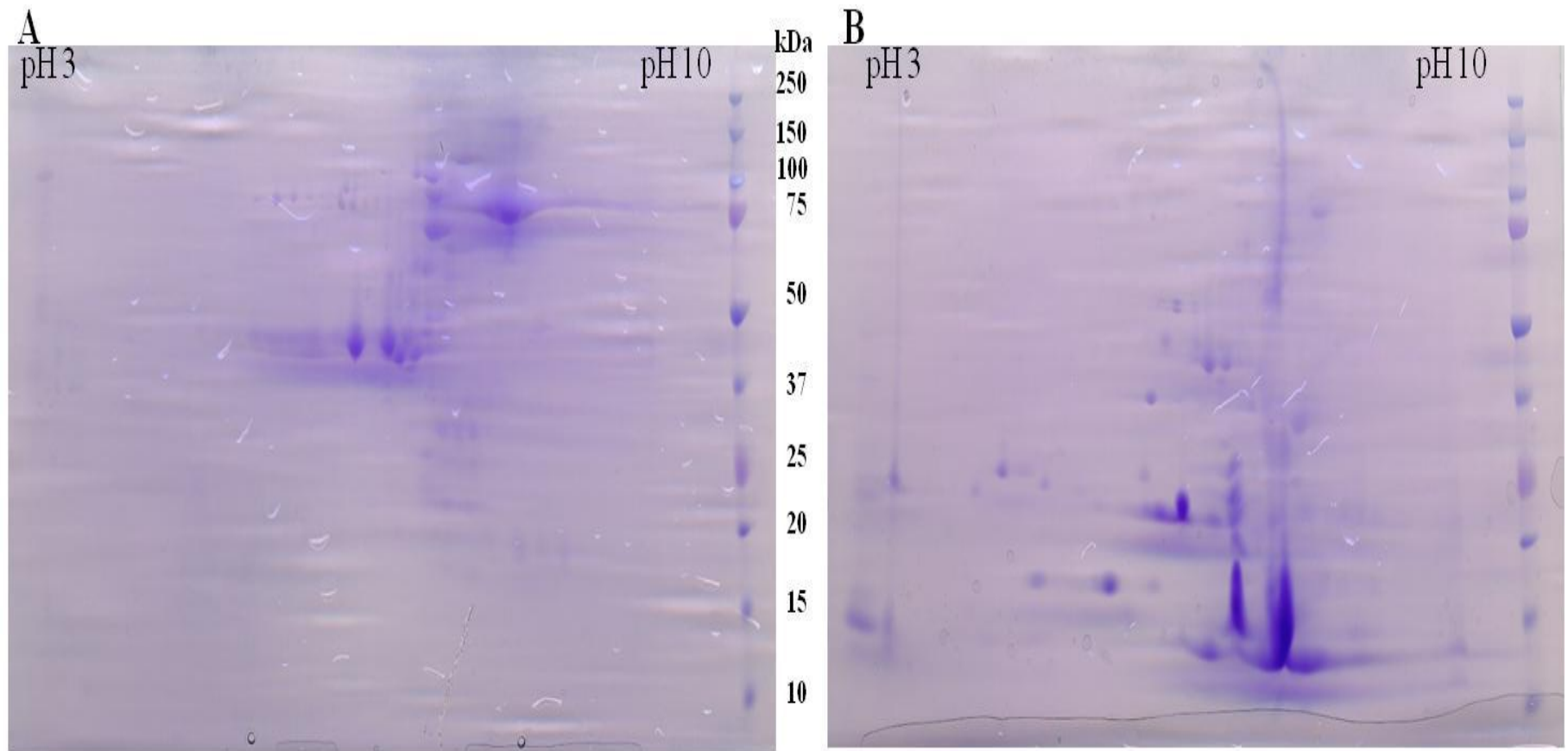


**Figure 3.6. 2DGE comparison of protein profiles of fraction 4 (A) and fraction 6 (B) from 32/98 isolate.** Hundred  $\mu$ g of protein was loaded from both fractions, Precision Plus Protein Standard (Lad) was used as marker ladder. Gels were stained with CBB R250. Proteins in fraction 6 have a wider range of MW and pH compared with proteins in fraction 4. Representative image is shown for two technical replicates.



### 3.3.2 Identification of virulence-related candidate proteins (VRCPs)

The 2DGE protein profiles of the culture filtrates from one of the least virulent isolates (08/08f) and one of the more virulent isolates (32/98) were compared and the overall protein patterns were quite similar in both isolates (Figure 3.7). The majority of proteins were between 10 and 75 kDa and more abundant at 10 to 25 kDa while protein *pI* were mostly in the range of 3.5 to 7.3. Two unique spots at 25 and 30 kDa were only present in the profile for the proteinaceous toxin mixtures extracted from the more virulent isolate (Figure 3.7A). LC-eSI-IT MS analysis of the two spots has identified three protein candidates (present in both spots) based on their peptide sequences (Table 3.5). These peptides shared most similarity with a cysteine hydrolase family annotated as an isochorismate hydrolase (XP\_001932705); an endo-1,4- $\beta$ -xylanase A of glycosyl hydrolase family 11 (XP\_001941158) and a conserved hypothetical protein (XP\_001933504) from *Ptr*, all of which match to proteins annotated as conserved hypothetical proteins in *Ptt* (Table 3.5). All identified proteins from *Ptt* had an N-terminal signal peptide sequence as predicted using SignalP (Bendtsen *et al.*, 2004), indicating that they were secreted proteins as expected.

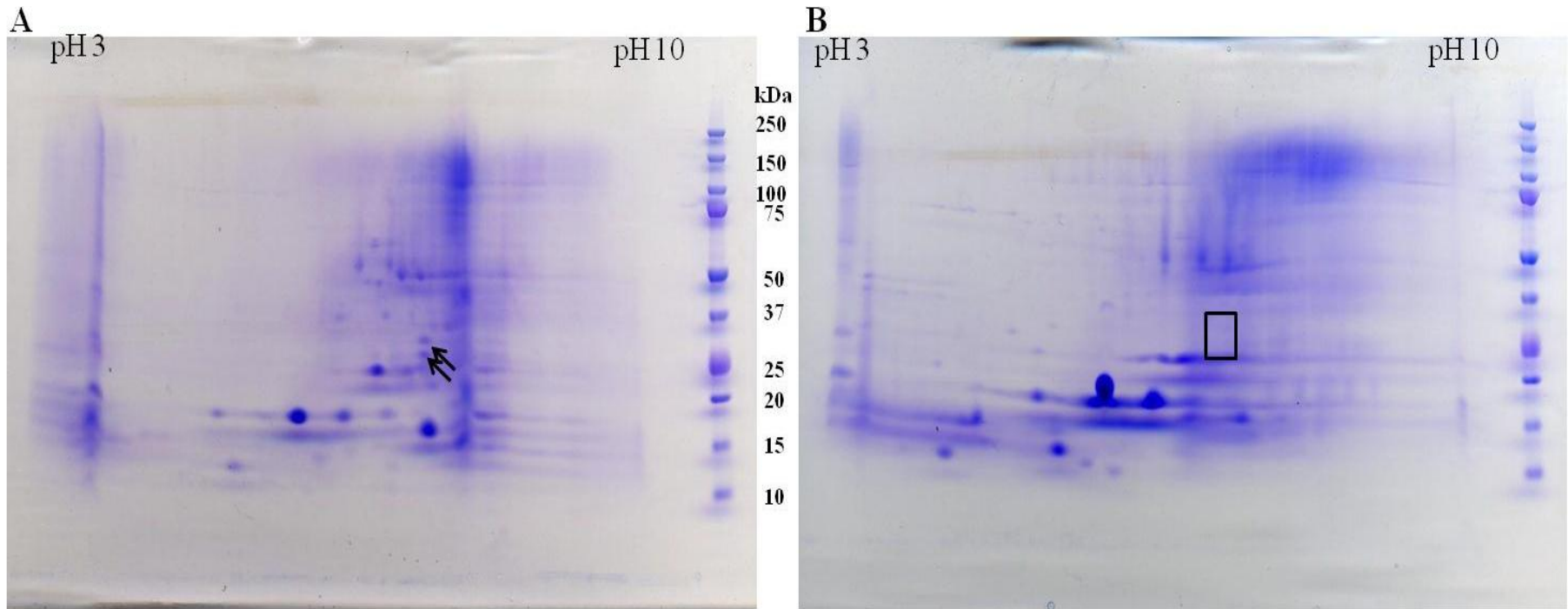


**Figure 3.7. Identification of proteins extracted from culture filtrates from the more virulent isolate 32/98 (A) and the least virulent isolate 08/08f (B) using 2-D gel electrophoresis.** Representative gel image for three biological replicates. Two unique spots (black arrows) were associated with the more virulent isolate were analysed using LC-eSI-IT MS (rectangled area highlights the lack of spots in the least virulent isolate) (Table 3.5), and Precision Plus Protein Standard (Lad) was used as marker ladder

**Table 3.5. Protein identification of differentially expressed two-dimensional gel electrophoresis (2DGE) protein spots (Figure 3.7).** Using LC-eSI-IT MS and MASCOT searches, two accession numbers for each protein represent those with the most similarity to two proteins from *P. tritici-repentis* (*Ptr*) and *P. teres f. teres* (*Ptt*) databases. The *Ptr* database was used to identify these proteins then a BLAST search identified *Ptt* proteins (as *Ptt* database was not available at the identification time).

Proteins identified (Figure 3.7)	Accession	Identified peptides	Observed/ theoretical MW(kDa) <sup>a)</sup>	Observed/ theoretical pI <sup>a)</sup>	IonScore (Identity / homology threshold) <sup>b)</sup>	E value <sup>b)</sup>	% Cover-age <sup>c)</sup>	Secre- ted <sup>d)</sup>
Isochorismatase, <i>Ptr</i>	XP_001932705	1.R.NGMPVLWTFWGLDGK.D	25-30/ 31.1	5.5/7.8	1. 70(44/29)	2e <sup>-165</sup>	14	S
Hypothetical protein, <i>Ptt</i>	XP_003303790	2.R.SALIIIDMQNFFLHPELTPSAEGGR.K			2. 128(40/30)			
Endo-1,4-β-xylanase A, <i>Ptr</i>	XP_001941158	1.K.GQVQSDGGTYDILQTTR.Y	25-30 /24.9	5.5/ 7.8	1. 128(43/34)	2e <sup>-129</sup>	16	S
Hypothetical protein, <i>Ptt</i>	XP_003306630	2.R.YNQPSIDGTQTFQQFWSVR.T			2. 105(43/-)			
Conserved hypothetical protein <i>Ptr</i>	XP_001933504	1.R.TSHVYQSYNIGDYC	25-30 /19.9	5.5/ 5.9	1. 52(44/34)	5e <sup>-101</sup>	15	S
Hypothetical protein <i>Ptt</i>	XP_003296828	2.R.QPSANLPVDSTK.L			2. 27(44/28)			

- a)** The predicted molecular weight (MW) and isoelectric point (pI) of the matched protein based on the values provided in the MASCOT summary report.  
**b)** The ion scores for each of the matched peptides and the cut off score for being considered as having extensive homology are shown in the brackets.  
**c)** The percent coverage of the matched protein by the LC-eSI-IT MS derived *de novo* peptide sequences.  
**d)** Signal peptide sequence predicted by SignalP ([http:// www.cbs.dtu.dk/services/SignalP/](http://www.cbs.dtu.dk/services/SignalP/)).

### 3.3.3 Characterisation of ICWFs and cell components from infected plants

The protein profiles of the ICWFs, chloroplast and mitochondria extractions from cv. Sloop infected with the 32/98 isolate and an uninfected control were compared to identify whether *Ptt* toxins were produced *in planta* and targeted to particular cell components. Thus, protein was extracted 6 and 9 dpi from ICWFs and cell components (chloroplast and mitochondria). The ICWF from infected plants (6 and 9 dpi) had unique proteins, approximately 30 kDa in size, that were not present in the control ICWF (Figure 3.8). However, the proteins from chloroplast and mitochondria extractions did not show any differences between infected and uninfected plants.

Proteins from ICWFs of infected and uninfected plants were compared with total crude toxin, protein fraction 4 and protein sub-fraction 4/2 of 32/98 isolate using PAGE. Interestingly there was the same size band (approximately 30-35 kDa) associated with all protein profiles (Figure 3.9). This band has been previously identified as being associated with symptoms (Figure 3.7, Table 3.4), therefore the band from the ICWF of infected plants at 9 dpi which associated with symptoms was analysed using LC-eSI-IT MS (Table 3.6). Although ICWF proteins shared the same size band with protein fraction 4 and sub-fraction 4/2 from the filtrates of *Ptt*, no *Ptt* protein was detected in the ICWFs. All identified peptides were matched to proteins in barley and were mainly pathogenesis-related proteins (PRs); glucanase, chitinase, peroxidase, PRB1-2, PRB1-3 and PR (Table 3.6).

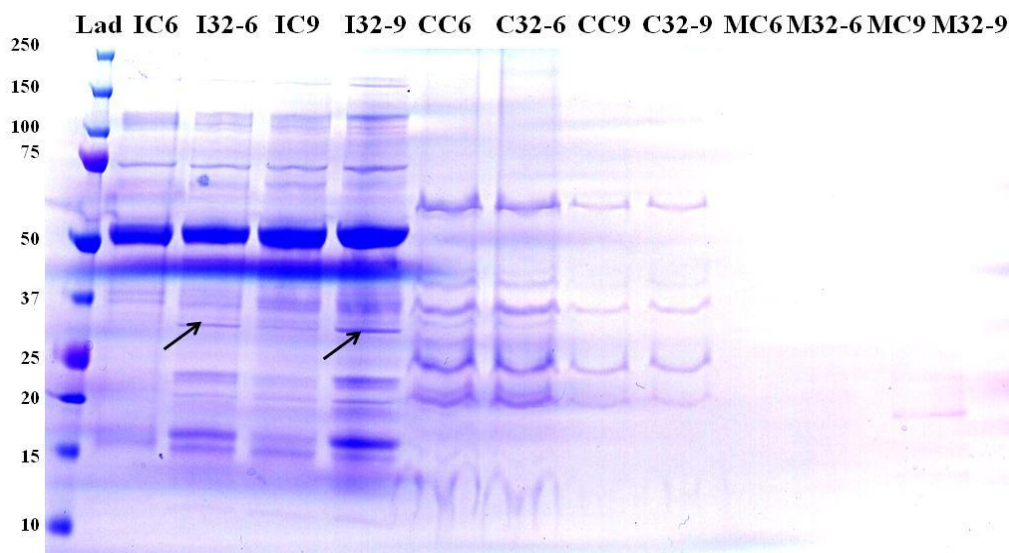


**Figure 3.8. PAGE for proteins extracted after 6 and 9 day post inoculation (dpi) from uninfected leaves (C) and leaves infected with 32/98 isolate (32) of *Ptt*.** Seven  $\mu$ g of total proteins was loaded from intercellular washing fluids (I), chloroplast (C) and mitochondria (M). I from uninfected leaves (IC-6, IC-9), I from leaves infected with 32/98 isolate (I32-6, I32-9), C from uninfected leaves (CC6, CC9), C from leaves infected with 32/98 isolate (C32-6, C32-9), M from uninfected leaves (MC6, MC9), M from leaves infected with 32/98 isolate (M32-6, M32-9). Precision Plus Protein Standard (Lad) was used as marker ladder, gels were stained with CBB R250. Arrows indicate differences between (I32-6, I32-9) and (IC-6, IC-9). Representative image for four technical replicates.

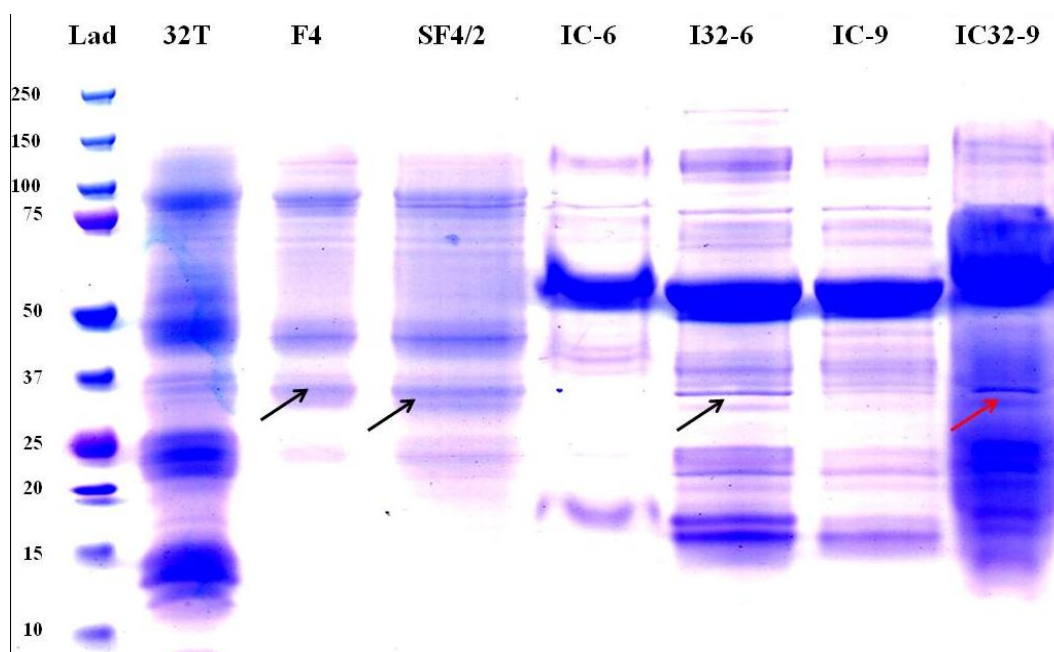


**Figure 3.9. Separation of proteins extracted from 32/98 crude toxin (32T), fraction 4 (F4), sub-fraction 4/2 (SF4/2) and intercellular washing fluids (ICWFs) using PAGE.** Fifteen  $\mu$ g of total protein was loaded from ICWFs of uninfected leaves after 6 and 9 day post inoculation (IC-6, IC-9), ICWFs from leaves infected with 32/98 isolate after 6 and 9 dpi (I32-6, I32-9), Precision Plus Protein Standard (Lad) was used as marker ladder. Gels were stained with CBB R250, arrows indicate bands which shared the same size (37 kDa) for F4, SF4/2, I32-6 and I32-9, red arrow shown the band that was sequenced using LC-eSI-IT MS (Table 3.6). Representative image for three technical replicates.

**Table 3.6. Protein identification of ICWFs from barley leaves infected with *Ptt* isolate 32/98 after 9 dpi.** LC-eSI-IT MS and MASCOT was used for searches, band present in the protein mixture of the ICWF of the more virulent isolate were selected and analysed after PAGE (Figure 3.9). Two accession numbers for each protein represent the most similarity to the plant species.

Protein identified (Figure 3.9)	Accession	Identified peptides	Observed/ theoretical MW (kDa)	IonScore (Identity / homology threshold) <sup>a)</sup>	E value <sup>a)</sup>	% Coverage <sup>b)</sup>	Secreted <sup>c)</sup>
β-1,3-glucanase II, <i>Hordeum vulgare</i> subsp. <i>vulgare</i> Chain A, The Three-Dimensional Structures Of Two Plant β-Glucan Endohydrolases With Distinct Substrate Specificities, <i>Hordeum vulgare</i>	AAM75342	1. R.SFGLFNPDKSPAYNIQF.	30/32.4	1. 54(55/42)	1e <sup>-26</sup>	64%	S
		2. K.VSTSIRFDEVANSFPSPAGVFK.N		2. 71(54/33)			
	1GHS_A	3. R.TYNQGLINHVGGGTPK.K		3. 71(55/31)			
		4. R.EALETYIFAMFNENQK.T		4. 78(55/48)			
		5. K.VVSVESGWPSAGGFAASAGNAR.T		5. 112(54/38)			
		6. R.DNPGSISLNYATFQPGTTVR.D		6. 100(54/41)			
		7. K.YIAAGNEVQGGATQSILPAMR.N		7. 135(54/-)			
		8. R.IYFADGQALSALR.N		8. 109(55/-)			
		9. R.FDEVANSFPSPAGVFK.N		9. 99(55/41)			
		10. R.LLASTGAPLLANVYPYFAYR.D		10. 97(54/-)			
		11. R.NLNAALSAAGLGAIK.V		11. 123(55/-)			
		12. K.YIAAGNEVQGGATQSILPAMR.N		12. 76(54/33)			
Endochitinase-antifreeze protein precursor, <i>Secale cereale</i> Chitinase, <i>Hordeum vulgare</i> subsp. <i>vulgare</i>	AAG53610	1. R.YCGMLGTATGGNLDCTQR.N	30/27.4	1. 92(54/35)	6e <sup>-32</sup>	51%	S
		2. R.GFYTYDAFIAAANTFPGFGTTGSADDIKR.E		2. 107(53/27)			
	CAA55344	3. R.YCGMLGTATGGNLDCTQR.N		3. 101(54/37)			
		4. K.DLVSNPDLVSTDAVVSFR.T		4. 117(54/50)			
		5. R.WTPTAADTAAGR.V		5. 51(56/39)			
		6. R.ELAAFFGQTSHETGGTR.G		6. 131(55/41)			
		7. R.SVYASMLPNR.D		7. 52(55/39)			
		8. R.SVYASMLPNR.D		8. 36(55/41)			
		9. R.AIGKDLVSNPDLVSTDAVVSFR.T		9. 55(54/22)			
		10. R.VPGYGVITNIINGGLECGMGR.N		10. 87(54/32)			
Chitinase I, <i>Triticum aestivum</i> Chitinase II, <i>Hordeum vulgare</i> subsp. <i>vulgare</i>	BAB82471	1. R.TAIWFWMTAQGNKPSHDVALGR.W	30/27.5	1. 59(53/21)	2e <sup>-18</sup>	44%	S
	CAB99486	2. R.YCGMLGTATGGNLDCTQR.N		2. 92(54/35)			
		3. R.YCGMLGTATGGNLDCTQR.N		3. 101(54/37)			
		4. K.DLVSNPDLVSTDAVVSFR.T		4. 117(54/50)			
		5. R.GPIQLTGQSNYDLAGR.A		5. 90(55/38)			
		6. R.WTPTAADTAAGR.V		6. 51(56/39)			
		7. R.ELAAFFGQTSHETGGTR.G		7. 131(55/41)			
		8. R.AIGKDLVSNPDLVSTDAVVSFR.T		8. 55(54/22)			

**Table 3.6 continued**

Protein identified (Figure 3.9)	Accession	Identified peptides	Observed/ theoretical MW (kDa)	IonScore (Identity / homology threshold) <sup>a)</sup>	E value <sup>a)</sup>	% Coverage <sup>b)</sup>	Secreted <sup>c)</sup>
Pathogenesis-related protein PRB1-2 Precursor pathogenesis-related protein, <i>Hordeum vulgare</i> subsp. <i>vulgare</i>	P35792	1. K.LQAFANQYANQR.I 2. R.SAVGVGAVSWSTK.L 3. K.LQHSGGPYGENIFWGSAGADWK.A	32/18.0	1. 87(55/46) 2. 102(55/49) 3. 109(54/36)	5e <sup>-27</sup>	49%	S
Pathogenesis-related protein PRB1-3, <i>Hordeum vulgare</i> subsp. <i>vulgare</i>	P35793	4. R.GVFITCNYEPR.G 5. K.AADAVNSWVNEK.K 6. K.VCGHYTQVVWR.A		4. 63(55/48) 5. 84(55/-) 6. 80(55/-)	4e <sup>-26</sup>		
Pathogenesis-related protein, <i>Triticum aestivum</i>	ACQ41879	1. R.AAVGVGAVSWSTKLQAYAQSYANQR.I 2. K.LQAYAQSYANQR.I	30/17.8	1. 73(53/35) 2. 102(55/46)	2e <sup>-40</sup>	48%	S
PR-1a pathogenesis related protein (Hv- 1a), <i>Hordeum vulgare</i> subsp. <i>vulgare</i>	CAA52893	3. R.AAVGVGAVSWSTK.L 4. K.LQHSGGPYGENIFWGSAGADWK.A 5. K.LWVDEKKDYDGSNTCAGGK.V 6. K.VCGHYTQVVWR.A		3. 90(55/49) 4. 109(54/36) 5. 52(54/24) 6. 80(55/-)	9e <sup>-38</sup>		
$\beta$ -1,3-glucanase precursor, <i>Triticum aestivum</i>	AAD28734	1. K.RSGAIEAYVFAMFNEDR.K 2. R.SAAVAWVQTNVQAHQGLNIK.Y	30/34.6	1. 18(54/40) 2. 120(54/39)	1e <sup>-25</sup>	28%	S
$\beta$ -1,3-glucanase 2a, <i>Hordeum vulgare</i>	AAU11328	3. K.YIAAGNEVGQGGDTGNLPAMQNLDAAALAAAGLGGIK.V 4. K.HFGLFNPDKSPAYPISF.- 5. K.RSGAIEAYVFAMFNEDR.K 6. R.SGAIEAYVFAMFNEDRK.G 7. R.SGAIEAYVFAMFNEDR.K 8. K.HFGLFNPDK.S		3. 81(52/20) 4. 87(53/35) 5. 48(54/33) 6. 17(54/28) 7. 103(55/38) 8. 47(56/44)	5e <sup>-20</sup>		
Basic pathogenesis-related protein PR5, <i>Hordeum vulgare</i> subsp. <i>vulgare</i>	CAA04642	1. R.LDPGQSWALNMPAGTAGAR.V 2. R.CSYTVWPGALPGGGVR.L	30/24.6	1. 101(55/39) 2. 46(55/35)	3e <sup>-20</sup>	36%	S
Thaumatococin-like protein TLP6, <i>Hordeum vulgare</i>	AAK55324	3. K.ELQVPGGCASACGK.F 4. R.CITGDCNGVLACR.V 5. R.LDPGQSWALNMPAGTAGAR.V 6. R.VSGQQPTTLAEYTLGQGANK.D		3. 73(55/39) 4. 81(55/35) 5. 118(54/40) 6. 109(54/39)	3e <sup>-20</sup>		
Hypothetical protein, <i>Hordeum vulgare</i>	CAA74594	1. K.QVLSDASTFIWNTFNQR.A	30/24.3	1. 100(54/36)	1e <sup>-17</sup>	34%	S
Hypothetical protein, <i>Sorghum bicolor</i>	XP_002467026	2. R.GTANGGLIEGIADYVR.L 3. K.SGYSDDFFAQILGK.N 4. R.FLDYCDLMPGFVAQLNAK.M 5. R.FDNAVGLAYSK.Q		2. 85(55/-) 3. 81(56/32) 4. 87(54/35) 5. 66(55/39)	2e <sup>-16</sup>		

**Table 3.6 continued**

Protein identified (Figure 3.9)	Accession	Identified peptides	Observed /theoretical MW (kDa)	IonScore (Identity / homology threshold) <sup>a)</sup>	E value <sup>a)</sup>	% Coverage <sup>b)</sup>	Secreted <sup>c)</sup>
Peroxidase, <i>Hordeum vulgare</i> Predicted protein, <i>Hordeum vulgare</i> subsp. <i>vulgare</i>	AAA32972 BAJ92911	1. R.DSVVALGGPSWTVPLGR.R	30/33.4	1. 57(54/38)	1e <sup>-22</sup>	24%	S
		2. R.NFASNPAAFSSAFTTAMIK.M		2. 82(54/35)			
		3. R.GFGVIDSIK.T		3. 46(56/53)			
		4. R.IYGGDTNINTAYAASLR.A		4. 120(55/43)			
		5. K.QTVSCADILTVAAR.D		5. 99(55/54)			
		6. R.NFASNPAAFSSAFTTAMIK.M		6. 77(54/40)			
Root peroxidase, <i>Triticum aestivum</i> Root peroxidase, <i>Triticum aestivum</i>	ACF70705 ACF70710	1. K.NLNTVDMVALSGAHTIGK.A	30/33	1. 98(54/48)	4e <sup>-16</sup>	25%	S
		2. R.DSVVALGGPSWTVPLGR.R		2. 57(54/38)			
		3. R.GFGVIDSIK.T		3. 46(56/53)			
		4. R.DSTTASAALANSIDLPGGSSR.S		4. 71(55/38)			
		5. K.QTVSCADILTVAAR.D		5. 99(55/54)			

**a)** The ion scores for each of the matched peptides and the cut off score for being considered as having extensive homology are shown in the brackets.

**b)** The percent coverage of the matched protein by the LC-eSI-IT MS derived *de novo* peptide sequences.

**c)** Signal peptide sequence predicted by SignalP ([http:// www.cbs.dtu.dk/services/SignalP/](http://www.cbs.dtu.dk/services/SignalP/)).



2DGE analysis was then used to investigate the presence of *Ptt* proteinaceous toxin in ICWF protein of infected and uninfected plants. Analysis showed differences between ICWF profiles (Figure 3.10) with two spots at 25 kDa (pI 5 and 5.5 respectively) only present in the profile for the protein mixtures extracted from infected plants (Figure 3.10A). LC-eSI-IT MS analysis of the two spots identified peptides matched to four proteins in *Hordeum vulgare* subsp. *vulgare* and *Aegilops speltoides*. However, *Ptt* toxins were not identified (Table 3.7).

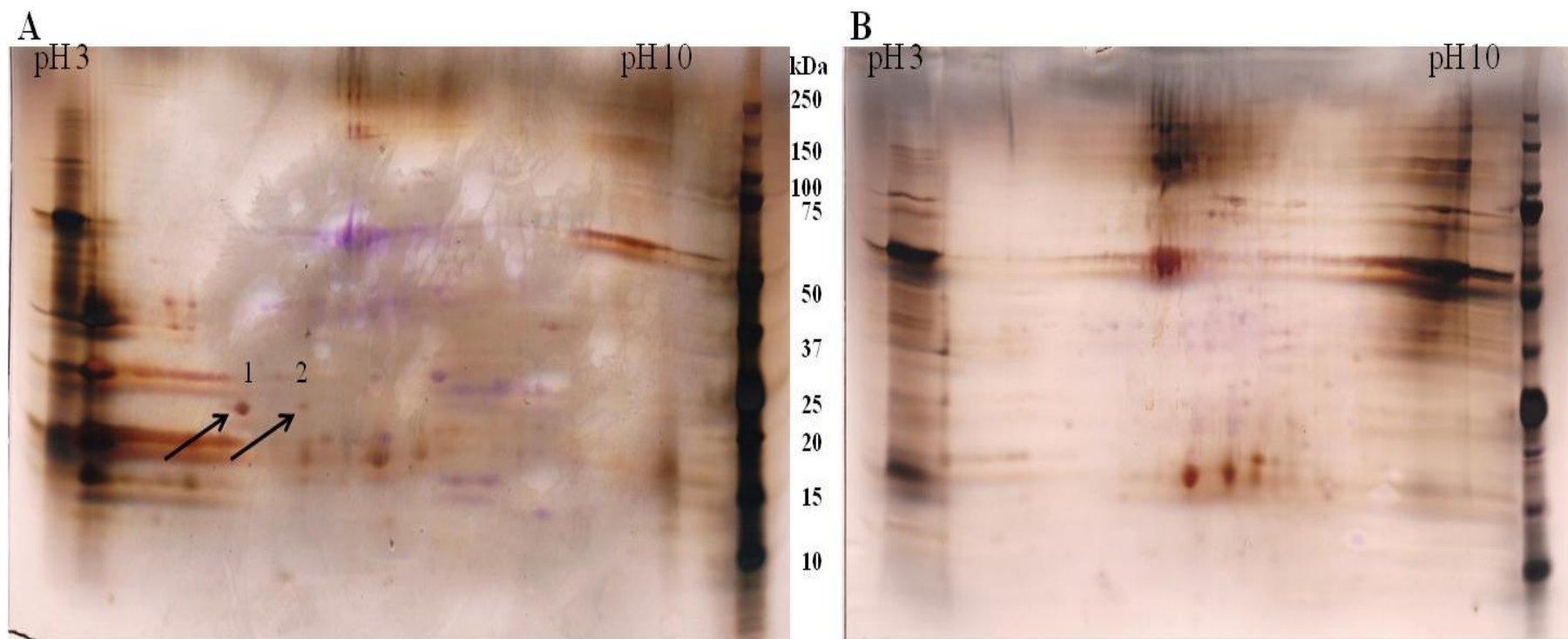


**Figure 3.10. 2DGE comparison of protein profiles of ICWFs from infected and uninfected plants.** Eighty seven  $\mu\text{g}$  (maximum total protein obtained) was loaded, protein extracted from ICWFs of Sloop inoculated with 32/98 isolate after 9 day post inoculation (A), uninfected leaves after 9 dpi (B), Precision Plus Protein Standard (Lad) was used as marker ladder. Gels were stained with CBB R250 and EBT, arrows indicate the two spots which present in infected leaf but not in uninfected, these spots were analysed using LC-eSI-IT MS (Table 3.7). Representative image for three technical replicates.

**Table 3.7. Protein identification of 2DGE comparison of ICWFs from infected and uninfected leaves after 9 dpi (Figure 3.10).** LCI-SI-S/MS and MASCOT was used for searches, two unique spots present in the protein mixture of the ICWF of the more virulent isolate were selected and analysed. Two accession numbers for each protein represent the most similarity to the plant species.

Spot number (Figure 3.10)	Protein identified	Accession	Identified peptides	Observed/ theoretical MW (kDa)	Observed/ theoretical pI <sup>a)</sup>	IonScore (Identity / homology threshold) <sup>b)</sup>	E value <sup>b)</sup>	% Cover-age <sup>c)</sup>	Secreted <sup>d)</sup>
Spot 1	Predicted protein, <i>Hordeum vulgare</i> subsp. <i>Vulgare</i>	BAJ90550	1. K.LPMFGCTDATQVLNEVEEVKK.E	24/19.7	6.5/9	1. 15(41/19)	2e <sup>-12</sup>	26%	NO
			2. K.VGFIFR.E			2. 43(41/40)			
	Predicted protein, <i>Hordeum vulgare</i> subsp. <i>vulgare</i>	BAJ89884	3. R.IIGFDNMR.Q			3. 30(42/35)	9e <sup>-12</sup>		
			4. R.SKWVPCLEFSK.V			4. 20(43/21)			
Spot 2	Ribulose-1,5-bisphosphate carboxylase/oxygenase, <i>Aegilops speltoides</i>	BAA35147	1. K.LPMFGCTDATQVLNEVEEVKK.E	24/19.7	6.5/9	1. 15(41/19)	7e <sup>-07</sup>	22%	NO
			2. K.VGFVFR.E			2. 37(41/37)			
	Ribulose bisphosphate carboxylase, <i>Brachypodium distachyon</i>	XP_003573911	3. R.SKWVPCLEFSK.V			3. 20(43/21)	8e <sup>-07</sup>		
Spot 2	Ribulose-1,5-bisphosphate carboxylase/oxygenase small subunit, <i>Aegilops sharonensis</i>	BAA35169	1. K.LPMFGCTDATQVLNEVEEVKK.E	25/19.7	7/9	1. 24(41/22)	5e <sup>-07</sup>	52%	NO
			2. K.VGFIFREHNASPGYYDGR.Y			2. 22(42/19)			
			3. K.QVDYLIR.S			3. 44(44/-)			
	Ribulose-1,5-bisphosphate carboxylase/oxygenase small subunit, <i>Aegilops sharonensis</i>	BAA35170	4. K.VGFIFR.E			4. 38(41/38)	5e <sup>-07</sup>		
			5. R.IIGFDNMR.Q			5. 47(42/-)			
			6. R.IIGFDNMR.Q			6. 18(43/30)			
			7. R.SKWVPCLEFSK.V			7. 38(43/36)			
			8. K.FETLSYLPPLSTEALLK.Q			8. 11(42/19)			
			9. K.EYPDAYVR.I			9. 23(43/30)			
			10. K.KFETLSYLPPLSTEALLK.Q			10. 11(42/22)			
Ribulose-1,5-bisphosphate carboxylase/oxygenase small subunit, <i>Aegilops speltoides</i>	BAA35147	1. K.LPMFGCTDATQVLNEVEEVKK.E	25/19.8	7/9	1. 24(41/22)	4e <sup>-07</sup>	41%	NO	
		2. K.QVDYLIR.S			2. 44(44/-)				
		3. K.VGFVFR.E			3. 43(41/40)				
Hypothetical protein, <i>Secale cereale</i>	CAA10496	4. R.SKWVPCLEFSK.V			4. 38(43/36)	6e <sup>-07</sup>			
		5. K.FETLSYLPPLSTEALLK.Q			5. 11(42/19)				
		6. K.KFETLSYLPPLSTEALLK.Q			6. 11(42/22)				
		7. K.EYPDAYVR.V			7. 23(43/30)				

**a)** The predicted molecular weight (MW) and isoelectric point (pI) of the matched protein based on the values provided in the MASCOT summary report.

**b)** The ion scores for each of the matched peptides and the cut off score for being considered as having extensive homology are shown in the brackets.

**c)** The percent coverage of the matched protein by the LC-eSI-IT MS derived *de novo* peptide sequences.

**d)** Signal peptide sequence predicted by SignalP ([http:// www.cbs.dtu.dk/services/SignalP/](http://www.cbs.dtu.dk/services/SignalP/)).

### 3.4 Discussion

Although protein mixtures from culture filtrates have been previously shown to induce symptoms on a susceptible barley cultivar (chapter 2) (Sarpeleh *et al.*, 2007; Sarpeleh *et al.*, 2008), the individual proteins responsible for toxic activity are not known. The research presented in this chapter therefore aimed to identify potential candidates for further characterisation. Several candidates were identified by looking at protein profiles and comparing the biological activity of fractions and sub-fractions of the proteins extracted from the culture filtrates of *Ptt*. The same protein fraction containing proteins from 37 to 150 kDa was biologically active regardless of the virulence of the isolate. Candidates were also identified as differentially expressed between the more and less virulent isolates. A number of these proteins appeared to be cell wall degradation enzymes but most were conserved hypothetical proteins with unknown functions.

Results in this chapter confirmed chapter 2 results that regardless of the virulence of the *Ptt* isolate, necrosis was induced by the same protein fraction from culture filtrates on a susceptible cultivar. The MW of biologically active fractions of proteinaceous toxins was between 37 and 150 kDa. Similarly, Sarpeleh *et al.* (2008) found that the MW of *Ptt* biologically active proteinaceous toxins appeared bigger than 30 kDa. Interestingly, the proteins in the active fractions from both isolates (32/98 and 08/08f) were of a similar MW and size (37 to 150 kDa) yet when the protein profile was compared only proteins at 25 kDa were identified as unique in the more virulent isolate. This may suggest other candidate

proteins might be present outside of the range of 37 to 150 kDa but that they might be at lower concentrations not able to be detected.

The susceptible cv. Sloop was sensitive to fractions 4, 5, 6, 9 and 10 (Figure 3.3) and sub-fractions (4/2, 4/3 and 4/4) compared with the resistant cultivars CI9214 and Beecher (Figure 3.4). Necrosis was also induced by fractions 9 and 10 even though their protein concentration was less than 1 µg per mL and difficult to visualise on a gel (Figure 3.5). Necrosis though can be induced at very low toxin concentrations. Sarpeleh *et al.* (2007) demonstrated that 0.2 µg of proteins extracted from *Ptt* induced symptoms in barley leaf, while Kim and Strelkov (2007) demonstrated that chlorosis was induced in wheat leaves with 33 pg of ToxB from *Ptr*. In addition, sub-fraction 4/4 induced necrosis only in cv. Sloop, suggesting that this sub-fraction might contain candidate effectors. The same response to *Ptt* proteinaceous toxin was reported for Sloop and CI9214 (Sarpeleh *et al.*, 2007), thus indicating that these fractions may contain host selective proteinaceous toxins that might interact with target proteins in the host. These target/s might only be available in the sensitive cultivar and/or internalised to their location in sensitive plants as has been shown for *Ptr* ToxA in the *Ptr*-wheat interaction (Manning and Ciuffetti, 2005; Manning *et al.*, 2007). In addition, the host target of the proteinaceous toxin could be different between cultivars in availability, quantity and type (Sarpeleh *et al.*, 2008). CI9214 responded to fraction 3 but other cultivars did not, suggesting that CI9214 might contain specific target/s to protein/s in this fraction. However, the specificity of targets needs to be confirmed in these cultivars.

PAGE analysis of the ICWFs, mitochondria and chloroplast cell components revealed a 37 kDa protein in each of the fungal fraction and ICWFs. 2DGE analysis revealed 24 kDa and 25 kDa proteins unique to the infected plant. However, no *Ptt* protein was detected in ICWFs profile of infected plants. Analysis of the unique spot from the 2DGE of ICWFs revealed the peptides were likely to be from the plant protein ribulose biphosphate carboxylase oxygenase (RUBISCO), while the proteins identified in the 30-35 kDa band on PAGE were likely to be PR proteins. Similarly, Sarpeleh (2007) found PR proteins were expressed in ICWFs of Sloop 48 hpi with *Ptt*. Even though, *Ptt* toxins were not detected, they might be at an undetectable level especially given that low quantity of toxins (even undetectable) was required to induce symptoms (Kim and Strelkov, 2007; Sarpeleh *et al.*, 2007). Alternatively, toxins might be present in other bands or spots which were not analysed, or they might have been internalised into the cell (Manning and Ciuffetti, 2005; Manning *et al.*, 2007). However, *Ptt* or many plant proteins were not detected in the chloroplast and mitochondria protein profile from a *Ptt*-infected plant suggesting that a higher quantity of protein is required for visualisation. Several PR proteins from barley were detected in ICWFs during the *Ptt*-barley interaction including glucanase, chitinase, peroxidase, PRB1-2, PRB1-3 and PR5. PRs are induced in response to pathogen attack (Kristensen *et al.*, 1999; Muthukrishnan *et al.*, 2001; Santén *et al.*, 2005; ScottCraig *et al.*, 1995). For example, a PR-1 protein accumulates in the outer cell wall layer and cytoplasm of primary hyphae of *Bipolaris sorokiniana* after invasion of barley (Santén *et al.*, 2005). Different functions have been suggested for

PR-1 including defence and/or as a senescence-related protein (Santén *et al.*, 2005), restricting fungal invasion (Benhamou *et al.*, 1991) and intercellular antimicrobial activity (Santén *et al.*, 2005; Van Loon, 1997). PR-2 has been reported as having an endo  $\beta$ -1,3-glucanase activity (Kauffmann *et al.*, 1987) while PR-3 has endochitinase activity (Legrand *et al.*, 1987). These glucanases and chitinases degrade (hydrolyse) the fungal cell wall (Adams, 2004) which mostly contain  $\beta$ -1,3-glucans or chitin (Bartnick, 1968). Peroxidase has been identified in barley leaf infected with *Blumeria graminis* (*Erysiphe graminis* f. sp. *hordei*), the casual agent of powdery mildew, after 24 hpi (Kristensen *et al.*, 1999; ScottCraig *et al.*, 1995).

As previously described a number of candidates were identified using LC-eSI-IT MS. Peptides were matched to proteins with theoretical MWs of between 15 and 64 kDa. Similarly, Sarpeleh *et al.* (2007) found that symptom induction was associated with fractions containing proteinaceous metabolites ranging between 20 and 100 kDa in *P. teres*. Seventeen candidates were identified in the culture filtrates of *Ptt*, all of them were annotated as conserved hypothetical proteins in *Ptt* database. However, these identified peptides matched to proteins in *P. teres-repentis* database that had been annotated as likely to have hydrolase, lactonase, peptidase or phosphatase activity (Table 3.8). The majority of identified proteins are likely to be hydrolase enzymes (Table 3.8) with them sharing similarity with endo-1, 4- $\beta$ -xylanase I precursor, glycoside hydrolase family 11 (GH11); glucan 1,3- $\beta$ -glucosidase precursor and GPI-anchored cell wall  $\beta$ -1,3-endoglucanase, GH17 family; or isochorismatase, cysteine hydrolase family. Other proteins included 6-phosphogluconolactonase, lactonase

family; carboxypeptidase S1, peptidase family; repressible acid phosphatase, histidine phosphatase superfamily; and a GPI anchored CFEM domain containing protein family. Most of the proteins were identified in more than one protein profile as summarised in Table 3.8. The frequent presence of these proteins suggested possible involvement in symptom induction.

Most of the candidates seem to have known function in fungal development or plant-pathogen interaction (Table 3.8) by affecting the cell wall or defence response. The analysis of the gene content of the *Ptt* genome assembly predicted the function of *Ptt* secreted proteins such as: mycelium development, 23 genes; pathogenesis, 9 genes; cell wall catabolic process, 6 genes; and protein modification process, 5 genes (Ellwood *et al.*, 2010). Xylanase is clearly involved in the metabolism of xylan in the plant cell wall (Beg *et al.*, 2001; Beliën *et al.*, 2006; Hartl *et al.*, 2011; Walton, 1994), suggesting a potential role in *Ptt* virulence. This virulence role has been well established for endoxylanase in *Cochliobolus carbonum* (Apel *et al.*, 1993; ApelBirkhold and Walton, 1996), *Sclerotinia sclerotiorum* (Ellouze *et al.*, 2011) and other fungi (Beliën *et al.*, 2006).



**Table 3.8. The most dominant proteins as identified in the biologically active protein profiles and their accession number, source, family and proposed function.**

Protein name	Code for selected protein	Accession number	Source of peptide	Protein family	Proposed function	Reference
<b>*Endo-1, 4-<math>\beta</math>-xylanase</b>	<b>PttXyn11A</b>	1. XP_001941158 2. XP_001939205 3. XP_001939862	1. 2DGE of 32/98 isolate (Table 3.5) 2. Active fraction 4, 32/98 isolate (Table 3.1) 3. Active fraction 4 and sub-fraction 4/2 of 32/98 isolate (Table 3.3)	Glycoside hydrolase family 11 (GH11)	Cell wall degradation	(Beg <i>et al.</i> , 2001; Beliën <i>et al.</i> , 2006; Tamano <i>et al.</i> , 2007; Walton, 1994)
<b>*Conserved hypothetical protein</b>	<b>PttSP1</b>	XP_003296828	1. Bands 3, 4 and 6 of active fraction of 08/08f (Table 3.1) 2. 2DGE of 32/98 isolate (Table 3.5)	Unknown	Unknown	-
<b>*Isochorismatase</b>	<b>PttCHFP1</b>	XP_001932705	1. 2DGE of 32/98 isolate (Table 3.5) 2. Active fraction number 4 (Table 3.4)	Cysteine hydrolase family	Host-pathogen interactions as phytotoxins or elicitors of plant defence responses, inhibits salicylic acid formation	(El-Bebany <i>et al.</i> , 2010; Keates <i>et al.</i> , 2003; Maruyama and Hamano, 2009; Rohe <i>et al.</i> , 1995)
<b>*GPI anchored CFEM domain containing protein</b>	<b>PttGPI-CFEM</b>	XP_001931262	1. Active fraction 4 (Table 3.4) 2. Active sub-fraction 4/2 (Table 3.4)	CFEM domain containing protein family	Cell adhesion (an important role in pathogenesis)	(DeZwaan <i>et al.</i> , 1999; Kershaw and Talbot, 1998; Kulkarni <i>et al.</i> , 2003)
<b>Glucan 1,3-<math>\beta</math>-glucosidase precursor</b>	-	XP_001931233	1. Active fraction 4 of 08/08f isolate (Table 3.1) 2. Active fraction 4 (Table 3.3) 3. Active sub-fraction 4/2 of 32/98 isolate (Table 3.3)	GH5 family	Cell wall degradation	(Beg <i>et al.</i> , 2001; Beliën <i>et al.</i> , 2006; Boonvitthya <i>et al.</i> , 2012; Tamano <i>et al.</i> , 2007; Walton, 1994)
<b>GPI-anchored cell wall <math>\beta</math>-1,3-endoglucanase</b>	-	XP_001934358	Active fraction 5 of 08/08f isolate (Table 3.1)	GH16 family	Cell wall construction and essential for cell separation in yeasts	(Baladrón <i>et al.</i> , 2002; Hartl <i>et al.</i> , 2011)
<b>6-phosphogluconolactonase</b>	-	XP_001938663	Active fraction 4, 32/98 isolate (Table 3.1)	Lactonase family	Mycelium development of <i>Magnaporthe oryzae</i>	(Gowda <i>et al.</i> , 2006)
<b>Carboxypeptidase S1</b>		XP_001932743 XP_001936980	Active fraction 4, 32/98 isolate (Table 3.4)	Peptidase family	Entomopathogen pathogenicity	(Stleger <i>et al.</i> , 1994)
<b>Repressible acid phosphatase</b>		XP_001937694	Active fraction 4, 32/98 isolate (Table 3.4)	Histidine phosphatase superfamily	Hydrolase, metabolism	(Kennedy <i>et al.</i> , 2005)
<b>Conserved hypothetical proteins (8)</b>		See Table 3.3 and Table 3.4	Active fraction 4 and sub-fraction 4/2 (Table 3.3 and Table 3.4)	Unknown	Unknown	-

\* Proteins were selected for further characterisation.

Glucan 1,3- $\beta$ -glucosidase (or  $\beta$ -1,3-endoglucanases), which affects cell wall  $\beta$ -1,3-glucan has been isolated and fully characterised in *Aspergillus oryzae* (Boonvitthya *et al.*, 2012; Chambers *et al.*, 1993; Tamano *et al.*, 2007).  $\beta$ -1,3-endoglucanase probably plays a role during germination and branching of hyphae by partially degrading the cell wall in order to obtain the required plasticity (Adams, 2004; Baladrón *et al.*, 2002; Martin-Cuadrado *et al.*, 2003). GPI-anchored cell wall  $\beta$ -endoglucanase has also been identified in the culture filtrates of *Leptosphaeria maculans* and *Aspergillus fumigatus* (Hartl *et al.*, 2011; Vincent *et al.*, 2009). This protein has been suggested to be unique to filamentous fungi (Hartl *et al.*, 2011) and probably affects fungal development by remodeling the cell wall structure through modification of cell wall  $\beta$ -glucan (Cabib *et al.*, 2007; Mouyna *et al.*, 2000). In addition,  $\beta$ -endoglucanases might have a role in the induction of the defence response of programmed cell death by allowing the release of elicitors from the cell wall (Okinaka *et al.*, 1995). Able (2003) demonstrated that reactive oxygen species (ROS), which have been implicated in the initiation of the hypersensitive reaction (Able *et al.*, 1998; 2000; Levine *et al.*, 1994), were produced in larger quantities during the barley-*R. commune* and barley-*P. teres* interactions in the susceptible response of barley leaves to these necrotrophic pathogens. In the biotrophic interactions between soybean and *Phytophthora megasperma* f. sp. *glycinea* (Okinaka *et al.*, 1995), and between wheat and leaf rust (*Puccinia recondita* f. sp. *tritici*) (Anguelova-Merhar *et al.*, 2001; Anguelova *et al.*, 1999), the hypersensitive reaction was associated with high levels of  $\beta$ -1,3-glucanase.

Isochorismatase has been identified in five plant pathogenic Ascomycetes including *B. cinerea*, *Gibberella zeae*, *Magnaporthe grisea*, *S. sclerotiorum* and *S. nodorum* (Soanes *et al.*, 2008) and has been suggested to have a role in the inhibition of plant defence systems (El-Bebany *et al.*, 2010; Kunkel and Brooks, 2002; Maruyama and Hamano, 2009; Soanes *et al.*, 2008; Wildermuth *et al.*, 2001). Thus, suggesting a similar role during the interaction of *Ptt* with barley.

The GPI-anchored CFEM domain-containing protein which is also cysteine rich has been linked to cell adhesion (Kershaw and Talbot, 1998; Kulkarni *et al.*, 2003) and might have a role in pathogenesis (DeZwaan *et al.*, 1999). 6-phosphogluconolactonase hydrolyses 6-phosphogluconolactone to 6-phosphogluconate and has been shown to be involved in the pentose phosphate pathway, a process that generates NADPH and pentoses (Stanford *et al.*, 2004), and necessary for mycelium development of *Magnaporthe oryzae* (Gowda *et al.*, 2006). However, nine conserved hypothetical proteins have been identified and they have not been annotated in any database, suggesting that they might have a unique role, previously not described, in symptom induction, virulence and or fungal development.

Four candidate proteins were selected for further characterisation based upon the biological activity of the corresponding protein fraction or sub-fraction, the frequency of presence in these profiles and the annotated function of the corresponding identified proteins (Table 3.8). *Ptt* conserved hypothetical proteins, XP\_003303790, XP\_003306630, XP\_003296828 and XP\_003295367

were highly similar to proteins annotated in *Ptr* as isochorismatase (XP\_001932705), endo-1,4- $\beta$ -xylanase A (XP\_001941158), conserved hypothetical protein (XP\_001933504) and GPI-anchored CFEM-domain containing protein (XP\_001931262) respectively. The xylanase and isochorismatase were selected as they were also present in the 2DGE profile of the more virulent isolate (32/98) (and not in the less virulent isolate, 08/08f). The conserved hypothetical protein (XP\_003296828) was identified in the active profiles of both the less and more virulent isolates and in the 2DGE of the more virulent isolate. The GPI-anchored CFEM domain-containing protein was also identified in the active fraction and sub-fraction. The results presented in later chapters detail the characterisation of these four candidate proteins.

## **Chapter 4 Isolation, characterisation and cloning of cDNA encoding for virulence-related candidate proteins (VRCPs) from *Pyrenophora teres f. teres (Ptt)***

### **4.1 Introduction**

Proteinaceous metabolites from *Ptt* culture filtrates induce brown necrotic lesions on barley with similarity to those that occur in natural infection by *Ptt* (chapter 2). These culture filtrates have also been shown to induce symptoms on susceptible barley cultivars, but not in wheat, triticale, rye and faba bean, in a light dependent manner (Sarpeleh *et al.*, 2008). Although Sarpeleh *et al.* (2007) found that the active proteins appeared bigger than 30 kDa, the diversity and the characteristic of these toxins was unknown (Liu *et al.*, 2011). The research presented in the previous chapter identified a number of candidate proteins (Table 3.8) for virulence or that might contribute to fungal growth *in planta*. Four proteins, previously suggested to be related to pathogenicity in other fungi (Table 3.8) were chosen: conserved hypothetical proteins in *Ptt* annotated in *P. tritici-repentis* as an endo-1, 4- $\beta$ - xylanase 11A, an isochorismatase, a GPI-anchored CFEM domain-containing protein and an unknown hypothetical protein. The full length of the cDNA needed to be isolated and analysed so that they might be correctly annotated in *Ptt*.

Protein bioinformatics, based on domain identification, phylogenetic analysis, secondary protein structure and three dimensional protein structure analyses, are important tools to identify protein characteristics and to predict the biological function (Xiong, 2006). This information provides reliable and relevant data to predict the nature of host–pathogen interactions and whether

one of the biological functions might be related to pathogenesis and the host (Bhadauria *et al.*, 2007). Due to the limited research characterising proteinaceous toxins/virulence factors in *Ptt*, bioinformatics analysis of the candidate proteins was used to identify the potential shared domains with already characterised proteins.

Several proteins have been identified as having a role in fungal pathogenesis including the necrosis-inducing toxin PtrToxA and the chlorosis-inducing toxin PtrToxB in *P. tritici-repentis* (Ciuffetti *et al.*, 2010; Ciuffetti and Tuori, 1999); proteinaceous host specific toxins (effectors) including; SnTox1, SnTox2, SnTox3 and SnTox4 in *Stagonospora nodorum* (Liu *et al.*, 2006); and hydrolytic enzymes that have a critical role in cell wall degradation (Gomez-Gomez *et al.*, 2001; Horbach *et al.*, 2011; Kikot *et al.*, 2009) such as endoxylanase. This enzyme has been considered essential for the infection of various plant pathogenic fungi (Jarozuk-Scisel and Kurek, 2012; Kikot *et al.*, 2009; Wu *et al.*, 1997) and has been identified in many fungal species including *Fusarium* spp. (Jarozuk-Scisel and Kurek, 2012), various formae speciales of the vascular wilt fungus *Fusarium oxysporum* (Alconada and Martinez, 1994; Gomez-Gomez *et al.*, 2001; Gomez-Gomez *et al.*, 2002; Jorge *et al.*, 2005; Ruiz-Roldan *et al.*, 1999; Ruiz *et al.*, 1997), *Cochliobolus carbonum* (Apel *et al.*, 1993), *Botrytis cinerea* (Brito *et al.*, 2006), and *Sclerotinia sclerotiorum* (Ellouze *et al.*, 2011). However, xylanase has not been previously identified in *Ptt*.

This study has also identified two proteins, an isochorismatase and a GPI-anchored CFEM domain-containing protein. Initial analysis showed that GPI-anchored CFEM domain-containing protein was rich in cysteine and might also play a role in virulence or host specificity. Cysteine-rich proteins with no known enzymatic activity are also often important in some host-pathogen interactions as phytotoxins or elicitors of plant defence responses (Keates *et al.*, 2003; Rohe *et al.*, 1995). Isochorismatase has been identified in five plant pathogenic Ascomycetes including *B. cinerea*, *Gibberella zaeae*, *Magnaporthe grisea*, *S. sclerotiorum* and *S. nodorum*, but not in non-pathogenic Ascomycetes (Soanes *et al.*, 2008). Similarly, the protein with similarity to a glycosylphosphatidylinositol (GPI)-anchored protein from *P. tritici-repentis* (Table 3.8) contains a CFEM (common in several fungal extracellular membrane) domain which is also cysteine rich but has been linked to cell adhesion (Kershaw and Talbot, 1998; Kulkarni *et al.*, 2003), and has been proposed to play an important role in pathogenesis (DeZwaan *et al.*, 1999). GPIs are often found in fungal proteins (Hartl *et al.*, 2011; Mouyna *et al.*, 2000) while the CFEM domain is common in several fungal extracellular membrane proteins (De Groot *et al.*, 2005). However, neither cysteine hydrolase family proteins nor GPI-anchored proteins have been reported in *Ptt* yet.

According to the previous research on similar proteins, the four candidates appear to be associated with virulence but whether they are produced by *Ptt* during the interaction with barley and have a potential role in symptom development is not known. Therefore, the aims of the research

presented in this chapter were to isolate the full length of the open reading frame of the cDNA for the endoxylanase (named PttXyn11A), the cysteine hydrolase family protein member isochorismatase (named PttCHFP1), the GPI-anchored CFEM domain-containing protein (named PttCFEM-GPI) and the conserved hypothetical protein (which because it is a secreted protein was named PttSP1), to analyse the possible functions of these candidates using bioinformatics and to investigate the probable presence of these proteins during the interaction by using semi-quantitative RT-PCR to detect their gene expression *in planta*.

## **4.2 Materials and methods**

### **4.2.1 Isolation of the full length of cDNA for virulence-related candidate gene transcripts (VRCGs)**

#### **4.2.1.1 Culturing the isolate**

The isolate 32/98 was provided by the South Australian Research and Development Institute (SARDI) (Table 2.1). Single spore colony was obtained as per section 2.2.2 and grown in FCM without trace elements as per section 2.2.6.1 for 10 days or 23 days at RT without shaking.

#### **4.2.1.2 Primer design**

Full lengths of VRCGs were isolated using the full length of the best hit for identified peptides in BLASTp at NCBI (section 3.2.5.3) in the *Ptt* database. Forward and reverse primers were designed for the *Ptt* sequence to amplify the open reading frame of identified genes from cDNA (Table 4.1); *PttXyn11A*, *PttCHFP1*, *PttGPI-CFEM* and *PttSPI*. The partial length of *PttGAPDH* was



used as an endogenous control for semi-quantitative RT-PCR (Wong, 2010). NetPrimer (Primer Analysis Software, PREMIER Biosoft. <http://www.premierbiosoft.com/netprimer/>) was used for analysing primers with recommended parameters. Annealing temperature was evaluated for each set of primers.

**Table 4.1. List of primers used in full length isolation and semi-quantitative RT-PCR to amplify the cDNA of the VRCGs *PttXyn11A*, *PttCHFPI*, *PttSP1*, *PttGPI-CFEM* and *PttGAPDH*.** Gene name, accession numbers, forward (FW) and reverse (RV) primers, annealing temperature (TM) and product length are indicated.

Genes	Accession number	Sequences of the primers 5'→3'	TM (°C)	Product length (bp)
<b>PttXyn11A</b>	XP_003306630	FW: ATGGTTGCCTTCTCTACTATCCTC	55	696 bp
		RV: TTAAGAGCTGCTGACAGTGATGG	55	
<b>PttCHFPI</b>	XP_003303790	FW: ATGAAGCTCGCTGCGCCCAT	54	906 bp
		RV: CTAGGAGAGTGCGGGTATGAT	54	
<b>PttSP1</b>	XP_003296828	FW: ATGCGCGCCTCAATCATCATC	55	537 bp
		RV: CTAGCAGTAATCGCCAATGTTGTAG	55	
<b>PttGPI-CFEM</b>	XP_003295367	FW: ATGAAGAGCTTCACCATCGC	54	624 bp
		RV: TTACAAGACGAGCATGGCAAG	54	
<b>PttGAPDH</b>	EF513236	FW: GGTC AATGGCAAGACCATCCGCTTC	55	156 bp
		RV: ACGACCTTCTTGGCTCCACCCTTC	55	

#### 4.2.1.3 RNA extraction, quantification and DNase treatment

Mycelium was harvested, obtained from culture grown as per section 4.2.1.1, after 10 days or 23 days and ground in liquid nitrogen using mortar and pestle. Total RNA was extracted using TriPure Isolation Reagent (Roche Applied Science, USA), following the manufacturer's protocol. The concentration of RNA was measured using a NanoDrop ND-100 Spectrophotometer (NanoDrop Technologies, USA) and quality of RNA was determined by gel electrophoresis. RNA samples (3 µg) were mixed with the desired amount of 6× Ficoll loading buffer (1 µL for every 5 µL RNA) before being loaded into a

horizontal 1% agarose gel (w/v) amended with ethidium bromide (0.5 µg/mL). Five µL of 1 Kb Plus DNA Ladder (Invitrogen, USA) was loaded as a molecular weight marker. The gels were run at 200 V for 33 min in 1 × Tris-acetate-EDTA (TAE) buffer. RNA quality was visualised using a UVP First Light UV Illuminator (BioDoc-It™ Imaging system, USA). RNA samples from *Ptt* mycelium grown for 23 days were discarded due to a high level of RNA degradation (data not shown). RNA from mycelium of 10 day old cultures was treated with RQ1 RNase-Free DNase (Promega, USA) following the manufacturer's protocol to remove any DNA contamination.

#### **4.2.1.4 Isolation of the full length of VRCGs**

cDNA was synthesised using SuperScript III First-Strand Synthesis System (Invitrogen, Life Technology) with an oligo (dT)<sub>12-18</sub> primer, according to the manufacturer's instructions, 70 ng cDNA template was used in RT-PCR reactions. RT-PCR amplification conditions were conducted under the following conditions: 95°C for 2 min, and 40 cycles of 15 s at 95°C and 30 sec at 55°C and 1 min at 70°C for *PttXyn11A*; 40 cycles for *PttSP1*; 40 cycles of 15 sec at 95°C and 30 sec at 54°C for *PttCHFPI* and *PttGPI-CFEM*, and last extension was 10 min at 70°C for all genes using a Bio-Rad thermocycler (DNA Engine, Dyad, Peltier thermal cycler). PCR amplicons were visualised on an agarose gel as per section 4.2.1.3.

#### **4.2.1.5 cDNA extraction from agarose gel and confirmation of sequences**

PCR amplicons were excised from the gels using a scalpel blade and cDNA fragments extracted using PureLink™ Quick Gel Extraction Kit (Invitrogen) according to the manufacturer's instructions. cDNA was eluted with 50 µL SNW and stored at -80°C. Cloning was conducted using Gateway cloning system (Invitrogen, USA) as per section 5.2.1, the sequences of amplicons were confirmed using the Australian Genome Research Facility Ltd (AGRF) protocol. PCR products were sequenced using the Purified DNA template (PD Service), where each PCR product and forward primer for the corresponding gene were pre-mixed in a total volume of 12 µL in a microfuge tube and all samples were run using AGRF cycling conditions for the PD sequencing service. Data was analysed for two replicates using Geneious software (Geneious Pro 5.4.6, Biomatters Ltd, Auckland, New Zealand).

#### **4.2.2 Bioinformatics analysis**

##### **4.2.2.1 Conserved domains analyses for VRCPs**

Domain detection in full length cDNA clones was performed using the NCBI

Conserved	Domain	Search	Tool
( <a href="http://www.ncbi.nlm.nih.gov/Structure/cdd/wrpsb.cgi">http://www.ncbi.nlm.nih.gov/Structure/cdd/wrpsb.cgi</a> ,		accessed	November
2012);	the	SMART	database
		( <a href="http://smart.embl-heidelberg.de/smart/set_mode.cgi?GENOMIC=1">http://smart.embl-heidelberg.de/smart/set_mode.cgi?GENOMIC=1</a> ,	accessed
		the European Bioinformatics Institute (EBI), InterProScan Sequence Search	November
		( <a href="http://www.ebi.ac.uk/Tools/pfa/iprscan/">http://www.ebi.ac.uk/Tools/pfa/iprscan/</a> ,	2012);
		and Apweiler, 2001) and PROSITE ( <a href="http://prosite.expasy.org/">http://prosite.expasy.org/</a> ,	

November 2012) using the default settings. Whether proteins had the N-terminal signal peptide sequence was predicted by SignalP (<http://www.cbs.dtu.dk/services/SignalP/>) (Bendtsen *et al.*, 2004).

#### 4.2.2.2 Alignment of individual VRCs

Alignments of VRCs were conducted using Geneious software, global alignment with free end gaps and MUSCLE matrix were used. For each of the four candidates the full length cDNA was used in multiple alignments with family members (as per Table 3.8), however sequences from *P. tritici-repentis* were not used as they had 100% similarity to each candidate of *Ptt*. The endoxylanase (named PttXyn11A and assigned accession number JX900133) was aligned with nine fungi sequences from the G11 family, to identify the active signature, including those that have been well characterised in pathogenicity (Table 4.2); *Trichoderma reesei* endoxylanase II (TrXyn11A, Q02244) (Saarelainen *et al.*, 1993) and *Botrytis cinerea* (also referred to as *Botryotinia fuckeliana*) endo- $\beta$ -1,4-Xylanase (BcXyn11A, DQ057980) (Brito *et al.*, 2006).

**Table 4.2. Selected proteins of GH11 family and their accession numbers and organisms which were used in multiple alignments with PttXyn11A (JX900133).**

Accession number	Organism
P33557	<i>Aspergillus kawachii</i>
1XYN_A	<i>Trichoderma reesei</i>
Q06562	<i>Cochliobolus carbonum</i>
1XYP_A	<i>Trichoderma reesei</i>
BAA07264	<i>Aspergillus kawachii</i>
AFA51067	<i>Aspergillus oryzae</i>
EIT80047	<i>Aspergillus oryzae</i>
Q02244	<i>Trichoderma reesei</i>
DQ057980	<i>Botrytis cinerea</i>

Because the isochorismatase (named PttCHFP1 and assigned accession number JX900134) belongs to a cysteine hydrolase superfamily, alignments and phylogenetic analysis were performed using selected proteins from each of the main member families including the isochorismatase family, CHase family, nicotinamidase family and nicotinamidase-related family (Table 4.3) However, fungal sequences were not included due to the lack of sequences available in the database.

**Table 4.3. Cysteine hydrolase families used in the alignments and phylogenetic analysis. Accession number for selected members and their corresponding organism names are shown.**

<b>Family name</b>	<b>Accession number</b>	<b>Organism</b>
<b>Isochorismatase</b>	AAG33854	<i>Listonella anguillarum</i>
	BAC16759	<i>Agrobacterium tumefaciens</i>
	Q51790	<i>Pseudomonas fluorescens</i>
	1NF8_A	<i>Pseudomonas aeruginosa</i>
<b>CHase</b>	NP_105355	<i>Mesorhizobium loti</i>
	NP_746071	<i>Pseudomonas putida</i>
	BAC000809	<i>Rhodococcus sp.</i>
<b>Nicotinamidase</b>	P53184	<i>Saccharomyces cerevisiae</i>
	XP_324893	<i>Neurospora crassa</i>
	ZP_00087981	<i>Pseudomonas fluorescens</i>
	NP_105653	<i>Mesorhizobium loti</i>
<b>Nicotinamidase-related</b>	AAL43057	<i>Agrobacterium tumefaciens</i>
	NP_791921	<i>Pseudomonas syringae</i>
	ZP_00085712	<i>Pseudomonas fluorescens</i>
	ZP_00086318	<i>Pseudomonas fluorescens</i>
	NP_104027	<i>Mesorhizobium loti</i>
	NP_637717	<i>Xanthomonas campestris</i>
	NP_791683	<i>Pseudomonas syringae</i>
ZP_00084792	<i>Pseudomonas fluorescens</i>	

The prediction of the C-terminal GPI-modification site for the GPI-anchored CFEM domain-containing protein (named PttGPI-CFEM and assigned accession number KC713871) was made using a selective fungal-specific algorithm Big-PI ([http://mendel.imp.ac.at/gpi/fungi\\_server.html](http://mendel.imp.ac.at/gpi/fungi_server.html), accessed October 2012) (Eisenhaber *et al.*, 2004). PttGPI-CFEM was aligned

with similar proteins from *Neurospora crassa* (Q9P3F4 and Q9C2R4), *Coccidioides immitis* (Q12295) and *S. cerevisiae* (EDN59294).

Although the conserved hypothetical protein, renamed to a *Ptt* secreted protein (named PttSP1 and assigned accession number JX900135), has an unknown function, a domain search was conducted using the database previously described in section 4.2.2.1. In addition, a search for potential effectors was conducted by looking for Y/F/WxC motifs for all candidates (Godfrey *et al.*, 2010; Morais do Amaral *et al.*, 2012).

#### **4.2.2.3 Phylogenetic analysis**

The full lengths of the candidate proteins were aligned using Geneious with the default of identity and global alignment with free end gap. Phylogenetic trees were built based upon the Neighbour-joining method and Jukes-Cantor method for the genetic distance model (Saitou and Nei, 1987). Branch support for the tree was evaluated using 10000 bootstrap replications.

#### **4.2.2.4 Secondary structure and three dimensional modelling of VRCPs**

Secondary structure was also predicted for proteins based on the EMBOSS prediction tool (Garnier, <http://helixweb.nih.gov/emboss/html/garnier.html>, accessed November 2012) using Geneious software. Three dimensional structure for VRCPs was predicted using the I-TASSER Server (Department of Computational Medicine and Bioinformatics, University of Michigan) (Roy *et*

*al.*, 2010; Zhang, 2008). Full length of amino acids was used to build the 3D structure for each protein by comparing multiple-threaded alignments by LOMETS and iterative TASSER assembly simulations. The confidence score (C-score) and accuracy of model (TM-score) were estimated by I-TASSER and the 3D structure was visualised using Geneious software. The C-score indicates the significance of threading template alignments and the convergence parameters of the structure assembly simulations, and C-score is typically in the range of -5 to 2, where a C-score of higher value signifies a model with a high confidence and vice-versa (Roy *et al.*, 2010; Zhang, 2008). TM-score is a known standard for measuring structural similarity between two structures and is usually used to measure the accuracy of structure modelling when the native structure is known (Zhang and Skolnick, 2004). When TM-score is between 0.0 and 0.17 there is random structural similarity between the two structures, while they are about the same structure if TM-score is between 0.5 and 1.00 (Zhang and Skolnick, 2004). The highest confidence score value was used to adopt the structure.

### **4.2.3 Semi-quantitative RT-PCR**

#### **4.2.3.1 *In vitro***

RNA extraction from six isolates of *Ptt* (Table 2.1) grown for 10 days and DNase treatment were conducted as per section 4.2.1.3, cDNA for each isolate was synthesised as per section 4.2.1.4. Partial length of *PttGAPDH* was used as an endogenous control. The PCR cycle number for each gene was optimised

using 27, 30, 33, 36 and 39 PCR cycles to ensure that amplification was in the linear range and the results were semi-quantitative (Appendix, Figure A2.1). Semi-quantitative RT-PCR was conducted using optimised cycle number (33 cycles for *PttXyn11A*; 40 cycles for *PttSPI*, *PttCHFP1* and *PttGPI-CFEM*) and PCR products were visualised as per section 4.2.1.3. *PttGAPDH* was amplified under the following conditions: 95°C for 2 min, and 33 cycles of 15 s at 95°C and 30 sec at 55°C and 1 min at 70°C and last extension was 10 min at 70°C.

#### **4.2.3.2 *In planta***

Inocula for six isolates (Table 2.1) were produced as per section 2.2.2. Four individual plants of barley cv. Sloop in each of two separate experiments were inoculated as per section 2.2.3 using a sprayer until run off. Plants were then grown as per section 2.2.1. Samples from infected and uninfected leaves were taken after 192 hpi, when the symptoms were severe, and immediately frozen in liquid nitrogen then ground and stored at -80°C until required. Ground material (500 to 600 mg) was used for RNA extraction and then DNase treatment as per section 4.2.1.3, cDNA for each isolate was synthesised as per section 4.2.1.4. Semi-quantitative RT-PCR was conducted and PCR products were visualised as per section 4.2.1.4.



### **4.3 Results**

#### **4.3.1 Isolation of the full length of cDNA for virulence-related candidate gene transcripts (VRCGs)**

The full length cDNAs for each VRCG were isolated and assigned a name based on their function and submitted to NCBI. They are referred to as *Ptt* endoxylanase 11A (*PttXyn11A*), *Ptt* cysteine hydrolase family protein (*PttCHFP1*), GPI-anchored protein containing a CFEM domains (*PttGPI-CFEM*) and *Ptt* secreted protein 1 (*PttSP1*) and have been assigned the accession numbers JX900133, JX900134, KC713871 and JX900135 respectively in the NCBI database.

#### **4.3.2 Conserved domains and phylogenetic analyses for VRCs**

##### **4.3.2.1 *PttXyn11A***

Sequencing analysis showed that the open reading frame of *PttXyn11A* cDNA contained 693 bp encoding a putative protein consisting of 231 amino acids (Figure 4.1A). SignalP 3.0 predicted that the N-terminal amino acid sequence has features of a signal peptide and the cleavage site was located between the 20<sup>th</sup> and 21<sup>st</sup> amino acids (Figure 4.1A). The peptides identified by LC-eSI-ITMS (Table 3.5) matched (100%) to the residues 144 to 181 of the open reading frame for *PttXyn11A*. The putative protein has a calculated molecular mass of 24.9 kDa. Conserved domain analysis revealed that the *PttXyn11A* amino acid sequence contains domains matched to the glycosyl hydrolase family 11 (GH11, EC:3.2.1) (Figure 4.1B). This family contains enzymes that hydrolyse the glycosidic bond between two or more carbohydrates, were formerly known

as cellulase family G (Davies and Henrissat, 1995), and have xylanase (EC:3.2.1.8) activity.

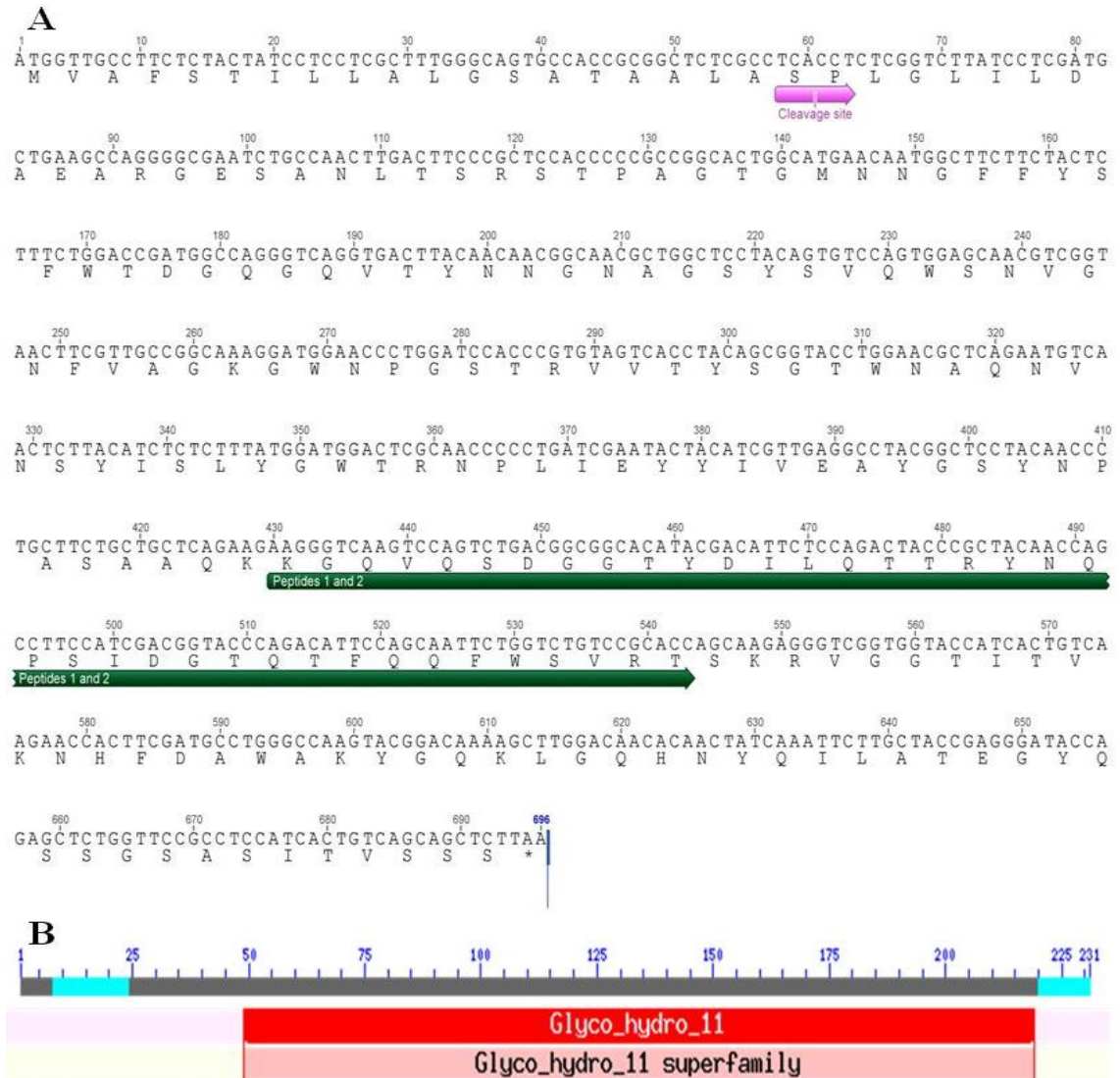
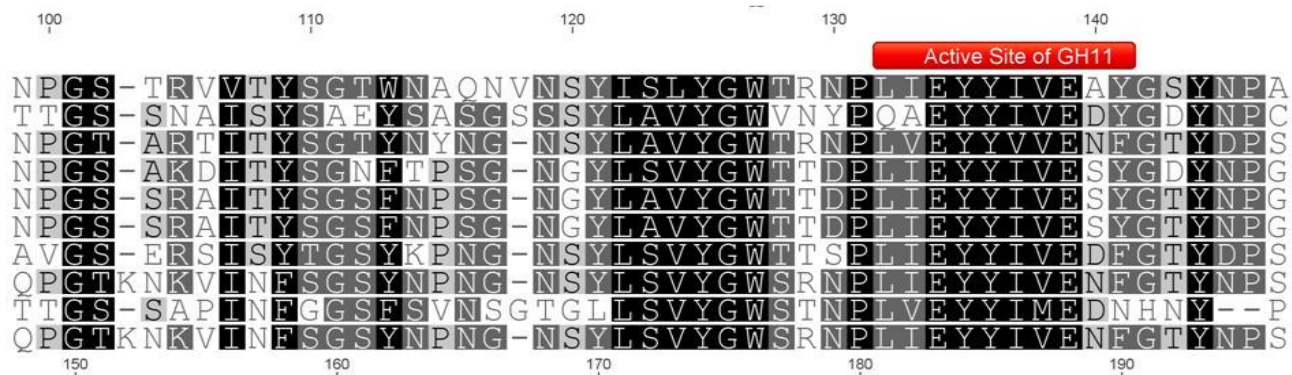


**Figure 4.1.** The full length of *PttXyn11A* cDNA and *PttXyn11A* protein (JX900133) (A). Cleavage site is shown in pink arrow below the sequence, identified peptides shown in green arrow below the sequence, star indicates stop codon. (B) Graphical summary of conserved domains identified on the full length of *PttXyn11A* amino acid sequence. Domains are colour coded according to families and superfamilies to which they have been assigned. Bar in red bright colour shows *PttXyn11A* sequence hits Glycosyl hydrolases family 11 with scores that pass a domain-specific threshold (specific hits). Bar in pink pastel colour shows superfamily Glycosyl hydrolases 11, low-complexity regions highlighted as solid cyan blocks.

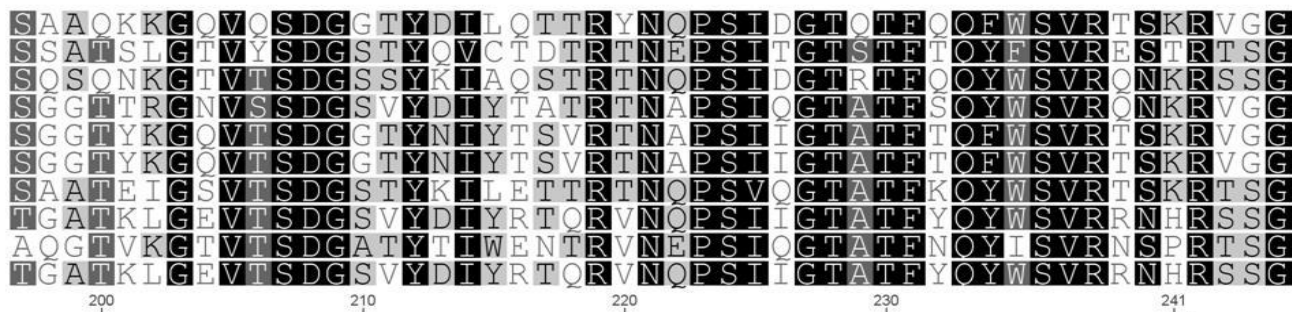
Multiple alignments of PttXyn11A with nine fungal sequences of GH11 family members (Table 4.2A) showed that PttXyn11A aligned with the active site signatures common for GH11, this site encodes in two regions (131 to 139 aa and 223 to 234 aa) (Brito *et al.*, 2006; Falquet *et al.*, 2002; Wakarchuk *et al.*, 1994). Most of the GH11 endoxylanases have been well characterised (Apel *et al.*, 1993; ApelBirkhold and Walton, 1996; Brito *et al.*, 2006; Ellouze *et al.*, 2011; Havukainen *et al.*, 1996; Noda *et al.*, 2010; Saarelainen *et al.*, 1993; Wu *et al.*, 1997). All amino acids that have been implicated in catalysis and/or are signatures of the endoxylanase enzyme are conserved at similar positions in PttXyn11A. Phylogenetic analysis of these sequences of the GH11 family and PttXyn11A amino acids showed that PttXyn11A shared most homology with *C. carbonum* (Q06562) and *A. kawachii* (BAA07264) (Figure 4.2B), however, *A. oryzae* was in a different clade.

A

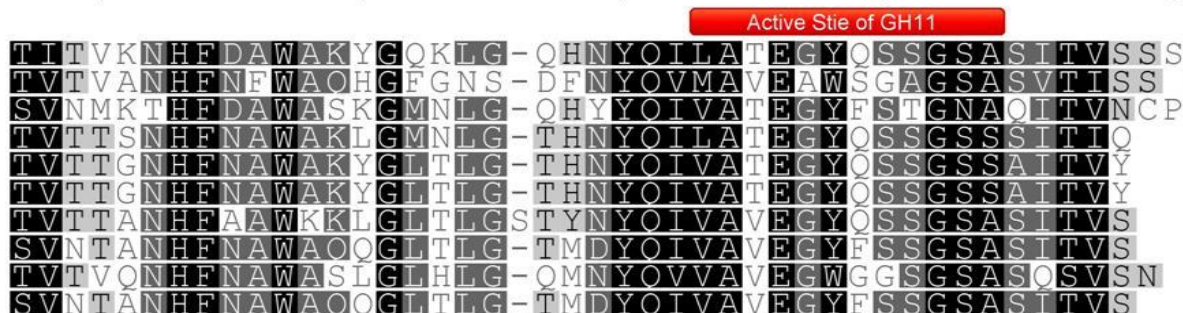
1. JX900133, *P. teres* f. *teres* (PttXyn11A)
2. P33557, *Aspergillus kawachii*
3. Q06562, *Cochliobolus carbonum*
4. BAA07264, *Aspergillus kawachii*
5. AFA51067, *Aspergillus oryzae*
6. EIT80047, *Aspergillus oryzae*
7. DQ057980, *Botrytis cinerea* (BcXyn11A)
8. 1XYP\_A, *Trichoderma reesei*
9. 1XYN\_A, *Trichoderma reesei*
10. Q02244, *Trichoderma reesei* (TrXyn11A)



1. JX900133, *P. teres* f. *teres* (PttXyn11A)
2. P33557, *Aspergillus kawachii*
3. Q06562, *Cochliobolus carbonum*
4. BAA07264, *Aspergillus kawachii*
5. AFA51067, *Aspergillus oryzae*
6. EIT80047, *Aspergillus oryzae*
7. DQ057980, *Botrytis cinerea* (BcXyn11A)
8. 1XYP\_A, *Trichoderma reesei*
9. 1XYN\_A, *Trichoderma reesei*
10. Q02244, *Trichoderma reesei* (TrXyn11A)



1. JX900133, *P. teres* f. *teres* (PttXyn11A)
2. P33557, *Aspergillus kawachii*
3. Q06562, *Cochliobolus carbonum*
4. BAA07264, *Aspergillus kawachii*
5. AFA51067, *Aspergillus oryzae*
6. EIT80047, *Aspergillus oryzae*
7. DQ057980, *Botrytis cinerea* (BcXyn11A)
8. 1XYP\_A, *Trichoderma reesei*
9. 1XYN\_A, *Trichoderma reesei*
10. Q02244, *Trichoderma reesei* (TrXyn11A)



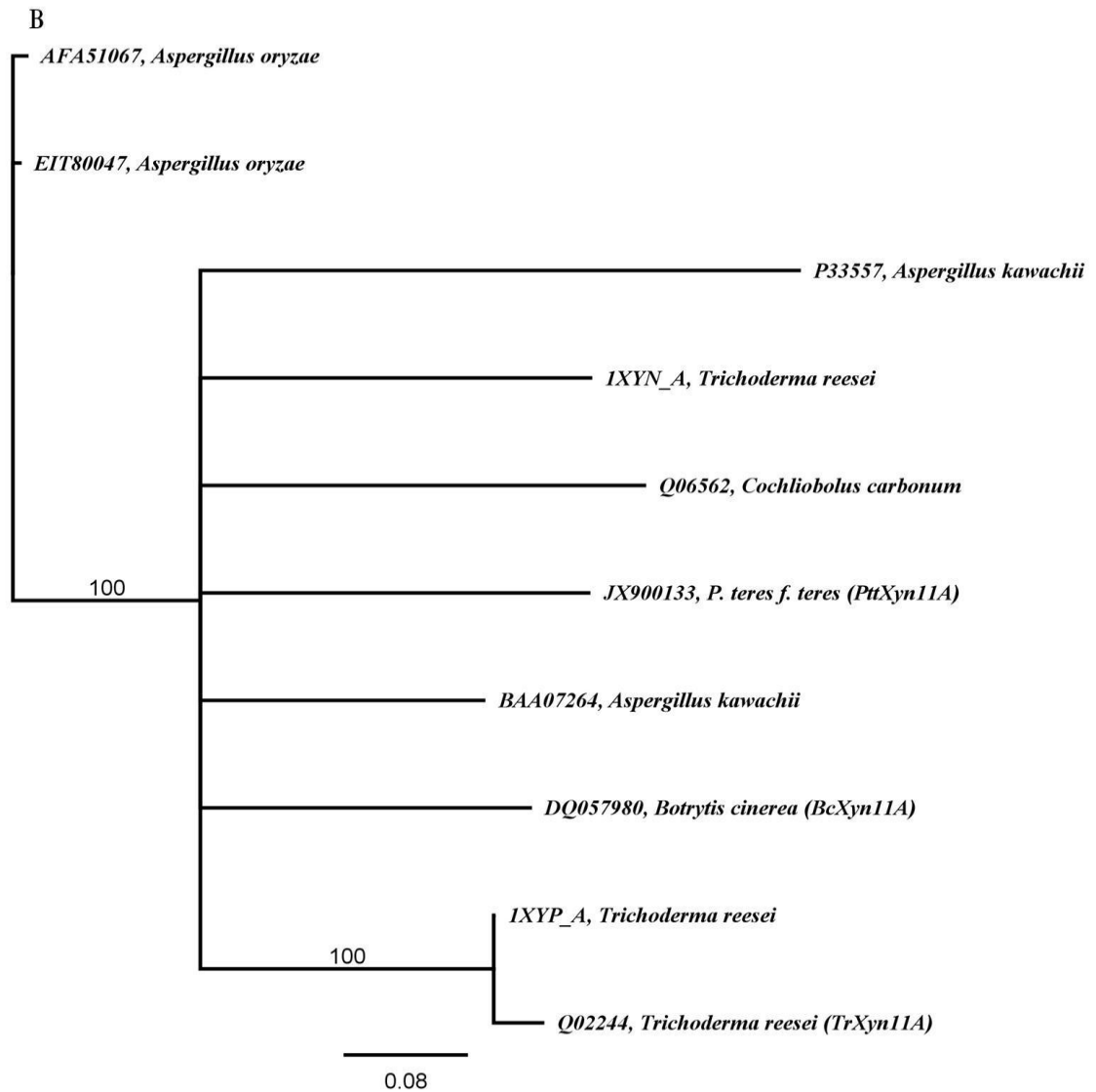


**Figure 4.2. Multiple alignment and phylogenetic analysis of PttXyn11A and proteins containing Glycosyl hydrolases family 11 domain.** (A) Multiple alignment of the full length of selected sequences which were obtained from NCBI database and aligned using Geneious. Selected regions of the proteins identified in the alignment are displayed. The accession numbers and species names of the sequences are indicated on the left side and the range of the residues from the original sequence is indicated at the top of the sequences. Active signature of GH11 is shown in red bars above the sequence, shared domains in the sequences are in boldface, conserved sequences shown in gray colour. Alignment was conducted when bases matched at least 75% of the sequences. (B) Phylogenetic analysis of PttXyn11A and its homologues from Glycosyl hydrolases family 11. Phylogenetic analysis was inferred using the Neighbor joining method. The bootstrap consensus tree from 10000 replicates was taken to represent the evolutionary history of 10 taxa. The percentage of replicate trees in which the associated taxa clustered together in the bootstrap test (10000 replicates) are shown next to the branches. The tree is drawn to scale, with branch lengths in the same units as those of the evolutionary distances used to infer the phylogenetic tree. Geneious was used to conduct phylogenetic analysis, 10 sequences from different species were used to construct the tree.

Further characterisation was conducted to identify domains and motifs in PttXyn11A that match to well characterised endoxylanase from other Ascomycetes species. Alignment of PttXyn11A, TrXyn11A and BcXyn11A of *Ptt*, *T. reesei*, and *B. cinerea* respectively (Brito *et al.*, 2006; Ellouze *et al.*, 2011) showed that *PttXyn11A* encodes two sites (LIEYYIVEDF and VAVEGYQSSGSA) which matched the conserved region (active site) of all xylanase proteins (Figure 4.3). The active sites of the protein are approximately located in the middle of the structure between residues 123 to 130 and 216 to 224. Rotblat *et al.* (2002) and Noda *et al.* (2010) also identified a necrosis-inducing region of 30 aa (aa residues 131 to 160) in the sequences of TrXyn11A and BcXyn11A of *T. reesei*, and *B. cinerea* respectively. This region shares some similarity in PttXyn11A (Figure 4.3), especially at the peptide TSDGS which has been proven to cause necrosis in tomato leaves (Noda *et al.*, 2010). The peptides TKLGE and TEIGS in the Xyn11A sequences for *T. reesei* and *B. cinerea* respectively, have been proven to induce necrosis *in planta* for both fungi (Noda *et al.*, 2010; Rotblat *et al.*, 2002). However, these peptides were substituted by the peptides QKKGQ in PttXyn11A.

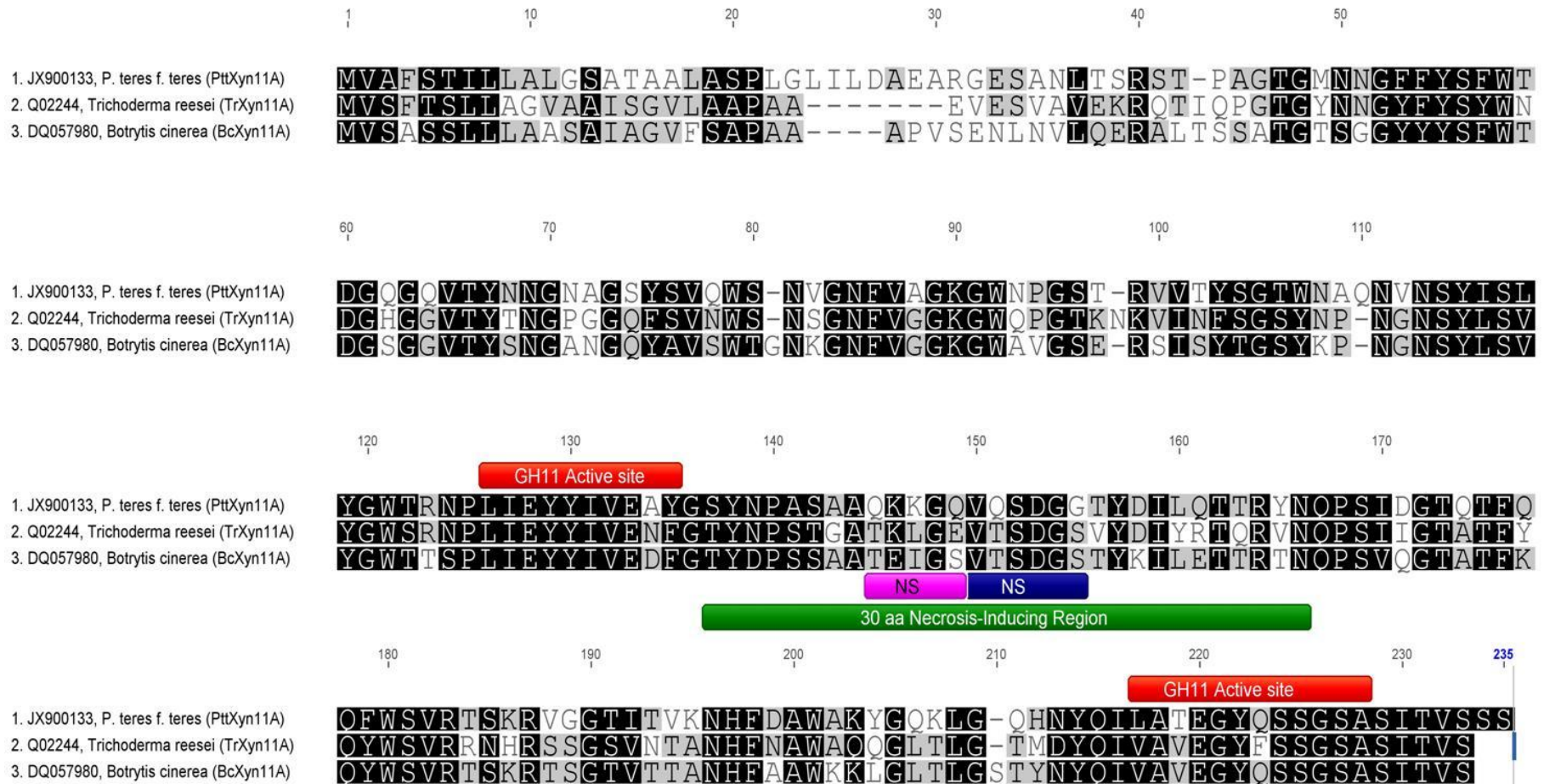


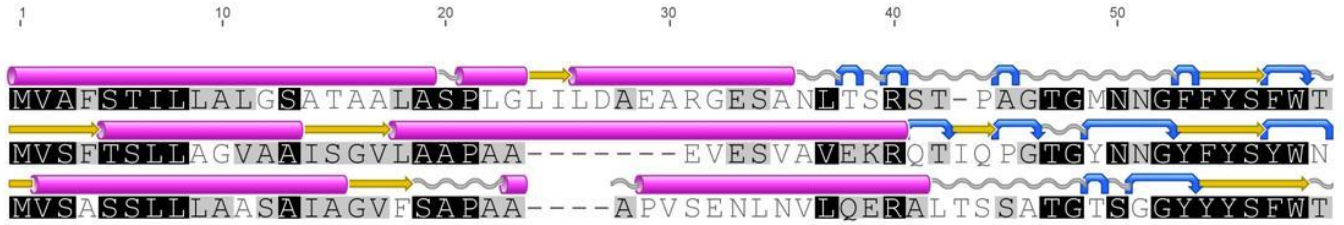
**Figure 4.3. Alignment of PttXyn11A of *Ptt* with TrXyn11A, *Trichoderma reesei* and BcXyn11A, *B. cinerea* (Brito *et al.*, 2006).** Accession number and species name are shown on the left side. Full length of these proteins were aligned using Geneious alignment with default; identity, global alignment with free end gap. Selected regions of the proteins identified in the alignment are displayed. Sequence identity shown in black bold and conserved in gray. The active signature of xylanase shown in red bars above the sequence, two necrosis-inducing sites (NS) shown in blue and purple bars below the sequence, 30 aa of necrosis-inducing region identified in *B. cinerea* (Noda *et al.*, 2010) is shown in green bar below the sequence.

Comparison of the predicted secondary structure of PttXyn11A, TrXyn11A and BcXyn11A demonstrated great similarity of the structure especially in the active sites of the enzyme (Figure 4.4A). PttXyn11A has also shown similarity in the structure in the necrosis-inducing region. Three dimensional structure of PttXyn11A was predicted with confidence score (-0.77) and TM-score ( $0.62 \pm 0.14$ ) indicating a strong similarity to the xylanase profile with three helices structures and the majority of the structure being beta sheets (Figure 4.4B). The active sites and necrosis-inducing region of the protein appeared as beta sheets in the structure (Figure 4.4C). PttXyn11A (Figure 4.4D and E) showed great similarity to the BcXyn11A in *B. cinerea* which was predicted by Noda *et al.* (2010) (Figure 4.4F and G). The predicted 30 aa necrosis-inducing region, which is similar to the region in BcXyn11A of *B. cinerea* (Noda *et al.*, 2010), was located at the surface of the protein. The two necrosis sites in PttXyn11A (Figure 4.4D and E), which were similar to VTSDGS and TEIGS in BcXyn11A of *B. cinerea* (Noda *et al.*, 2010) (Figure 4.4F and G), displayed as beta sheets on the surface of the enzyme.

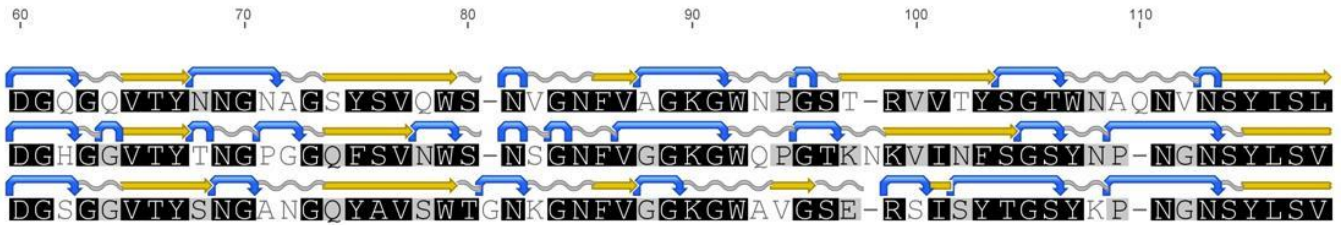


# A

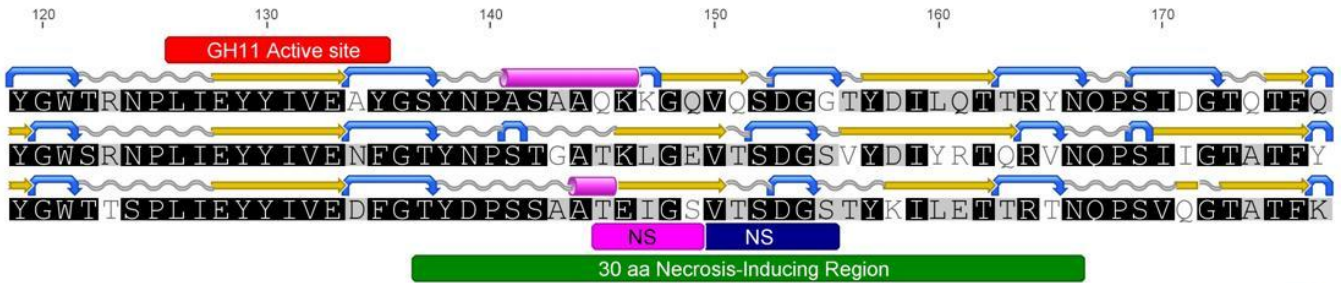
1. JX900133, *P. teres* f. *teres* (PttXyn11A)
2. Q02244, *Trichoderma reesei* (TrXyn11A)
3. DQ057980, *Botrytis cinerea* (BcXyn11A)



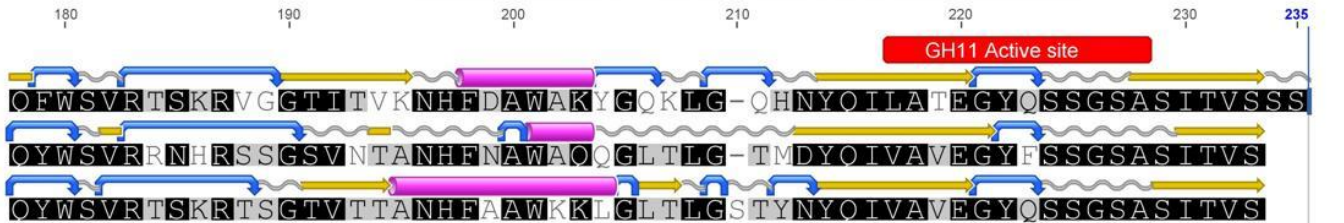
1. JX900133, *P. teres* f. *teres* (PttXyn11A)
2. Q02244, *Trichoderma reesei* (TrXyn11A)
3. DQ057980, *Botrytis cinerea* (BcXyn11A)



1. JX900133, *P. teres* f. *teres* (PttXyn11A)
2. Q02244, *Trichoderma reesei* (TrXyn11A)
3. DQ057980, *Botrytis cinerea* (BcXyn11A)



1. JX900133, *P. teres* f. *teres* (PttXyn11A)
2. Q02244, *Trichoderma reesei* (TrXyn11A)
3. DQ057980, *Botrytis cinerea* (BcXyn11A)



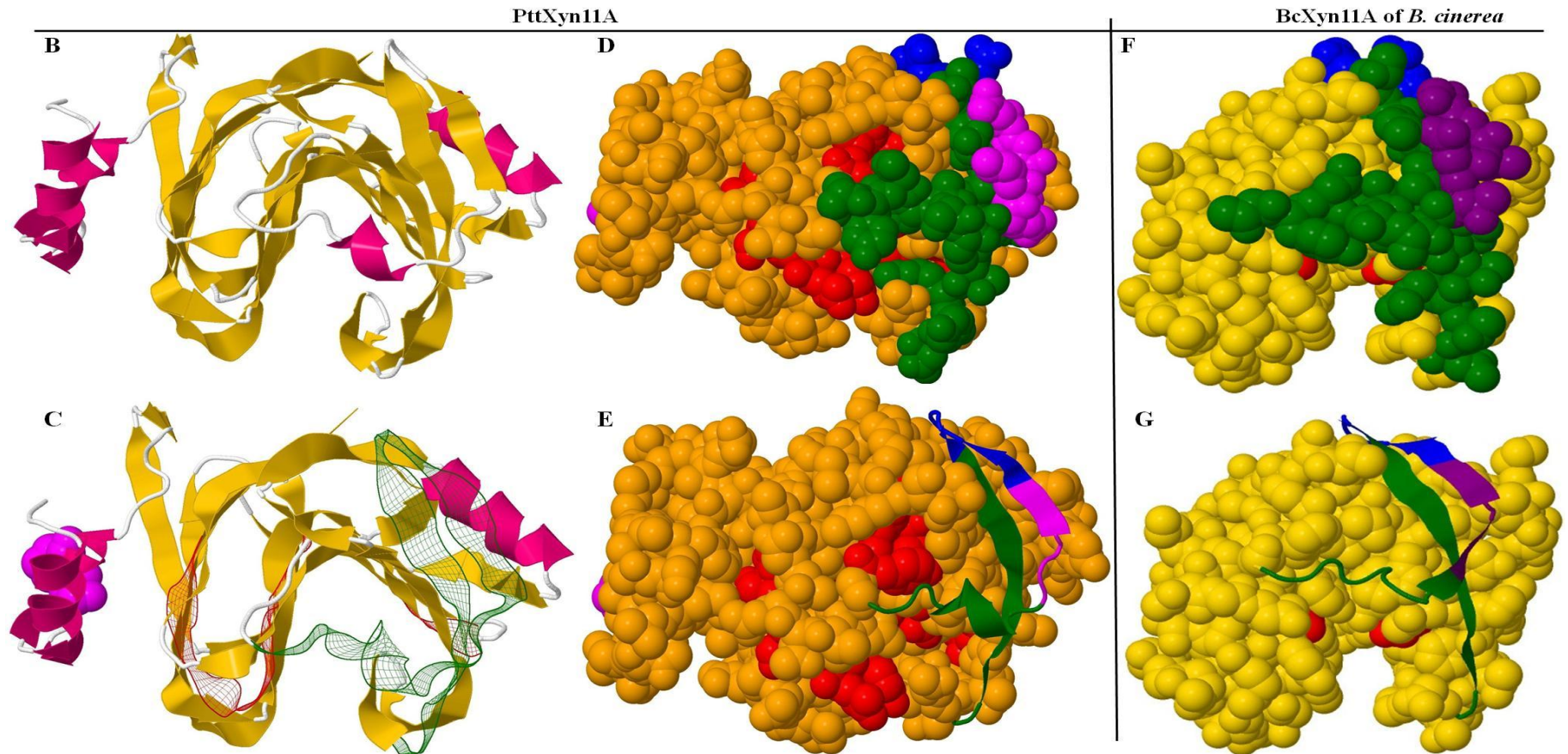


**Figure 4.4. Secondary and three dimensional structure of PttXyn11A of *Ptt*.** (A) The predicted secondary structure of PttXyn11A, TrXyn11A and BcXyn11A of *Ptt*, *T. reesei* and *B. cinerea* respectively. Alignment and prediction conducted using Genieous software, secondary structure predicted based on the EMBOSS prediction tool (Garnier). Alpha helice (purple cylinders), coil (gray curve shapes), Beta strand (yellow arrows) and turn (blue curves) are shown for the secondary structure above the sequence. Sequence identity shown in black bold and conserved in gray, shared motifs (active site of GH11 family) shown in red bars above the sequence, the 30 amino acid necrosis-inducing region (green bar) and necrosis sites (NS) (blue and purple) are shown below the sequence. Accession number and organism names are shown on the left. (B) The predicted three dimensional structure of PttXyn11A of *Ptt*, the model shows the alpha helical (deep pink), beta strand (orange) and turns (white) in the secondary structure. (C) the active site of PttXyn11A shown in red mesh ribbon, the 30 amino acids necrosis inducing site shown in green mesh ribbon, purple balls show the cleavage site of the protein. (D and E) Space filling predicted 3D structure of PttXyn11A showing similarity to BcXyn11A of *B. cinerea* (Noda *et al.*, 2010) (F and G), GH11 active site, 30 aa necrosis inducing region and necrosis-inducing sites are shown in red, green, blue and purple respectively.

#### 4.3.2.2 PttCHFP1

The isolated open reading frame of *PttCHFP1* cDNA contained 903 bp which encodes a putative protein consisting of 301 amino acids (Figure 4.5A). A signal peptide and cleavage site were identified and located between amino acids 19 and 20 (Figure 4.5A). The peptides identified by LC-eSI-IT MS analysis (Table 3.2) have matched approximately to the middle of the protein at residue 57 to 110. Conserved domain analysis suggested that PttCHFP1 belongs to the cysteine hydrolase family and that it contains the conserved *cis*-peptide bonds considered to be a conserved feature (catalytic triad) in this family (Figure 4.5B). Although PttCHFP1 belongs to cysteine hydrolase superfamily, the amino acid sequence shared similarity with a number of families in that superfamily, including isochorismatase and CSHase (N-carbamoylsarcosine amidohydrolase).

Phylogenetic analysis of selected members of cysteine hydrolase families (Table 4.3) suggested that PttCHFP1 was most likely a homolog to the isochorismatase family (Figure 4.6). Interestingly, multi-domains were identified in PttCHFP1. One of these shared homology to the isochorismatase family (spfam00857), which contains hydrolase enzymes that have more than one domain. BLASTp analysis also showed that PttCHFP1 matched to *P.tritici-repentis* protein annotated as an isochorismatase. However, there was one main shared domain between other families (CSHase, nicotinamidase and nicotinamidase-related amidohydrolases) (Appendix; Figure A2.2, Figure A2.3, Figure A2.4 and Figure A2.5).

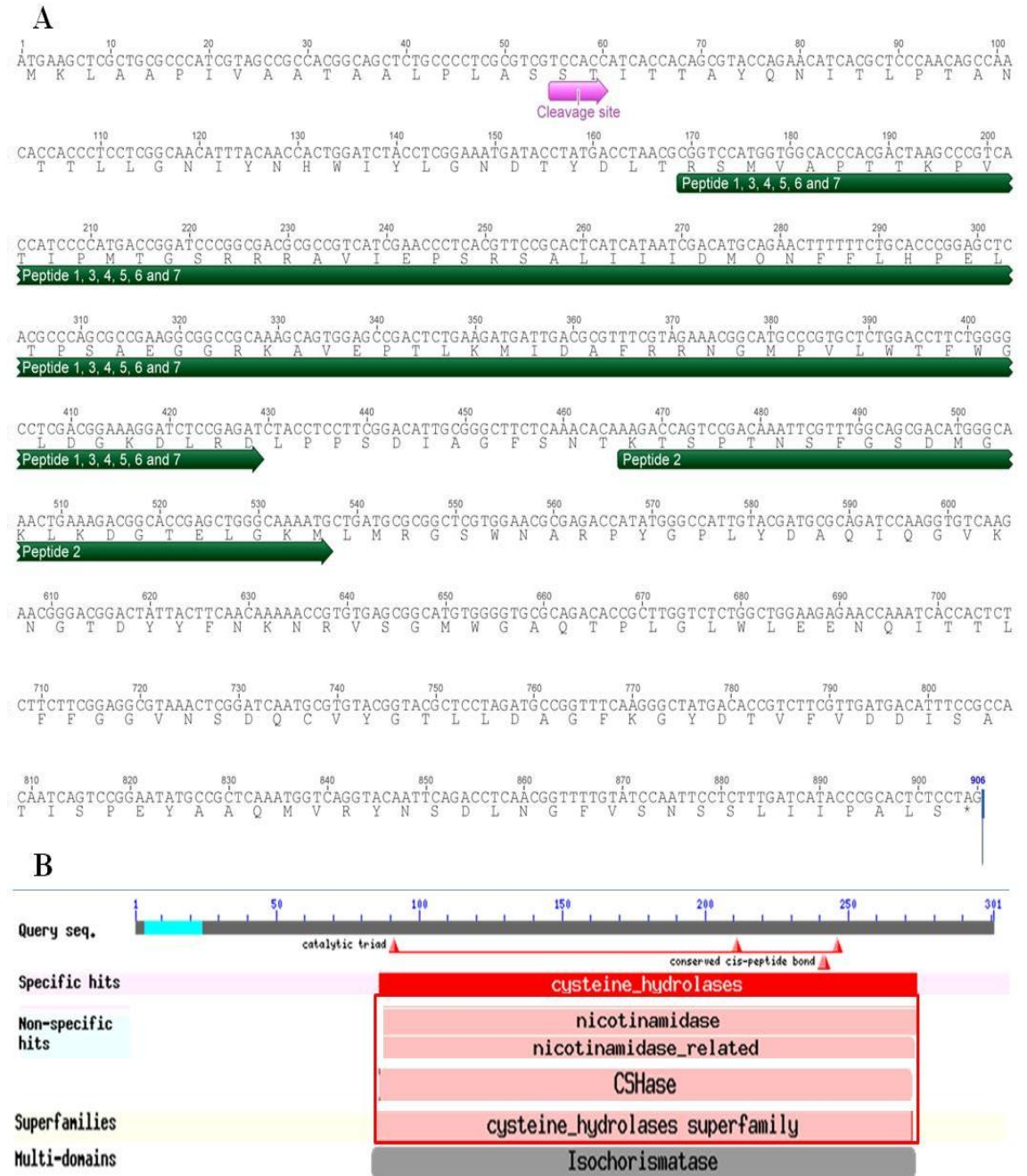


**Figure 4.5. The full length of *PttCHFP1* cDNA and *PttCHFP1* protein (JX900134).** (A) Cleavage site is shown in pink arrow below the sequence, seven identified peptides shown in green arrows below the sequence, star indicates stop codon below the sequence. (B) Graphical summary of conserved domains identified on the full length of *PttCHFP1* amino acid sequence. Domains are colour coded according to families to which they have been assigned. Hits with scores that pass a domain-specific threshold (specific hits) are drawn in bright red colours. Superfamily placeholders (non-specific hits) and are drawn in pastel pink colours. Grey colored bars shows multi-domains which they were computationally detected and are likely to contain multiple single domains. Triangles indicate conserved cis-peptide bonds (as conserved feature) in cysteine hydrolase family.

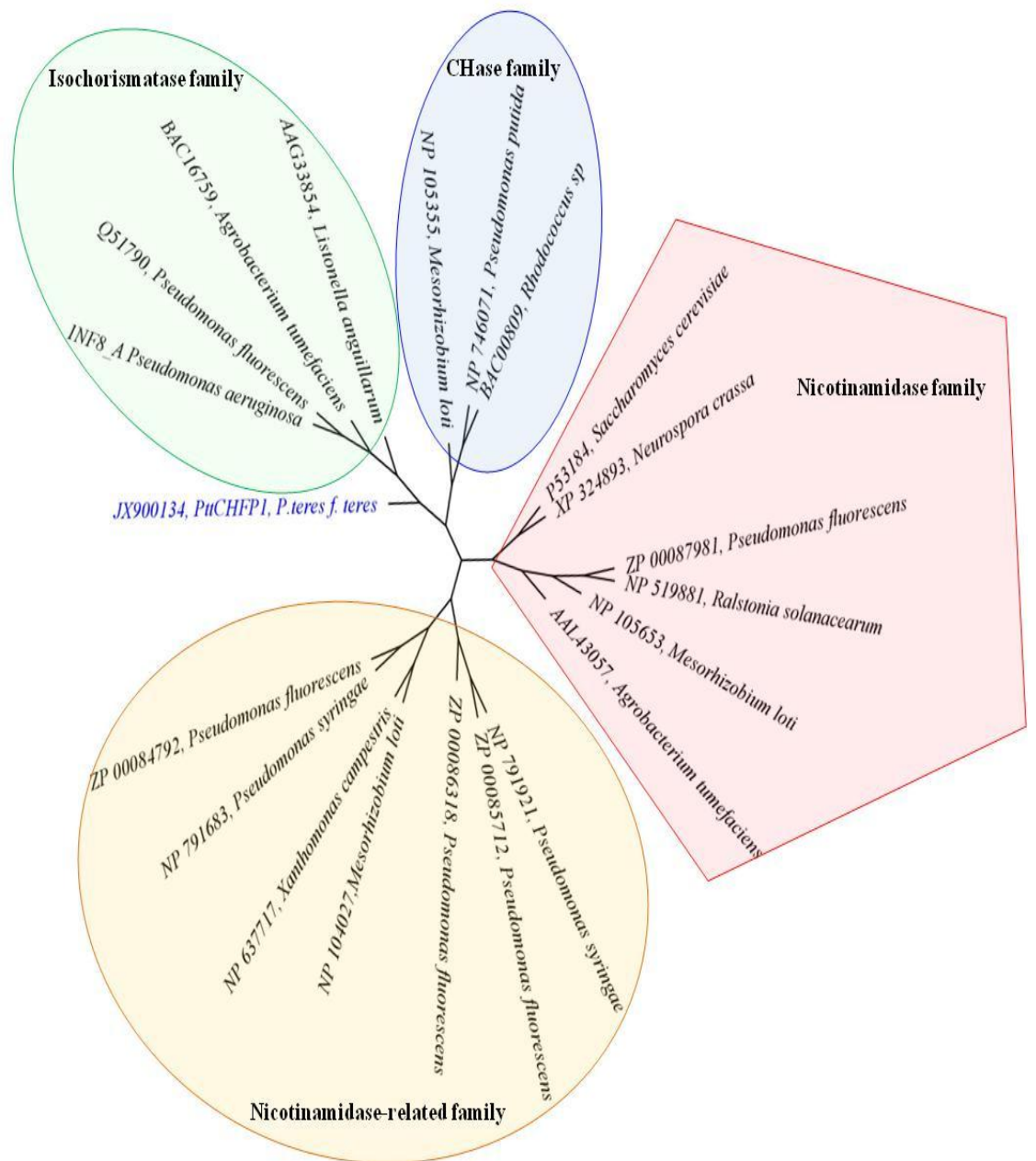


**Figure 4.6. Phylogenetic tree of selected members of cysteine hydrolase superfamily.** Phylogenetic analysis was inferred using the Neighbor joining method. The bootstrap consensus tree from 10000 replicates is taken to represent the evolutionary history of different taxa in each family. Geneious was used to conduct phylogenetic analysis for 4 families (Table 4.3) from different species were aligned using Geneious with MUSCLE used to construct the tree.

Multiple alignment of selected members of the isochorismatase family (pfam00857) (Table 4.3) (Parsons *et al.*, 2003) showed that PttCHFP1 protein matched to several domains, the most common and longest, from this family was highlighted as MD1, MD2 and MD3 (Figure 4.7). This family includes an isochorismatase and other related enzymes with unknown function (Sonoda *et al.*, 2002; Zajc *et al.*, 1996). PttCHFP1 have shown homology to the probable isochorismatase from *P. fluorescens* (Q51790), an enzyme which is involved in the biosynthesis of the broad-spectrum antibiotic phenazine-1-carboxylic acid (PCA) (Mavrodi *et al.*, 1998).

Because the similarity of PttCHFP1 was only in the active site of the isochorismatase, the secondary structure was quite different (data not shown). Three dimensional model of PttCHFP1 was predicted with confidence score (-2.69) and TM-score (0.40±0.14) indicating a random similarity to isochorismatase and it contains 7 helices, 6 beta sheets and several turns (Figure 4.8A). The shared domains of the protein distributed across the structure and PttCHFP1 showed similarity to the three dimensional structure of *P. aeruginosa* 1NF8 protein (Figure 4.8B) (Parsons *et al.*, 2003)

1. JX900134, PttCHFP1. *P. teres* f. *teres*
2. AAG33854 *Listonella anguillarum*
3. BAC16759, *Agrobacterium tumefaciens*
4. 1NF8\_A, *Pseudomonas aeruginosa*
5. Q51790, *Pseudomonas fluorescens*

1. JX900134, PttCHFP1. *P. teres* f. *teres*
2. AAG33854 *Listonella anguillarum*
3. BAC16759, *Agrobacterium tumefaciens*
4. 1NF8\_A, *Pseudomonas aeruginosa*
5. Q51790, *Pseudomonas fluorescens*

1. JX900134, PttCHFP1, *P. teres* f. *teres*
2. AAG33854 *Listonella anguillarum*
3. BAC16759, *Agrobacterium tumefaciens*
4. 1NF8\_A, *Pseudomonas aeruginosa*
5. Q51790, *Pseudomonas fluorescens*

1. JX900134, PttCHFP1 *P. teres* f. *teres*
2. AAG33854 *Listonella anguillarum*
3. BAC16759, *Agrobacterium tumefaciens*
4. 1NF8\_A, *Pseudomonas aeruginosa*
5. Q51790, *Pseudomonas fluorescens*

1. JX900134, PttCHFP1, *P. teres* f. *teres*
2. AAG33854 *Listonella anguillarum*
3. BAC16759, *Agrobacterium tumefaciens*
4. 1NF8\_A, *Pseudomonas aeruginosa*
5. Q51790, *Pseudomonas fluorescens*

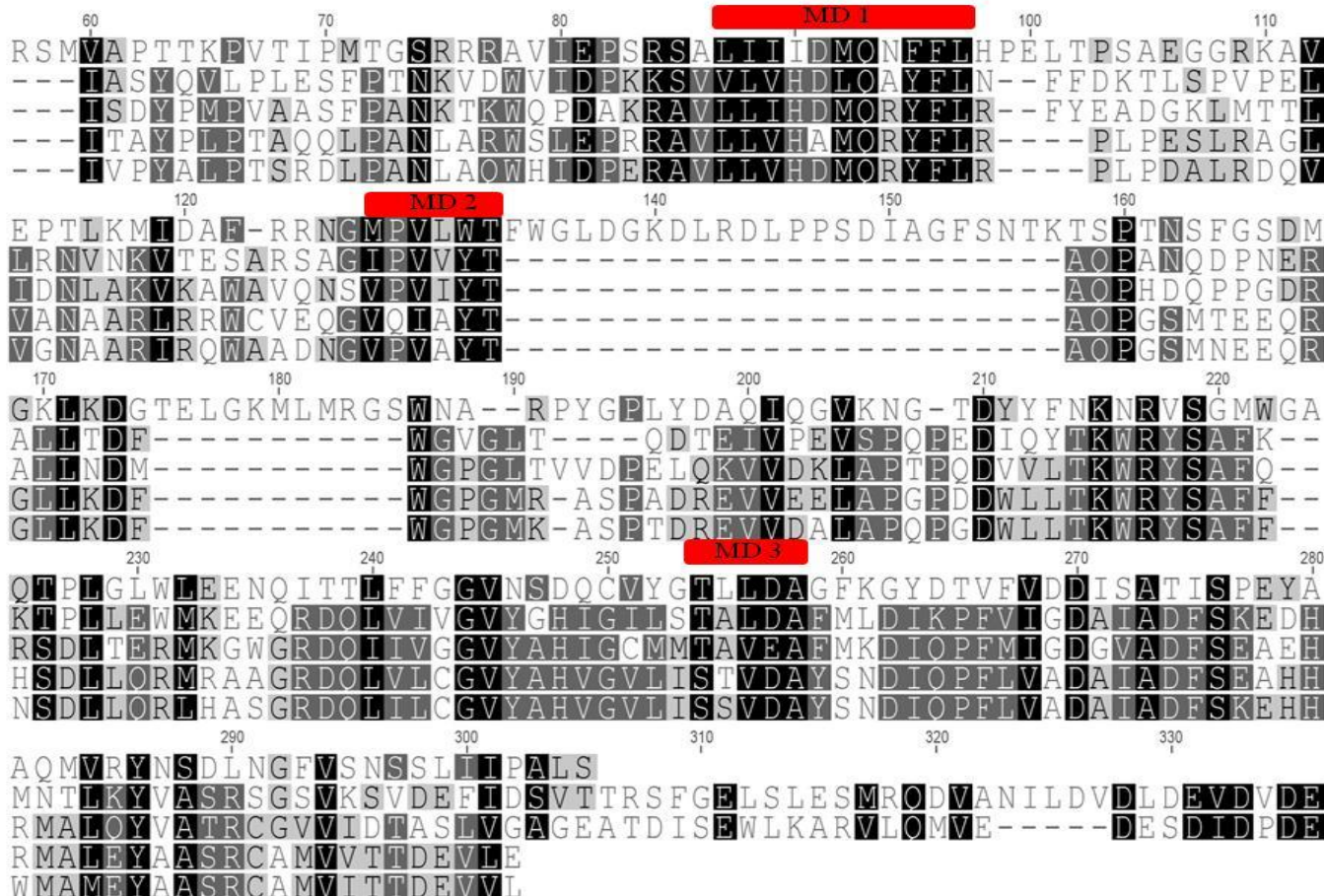


**Figure 4.7. Multiple alignment of PttCHFP1 and selected members of isochorismatase family proteins.** Multiple alignment of the full length of selected sequences which were obtained from NCBI database and aligned using Geneious. Selected regions of the proteins identified in the alignment are displayed. The accession numbers and species names of the sequences are indicated on the left side and the range of the residues from the original sequence is indicated at the top of the sequences. MD, multi domains (1, 2 and 3) are shown in red bars above the sequence, sequence identity shown in black bold and conserved in gray, 5 sequences from different species were aligned using MUSCLE in Geneious software.

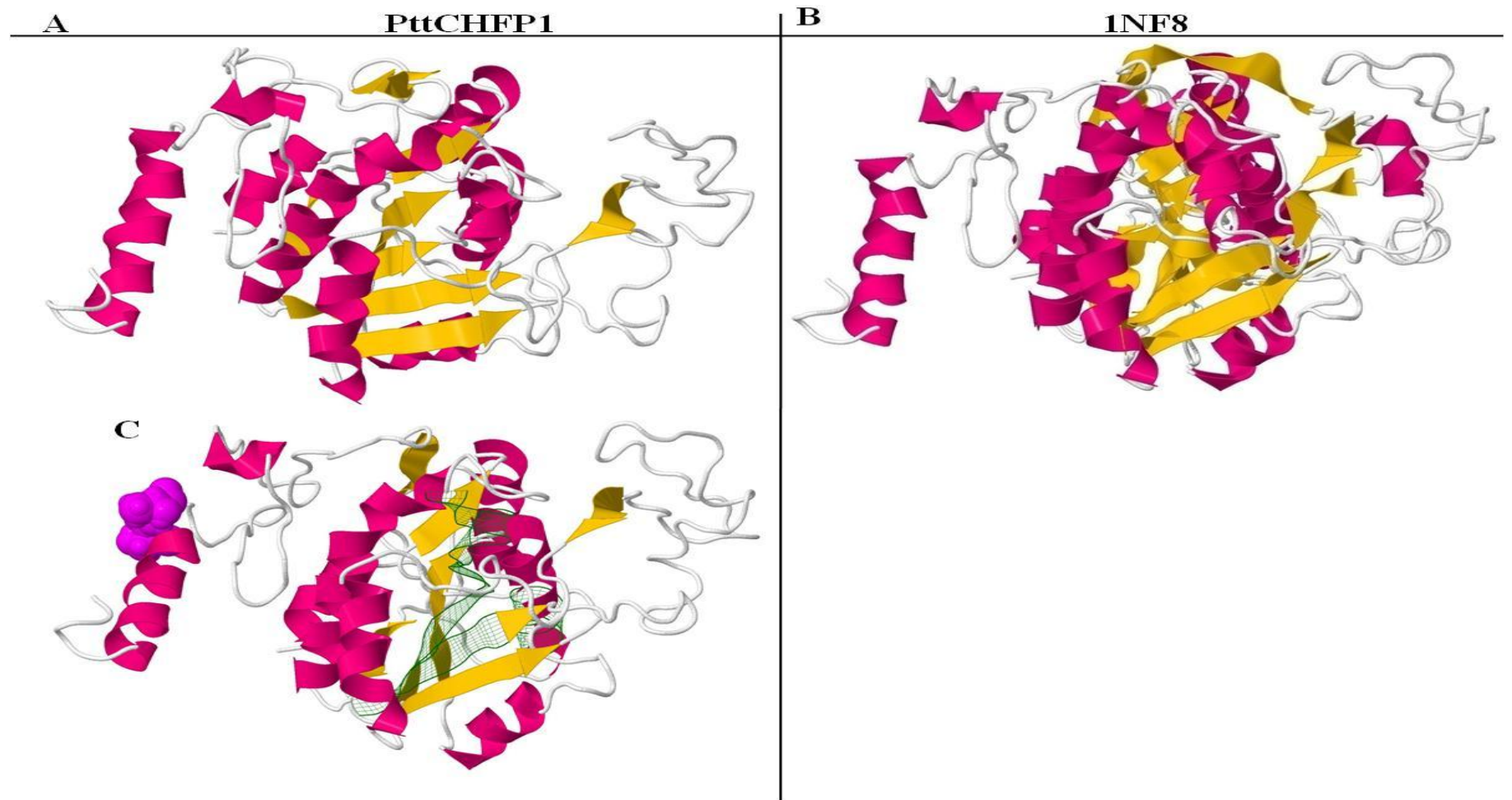


**Figure 4.8.** The predicted three dimensional structure of PttCHFP1 of *Ptt* (A) and *P. aeruginosa* 1NF8 protein (B). The model shows the alpha helical (deep pink), beta strand (orange) and turns (white) secondary structure. (B) the 3D structure of 1NF8, an isochorismatase from *P. aeruginosa* (Parsons *et al.*, 2003). (C) Selected domains (MD1, MD2 and MD3) of PttCHFP1 shown in green mesh, purple balls and sticks indicates the cleavage site.



#### 4.3.2.3 PttGPI-CFEM

The isolated open reading frame of *PttGPI-CFEM* cDNA contained 621 bp that encodes a putative protein consisting of 207 amino acids (Figure 4.9A). SignalP 3.0 showed that PttGPI-CFEM has features of a signal peptide and a cleavage site was located between the 18<sup>th</sup> and 19<sup>th</sup> amino acids (Figure 4.9A). C-terminal GPI-modification site prediction for PttGPI-CFEM was made using a selective fungal-specific algorithm Big-PI ([http://mendel.imp.ac.at/gpi/fungi\\_server.html](http://mendel.imp.ac.at/gpi/fungi_server.html)) (Eisenhaber *et al.*, 2004). The best potential C-terminal GPI-modification sites was predicted at sequence position of the omega-site (aa 185), score of the best site was 18.48 (PValue = 1.330763e-06) (Figure 4.9A). Bioinformatics analysis of PttGPI-CFEM identified CFEM domain which belongs to CFEM superfamily (cl02770) and specifically to family smart 00747 (Figure 4.9B) (Kulkarni *et al.*, 2003).

PttGPI-CFEM easily aligned with four other fungal sequences that also contained the CFEM domain (Figure 4.10A). This domain was identified in the first 95 amino acids of the sequence of the open reading frame. Normally this domain is presented in one copy at the N terminus of fungal membrane protein (Kulkarni *et al.*, 2003). The phylogenetic analysis of PttGPI-CFEM and its homologues from CFEM family showed that the CFEM-containing protein in *C. immitis* and *N. crassa* are the most related species to *Ptt* fungus (Figure 4.10B).

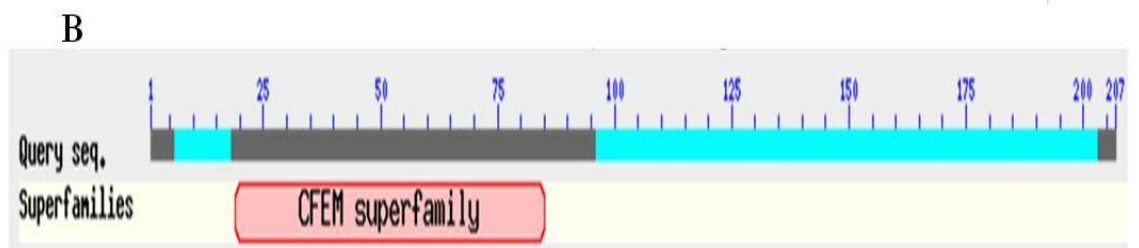
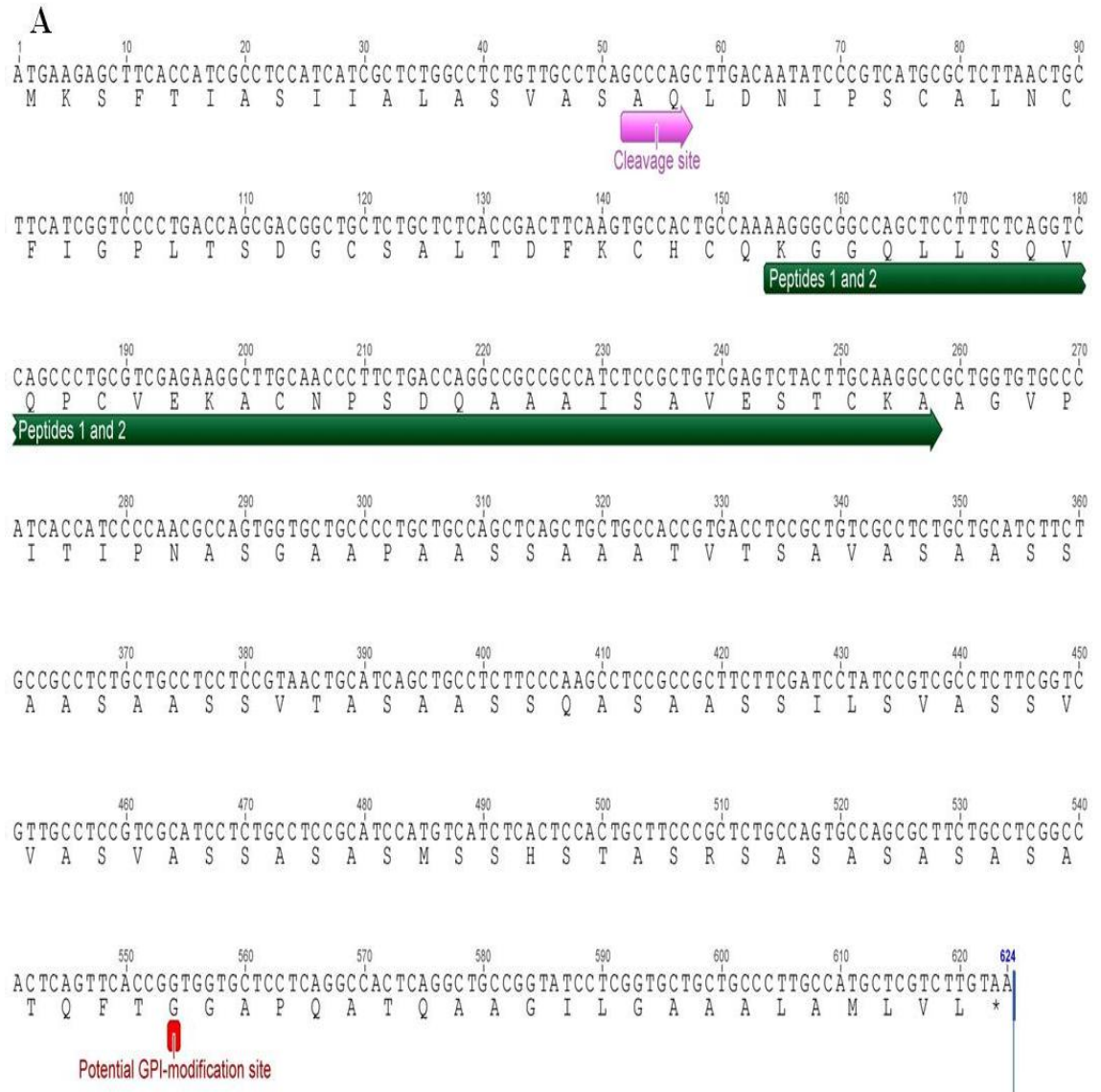


**Figure 4.9. The full length of *PttGPI-CFEM* cDNA and *PttGPI-CFEM* protein (A).** Cleavage site is shown in pink arrow, identified peptides shown in green arrow below the sequence, red square below the sequence shown the potential GPI modification site and star indicates stop codon below the sequence. (B) Graphical summary of conserved domains identified on the full length of *PttGPI-CFEM* amino acid sequence. Domains are colour coded according to superfamilies to which they have been assigned. Superfamily placeholders are drawn in pastel pink colours. Low-complexity regions highlighted as solid cyan blocks.

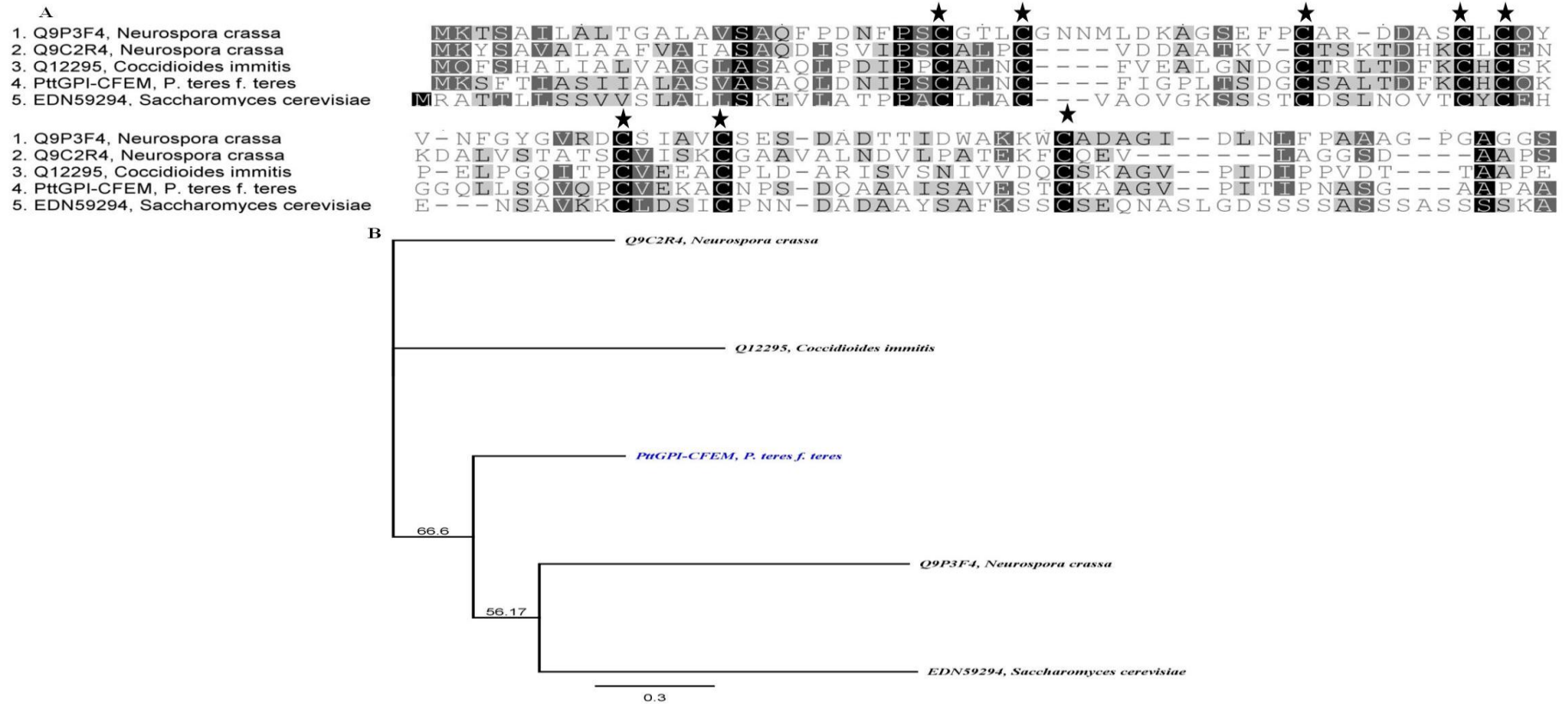


**Figure 4.10. Multiple alignment of PttGPI-CFEM and fungal proteins showing the eight cysteine-containing CFEM domain (A).** Multiple alignment of the full length of selected sequences which were obtained from NCBI database and aligned using Geneious. Selected regions of the proteins identified in the alignment are displayed. CFEM domain (which includes eight cysteine) is indicated by stars, the accession numbers and species names of the sequences are indicated on the left side and the range of the residues from the original sequence is indicated at the top of the sequences. Sequence identity shown in black bold and conserved in gray, 5 sequences from different species were aligned. (B) The evolutionary history of PttGPI-CFEM and its homologues from CFEM family. Phylogenetic analysis was inferred using the Neighbor joining method. The bootstrap consensus tree from 10000 replicates is taken to represent the evolutionary history of 5 taxa. The percentage of replicate trees in which the associated taxa clustered together in the bootstrap test (10000 replicates) are shown next to the branches. The tree is drawn to scale, with branch lengths in the same units as those of the evolutionary distances used to infer the phylogenetic tree. Geneious was used to conduct phylogenetic analysis.

The prediction of secondary structure for PttGPI-CFEM was not similar to the four other members of the CFEM family (Appendix, Figure A2.6). Three dimensional structure modelling of PttGPI-CFEM was predicted with the confidence score (-4.12) and TM-score ( $0.28 \pm 0.09$ ) indicating random similarity to structure template and it contains 7 helices structures, 9 beta sheets and 16 turns (Figure 4.11). The eight cysteine domain was located at the residue numbers 30, 40, 48, 50, 63, 68 and 84. However, the 3D structure has not been determined for any CFEM protein such that a comparison could not be made for the PttGPI-CFEM protein.

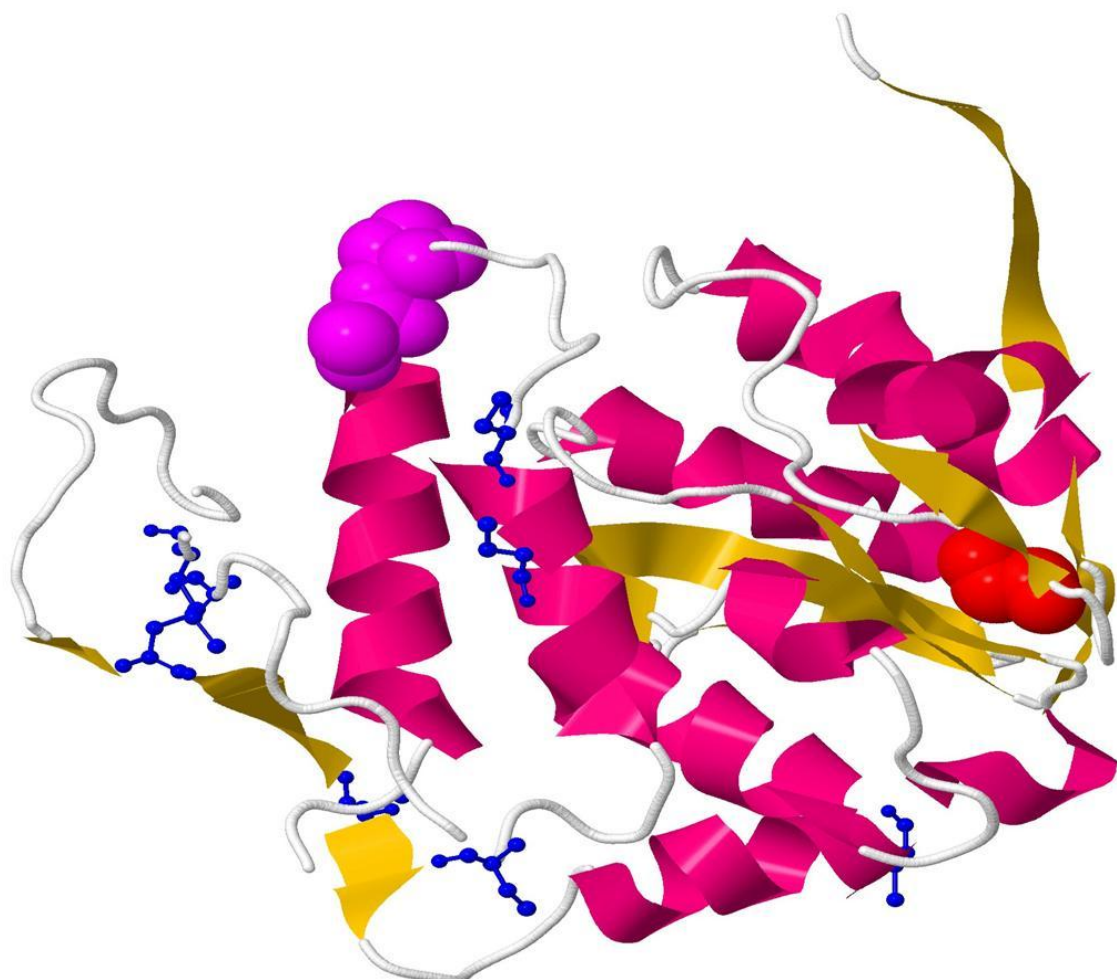


**Figure 4.11.** The predicted three dimensional structure of PttGPI-CFEM of *Ptt*. The model shows the alpha helical structure (deep pink), beta strand (orange) and turns (white) secondary structure, the 8 cysteine residues of PttGPI-CFEM are shown in balls and sticks coded with blue colour. Predicted cleavage and GPI sites are shown in purple and red balls respectively.

#### 4.3.2.4 PttSP1

The isolated full length of *PttSP1* cDNA contained 534 bp that encodes a putative protein consisting of 178 amino acids (Figure 4.12A). The cleavage site for the signal peptide of the protein was located between amino acids 18 and 19 (Figure 4.12A). In addition, a BLASTp search identified homology to this protein, mainly from Ascomycetes, but with unknown function (Appendix, Figure A2.7). PROSITE identified a prokaryotic membrane lipoprotein lipid attachment site (PS51257, PROKAR\_LIPOPROTEIN) in the first 19 aa of the protein (Figure 4.12B). Multiple alignments of PttSP1 with selected sequences, which have this particular site, have shown homology to a bacterial 17 kDa surface antigen protein from *Rickettsia* spp (Figure 4.13). However, all other domain searching tools, NCBI Conserved Domain Search and SMART, did not identify any domain in this protein. In addition, the number of cysteine residues within the mature peptide was 4.4% while the recommended percentage for cysteine in most fungal effectors is 5% (Morais do Amaral *et al.*, 2012). The search for potential degenerative Y/F/WxC motifs often identified in effectors (Godfrey *et al.*, 2010; Morais do Amaral *et al.*, 2012), identified the YxC motif within the first 46 amino acids of the N-terminal methionine. Secondary structure and the three dimensional structure of PttSP1 showed 4 helices, several beta strand sheets and several turns (Figure 4.14). The confidence score of three dimensional structure model of PttSP1 was (-3.43) and TM-score ( $0.34 \pm 0.11$ ) indicating random similarity to the structure template. However, due to the limited information about the homologues of this protein no comparison was made with other 3D structures.

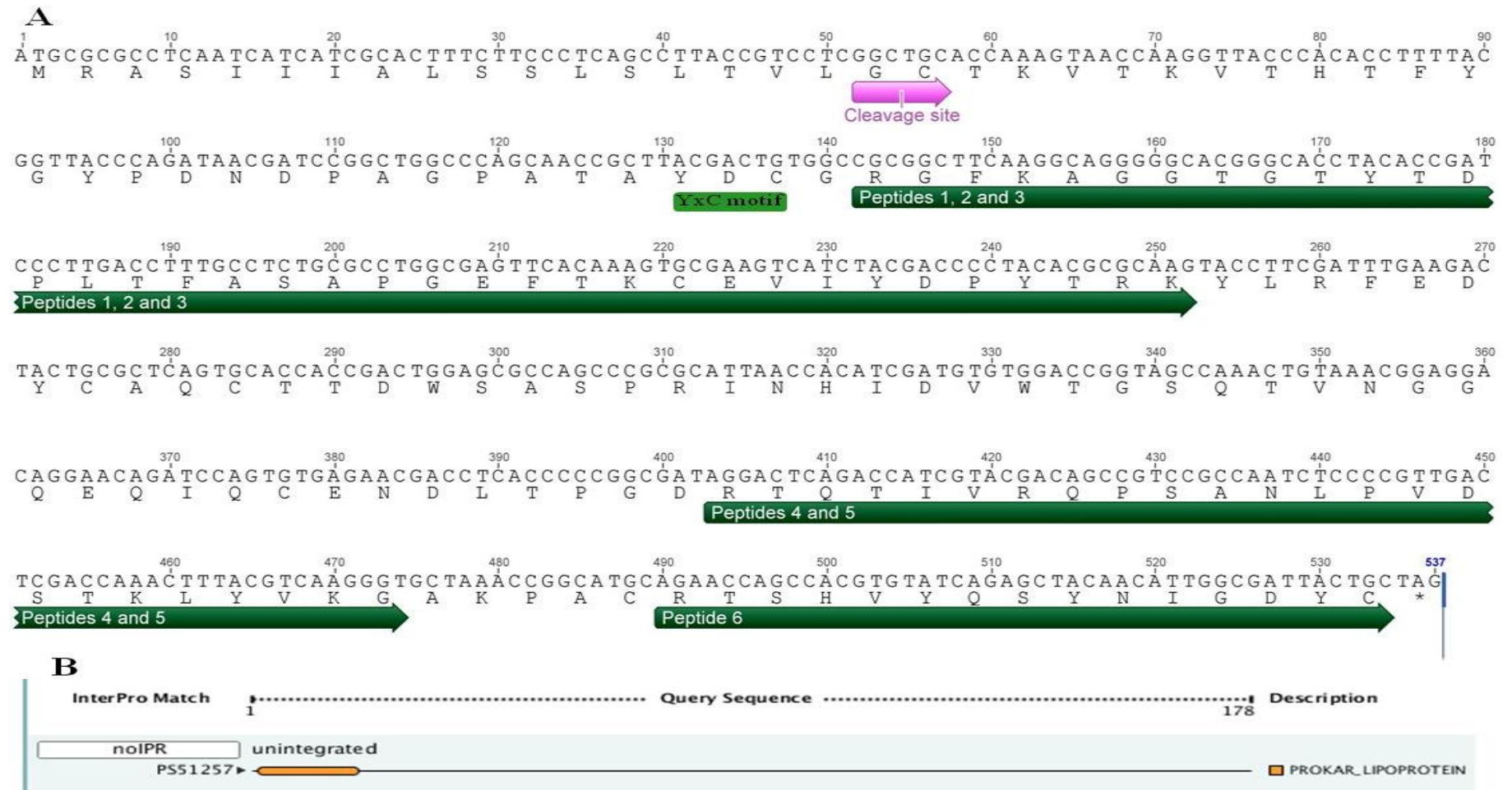


**Figure 4.12. The full length of *PttSP1* cDNA and PttSP1 protein (A).** Cleavage site is shown in pink arrow below the sequence, six identified peptides shown in green arrows below the sequence, YxC motif shown in light green bar, star indicates stop codon. (B) Graphical summary of conserved domains identified on the full length of PttSP1 amino acid sequence. Domain are colour coded according to PROSITE.



**Figure 4.13. Multiple alignment of PttSP1 and bacterial proteins showing lipid attachment site.** Multiple alignment of the full length of selected sequences which were obtained from NCBI database and aligned using Geneious. Selected regions of the proteins identified in the alignment are displayed. The accession numbers and species names of the sequences are indicated on the left side and the range of the residues from the original sequence is indicated at the top of the sequences. Sequence identity shown in black bold and conserved in gray, 4 sequences from different species were aligned.

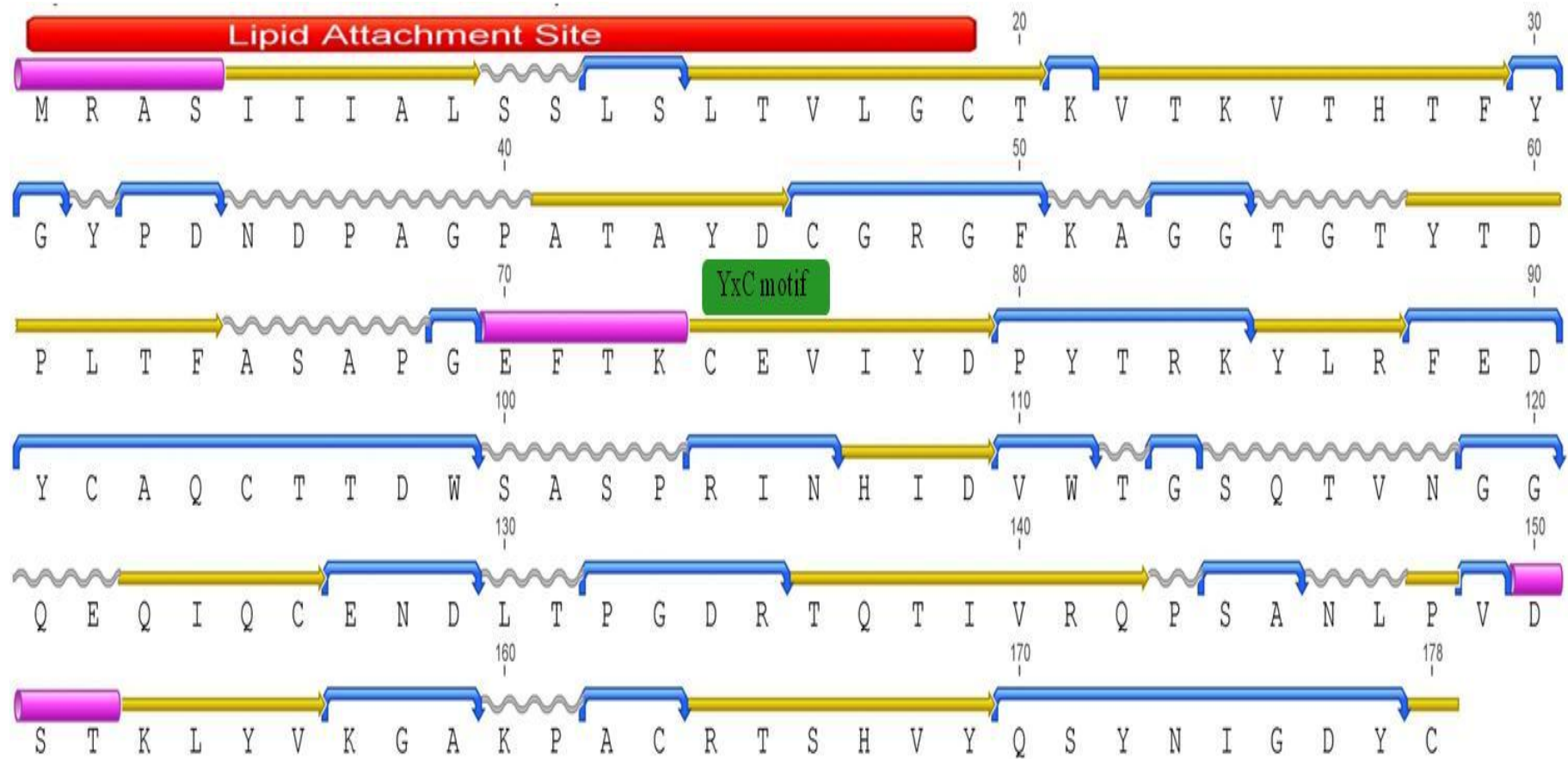


**Figure 4.14. Secondary and three dimensional structure of PttSP1.** Secondary structure predicted based on the EMBOSS prediction tool (Garnier). Alpha helices (purple cylinders), coil (gray curve shapes), Beta strand (yellow arrows) and turn (blue curves) are shown the secondary structure. Potential YxC motif shown in green bar below the sequence.



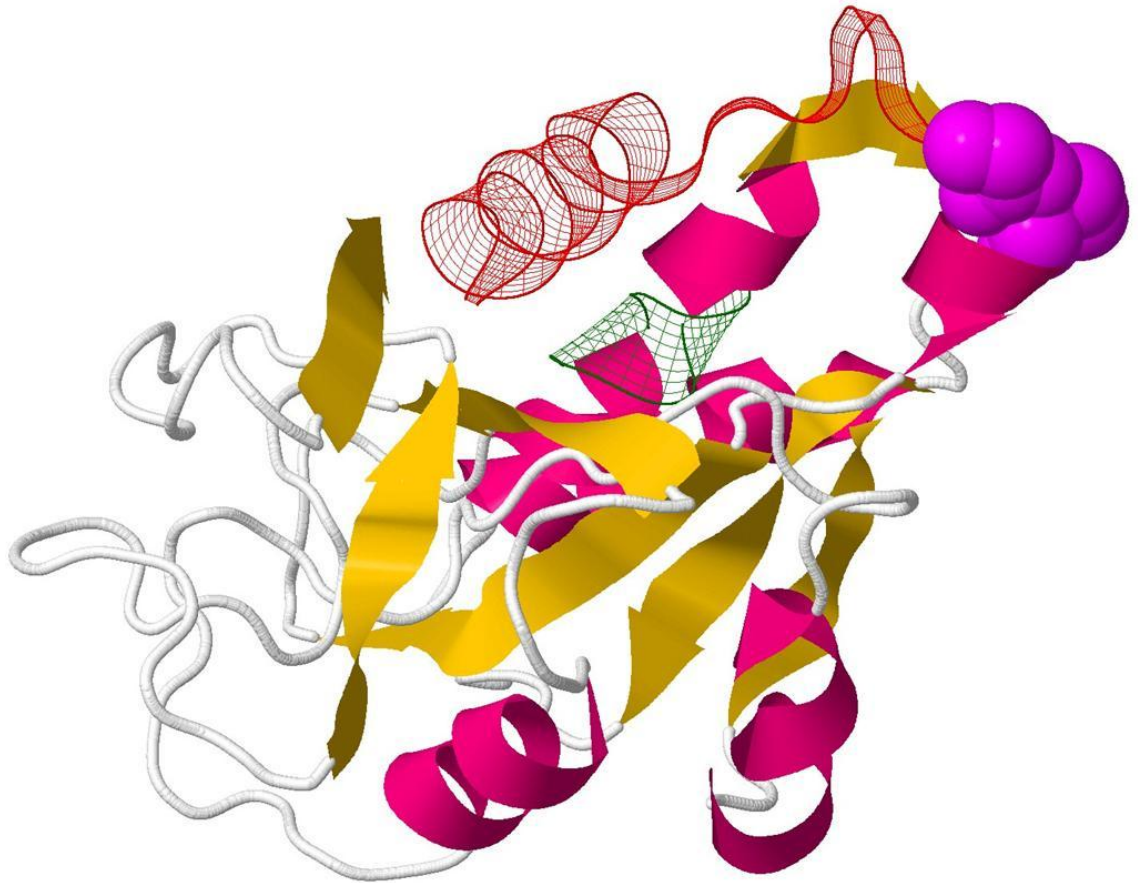


**Figure 4.15. The predicted three dimensional structure of PttSP1 of *Ptt*.** The model shows the alpha helical structure (deep pink), beta strand (orange) and turns (white) secondary structure. The predicted cleavage site is shown as purple ball, lipid attachment site is shown in red mesh and YxC motif shown in green mesh.

### 4.3.3 Semi-quantitative RT-PCR

#### 4.3.3.1 *In vitro*

Expression of the genes encoding the four VRCs (*PttXyn11A*, *PttCHFPI*, *PttSP1* and *PttGPI-CFEM*) was compared in six isolates of *Ptt in vitro* using semi-quantitative RT-PCR after 10 days of culture growth (Figure 4.16). The isolates 08/08f, 32/98 and 152/09 expressed *PttXyn11A* more abundantly compared with the other isolates. *PttCHFPI* was also expressed at a greater level in the most virulent isolates (123/09, 32/98 and 152/09) compared with other isolates. *PttSP1*, *PttGPI-CFEM* and *PttGAPDH* were constitutively expressed but at similar levels for all isolates.

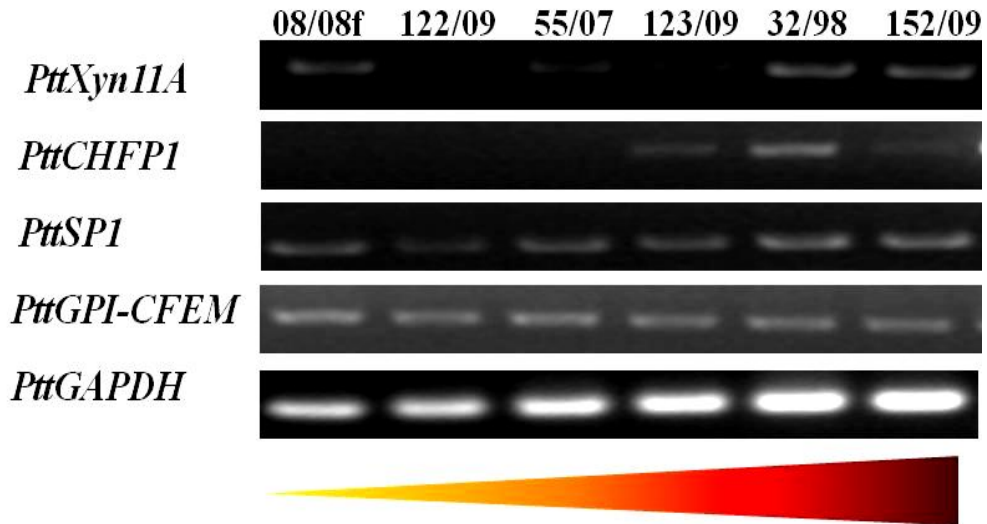


**Figure 4.16. Differences in the expression level of VRCGs for six isolates (*in vitro*) growing for 10 days in FCM.** Using semi-quantitative Reverse Transcription Polymerase Chain Reaction (RT-PCR), *PttXyn11A*, *PttCHFP1*, *PttSP1*, *PttGPI-CFEM* and *PttGAPDH* expression was determined. Red bar indicates the isolates ordered according to the virulence from low to high. Representative image from four biological replicates.

#### 4.3.3.2 *In planta*

Expression of the genes encoding the four VRCs by *Ptt* *in planta* during the interaction was confirmed using semi-quantitative RT-PCR at 192 hpi (Figure 4.17). *PttXyn11A* was expressed more abundantly in barley infected with the most virulent isolates (32/98 and 152/09) compared with the other isolates. *PttCHFP1*, *PttSP1* and *PttGPI-CFEM* were constitutively expressed but at similar levels for all isolates. Although *PttGAPDH* was used as a housekeeping gene, expression differed between isolates probably reflecting the amount of fungus present during the interaction.

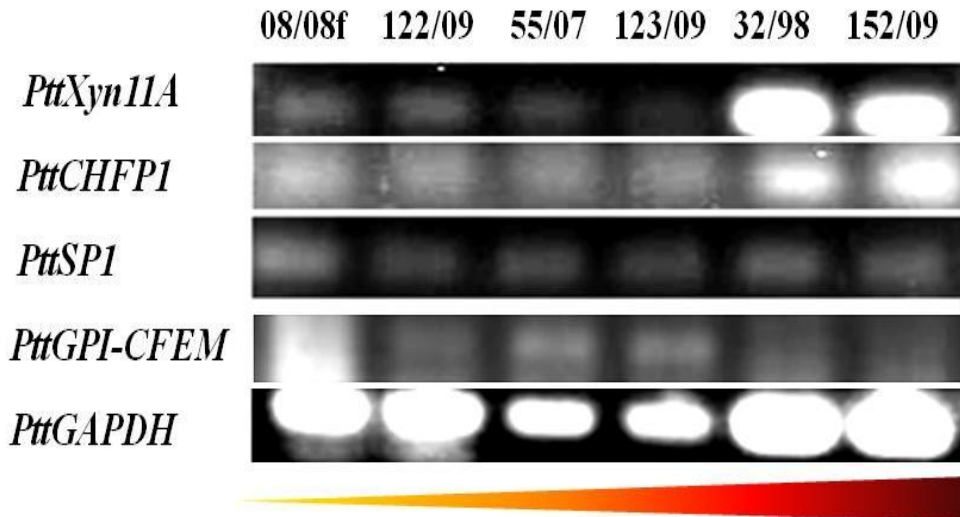


**Figure 4.17. Differences in the expression level of VRCGs for six isolates *in planta* at 192 hours post inoculation.** Using semi-quantitative Reverse Transcription Polymerase Chain Reaction (RT-PCR), *PttXyn11A*, *PttCHFPI*, *PttSP1*, *PttGPI-CFEM* and *PttGAPDH*. Red bar indicates the isolates ordered according to the virulence from low to high (Figure 2.2). Representative image four biological replicates.

#### 4.4 Discussion

The full length of the cDNA for the four candidate virulence genes were successfully isolated using RT-PCR and bioinformatics analysis confirmed that they were encoding an endo 1, 4- $\beta$ -xylanase (*PttXyn11A*), a cysteine hydrolase family protein (*PttCHFPI*), a GPI-anchored CFEM domain-containing protein (*PttGPI-CFEM*) and a secreted protein with unknown function (*PttSP1*) respectively. Regardless of isolate, transcripts of *PttXyn11A*, *PttCHFPI*, *PttSP1* and *PttGPI-CFEM* were detected *in planta* suggesting the potential role of proteinaceous toxins in fungal growth and therefore the infection process of *Ptt*. In particular, transcripts of *PttXyn11A* and *PttGAPDH* were abundantly expressed in the more virulent isolates (32/98 and 152/09). The more virulent isolates may have greater fungal growth (Figure 2.6, 2.8A and B) because of the presence of *PttXyn11A*. Greater fungal growth was confirmed by the abundance of *PttGAPDH* in

more virulent isolates (Figure 4.16 and Figure 4.17) *in planta*. Solomon and Rathjen (2010) and Tan *et al.* (2010) suggest that colonising the tissue and secreting pathogenic proteins are key for successful infection by virulent isolates.

Increasing the number of fully sequenced fungal genomes has provided researchers with powerful comparative analysis options which might help identify proteins produced by phytopathogenic fungi, especially virulence factors or effectors (Ellwood *et al.*, 2010). When this study was initiated, there was limited information about *Ptt* but the *P. tritici-repentis* database helped to indentify candidates and design primers for cDNA isolation. The protein function was predicted by identifying the conserved region in the open reading frame from the cDNA isolated from *Ptt*. Phylogenetic and conserved domain analysis revealed that PttXyn11A shares similarity to the glycosyl hydrolase 11 (GH11) family and has strong homology to the well characterised TrXyn11A and BcXyn11A (Brito *et al.*, 2006; Ellouze *et al.*, 2011; Noda *et al.*, 2010). Moreover, PttXyn11A showed all the characteristics of the GH11 endo- $\beta$ -1,4-xylanases, including the basic pI and low molecular weight that are common for this group (Bailey *et al.*, 1992); the typical jelly-roll topology structure of the GH11 family with two twisted  $\beta$ -sheets enclosing a substrate-binding cleft (Hakulinen *et al.*, 2003); and a 30 aa necrosis-inducing region (Noda *et al.*, 2010; Saarelainen *et al.*, 1993). Xylanase is an important member of this family which is clearly involved in the degradation of plant cell walls (Beg *et al.*, 2001; Beliën *et al.*, 2006; Walton, 1994). This enzyme has been

confirmed as a virulence factor in many fungal species (Gomez-Gomez *et al.*, 2001; He *et al.*, 2009; Jaroszuk-Scisel and Kurek, 2012; Torronen *et al.*, 1992) and mutation of this enzyme in *B. cinerea* resulted in reduction of secondary lesions on tomato leaves (Brito *et al.*, 2006). The necrosis-inducing region in BcXyn11A of *B. cinerea* and TrXyn11A of *T. reesei* showed similarity in the primary, secondary and tertiary structure to PttXyn11A (Brito *et al.*, 2006; Noda *et al.*, 2010). In addition, this region was located at the surface of the enzyme confirming similarity to the well characterised BcXyn11A of *B. cinerea* (Noda *et al.*, 2010). However, catalytic and necrosis-inducing activities need to be confirmed through mutation of the *PttXyn11A* gene in *Ptt*.

PttCHFP1 belongs to the cysteine hydrolase super family and appeared more closely related to the isochorismatase family by having homology to multi domains (Figure 4.7). In addition, PttCHFP1 showed homology to another member of the cysteine hydrolase super family, CSHase (N-carbamoylsarcosine amidohydrolase), which is involved in creatine metabolism and nicotinamidase, converting nicotinamide to nicotinic acid and ammonia in the pyridine nucleotide cycle. Gardiner *et al.* (2012) more recently reported that cereal pathogens produce amidohydrolase proteins that might have a role in pathogenicity towards plants. These proteins are believed to have been horizontally transferred from bacteria (Gardiner *et al.* 2012). Bioinformatic analysis showed that PttCHFP1 has also shared homology with bacterial amidohydrolase proteins (Appendix, Figure A2.2 and Figure A2.3), supporting the Gardiner *et al.*

(2012) findings. The isochorismatase enzyme, also known as phenazine biosynthesis protein (PhzD) and as 2,3 dihydro-2,3 dihydroxybenzoate synthase (Mavrodi *et al.*, 1998; Parsons *et al.*, 2003), is involved in phenazine biosynthesis (Parsons *et al.*, 2003). Several functions have been suggested for this enzyme including antibiotic activity, where *PhzD* along with 3 other genes from the same family have been shown to be involved in the production of PCA (Mavrodi *et al.*, 1998). PCA has antibiotic ability against a variety of fungal root pathogens and the phenazines might provide *Pseudomonas* spp. with a competitive advantage (Parsons *et al.*, 2003). However, whether this compound would be produced by a fungal leaf pathogen such as *Ptt* and therefore be used to provide a competitive advantage against other pathogens needs to be established. Isochorismatase has been shown to inhibit salicylic acid production through the removal of the precursor isochorismate to repress plant defences (El-Bebany *et al.*, 2010; Kunkel and Brooks, 2002; Soanes *et al.*, 2008; Wildermuth *et al.*, 2001), suggesting that *PttCHFPI* might have a similar function during the interaction with barley. RT-PCR results showed that *PttCHFPI* was expressed constitutively at similar levels for all *Ptt* isolates *in vitro*, however there was a different level of expression *in planta* at 192 hpi especially in the more virulent isolates. This difference was probably due to the amount of fungus present *in planta* as evidenced by *PttGAPDH* expression level of these isolates (Figure 4.17). Whether *PttCHFPI* is expressed in the early stages needs to be investigated.

The GPI-modification site was identified in the *PttGPI-CFEM* protein in *Ptt* metabolites. The first GPI protein was characterised in *F.*

*oxysporum* f. sp. *lycopersici* (Schoffemeer *et al.*, 1999; Schoffemeer *et al.*, 2001) and has been shown to be required for morphogenesis, plant-pathogen interactions, virulence (Castro *et al.*, 2005), cell wall polysaccharide remodeling (Hartl *et al.*, 2011) and cell wall construction (Cabib *et al.*, 2007; Mouyna *et al.*, 2000). Conserved domain alignment of PttGPI-CFEM with CFEM family members showed an eight cysteine domain (CFEM domain), which has been proposed to have a role in pathogenesis (DeZwaan *et al.*, 1999; Kulkarni *et al.*, 2003). Several functions were suggested for CFEM proteins including appressorium development (DeZwaan *et al.*, 1999), acting as cell-surface receptors or signal transducers, or as adhesion molecules (Kulkarni *et al.*, 2003). Fungal-secreted hydrophobins, containing eight cysteines in the mature protein sequence, facilitate attachment to hydrophobic surfaces (Bayry *et al.*, 2012). Kulkarni *et al.* (2003) analysed 25 fungal membrane sequences and found that most of the proteins had one copy of the CFEM domain, a few of them had more than one copy and no other domains were detected with CFEM-containing proteins. This study found that PttGPI-CFEM has one copy of this domain, and also had a GPI-anchor domain. RT-PCR results showed great similarity in the expression profile of *PttGPI-CFEM* in six isolates of *Ptt* both *in vitro* and *in planta*, which was not surprising as CFEM-domain containing proteins appear to be required for essential pathogenesis processes like adhesion and networking (DeZwaan *et al.*, 1999; Kulkarni *et al.*, 2003). Therefore, all *Ptt* isolates expressed this protein, probably allowing growth and infection in barley, regardless of their virulence (Figure 2.2).

PttSP1 did not have any conserved domains except the membrane lipoprotein lipid attachment site, this site includes signal peptide cleavage and attachment of glyceride-fatty acid lipids which have been proposed to anchor proteins in the membrane as a part of membrane lipoprotein synthesis (Hayashi and Wu, 1990). In addition, PttSP1 has showed homology to a 17 kDa surface antigen protein from bacterial species. Ellwood *et al.* (2010) predicted several secreted surface antigens using both WolfPSORT and SignalP in the *Ptt* genome and these proteins were annotated as pathogenesis proteins. The YxC motif, commonly found in effectors, was identified at 44 to 46 aa. However, the motif must be within the first 45 amino acids from the cleavage site to be considered as an effector (Brown *et al.*, 2012; Godfrey *et al.*, 2010; Morais do Amaral *et al.*, 2012). RT-PCR at 192 hpi did not show differences in the level of *PttSP1* between isolates *in vitro* and *in planta*, however whether PttSP1 is produced in the early stages of infection needs to be established.

Identification and characterisation of PttXyn11A, PttCHFP1, PttGPI-CFEM and PttSP1 in the mixture of *Ptt* culture filtrates might provide a better understanding of the *Ptt*-barley interaction. In addition, the observation that proteins similar to other fungi have been shown to be induced in virulence (as discussed above) has promoted further investigations into possible function. Therefore, timing of expression of VRCs needs to be established as well as whether they induce symptoms observed in NFNB.



## Chapter 5 Heterologous expression and bioassays of virulence-related candidate proteins (VRCs)

### 5.1 Introduction

*Pyrenophora teres* produces several proteins with phytotoxic activity (Liu *et al.*, 2011; Sarpeleh *et al.*, 2007; 2008; Wong, 2010; Wong *et al.*, 2012), that may induce cell necrosis (Sarpeleh *et al.*, 2007; Turkkan and Dolar, 2008) by interacting with a specific plant target (Manning and Ciuffetti, 2005; Manning *et al.*, 2007). Other proteins might suppress the plant defence systems (Templeton *et al.*, 1994); modify the structure of the plant cellular membrane (Carresi *et al.*, 2006); or act as elicitors that stimulate plant defence (Angelova *et al.*, 2006; He *et al.*, 2007; Templeton *et al.*, 1994). Research presented in an earlier chapter identified several candidate proteins from *Ptt* (Table 3.8) and bioinformatics analysis suggested that some of these toxins might have a role in their pathogenesis and/or virulence (Section 4.4). PttXyn11A, a homolog to endo 1, 4- $\beta$ -xylanase, has suggested roles in plant cell wall degradation (Beg *et al.*, 2001; Jaroszuk-Scisel and Kurek, 2012) and as a necrosis-inducing agent (Nguyen *et al.*, 2011; Rotblat *et al.*, 2002). The potential function of PttCHFP1, homolog to isochorismatase, may be to repress the plant defence system (El-Bebany *et al.*, 2010; Kunkel and Brooks, 2002; Soanes *et al.*, 2008; Wildermuth *et al.*, 2001), while PttGPI-CFEM may have a role in cell adhesion (Bayry *et al.*, 2012; Kershaw and Talbot, 1998; Kulkarni *et al.*, 2003), appressorium development (DeZwaan *et al.*, 1999) and fungal membrane modification which might contribute to pathogenesis (DeZwaan *et al.*, 1999). PttSP1 was not homologous with any known protein, but contains an unconfirmed

effector motif suggesting a potential contribution to fungal development (Hayashi and Wu, 1990). However, the function of each of these *Ptt* proteinaceous toxins requires confirmation.

Several fungal toxins have been expressed heterologously and biologically tested including Ptr ToxB and Ptr ToxA of *P. tritici repentis* (Kim and Strelkov, 2007; Tuori *et al.*, 2000); SnToxA, SnTox1, SnTox2 and SnTox3 (Friesen and Faris, 2010; Friesen *et al.*, 2008b); and endo-1,4- $\beta$ -xylanase of *Phanerochaete chrysosporium* (Khan *et al.*, 2002). Heterologous expression for these proteins was conducted using either *Escherichia coli* or *Pichia pastoris* (Carresi *et al.*, 2006; Hartl *et al.*, 2011; He *et al.*, 2009; Kars *et al.*, 2005; Tanaka *et al.*, 2004). Having a pure source of the enzymes also allows their biochemical function to be explored, such as has been done for heterologously expressed endoxylanase previously (Bailey *et al.*, 1992; Jun *et al.*, 2009). Therefore, the aims of research presented in this chapter were to heterologously express the four VRCGs (Table 3.8) using *E. coli*, the most common heterologous protein expression system (Carresi *et al.*, 2006), and to assess the toxicity of these recombinant proteins on barley. In addition, endoxylanase activity was evaluated for *Ptt* isolates using a xylanase assay.

## **5.2 Material and methods**

### **5.2.1 Cloning of cDNA of VRCGs**

Cloning was conducted using the Gateway cloning system (Invitrogen, USA) with ligation of PCR products into pCR<sup>®</sup>8 which was then

transformed into the TOPO10 strain of *E. coli*. Four cDNA clones (*PttGPI-CFEM*, *PttXyn11A*, *PttCHFPI* and *PttSPI*) encoding candidate proteins were used for transformation. The full length of cDNA was amplified using RT-PCR from RNA extracted from 10 day old cultures of *Ptt* as per section 4.2.1.4. PCR products for these genes were extracted from gels as per section 4.2.1.5 and then transformed into the pCR<sup>®</sup>8 vector using the pCR<sup>®</sup>8/GW/TOPO<sup>®</sup> TA Cloning Kit (Invitrogen, USA) following the manufacturer's protocol. Genes were transformed into the heat-shock competent TOPO10 strain of *E. coli*, and incubated at 37°C for 3 h. Cells being transformed were placed onto Luria Bertani (LB) agar plates containing 100 µg/mL spectinomycin (Sigma-Aldrich) and incubated at 37°C overnight. Ten colonies were then picked using sterilised pipette tips and dipped into a PCR reaction master mix before being transferred into 25 mL of LB media amended with 100 µg/mL spectinomycin and incubated overnight at 37°C. Each PCR reaction contained 2.5 µL of 10x PCR buffer minus Mg<sup>++</sup>, 0.75 µL of 50 mM MgCl<sub>2</sub>, 0.5 µL of 10 mM dNTP mix, 1 µL of 10mM of each corresponding forward and reverse primers (Table 4.1), 0.1 µL of Taq<sup>®</sup> DNA polymerase (5 units/µL) and 19.15 µL of SNW (Invitrogen, USA). PCR reactions were placed into the BioRad DNA Engine Dyad Cycler and DNA amplification was conducted as per section 4.2.1.4, and PCR products were visualised as per section 4.2.1.3 where the PCR product was the expected size (*PttCHFPI*, 906 bp; *PttXyn11A*, 696 bp; *PttGPI-CFEM*, 625 bp; and *PttSPI*, 537 bp) (Table 4.1). A small volume of each overnight colony (grown in LB media) was stored as a 50% glycerol

stock while the remainder was used to extract the plasmid with the PureLink™ Quick Plasmid Miniprep Kit (Invitrogen) according to the manufacturer's instructions. Plasmid concentration was measured as per 4.2.1.3. All plasmids were sequenced and analysed as per section 4.2.1.5 using the M13 forward and reverse primers and the in frame orientation was confirmed within the pCR®8 vector. The vectors where the ORF of interest was confirmed to be in frame were then used for heterologous expression using the pDEST17 vector system which allows protein expression and purification [due to the 6xHis tag at the 5' end of the multiple cloning site (MCS)].

## **5.2.2 Heterologous expression of candidate proteins**

VRCGs were ligated into the pDEST17 (Invitrogen) vector before being transformed into *E. coli* for heterologous expression.

### **5.2.2.1 Ligation of PCR amplicons in pDEST17 vector**

The appropriate volume containing 150 ng of pCR®8 plasmid (for each individual VRCG) was used for ligation according to the manufacturer's protocol using the LR Clonase™ II enzyme mix (Invitrogen) and DH5α™ *E. coli* cells (used as a host for cloning and to enable sequencing). After recombination, cells were incubated at 37°C for 3 h and then plated onto LB agar containing 100 µg/mL ampicillin (AMRESCO, USA) and grown at 37°C overnight. Successfully transformed colonies were confirmed using colony PCR and the plasmid extracted as per section 5.2.1, and then sequenced using the AGRF protocol as per section 4.2.1.5 using T7 forward

primer. Geneious software was used to confirm the sequence and the VRCGs were in-frame and correctly oriented before expression.

#### **5.2.2.2 Expression of recombinant protein**

The expression plasmid (pDEST17) was then transformed into BL21-AI™ one shot® chemically competent *E. coli* (Invitrogen, USA) as per the manufacturer's protocol. Colony PCR was used to confirm the positively transformed colonies as per section 5.2.1 and cells were kept at -80°C in 50% glycerol until required. For heterologous expression, two positive colonies were each cultured in 5 mL of LB medium containing 100 µg/mL ampicillin and grown at 37°C and 180 rpm overnight. These cultures were then used to inoculate fresh LB medium containing 100 µg/mL ampicillin before incubating at 37°C until OD<sub>600</sub> reached 0.6 as measured using a Metertech UV/Vis SP8001 spectrophotometer (Metertech Inc., Taiwan). L-arabinose (Sigma-Aldrich) (0.2% or 0.4% w/v) and isopropyl β-D-1-thiogalactopyranoside (IPTG) (Sigma-Aldrich) (100 mM final concentration) were added to one of the cultures (as induced cells), and 0.4% (w/v) D(+)-glucose (MERCK, Germany) to another (as non-induced cells). Induced and non-induced cells were incubated at either 16°C, 23°C or 37°C for either 2 h, 4 h or 6 h at 180 rpm before purification of recombinant protein.

#### **5.2.2.3 Purification of heterologously expressed proteins**

Induced and non-induced cells were harvested by centrifuging the cell culture at 7000 g for 10 min and the wet weight of cell pellets recorded.

Pellets and 1 mL of the supernatant were kept at -80°C until required for protein purification using either denaturing or native conditions. Although denaturing conditions allow the 6xHis-Tag to be exposed to the Ni-NTA matrix ensuring better purification (Crowe *et al.*, 1995), native purification was also necessary to preserve the biological activity of the recombinant proteins for use in the bioassay.

#### **5.2.2.3.1 Purification under denaturing conditions**

Cell pellets were dissolved in buffer B (8 M, urea; 0.1 M, NaH<sub>2</sub>PO<sub>4</sub>; and 0.01 M, Tris HCL; pH 9) on a rotating wheel at room temperature (RT) for 1 h before being sonicated for six times in 10 sec bursts at power output 4 (25 W) (Branson Sonicator B-12, USA) for complete lysis. Lysates were adjusted to pH 9 using concentrated Tris base before loading onto Ni-NTA Spin Columns (Qiagen, Germany). 6xHis-Tag recombinant proteins were bound, washed and eluted as recommended by the manufacturer. Washing and elution steps were conducted using buffers C1, C2, D and E. These buffers were identical to buffer B except the pH was 7.1, 6.3, 5.9 and 4.5 respectively. Fractions from each purification step were kept at -20°C for comparison using PAGE.

#### **5.2.2.3.2 Purification under native conditions**

Native purification buffers were immediately prepared prior to use by making a stock solution (300 mL) of 50 mM NaH<sub>2</sub>PO<sub>4</sub> and 300 mM NaCl which was then divided into three 100 mL aliquots to which 10 mM, 20 mM

or 500 mM of imidazole (Sigma, Aldrich) was added (buffers NP10, NP20 and NP500 respectively). Cell pellets were dissolved in buffer NP10 (pH 9), sonicated, adjusted to pH 9 and then purified using Ni-NTA Spin Columns as per section 5.2.2.3.1. Fractions from each purification step were kept at -20°C for comparison using PAGE and in bioassay tests. Due to a high concentration of salt in purified recombinant proteins, two additional washing steps were conducted using SNW and an Amicon YM-10 filter at 6000 *g* for 10 min before bioassay only.

#### **5.2.2.4 Visualisation and LC-eSI-IT MS identification of expressed recombinant proteins**

To confirm the expression of recombinant proteins, PAGE was performed as per section 2.2.6.3 using NuPAGE<sup>®</sup> Novex<sup>®</sup> Bis-Tris Mini Gels (Invitrogen) by loading 11.5 µL of fractions extracted from each purification (sections 5.2.2.3.1 and 5.2.2.3.2). Coomassie Brilliant Blue staining was conducted as per section 2.2.6.3.1. Bands, that had migrated to the approximate expected size of recombinant proteins, were sent to Adelaide Proteomics Centre (The University of Adelaide) for peptide analysis using LC-eSI-IT MS as described in section 3.2.5.3. The sequence of identified peptides were analysed as per section 3.2.5.3.

#### **5.2.2.5 The effect of recombinant protein on the viability of *E. coli***

Given that some gene products can be toxic to *E. coli* (Saïda, 2001), the effect of successfully expressed recombinant proteins (PttXyn11A, PttCHFP1 and PttSP1) on BL21-AI<sup>™</sup> cell growth was evaluated. Cells were

cultured as described in section 5.2.2.2 and incubated at 37°C and 180 rpm until OD<sub>600</sub> was 0.6. Small aliquots (500 µL) were taken from these cultures (before induction) and serial dilutions (10<sup>-1</sup> to 10<sup>-6</sup>) were made using SNW, one hundred µL of each dilution was spread onto LB agar plates containing 100 µg/mL ampicillin and incubated overnight at 37°C. Colonies were then counted in the 10<sup>-6</sup> dilution because they were easily distinguishable. The cell cultures were either induced with 0.4% (w/v) L-arabinose and 100 mM IPTG or repressed with 0.4% D(+)-glucose as per section 5.2.2.2 and the same dilution as described earlier was also done for cells from induced and non-induced cultures after 2 h incubation at 23°C. The same volume was plated onto LB agar containing 100 µg/mL ampicillin and plates were incubated overnight at 37°C. The number of viable cells was estimated by counting the number of colonies on the plate containing the 10<sup>-6</sup> dilution and multiplying by the dilution factor. Three biological replicates were used.

### **5.2.3 Bioassay of heterologously expressed proteins**

To evaluate the biological activity of expressed recombinant proteins, washed and unwashed purified proteins were injected into barley leaves using several concentrations. Clear lysate fractions (10 µg, 20 µg and 60 µg total protein) and elution fractions (3 µg, 5 µg, 10 µg and 20 µg) were injected into the second leaf at Zadoks' growth stage 14 in a total volume of 200 µL using a Hagborg device as per section 2.2.6.4. Where washed proteins were used, due to low concentrations, 200 µL of protein solution was injected. A mixture of elutions from candidate proteins was also injected to investigate their activity when combined. Symptoms were then



monitored and compared every 24 h up to 10 days post injection. Three individual plants of cv. Sloop, CI9214 and Beecher were used in each experiment and representative leaves were imaged.

Given that PttXyn11A could not be expressed heterologously at high levels using *E. coli*, due to toxic activity, a commercial xylanase [endo-1,4- $\beta$ -xylanase of *Aspergillus niger* (Megazyme International Ireland Limited, Ireland)] was also used in the bioassay. Three concentrations of xylanase from *A. niger* (5  $\mu$ g, 20  $\mu$ g and 76  $\mu$ g), and a mixture of *A. niger* xylanase (5  $\mu$ g), PttCHFP1 (2.4  $\mu$ g) and PttSP1 (20  $\mu$ g) were injected in cv. Sloop as per section 2.2.6.4. SNW and corresponding buffers were used as controls. The volume of buffer required for injection was always determined by the final volume of the recombinant protein. Three biological replicates were used for all treatments and representative leaves were taken after either 4, 5 or 7 days post injection and image captured as per section 2.2.3.

#### **5.2.4 Activity of xylanase in six isolates of *Ptt in vitro***

To measure xylanase activity in the filtrate of *Ptt* isolates and of heterologously expressed PttXyn11A, the XYLAZYME AX kit (Megazyme) was used. Six isolates (Table 2.1) were grown in FCM without trace elements for 15 days at RT without shaking as per section 2.2.6.1. Proteinaceous toxins were extracted using UFP as described in section 2.2.6.2.1 after 10 and 15 days growth. Protein extracted from culture filtrates for each isolate and cell lysates from induced and non-induced cells of recombinant protein PttXyn11A, that had been extracted using native

purification as per section 5.2.2.3.2, were placed in 5 mL yellow capped tubes and mixed with SNW to a final protein concentration of 0.4 µg/µL in a total volume of 300 µL. Three biological replicates of each protein extract were used.

Three hundred µL of SNW was added to 200 µL of control xylanase solution (*A. niger*) (approx. 275 mU/mL) as a positive control. Solutions were vigorously and immediately stirred on a vortex mixer until thoroughly combined. A XYLAZYME AX tablet was placed in each tube and transferred without stirring, to a water bath at 50°C and incubated for 30 min. Five mL of Tris Base solution (1.5 M, pH 9 with HCl) was added and stirred vigorously and incubated at RT for 5 min to terminate the reaction. Solutions were stirred prior to filtration using Whatman No.1 filter paper and then measurements of the absorbance of the filtrates at 590 nm were conducted using a Metertech UV/Vis SP8001 spectrophotometer against a reaction blank. The reaction blank was prepared by the same method but using 0.5 mL SNW instead of the sample. The activity of xylanase in the filtrates of isolates from *Ptt* and recombinant PttXyn11A was calculated using the following equation:

$$\text{Xylanase activity} = \text{Added activity} \times \frac{\text{SA}}{\text{TA} - \text{SA}}$$

Where the added activity = the amount of xylanase added to the water sample (55 mU in the control xylanase solution in 200 µL), SA = sample absorbance obtained for extracts to which no control xylanase was added, TA = the total absorbance to which the control xylanase was added.

### **5.2.5 Statistical analysis and photography**

GenStat was used to analyse three biological replicates as per section 2.2.7.

Photos were taken for representative leaves and gels as per section 2.2.3.

## **5.3 Results**

### **5.3.1 Heterologous expression of VRCPs**

Optimisation was necessary for each of the four candidate proteins to maximise protein yield including cell incubation temperature, the concentration of L-arabinose in LB media and culture incubation time.

#### **5.3.1.1 PttGPI-CFEM**

Denaturing conditions for PttGPI-CFEM purification showed unsuccessful expression for recombinant PttGPI-CFEM. Although, optimised heterologous expression conditions were trialled, clear lysate, flow through, washing and elution fractions did not show differences between induced and non-induced *E. coli* (Figure 5.1).

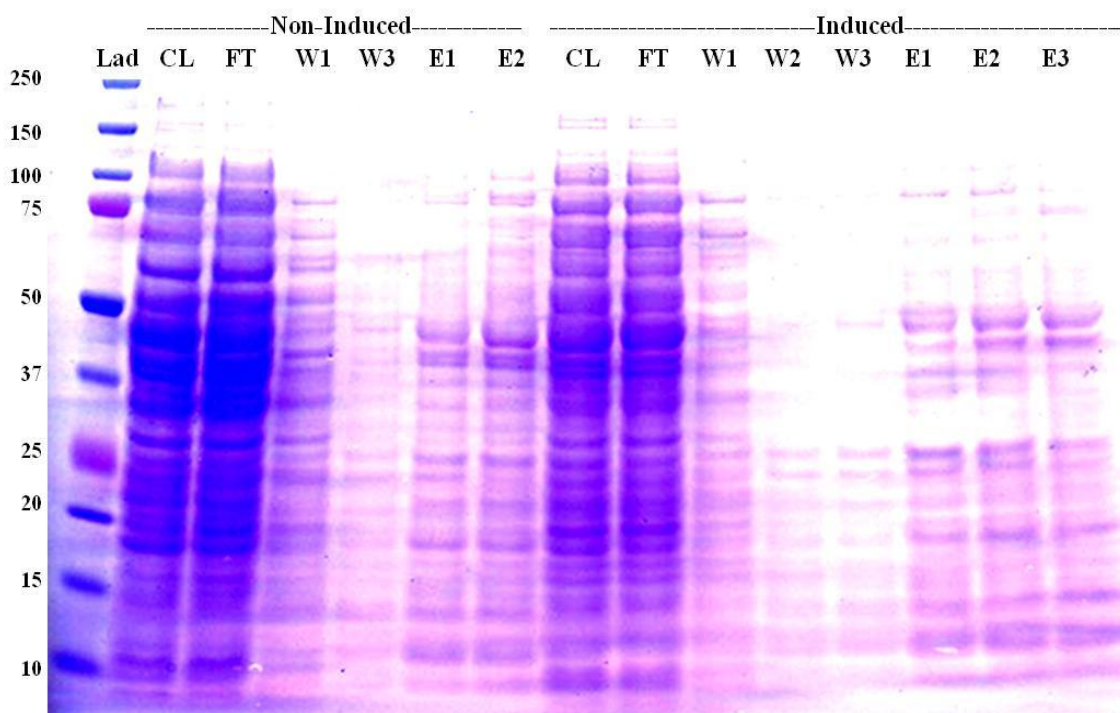


**Figure 5.1. Denaturing purification of PttGPI-CFEM heterologously expressed in *E. coli*.** L-arabinose (0.4%) was added to LB media for induction and D (+)-glucose for repression of recombinant protein, cells incubated at 23°C for 6 h. CL, clear lysate; FT, flow through fractions; W, washing fractions; E, elution fractions. Precision Plus Protein Standard (Lad) was used as marker ladder. Unsuccessful expression of candidate protein, representative image for three gels.

### 5.3.1.2 PttXyn11A

Several optimisations were conducted to express PttXyn11A including the concentration of L-arabinose, incubation time, incubation temperature and protein purification. Using the conditions recommended by the manufacturer, there was no difference between the protein profiles of clear lysate, washing and elution fractions of induced and non-induced cells under denaturing conditions (Figure 5.2A, B) or native conditions at both 16°C and 23°C (Appendix, Figure A3.1). Even though different transformants were used, there was no detected expression (Appendix, Figure A3.2). Potentially, the overexpression of PttXyn11A was toxic to the cells, therefore the expression was compared at three timepoints (2 h, 4 h and 6 h) of incubation at 23°C with either 0.2 or 0.4% L-arabinose, as an attempt to

purify recombinant protein before being degraded. By 6 h incubation, cell lysates had proteins at the expected weight of 30 kDa (Figure 5.3), given that 6xHis tag increases the MW of recombinant protein. The clear lysate fraction after 6 h growth with 0.4% L-arabinose was used to purify the recombinant protein. PAGE showed a band specific to the elution from induced cells (Figure 5.4). This band was sent for sequencing and LC-eSIT MS identified proteins annotated as endogenous *E. coli* proteins (30S ribosomal protein S2, NP\_285863, *E. coli*; 30S ribosomal protein S2, YP\_003611483, *Enterobacter cloacae*; Chain A, X-Ray Crystal Structure Of Tem-1  $\beta$ -Lactamase in Complex With A Designed Boronic Acid Inhibitor (1r)-2- Phenylacetamido-2-(3-Carboxyphenyl)ethyl Boronic Acid, 1ERO\_A, *E. coli*), however, no *Ptt* protein was identified.

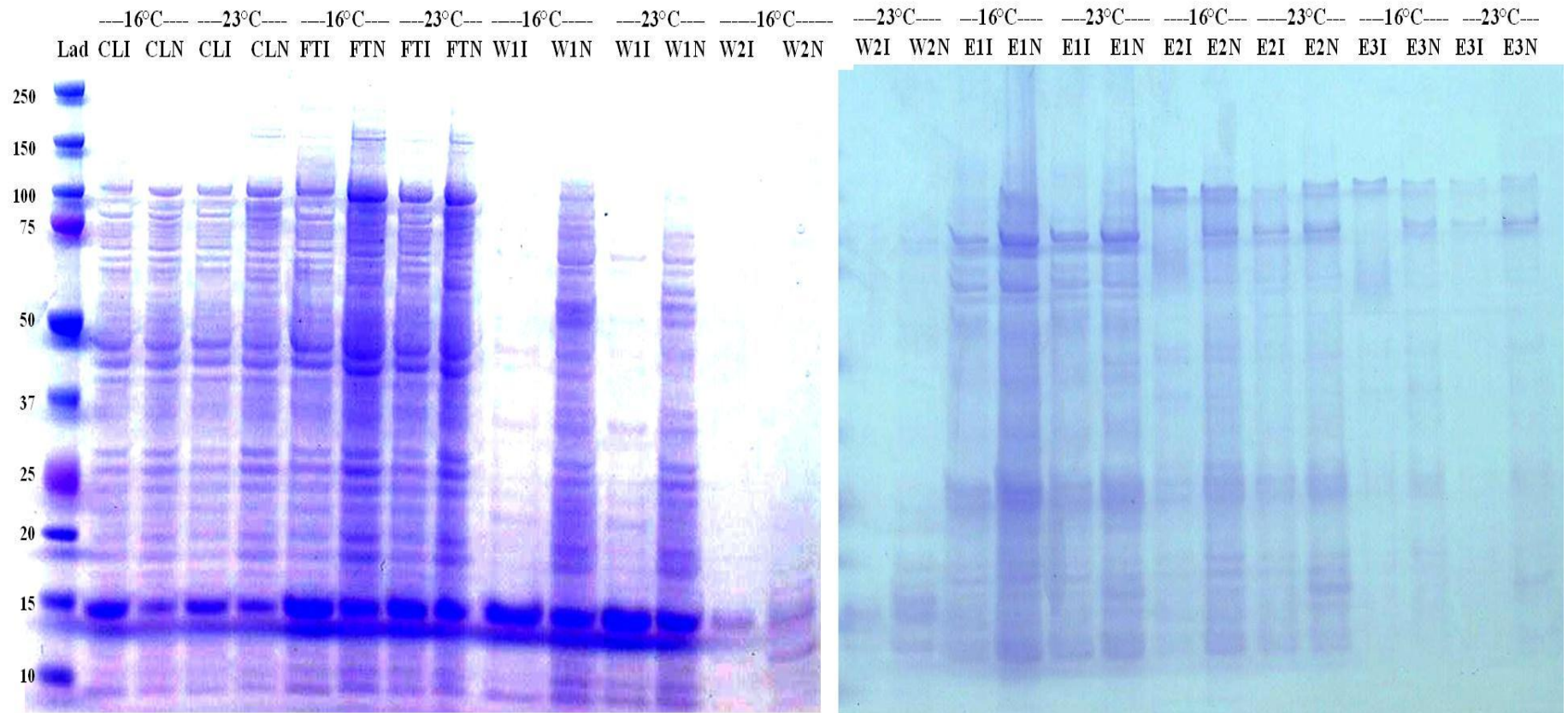


**Figure 5.2. Optimisation of heterologous expression of PttXyn11A in *E. coli* with different temperatures.** Two incubation temperature (16°C and 23°C) were used, L-arabinose (0.4%) was added to LB media for induction and D (+)-glucose for repression of recombinant protein, cells incubated for 6 h. Denaturing conditions were used for protein purification. CLI, clear lysate fractions for induced cells; and CLN, non-induced; FTI, flow through fraction for induced cells; FTNI, flow through non-induced; WI, two washing fraction for induced; WN, two washing for non-induced; EI, three elutions fractions for induced cells; and EN, two elutions non-induced. Precision Plus Protein Standard (Lad) was used as marker ladder, representative gel for two replicates.

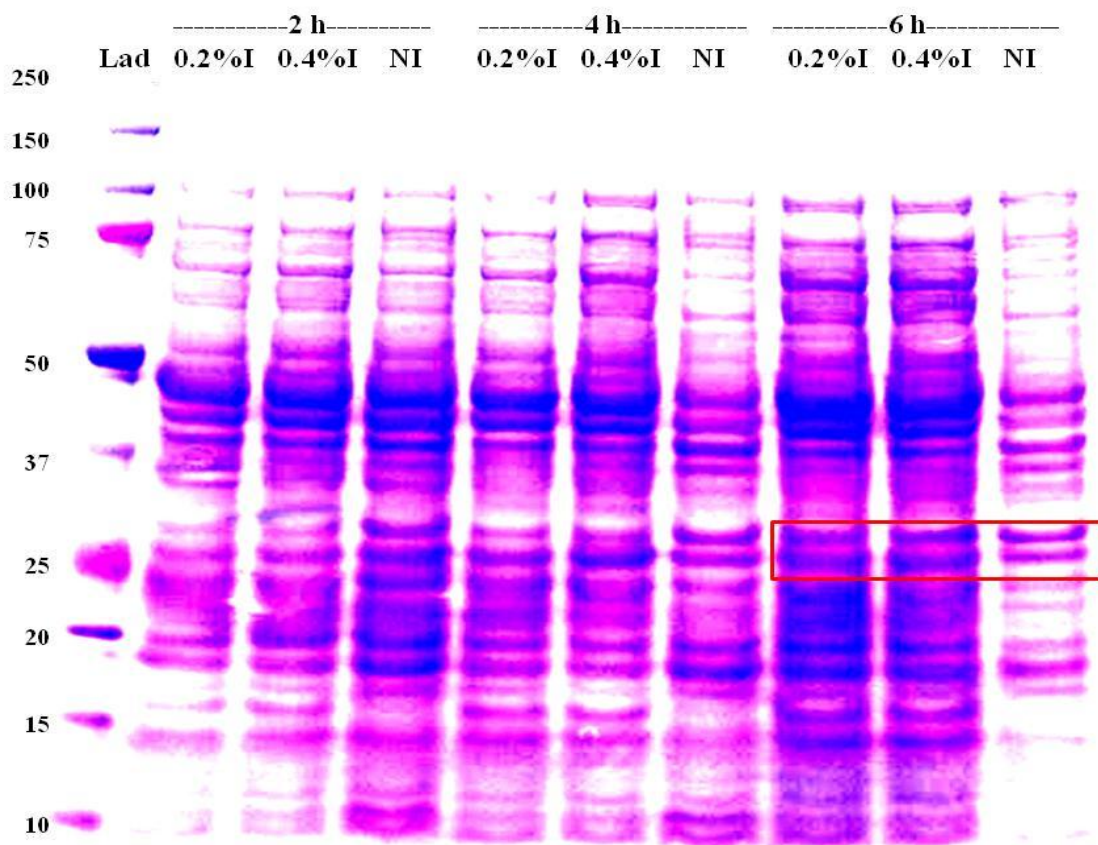


**Figure 5.3. Optimisation of heterologous expression of PttXyn11A in *E. coli* with different incubation time and L-arabinose concentration.** Three incubation times (2 h, 4 h and 6 h) and two concentrations of L-arabinose (0.2% and 0.4%) at 23°C were used. D (+)-glucose was used to repress the expression of recombinant protein. Denaturing conditions were used for protein purification. I, clear lysate fractions for induced cells; and NI, non-induced were loaded in PAGE, Precision Plus Protein Standard (Lad) was used as marker ladder. Red rectangle indicates the increased density of two bands in which the PttXyn11A was potentially differently expressed in induced cells. Incubation for 6 h with 0.4% L-arabinose was used for heterologous expression. Representative gel for two replicates.

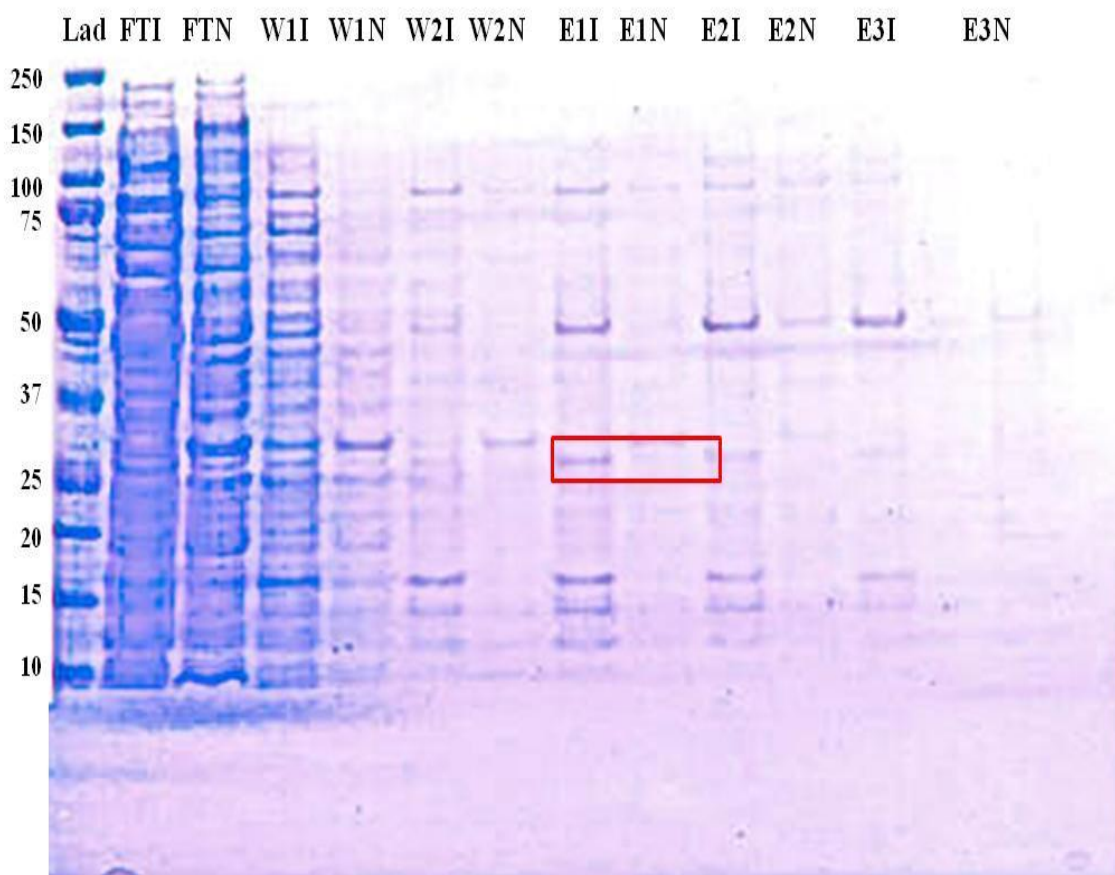


**Figure 5.4. Heterologous expression of PttXyn11A in *E.coli*.** L-arabinose (0.4%) was added to LB media for induction and D (+)-glucose for repression of recombinant protein, cells incubated at 23°C for 6 h. Denaturing conditions were used for protein purification from clear lysate of cell grown for 6 h with 0.4% L-arabinose (Figure 5.3), FTI, flow through fraction for induced cells; FTNI, flow through non-induced; WI, two washing fractions for induced; WN, two washing fractions for non-induced; EI, two elutions fractions for induced cells; and EN, two elutions fractions non-induced. Precision Plus Protein Standard (Lad) was used as marker ladder. Red rectangle indicates the protein which was differentially expressed in induced cells but not in non-induced, this band was sequenced using LC-eSI-IT MS. Representative gel for two replicates.

Given that *E. coli* appeared incapable of expressing PttXyn11A at a detectable level, a viability test was conducted to investigate the toxicity of PttXyn11A to *E. coli*. The number of viable cells was significantly lower after 2 h of induction compared with before the induction ( $P < 0.001$ ,  $LSD = 5.47E+08$ ) (Figure 5.5), suggesting that PttXyn11A may have been produced.



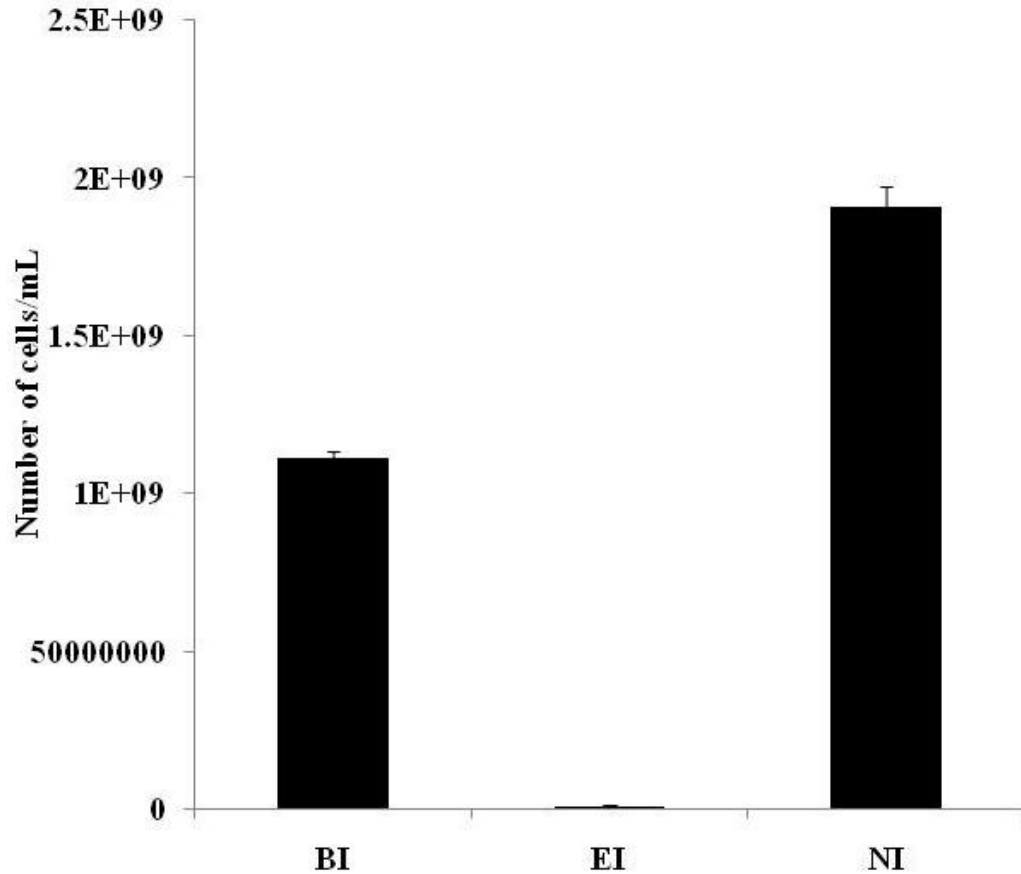


**Figure 5.5. The effect of overexpression of PttXyn11A on the viability of *E. coli*.** Graph shows BI, number of living cells before the induction; and EI, at the end of the induction compared with NI, non-induced cells. Three replicates in two individual experiments, ( $P < 0.001$ ,  $LSD = 5.47E+08$ ). Error bars represent the standard error of the mean of three replicates.

### 5.3.1.3 PttCHFP1

Incubating *E. coli* for 6 h at 23°C induced expression of a protein with the approximate molecular size of PttCHFP1 (30-37 kDa) (Figure 5.6). Level of L-arabinose (0.2% or 0.4%) had no obvious effect on the expression of PttCHFP1 while incubation for 6 h increased the expression of proteins compared with 4 h at both temperatures (23°C and 37°C). However, incubation at 16°C produced a lower amount of proteins (appendix, Figure A3.3). Therefore, heterologous expression of PttCHFP1 was carried out using 0.4% L-arabinose at 23°C for 6 h (Figure 5.7). PAGE analysis

demonstrated that elution 2 and 3 from induced cells contained proteins which migrated to a molecular weight of 37 kDa. LC-eSI-IT MS analysis confirmed that the differentially expressed protein contained peptides which matched to protein annotated as isochorismatase (XP\_001932705 in *P. tritici-repentis*) and PttCHFP1 (JX900134 in *Ptt*, chapter 4). Native purification of PttCHFP1 also confirmed the expression of this protein evidenced by large bands present at the same molecular weight in both elution 1 and 2 from induced cells (Figure 5.8).

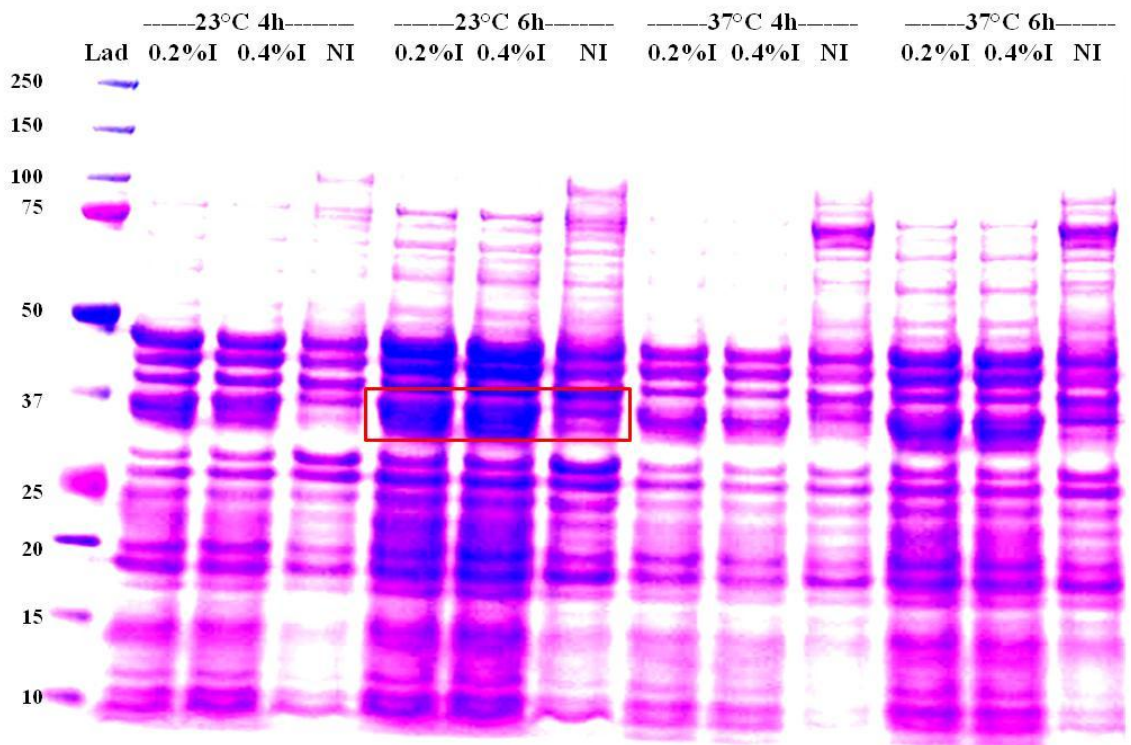


**Figure 5.6. Optimisation of heterologous expression of PttCHFP1 in *E. coli* with different incubation conditions and L-arabinose concentration.** Two incubation times (4 h and 6 h) and two concentrations of L-arabinose (0.2% and 0.4%) at two incubation temperatures (23°C and 37°C) were used, D (+)-glucose was used to repress the expression of recombinant protein. Denaturing conditions were used for protein purification. I, clear lysate fractions for induced cells; and NI, non-induced were loaded in PAGE. Precision Plus Protein Standard (Lad) was used as marker ladder. Red rectangle indicates the increased density of two bands in which the PttCHFP1 appeared to be differentially expressed in induced cells but not in non-induced.

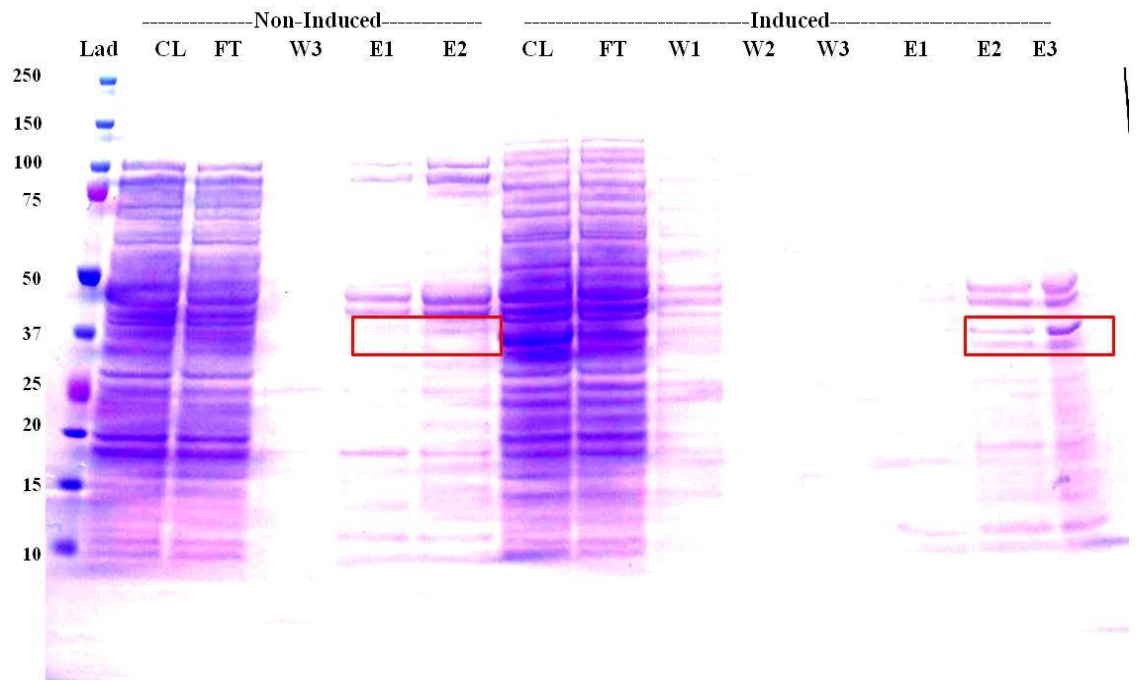


**Figure 5.7. Heterologous expression and denaturing purification of PttCHFP1 in *E.coli*.** L-arabinose (0.4%) was added to LB media for induction and D (+)-glucose for repression of recombinant protein, cells incubated at 23°C for 6 h. Denaturing conditions were used for protein purification: CL, clear lysate; FT, flow through fraction; W, washing fraction; E, elutions fractions. Precision Plus Protein Standard (Lad) was used as marker ladder. Red rectangles indicate the protein which was differentially expressed in induced cells but not in non-induced, this band was sequenced using LC-eSI-IT MS.

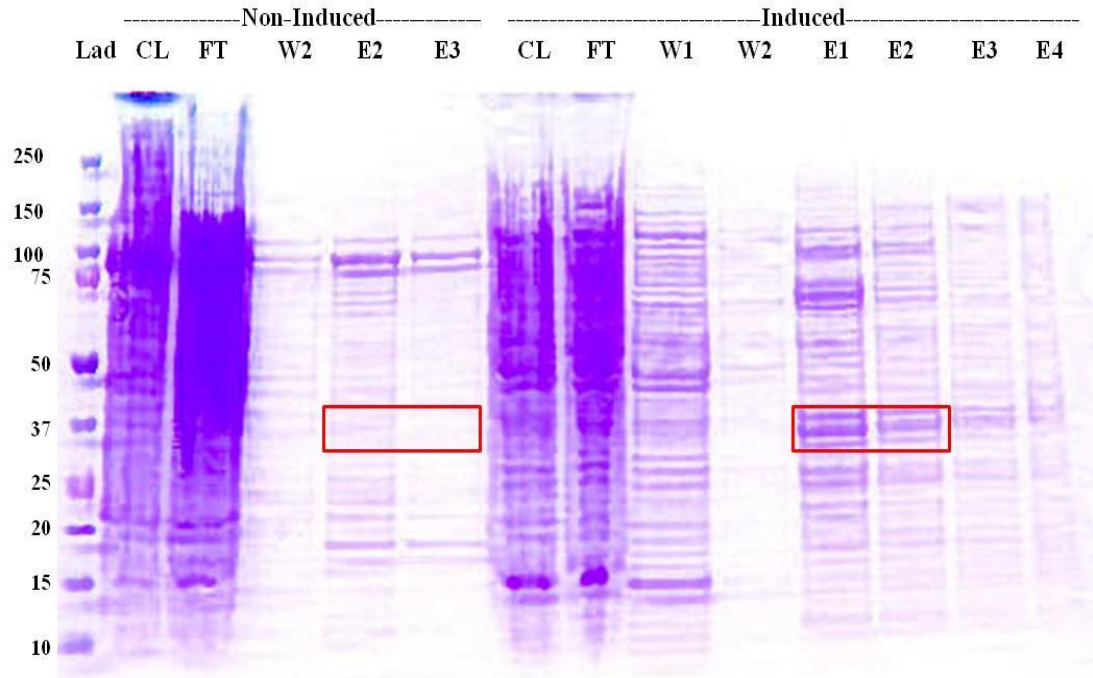


**Figure 5.8. Heterologous expression and native purification of PttCHFP1 in *E.coli*.** L-arabinose (0.4%) was added to LB media for induction and D (+)-glucose for repression of recombinant protein, cells incubated at 23°C for 6 h. CL, clear lysate; FT, flow through fraction; W, washing fraction; and E, elutions fractions. Precision Plus Protein Standard (Lad) was used as marker ladder. Red rectangles indicate the protein which was differentially expressed in induced cells but not in non-induced.

Overexpression of recombinant PttCHFP1 increased the number of viable cells of *E. coli*, however viability of non-induced cells was greater compared with induced cells (Figure 5.9). Cell growth increased significantly ( $P<0.001$ ,  $LSD= 1.35E+08$ ) from  $1.15\times 10^9$  cells/mL before induction to  $2\times 10^9$  cells/mL after induction compared with the growth of the cells without induction at  $2.8\times 10^9$  cells/mL. Even though the expression of recombinant protein (PttCHFP1) affected the viability of *E. coli*, cells were capable of expressing the protein at easily extractable levels.

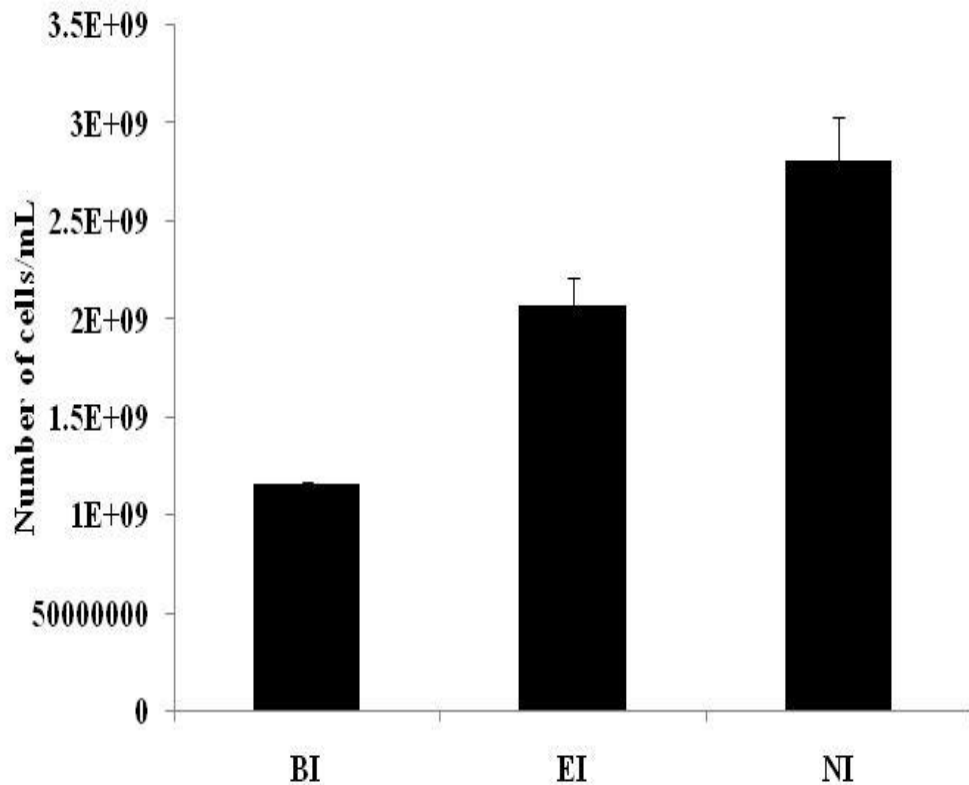


**Figure 5.9. The effect of overexpression of PttCHFP1 on the viability of *E. coli*.** Graph shows BI, mean number of viable cell before the induction; and EI, at the end of the induction compared with NI, non-induced cell. Three replicates in two individual experiments were used, ( $P<0.001$ ,  $LSD=1.35E+08$ ). Error bars represent the standard error of mean of three replicates.

#### 5.3.1.4 PttSP1

Regardless of L-arabinose concentrations (0.2% and 0.4%), incubation temperature (23°C and 37°C) and incubation time (4 h and 6 h), overproduction of potential 6×His-tagged PttSP1 was detected in clear lysate of induced *E. coli* cells compared with non-induced lysate (Figure 5.10). Incubation of cells at 16°C for 6 h with 0.4% L-arabinose has also produced the candidate recombinant protein in the same magnitude as previous conditions (Appendix, Figure A3.4). Downstream heterologous expression was conducted using 0.4% L-arabinose at 23°C for 6 h before denaturing and native purification conditions were used to extract 6×His-tagged PttSP1 protein. Elution fractions 1, 2 and 3 in induced cells, from both denaturing and native purification conditions, contained proteins which had migrated to the predicted molecular size of 6×His-tagged PttSP1 protein (25 kDa), while they were absent in non-induced elution fractions (Figure 5.11 and Figure 5.12). Proteins were extracted from these bands and identified using LC-eSI-IT MS, analysis revealed that the differentially expressed protein (size 25 kDa) contained peptides that matched to proteins annotated as conserved hypothetical proteins in *P. tritici-repentis* and PttSP1 in *Ptt* (XP\_001933504 and XJ900135 respectively). The theoretical molecular weight for this protein was above 24 kDa, more than likely because of the 6×His-tag.

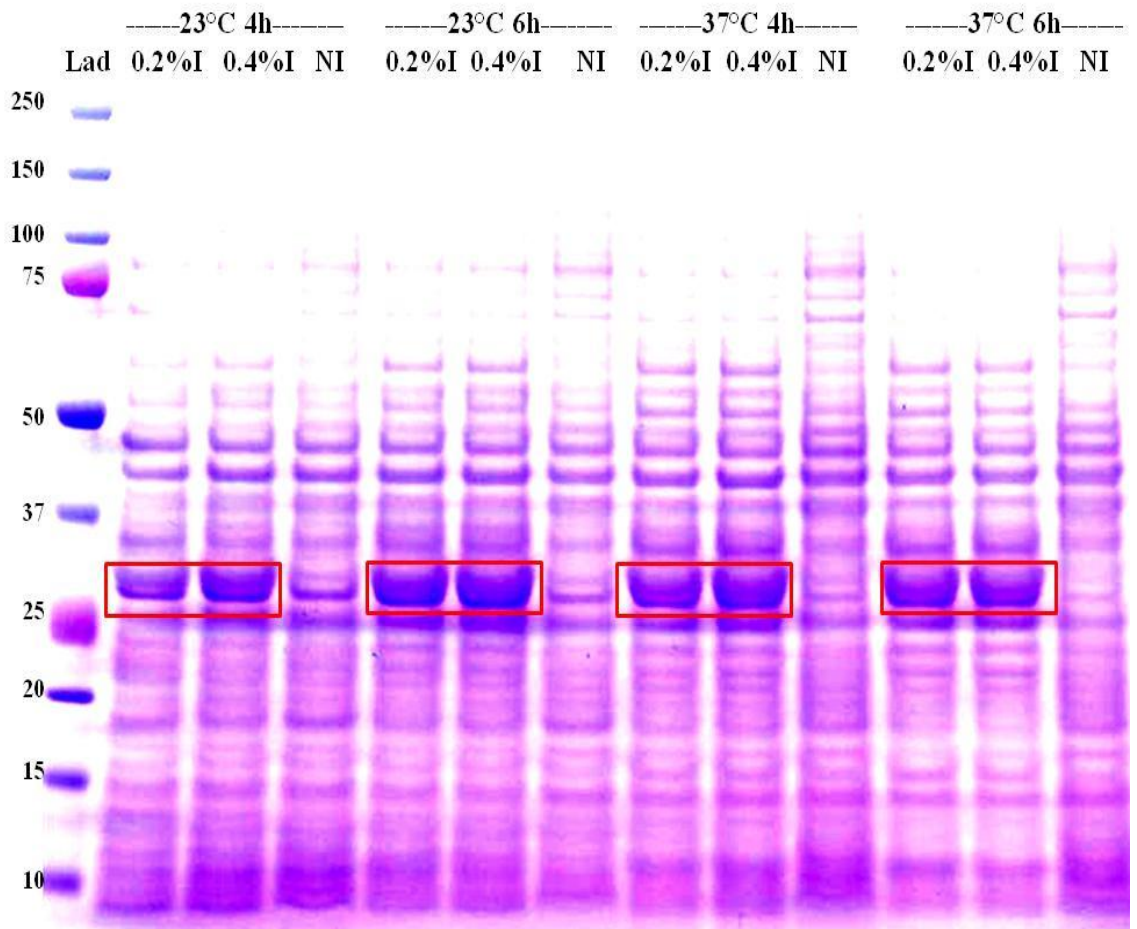


**Figure 5.10. Optimisation of heterologous expression of PttSP1 in *E. coli* with different incubation conditions and L-arabinose concentration.** Two incubation time (4 h and 6 h) and two concentrations of L-arabinose (0.2% and 0.4%) at two incubation temperatures (23°C and 37°C) were used, D (+)-glucose was used to repress the expression of recombinant protein. Denaturing conditions were used for protein purification. I, clear lysate fractions for induced cells; and NI, non-induced were loaded in PAGE. Precision Plus Protein Standard (Lad) was used as marker ladder. Red rectangles indicate the presence of two bands in both L-arabinose concentrations in which the PttSP1 was differentially expressed in induced cells but not in non-induced.

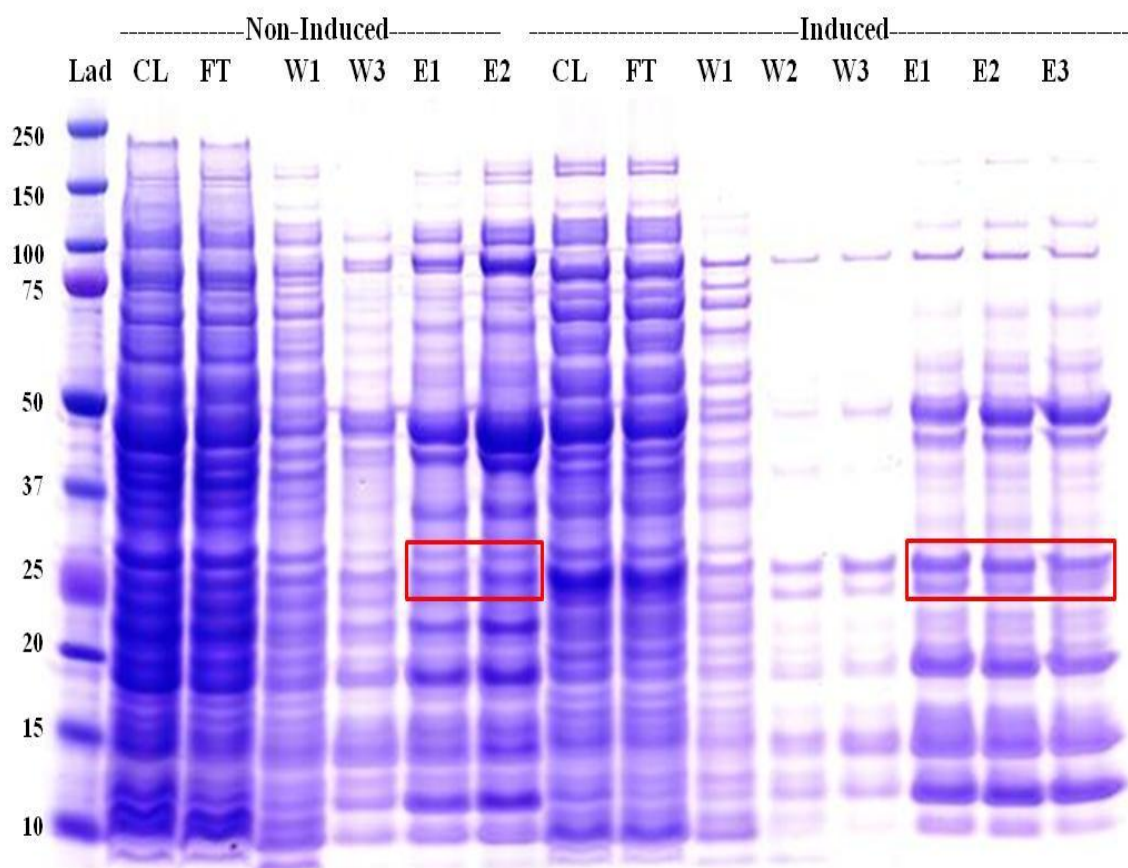


**Figure 5.11. Heterologous expression and denaturing purification of PttSP1 in *E. coli*.** L-arabinose (0.4%) was added to LB media for induction and D (+)-glucose for repression of recombinant protein, cells incubated at 23°C for 6 h. CL, clear lysate; FT, flow through fractions; W, washing fractions; and E, elution fractions. Precision Plus Protein Standard (Lad) was used as marker ladder. Red rectangles indicate the protein which was differentially expressed in induced cells but not in non-induced, protein from this band was sequenced using LC-eSI-IT MS.

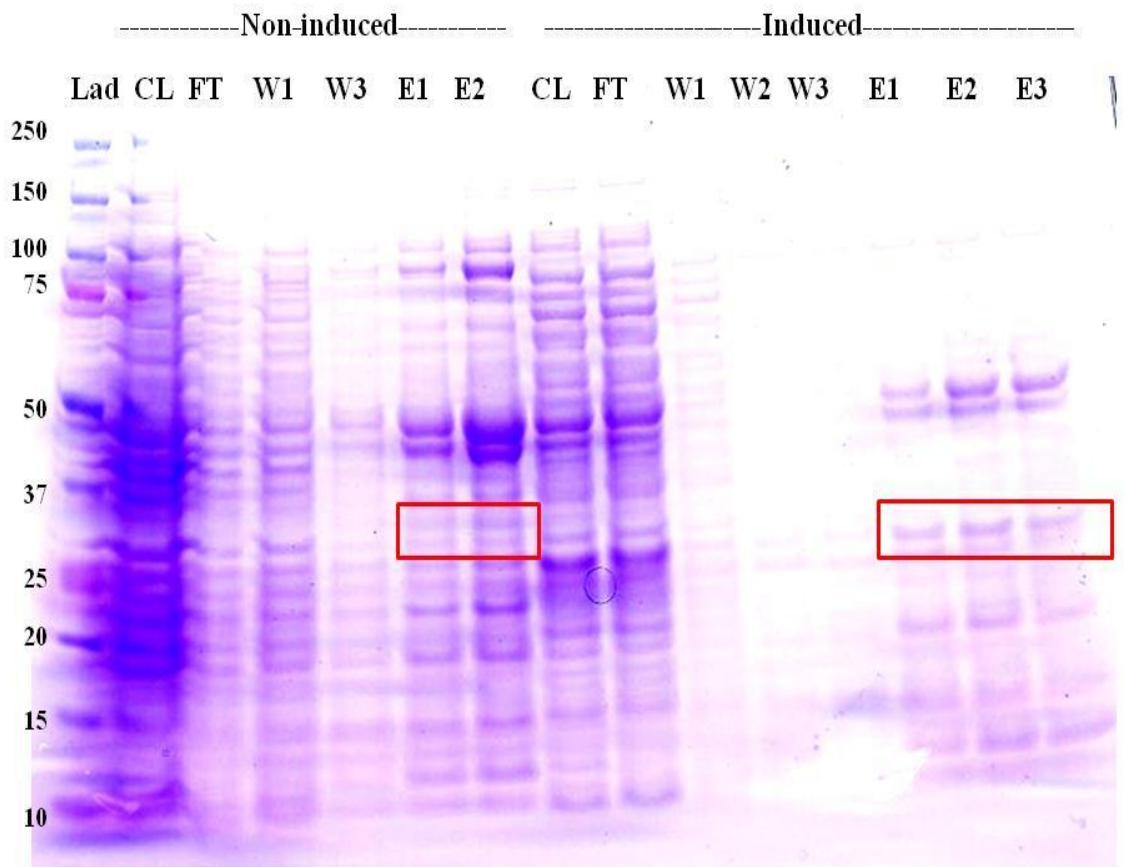


**Figure 5.12. Heterologous expression and native purification of PttSP1 in *E. coli*.** L-arabinose (0.4%) was added to LB media for induction and D (+)-glucose for repression of recombinant protein, cells incubated at 23°C for 6 h. CL, clear lysate; FT, flow through fraction; W, washing fraction; and E, elutions fractions. Precision Plus Protein Standard (Lad) was used as marker ladder. Red rectangles indicate the protein which has been differentially expressed in induced cells but not in non-induced.

Viability of induced *E. coli* cells decreased significantly ( $P < 0.001$ ,  $LSD = 2.68E+08$ ) after 2 h of overexpression of recombinant 6×His-tagged PttSP1 protein, compared with non-induced cells (Figure 5.13). Cell growth declined significantly from  $1.21 \times 10^9$  cells/mL before induction to  $7.43 \times 10^8$  cells/mL after 2 h of induction compared with the growth of the cells without induction ( $2.1 \times 10^9$  cells/mL). Even though the expression of recombinant protein (PttSP1) affected the viability of *E. coli*, cells were capable of expressing the protein at detectable level.



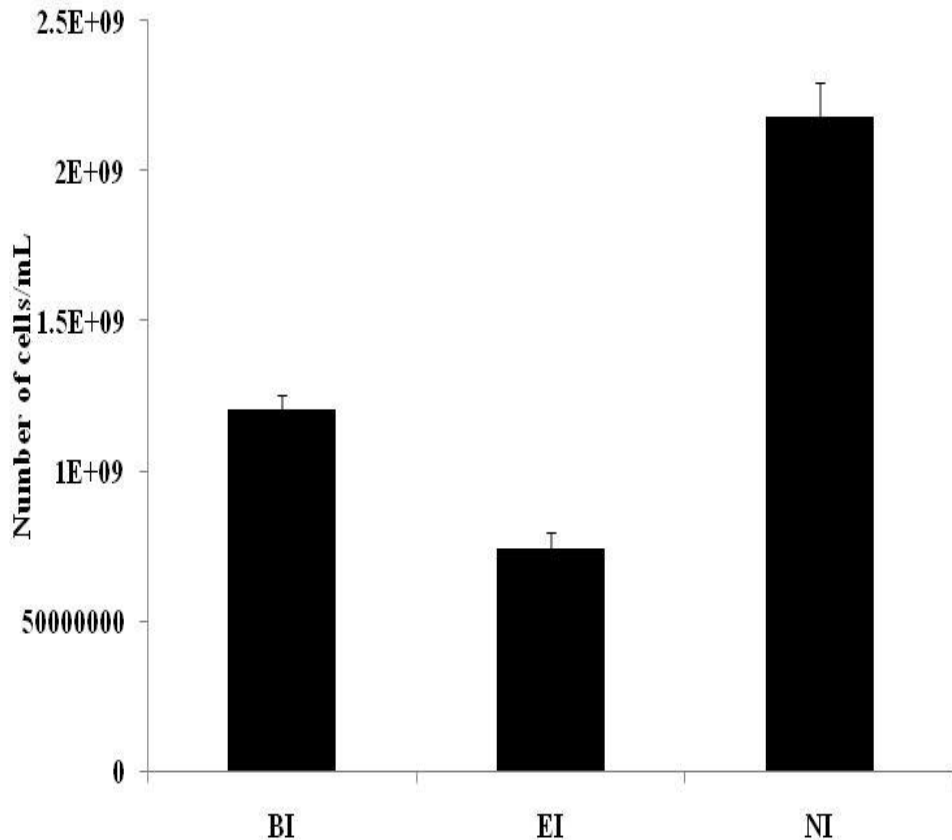


**Figure 5.13. The effect of overexpression of PttSP1 on the viability of *E.coli*.** Graph shows BI, mean number of viable cell before the induction and EI, at the end of the induction compared with non-induced cell. Three replicates in two individual experiments, ( $P < 0.001$ , LSD= 2.68E+08). Error bars represent the standard error of mean of three replicates.

### 5.3.2 Bioassay for candidate proteins

PttCHFP1 and PttSP1 were successfully expressed in *E. coli*. However PttXyn11A might be expressed at very low levels because it caused toxicity to the cells and remained in the cell lysate. PttGPI-CFEM could not be expressed, therefore PttCHFP1, PttSP1 and PttXyn11A were used for bioassays.

#### 5.3.2.1 Biological activity of recombinant proteins on barley cultivars

Biological activity of recombinant proteins, purified using native conditions, were tested against different barley cultivars at different protein

concentrations using cell clear lysate or elution fractions for plant injection. When using unwashed proteins (Figure 5.14), the eluted PttCHFP1 (10 µg) induced yellow lesions in the susceptible cv. Sloop but not in cv. CI9214 and cv. Beecher (Figure 5.14). The eluted PttXyn11A (albeit at very low levels due to the toxicity, section 5.3.1.2), did not cause symptoms on any of the cultivars tested. Due to a low concentration of PttSP1 in the elution (less than 1 µL/mL), a large volume was injected into leaves and all leaves had some symptoms. However, the purification buffer used to elute the recombinant protein (NP-500) caused leaf burning for all cultivars.

Proteins were therefore washed twice with SNW using Amicon YM-10 filter to remove imidazole and other salts from the purified proteins. However, the protein concentration of the elution fraction was significantly decreased by washing to undetectable levels. Hence, 200 µL of each total elution was injected in each leaf but after 4 days post injection, both cultivars Sloop and CI9214 had chlorosis symptoms caused by non-induced cells containing *PttSP1* (Figure 5.15). In addition, elutions from both induced and non-induced cells containing *PttXyn11A* caused chlorosis on leaves from CI9214. Eluted PttCHFP1 caused chlorosis on Sloop and CI9214 but no symptoms were detected on Beecher (Figure 5.15).

The expressed proteins (in elutions) were also combined and used in the bioassay. Ten µg for each protein (PttXyn11A, PttCHFP1 and PttSP1) or a mixture of 10 µg of PttXyn11A; 10 µg PttCHFP1 and 3 µg of PttSP1 (due to low concentration) were injected (Figure 5.16). Given that PttSP1 was expressed in a very low level in *E. coli* and the protein yield was very limited, CI9214 and Beecher were not tested with PttSP1 recombinant

protein alone. The PttCHFP1 elution showed biological activity in both cultivars Sloop and CI9214 as indicated by chlorosis while Beecher was less sensitive. The elution fraction for PttXyn11A did not induce necrosis in any of the cultivars while cv. Sloop did not respond to injection with the eluted PttSP1. The mixture of elutions of the three proteins indicated that some necrosis was induced in Sloop and CI9214 compared with Beecher (Figure 5.16), suggesting that these symptoms were caused by PttCHFP1.

The previous bioassay was repeated using clear lysates, in case recombinant proteins had been lost during purification. By 5 days post injection, all cultivars showed no response for three injected proteins (Figure 5.17). Although 20 µg was injected for each clear lysate, the corresponding amount for each individual recombinant protein might have been insufficient.

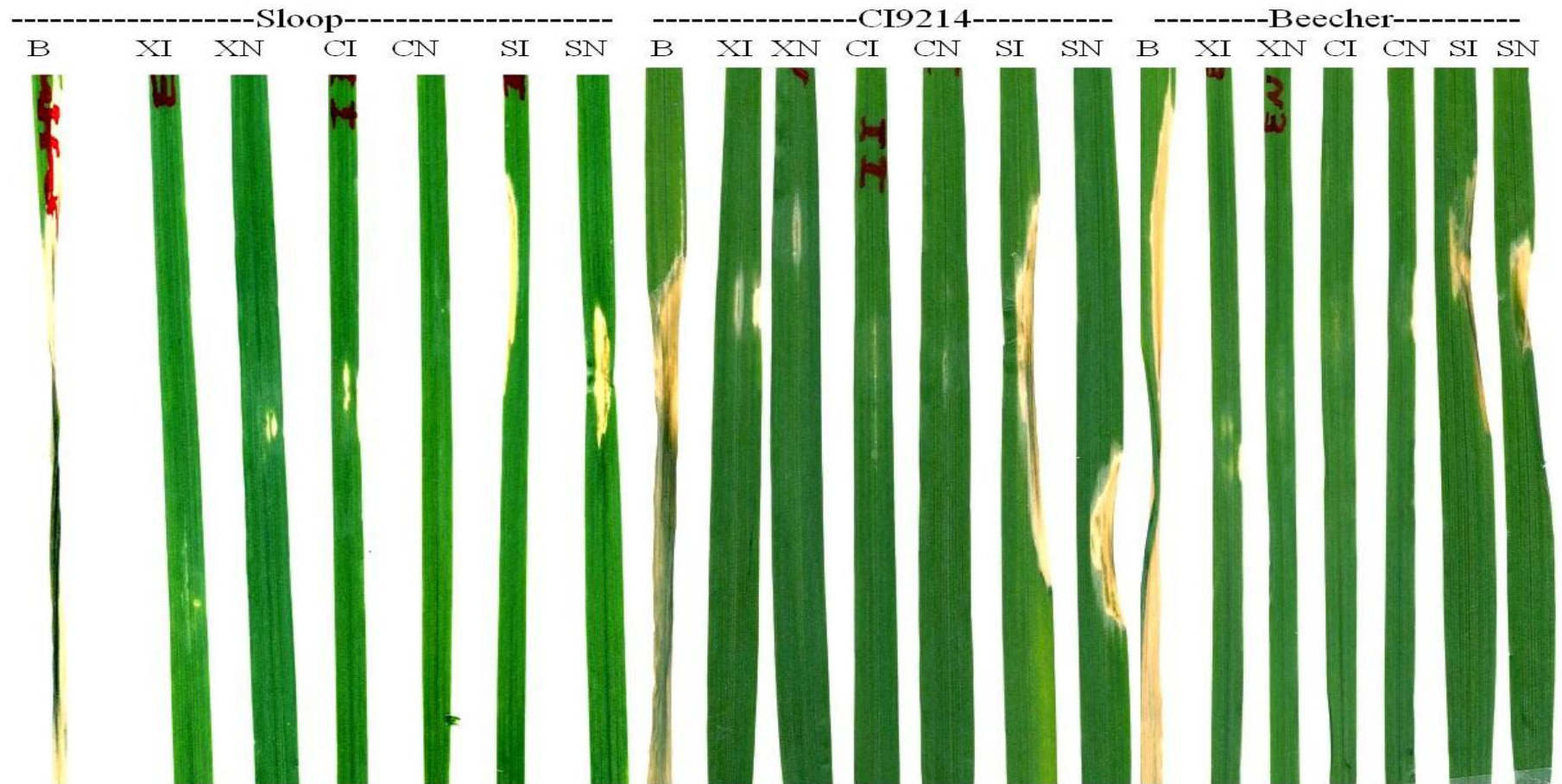


**Figure 5.14. Bioassay of heterologously expressed PttXyn11A (X), PttCHFP1 (C) and PttSP1 (S) (expressed in *E. coli*) unwashed protein.** Ten  $\mu\text{g}$  of purified protein elutions and control buffer (B) (similar volume to recombinant protein) were injected from I, induced cells; and N, non-induced in three barley cultivar. Representative leaves were imaged after 4 days post injection, three biological replicates were used.

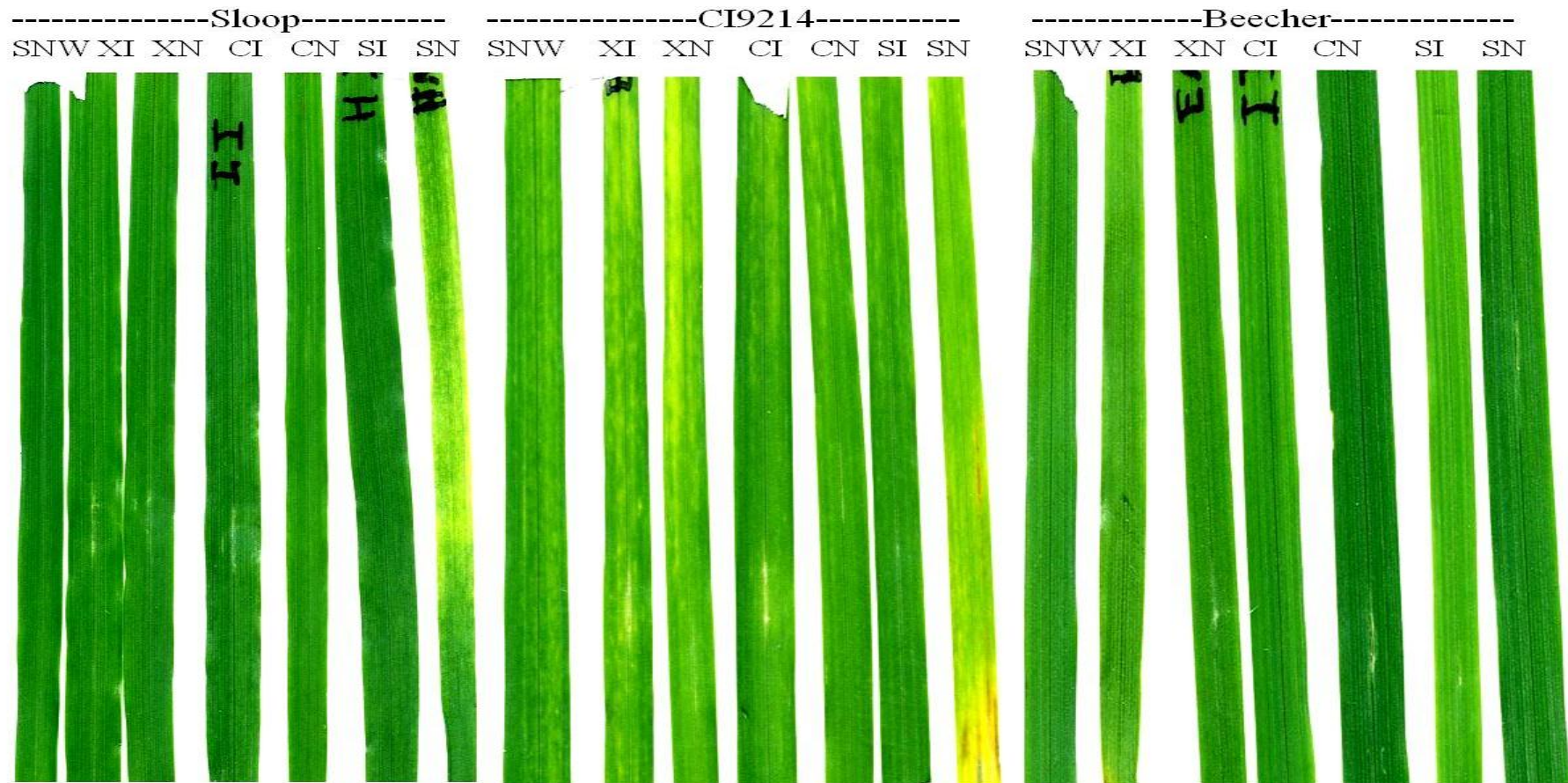


**Figure 5.15. Bioassay of heterologously expressed PttXyn11A (X), PttCHFP1 (C) and PttSP1 (S) (expressed in *E. coli*) washed protein.** Purified protein elution was washed with sterilised nanopure water (SNW) and 200  $\mu$ L of solution was injected from I, induced cells; and N, non-induced in three barley cultivar, 200  $\mu$ L of SNW, Sterilised nanopure water was injected as a control. Representative leaves were taken after 4 days post injection, three biological replicates were used.

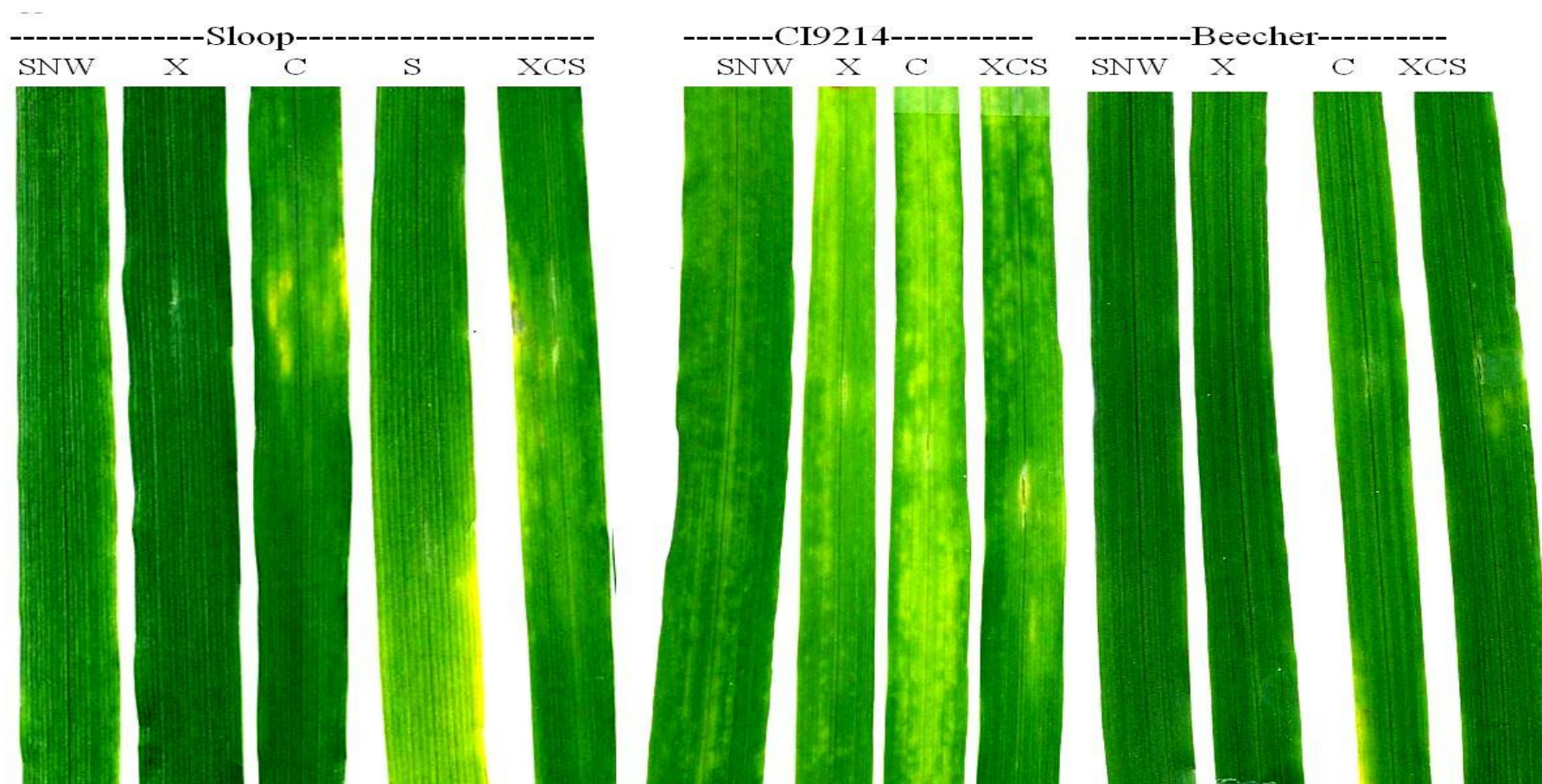


**Figure 5.16. Bioassay of heterologously expressed PttXyn11A (X), PttCHFP1 (C) and PttSP1 (S) (expressed in *E. coli*) on three cultivars.** Ten  $\mu\text{g}$  of purified protein of combined elutions 1 and 2 for each protein from induced cells (X, C and S) was injected; XCS, a mixture of 10  $\mu\text{g}$  of (X and C) and 3  $\mu\text{g}$  of (S) was mixed together and injected. SNW, sterilised nanopure water as a control. Representative leaves were taken after 5 days post injection, three biological replicates were used.

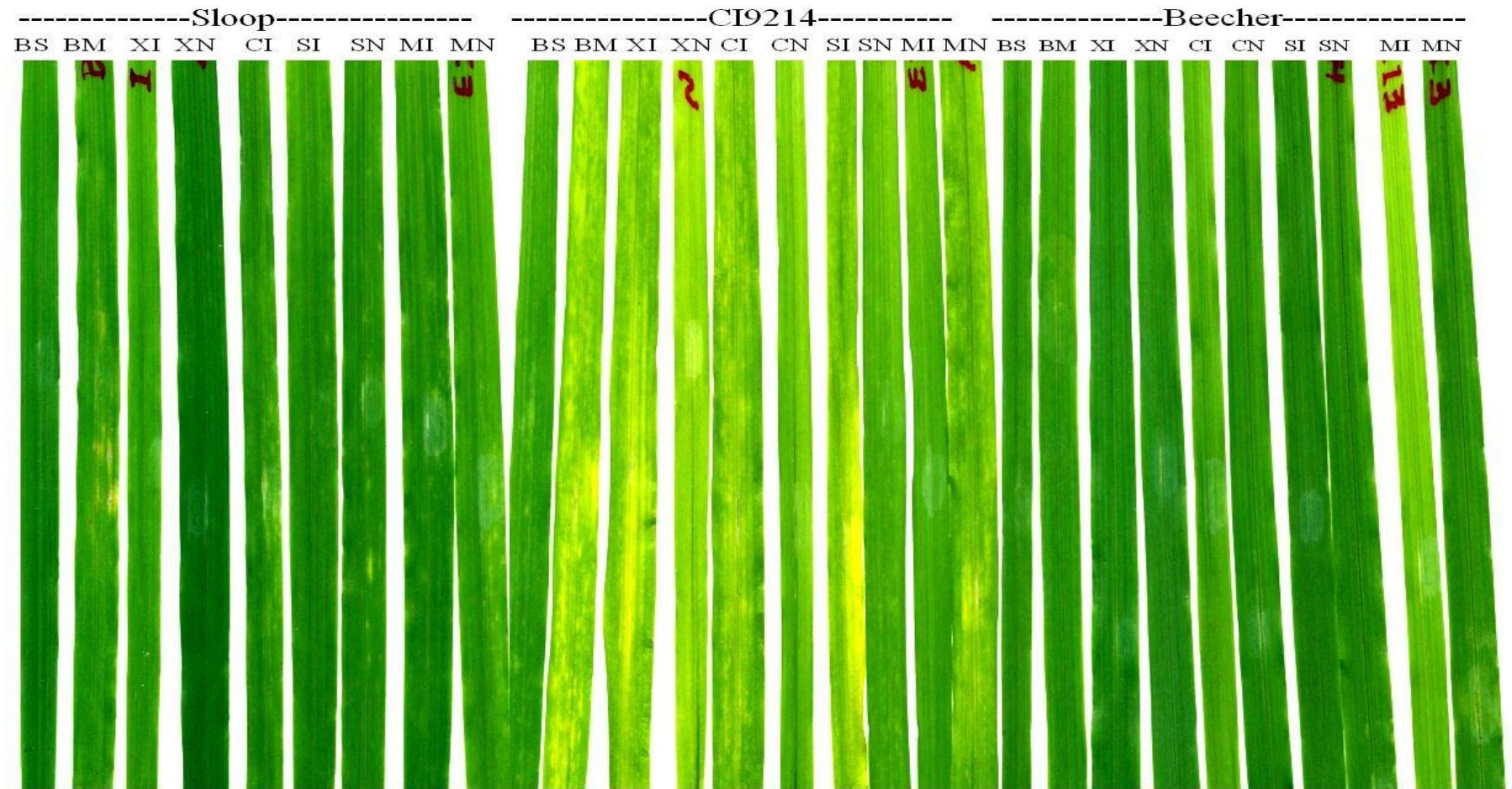


**Figure 5.17. Bioassay of heterologously expressed PttXyn11A (X), PttCHFP1 (C) and PttSP1 (S) (expressed in *E. coli*), clear lysate on three cultivars.** Twenty  $\mu\text{g}$  of clear lysate of single protein and for each in a mixture of clear lysate (M) were injected. Control buffer (similar volume to recombinant protein) of BS, buffer for single protein; BM, buffer for mixture of proteins were injected. Representative leaves were taken after 5 days post injection, three biological replicates were used.

### **5.3.2.2 Biological activity of recombinant proteins on cv. Sloop**

CI9214 and Beecher appeared to be less sensitive to recombinant PttCHFP1 while the results for PttSP1 are inconclusive due to low quantities. In addition, PttXyn11A could not be expressed by the bacteria due to toxicity. Therefore, PttCHFP1 and PttSP1 were expressed on a large scale (to concentrate the recombinant protein and ultimately reduce the required volume of injected buffer) and tested against Sloop. Two concentrations of recombinant protein (PttCHFP1) clear lysate (20 µg and 60 µg) and 20 µg of elution were used. Clear lysate of PttCHFP1 from induced and non-induced cells did not show symptoms (Figure 5.18), while elution 1 from induced cells produced symptoms to a great extent than non-induced cells. Although the same volume of buffers was injected in both protein and control treatments, symptoms often appeared more extensive in the buffer control especially in the elution buffer as it contained larger volume (160 µL of NP500 with 40 µL SNW) compared with clear lysate buffer (8 µL of NP10 with 192 µL SNW).

Bioassay of recombinant PttSP1 was conducted using two concentrations of clear lysate (20 µg and 60 µg) and 20 µg of protein elution 1 and 2. Elution 1 and 2 from induced cells caused symptoms but elutions from non-induced cells did not (Figure 5.19). Clear lysate in both concentrations from both induced and non-induced cells did not cause symptoms on leaves. In addition, the buffers did not cause symptoms in this experiment as less volume was injected compared with the previous experiment.



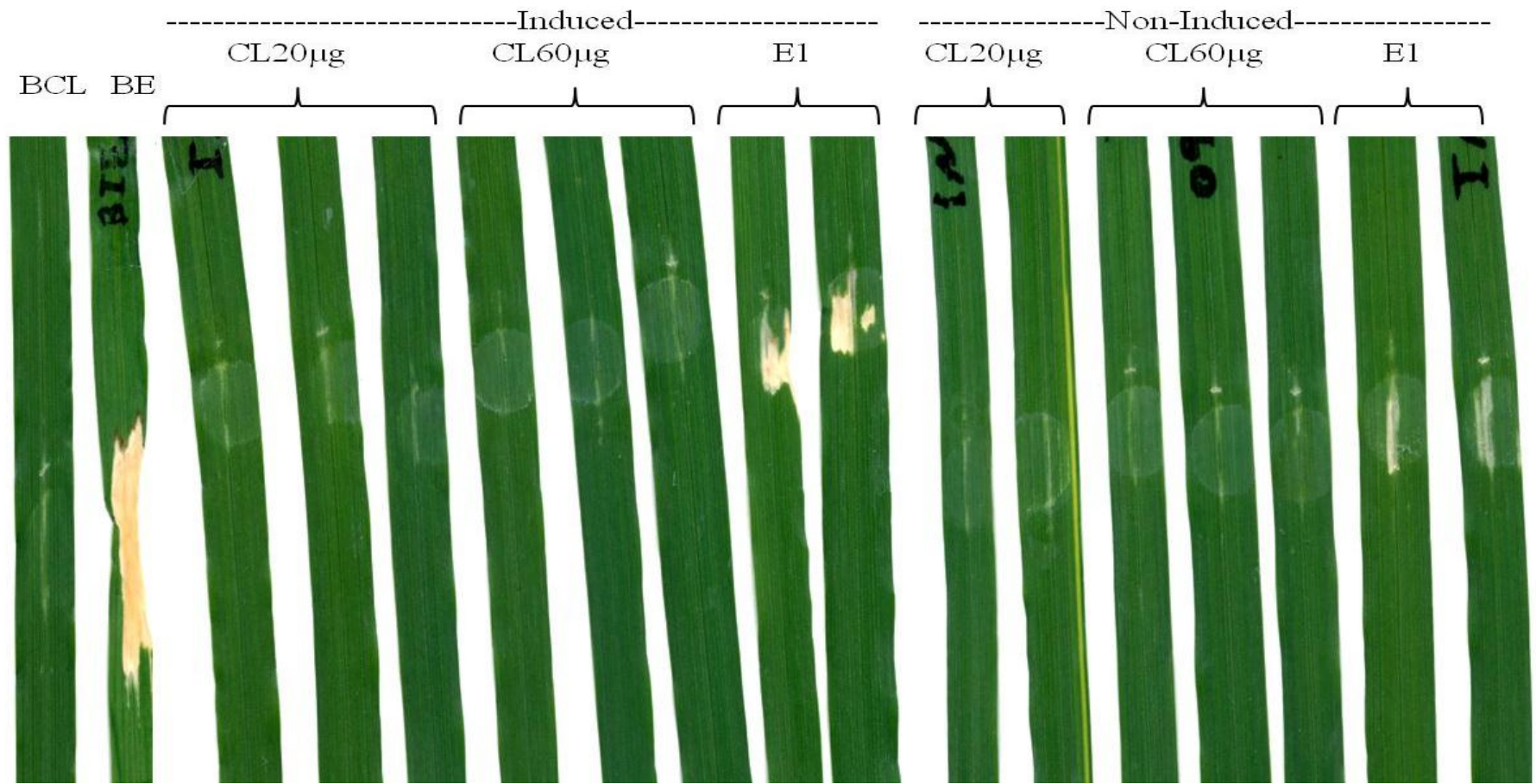


**Figure 5.18. Effect of protein concentration on the bioassay of heterologously expressed PttCHFP1 (expressed in *E. coli*) on cv. Sloop.** Twenty and sixty µg of clear lysate of protein of CL, clear lysate; and E1, 20 µg of elution 1 of both induced and non-induced were injected. Control buffer (similar volume to recombinant protein) BCL, buffers NP10 (8 µL of NP10 with 192 µL SNW); and BE, NP500 (160 µL of NP500 with 40 µL SNW). Representative leaves were taken after 7 days post injection, three biological replicates were used.

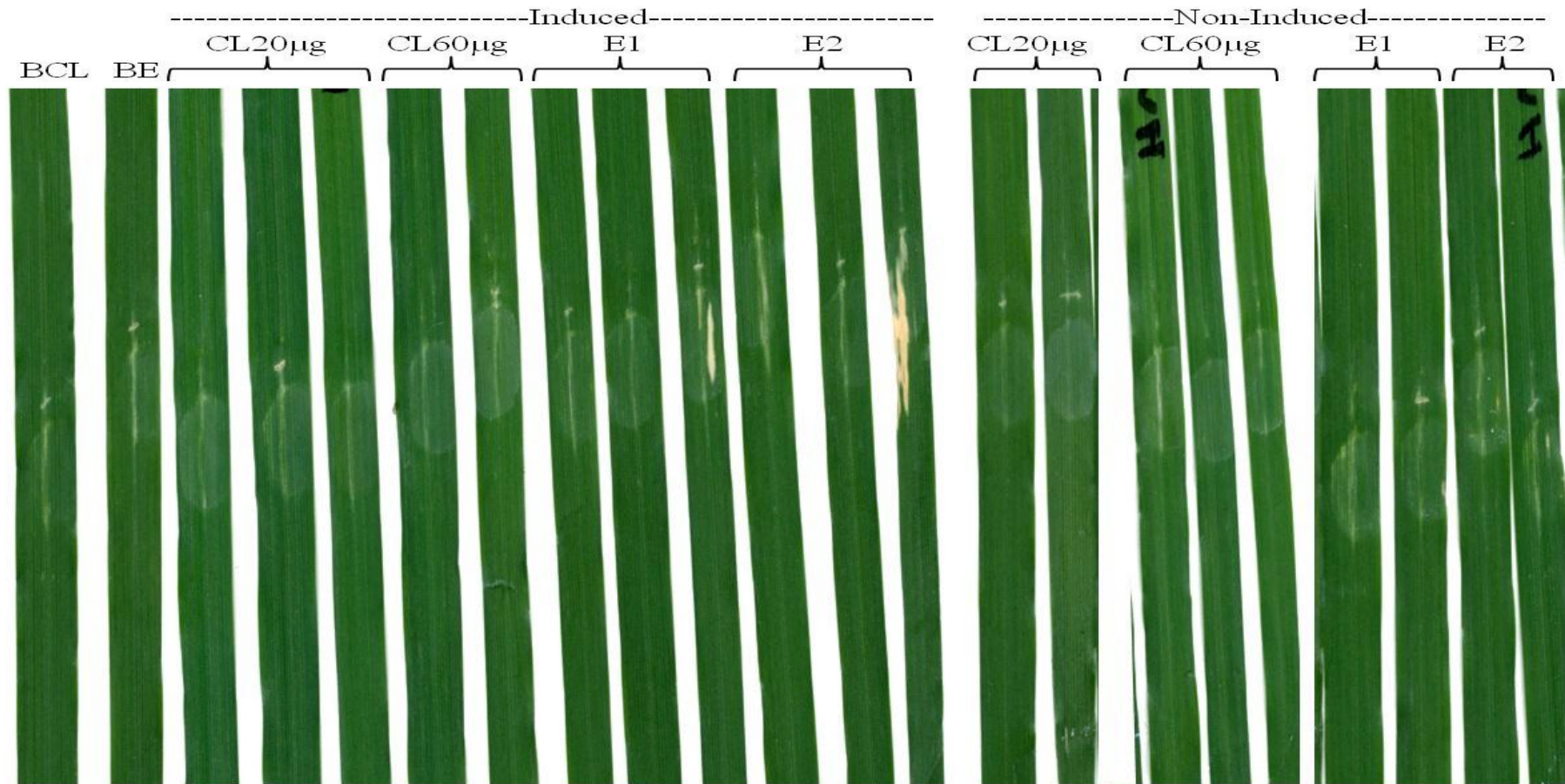


**Figure 5.19. Bioassay of heterologously expressed PttSP1 (expressed in *E. coli*) on cv. Sloop.** Twenty and sixty µg of CL, clear lysate; and 20 µg of E1, E2, elution 1 and 2; of both induced and non-induced were injected. Control buffer (similar volume to recombinant protein) BCL, buffers NP10 (8 µL of NP10 with 192 µL SNW); and BE, NP500 (22 µL of NP500 with 178 µL SNW) were injected. Representative leaves were taken after 7 days post injection, three biological replicates were used.

### 5.3.3 Biological activity of commercial xylanase

Necrosis symptoms appeared 7 days post injection when 76  $\mu\text{g}$  of *A. niger* xylanase was injected into leaves from cv. Sloop. Injection with 5  $\mu\text{g}$  or 20  $\mu\text{g}$  of *A. niger* xylanase did not cause symptoms (Figure 5.20). The mixture of *A. niger* xylanase (5  $\mu\text{g}$ ), PttCHFP1 (2.4  $\mu\text{g}$ ) and PttSP1 (20  $\mu\text{g}$ ) also induced symptoms after 7 days post injection even though 5  $\mu\text{g}$  xylanase did not induce necrosis.

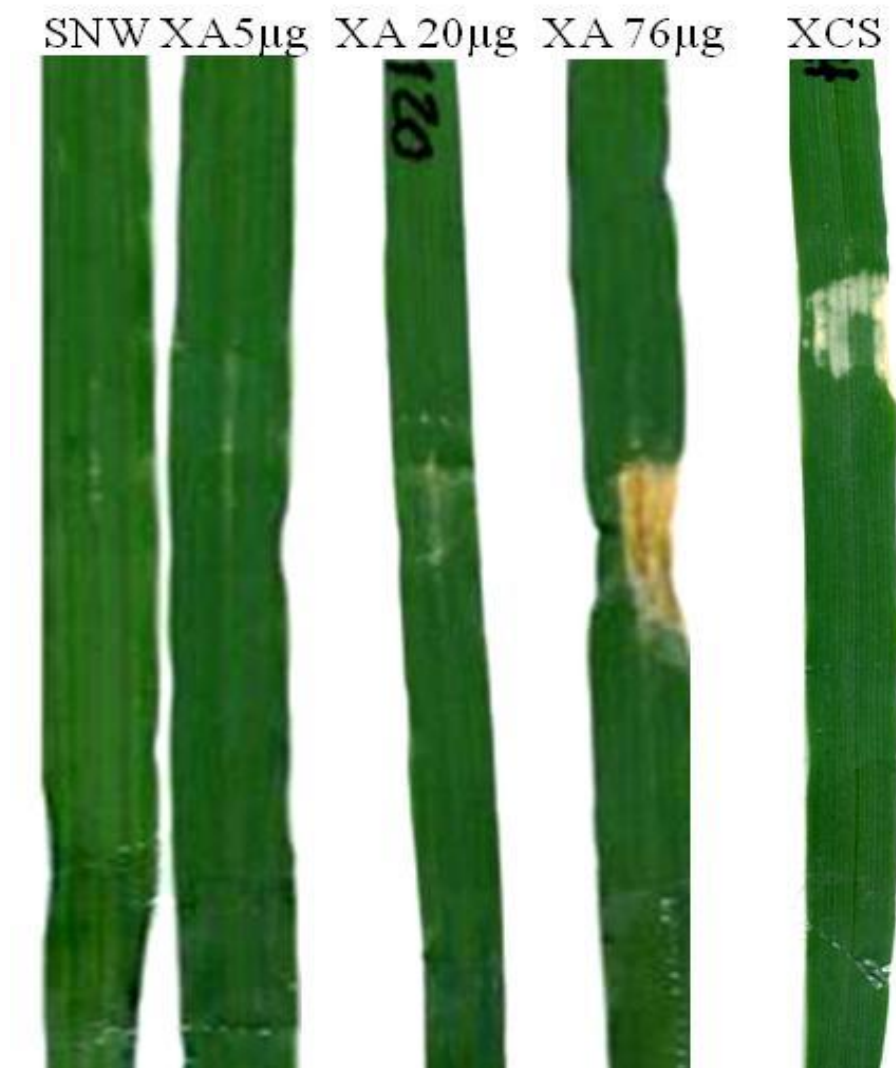


**Figure 5.20. Bioassay of commercial xylanase on cv. Sloop.** Three concentration of *Aspergillus niger* xylanase (XA 5  $\mu\text{g}$ , XA 20  $\mu\text{g}$  and XA 76  $\mu\text{g}$ ); SNW, sterilised nanopure water; and XCS, a protein mixture of *A. niger* xylanase (5  $\mu\text{g}$ ), PttCHFP1 (2.4  $\mu\text{g}$ ) and PttSP1 (20  $\mu\text{g}$ ). Representative leaves were taken after 7 days post injection, three biological replicates were used.

#### **5.3.4 Xylanase activity in isolates of *Ptt* with different virulence**

A xylanase assay was designed to investigate the enzymatic activity of the culture filtrate of five isolates with different virulence (Table 2.1, 55/07 had abnormal colony colour and shape, therefore was discarded in this assay). The activity of xylanase after both 10 and 15 days, was significantly higher ( $P < 0.001$ ,  $LSD = 0.71$ ) in the more virulent isolates (32/98 and 152/09) compared with the isolates with lower virulence (08/08f and 122/09) (Figure 5.21). Although the 123/09 isolate had significantly lower activity at 10 days, by 15 days the activity had increased by almost three-fold. In addition, the activity of xylanase in 32/98 isolate was the greatest after 15 days and significantly different from 10 days. However, there were no significant differences in the activity between culture filtrates after 10 and 15 days for 08/08f, 122/09 and 152/09 (Figure 5.21). Clear lysate from induced heterologously expressed PttXyn11A (xylanase) and non-induced cells were also tested and showed activity in the induced cells compared with non-induced, indicating that cells might express PttXyn11A at a low level.

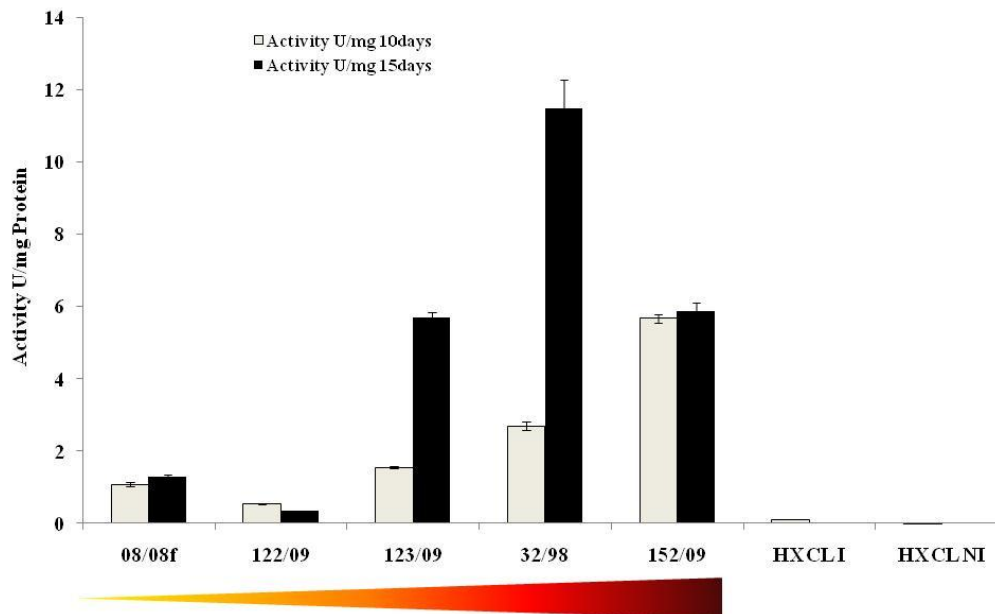


**Figure 5.21. Activity of xylanase (X) in the culture filtrate of six isolates of *Ptt* grown at FCM for 10 and 15 days.** The activity was measured by enzyme U for each mg of protein. Red bar indicates the isolates ordered according to the virulence from low to high. HXCLI, clear lysate from induced heterologously expressed PttXyn11A; and HXCLNI, non-induced. Three biological replicates, the least significant difference (LSD=0.71) at  $P<0.001$ . Error bars represent the standard error of three replicates.

#### 5.4 Discussion

Heterologous expression experiments showed that *E. coli* was able to produce PttCHFP1 and PttSP1 but PttXyn11A and PttGPI-CFEM were not expressed at detectable levels in this system. Bioassay of recombinant PttCHFP1 and PttSP1 showed that these proteins have some biological activity on the susceptible barley cultivar (Sloop) suggesting a role in virulence and/or symptom development. However, this biological activity needs to be confirmed as the buffers used for protein purification could also induce some symptoms. The detection of some xylanase activity in induced cells and the high levels of toxicity suggest that PttXyn11A was expressed, albeit at very low levels. The observation that the more virulent isolates had significantly greater activity compared with less virulent isolates also suggests a role for PttXyn11A in virulence. Although the

bioassay of PttGPI-CFEM was not performed during this research, due to time constraints, further optimisation of the heterologous expression and bioassay to confirm the results presented herein is necessary.

Denaturing conditions for PttGPI-CFEM purification showed unsuccessful expression for recombinant PttGPI-CFEM. GPI-anchored proteins are often linked to the plasma membrane via a preformed GPI anchor that is added to the protein in the endoplasmic reticulum (ER, predicted by <http://psort.hgc.jp/form.html>)(Plaine *et al.*, 2008; Tiede *et al.*, 1999). Hamada *et al.* (1999) suggested that in some fungi a subset of GPIs are cleaved from the membrane and translocated to the cell wall where they are linked covalently to  $\beta$ -1, 6-glucan. GPI attachment to the plasma membrane and/or cell wall might suggest that GPI could not be secreted into the media and therefore cannot be purified. In addition, fungal cell wall glycoproteins (including GPI-anchored proteins) have various posttranslational modifications (de Groot *et al.*, 2009; De Groot *et al.*, 2005), suggesting that these proteins can be changed or integrated on their arrival at the cell surface according to the proposed biological function (de Groot *et al.*, 2009; Varki *et al.*, 1999). The machinery of post-translational modification of proteins might vary between organisms (Schumacher *et al.*, 2010). Therefore, PttGPI-CFEM might have misfolded when it was expressed by the bacteria, or might not have been translated because the GPI signal might not be recognised by the ER of *E. coli* (Varki *et al.*, 1999). In addition, many membrane proteins, even from *E. coli*, are toxic when overexpressed in bacteria (Frommer and Ninnemann, 1995;

Schertler, 1992). Removing the anchor region and re-expressing might help to produce this protein (Ahmad *et al.*, 2012) but it might cause loss of its function. Alternatively, using another expression system which is more closely related to the fungus such as *P. pastoris* might allow the heterologous expression. However, due to the time constraints, toxicity and heterologous expression assays using *P. pastoris* were not conducted.

Even though L-arabinose concentration, incubation time and temperature, and different transformants of *E. coli* were used to optimise induction and purification methods (denaturing and native conditions) were optimised, *E. coli* cells were not able to express the recombinant PttXyn11A at a detectable level probably because of its toxicity to the *E. coli* (Figure 5.5). Many authors have reported similar problems with many genes from different organisms (Frommer and Ninnemann, 1995; Saïda, 2001). Khan *et al* (2002) reported that the number of generations has to be kept to a minimum to reduce the toxicity of xylanase to cells. Using lower number of cell generations was also trialled in this study (Figure 5.3) using a series of incubation times but was not successful. The observation that induced cells produced more endogenous proteins compared with non-induced cells (Figure 5.3 and Figure 5.4) was probably due to the stress caused by the overexpression of PttXyn11A. Some of the endogenous proteins of *E.coli* (30S ribosomal protein S2, Tem-1  $\beta$ -Lactamase) identified especially after 4 h induction (Figure 5.3) have been shown to be usually induced as a response to stress (Petrosino and Palzkill, 1996; Toone *et al.*, 1991). The presence of native *E. coli* proteins in the elution

of recombinant proteins is a common problem for purification especially using a high affinity ion for divalent cations such as nickel (Bolanos-Garcia and Davies, 2006). Many *E. coli* native proteins are commonly co-purified by immobilised-metal affinity chromatography (IMAC), the same system been used in this research, as they bind to the column (Bolanos-Garcia and Davies, 2006). However, *E. coli* was capable of producing enough recombinant endoxylanase to be detected in the activity assay (Figure 5.21), confirming that recombinant PttXyn11A has xylanase activity.

Endo- $\beta$ -1,4-xylanase has been shown to be involved in the degradation of plant cell walls (Beg *et al.*, 2001; Beliën *et al.*, 2006; Walton, 1994), and has been confirmed as a virulence factor in many fungal species (Gomez-Gomez *et al.*, 2001; He *et al.*, 2009; Jaroszuk-Scisel and Kurek, 2012; Torronen *et al.*, 1992). Xylanase activity was therefore evaluated in the culture filtrates of *Ptt* isolates with varying virulence (Bailey *et al.*, 1992; Jun *et al.*, 2009). The greatest activity of xylanase was recorded for the most virulent isolates of *Ptt* compared with less virulent isolates, suggesting that the endoxylanase might play a role in virulence in NFNB. Indeed, injection of barley leaves with commercial xylanase caused extensive necrosis around the injected area. However, the role that xylanase might play as a virulence factor for *Ptt* would need to be confirmed by mutant analysis. Further analysis of endoxylanase production or *PttXyn11A* gene expression during the interaction might also help to confirm its role in virulence.



Regardless of the concentration of L-arabinose, *E. coli* expressed PttCHFP1 and PttSP1, suggesting they were less toxic to *E. coli* than endoxylanase. Unwashed elutions of recombinant proteins, containing PttCHFP1 and PttSP1, caused chlorosis to injected leaves (Figure 5.14), but this chlorosis was due to the high concentration of salt in the elution buffer, especially NaCl and imidazole (Haddad and Mazzafera, 1999; Turkyilmaz *et al.*, 2011). However, washing the proteins with SNW using UFP decreased their concentration and consequently no symptoms appeared (Figure 5.15). Large scale protein production was therefore conducted to minimise the volume of injected buffer. Injecting 10 µg or 20 µg of the PttCHFP1 elution induced light necrosis in cv. Sloop but not in CI9214 and Beecher, thus suggesting that cv. Sloop may contain target protein(s) not present in other cultivars (Manning and Ciuffetti, 2005; Sarpeleh *et al.*, 2008) as discussed in section 3.4. However, the chlorotic symptoms, probably caused by the buffer, made the symptoms difficult to visualise. Lower concentration of PttSP1 (<10 µg) did not cause any symptoms on barley leaves (Figure 5.16) but 20 µg of PttSP1 elution induced chlorosis in cv. Sloop (Figure 5.19). These symptoms were not expected as the proteinaceous toxins from *Ptt* usually cause necrosis (Sarpeleh *et al.*, 2007; 2008). However, the need for high concentrations associated with a high volume of buffer might suggest that PttCHFP1 does not act directly as a toxin.

In summary, PttGPI-CFEM was not detected in PAGE because either it might be linked to the plasma membrane and/or to the cell wall via

GPI anchor if it was expressed or *E. coli* was not able to express PttGPI-CFEM because the GPI signal was unrecognisable by the bacteria. PttXyn11A also was not expressed at detectable levels because it was toxic to the cells. However commercial xylanase showed biological activity in barley similar to the natural necrosis which was induced by the *Ptt* isolates (Figure 2.2). In addition, the filtrates of more virulent isolates had a greater xylanase activity compared with the less virulent isolates. Thus, suggesting that PttXyn11A might have a xylanase activity and a role in virulence. The induction of symptoms in cv. Sloop by recombinant PttSP1 and PttCHFP1, suggests these proteins may also play some role in virulence. However, further research is required to confirm their role in virulence and/or development of symptoms. Given time constraints and lack of a reliable transformation system for *Ptt*, the expression of all candidate genes at different times of the interaction between *Ptt* and barley might uncover the nature of their role and thus was investigated in chapter 6.

## **Chapter 6 Expression of virulence-related candidate genes (VRCG) during the interaction between barley and isolates of *P. teres* f. *teres* with different virulence**

### **6.1 Introduction**

Studying interactions between *P. teres* f. *teres* (*Ptt*) and barley is an important step in understanding the nature of infection and ultimately building disease control strategies. Many studies have grouped *Ptt* isolates according to their virulence (Afanasenko *et al.*, 2007a; Afanasenko *et al.*, 2009; Afanasenko *et al.*, 2007b; Bogacki *et al.*, 2010; Bouajila *et al.*, 2011; 2012). However, limited information is available about the virulence factors produced by these isolates. Bogacki *et al.* (2010) reported that three populations of *Ptt* isolates in South Australia have genetic differences, however these differences were only attributed to the location of the isolates. Therefore, identification of genes responsible for virulence might be useful to identify the potential virulence factors.

Gene expression analysis provides useful information about the involvement of particular fungal genes in the interaction. Conventional PCR techniques (end point PCR, such as RT-PCR) (Hu *et al.*, 1993) and reverse-transcription quantitative PCR (RT-qPCR; real time PCR) (Bates *et al.*, 2001; Leisova *et al.*, 2006) can both be used to study gene expression. However, conventional PCR is time consuming and does not give an accurate quantification especially in the log-linear phase of amplification (VanGuilder *et al.*, 2008). RT-qPCR, however, allows accurate and sensitive measurements as well as the detection of multiple products in the reaction by providing a melting curve profile for each reaction at the end of the cycling (Fraga *et al.*, 2008; Ririe *et al.*, 1997). RT-qPCR uses several

dyes to detect the double stranded DNA (VanGuilder *et al.*, 2008), but the most common is SYBR Green which enables the quantification of nucleic acids in unknown samples by a direct comparison to amplified standards (Bates *et al.*, 2001; Wittwer *et al.*, 1997). This dye has been used to detect genes involved in the pathogenesis in several fungal pathogens (Fraaije *et al.*, 2002; Schena *et al.*, 2004). RT-qPCR data can be analysed using either absolute or relative quantification (VanGuilder *et al.*, 2008). The most common method for relative quantification is the  $2^{-\Delta\Delta CT}$  method (Livak and Schmittgen, 2001), which is used to calculate relative changes in gene expression determined from RT-qPCR experiments. However, this method relies on the assumption that there is a gene (or genes) that is expressed at a constant level between the samples (called a reference or housekeeping endogenous gene) (VanGuilder *et al.*, 2008). That assumption cannot be met in our research as the growth of *Ptt* isolates *in planta* was quite different and associated with their virulence (Figure 2.6 and 2.8). Therefore, absolute analysis of RT-qPCR was used in the research presented in this chapter to investigate the expression profile of the four VRCGs as well as the endogenous fungal gene *PttGAPDH*. *GAPDH* has been previously used as a reference gene for the necrotroph *Alternaria brassicicola*, in RT-qPCR experiments (Kim *et al.*, 2009). A real-time quantitative PCR technique has been used to quantify the upregulation of various fungal transcripts during the interaction of *P. teres* with barley (Bates *et al.*, 2001; Dilger *et al.*, 2003; Leisova *et al.*, 2006) and during conidial germination *in vitro*, however none of these fungal genes were candidates in virulence. Leisova *et al.* (2006) used real-time PCR to measure the amount of fungus and to differentiate

between the two forms of *P. teres* (*Ptt* and *P. teres* f. *maculata*) in infected leaves.

In research presented in previous chapters, the expression of virulence candidate genes *PttXyn11A*, *PttCHFP1*, *PttSP1* and *PttGPI-CFEM* during the course of the interaction between barley and *Ptt* isolates with different virulence appeared to be differential at 192 hour post inoculation (hpi) using semi-quantitative RT-PCR (chapter 4). In addition, the ability of heterologously expressed recombinant proteins (*PttCHFP1* and *PttSP1*) to cause symptoms was not conclusive (chapter 5). Therefore, using RT-qPCR might provide quantitative information about the potential contributions of these proteins in *Ptt* virulence on the barley cultivar Sloop.

Comparative genomics studies have demonstrated that genes encoding cell wall degrading enzymes, including endo- $\beta$ -1,4-xylanases (EC 3.2.1.8) were generally upregulated in phytopathogenic fungi compared with saprobic fungi, thus indicating a potential role in pathogenesis (Nguyen *et al.*, 2011). This role was confirmed by gene disruption in various pathogenic fungi, such as *Botrytis cinerea* (Brito *et al.*, 2006; Nguyen *et al.*, 2011), *Cochliobolus carbonum* (Apel *et al.*, 1993; ApelBirkhold and Walton, 1996), *Fusarium oxysporum* (Ruiz-Roldan *et al.*, 1999) and *Magnaporthe grisea* (Wu *et al.*, 1997). Xylanase may play this role either through the breakdown of the cell wall (Walton, 1994, Beg *et al.*, 2001, Beliën *et al.*, 2006), which could elicit plant defence responses (Beliën *et al.*, 2006) or by inducing necrosis (Noda *et al.*, 2010). Concrete evidence has not been reported yet about the direct involvement of isochorismatase in

pathogenesis other than its potential role in plant defence through reduction of salicylic acid (van Tegelen *et al.*, 1999). PttGPI-CFEM and PttSP1 are both rich in cysteine and may have a role in the fungal growth and development (Bayry *et al.*, 2012; DeZwaan *et al.*, 1999; Hayashi and Wu, 1990; Kershaw and Talbot, 1998; Kulkarni *et al.*, 2003), which might suggest a contribution to pathogenesis. However, whether any of these proteins have a direct role during the *Ptt*-barley interaction remains to be established. Correlation of gene expression with the time course of fungal growth may help to provide a greater understanding. The aim of this research, therefore, was to quantify the gene expression of *Ptt PttXyn11A*, *PttCHFPI*, *PttSP1*, *PttGPI-CFEM* and *PttGAPDH* during the interaction of six *Ptt* isolates of different virulences with a susceptible barley cultivar.

## **6.2 Material and methods**

### **6.2.1 Quantification of expression of VRCGs in six isolates of *Ptt***

The expression profile of *PttXyn11A*, *PttCHFPI*, *PttSP1*, *PttGPI-CFEM* and *PttGAPDH* was explored during the interaction between six isolates of *Ptt* and barley cv. Sloop using quantitative reverse transcriptase PCR (RT-qPCR).

#### **6.2.1.1 Primer design for RT-qPCR**

Primers for RT-qPCR (Table 4.1), to amplify products of an appropriate length, were designed using the full length of cDNA of VRCGs and analysed using Primer3 (<http://www.ncbi.nlm.nih.gov/tools/primer-blast/>), NetPrimer (<http://www.premierbiosoft.com/netprimer/>) and BLASTn.

Conventional RT-PCR using the RT-qPCR primers was performed using DNase-treated RNA extracted from the mycelium of the 32/98 isolate (as this isolate had greater virulence and has been previously shown to express all four genes at high level, Figure 4.16) grown in FCM at 23°C for 10 days as per section 4.2.1.1. cDNA was synthesised as per section 4.2.1.4, PCR amplicons were visualised as per sections 4.2.1.3, and PCR products extracted and confirmed using the AGRF sequencing facility as per section 4.2.1.5. The target regions of VRCGs were successfully isolated and sequences of RT-qPCR primer products were confirmed (Appendix, Figure A4.1 and Figure A4.2).

**Table 6.1. List of primers used in RT-qPCR to amplify the partial length of cDNA of VRCGs *PttSPI*, *PttXyn11A*, *PttCHFP1*, *PttGPI-CFEM* and *PttGAPDH*.** Gene name, accession numbers, forward (FW) and reverse (RV) primers, annealing temperature (TM) and product length are indicated.

Genes	Accession number	Sequences of the primers 5'→3'	TM (°C)	Product length (bp)
<i>PttSPI</i>	JX900135	FW:AATCATCATCGCACTTTCTTCC	55	225
		RV:TCGTAGATGACTTCGCACTTTG	55	
<i>PttXyn11A</i>	JX900133	FW:ATGGCTTCTTCTACTCTTTCTGGAC	55	184
		RV:GAGTTGACATTCTGAGCGTTCC	55	
<i>PttCHFP1</i>	JX900134	FW:CGGAAATGATACCTATGACCTAACG	54	202
		RV:AGTCGGCTCCACTGCTTTGC	54	
<i>PttGPI-CFEM</i>	KC713871	FW:GACGGCTGCTCTGCTCTCAC	54	232
		RV:CGACAGCGGAGGTCACGGT	54	
<i>PttGAPDH</i>	EF513236	FW:GGTCAATGGCAAGACCATCCGCTTC	55	156
		RV:ACGACCTTCTGGCTCCACCCTTC	55	

### **6.2.1.2 Plant inoculation and *in planta* cDNA synthesis**

Six isolates (Table 2.1) were induced to produce conidia as per section 2.2.2. Four individual plants (cv. Sloop) (grown as per section 2.2.1) per treatment were inoculated with conidia (section 2.2.3) in each of three biological replicates. SNW was sprayed as a control. Plants were scored at 64, 98, 120, 144, 168 and 192 hpi using a numerical scale (0-10) adapted from Tekauz (1985) (Appendix, Figure A1.1). Photos were taken for representative leaves and leaf samples were also collected at 40, 64, 98, 120, 144, 168 and 192 hpi; frozen in liquid nitrogen and stored until required. RNA was extracted from infected and control leaves (500-600 mg) at each time point for all three biological replicates and DNase treated as described in section 4.2.1.3. cDNA was prepared as per section 4.2.1.4 and stored at -80°C until required.

### **6.2.1.3 Optimisation of RT-qPCR for VRCGs gene expression**

Gene expression can be analysed using either relative or absolute quantification (Brankatschk *et al.*, 2012; VanGuilder *et al.*, 2008). Relative quantification such as comparative C<sub>T</sub> ( $\Delta\Delta C_T$ ) provides a relative value presented as a ratio of the amount of initial target sequence and control (reference sample) (Livak and Schmittgen, 2001). This ratio is usually normalised to an internal standard such as the expression of a housekeeping (or reference gene) (Fraga *et al.*, 2008; VanGuilder *et al.*, 2008). Absolute quantification measures the amount of a target sequence in the sample as either copy number or concentration (Bustin and Nolan, 2004; Fraga *et al.*, 2008) relative to a standard cDNA curve. Both methods of quantification were trialled and all real-time RT-PCR experiments included the following



controls: negative controls (no-template control and no-reverse-transcriptase control) and a positive control included plasmids with corresponding genes (section 5.2.1) (Bustin *et al.*, 2009).

#### **6.2.1.3.1 VRCGs expression using Comparative C<sub>T</sub> ( $\Delta\Delta C_T$ )**

Comparative C<sub>T</sub> ( $\Delta\Delta C_T$ ) analysis was initially conducted using 64000 pg final concentration of cDNA from six isolates at 40 hpi and 192 hpi to optimise the analysis. RT-qPCR was conducted using the Applied Biosystems ViiA™ 7 Real-Time PCR System and ViiA™ 7 Software (Applied Biosystems, Life Technology) and SYBR Green (iQ™ SYBR® Green supermix, Bio-Rad). Each amplification was performed in 10 µL reaction volumes and amplification conditions of RT-qPCR were conducted as per section 4.2.1.4 and relative quantification (RQ) was calculated using the software default. The expression of *PttXyn11A*, *PttCHFPI*, *PttSP1* and *PttGPI-CFEM* was normalised using the comparative CT ( $\Delta\Delta C_T$ ) method using 08/08f (less virulent isolate) as the reference sample and *PttGAPDH* as the reference gene. However, because the software could only use one isolate as reference sample (the less virulent isolate 08/08f was used), and this is likely to have much lower levels of *PttGAPDH* expression due to the lower amount of fungus (Figure 4.17), absolute quantification was considered more suitable than the Comparative CT ( $\Delta\Delta C_T$ ) method. The RT-qPCR was therefore optimised using absolute quantification after confirmation of the gDNA quantities between isolates at 192 hpi.

#### **6.2.1.3.2 qPCR for genomic DNA for six isolates of *Ptt* at 192 hpi**

To confirm that the variable levels of *PttGAPDH* expression across isolates could be related to the different amounts of fungus during the interaction, genomic DNA from six isolates at 192 hpi was used to run qPCR. DNA was extracted using a Nucleon Phytopure Genomic DNA Extraction Kit (GE, HealthCare) according to the manufacturer's protocol and 23000 pg of DNA was used (Eshraghi *et al.*, 2011). Amplification conditions (using the same set of primers in Table 4.1) of qPCR were conducted as per section 4.2.1.4 and fluorescent values were collected at 40 cycles for all genes with three technical replicates being used.

#### **6.2.1.3.3 VRCGs expression using absolute quantification**

To optimise amplification efficiency for the absolute quantification of VRCGs expression during the interaction of *Ptt* with barley, a number of variables were examined using cDNA of the VRCGs *PttSPI*, *PttXyn11A*, *PttCHFPI* and *PttGPI-CFEM* including primer concentration and cDNA template. cDNA was obtained as per section 4.2.1.4 from RNA of the 32/98 isolate grown for 10 days in FCM as per sections 4.2.1.1 and 4.2.1.3.

##### **6.2.1.3.3.1 Primer efficiency**

To make accurate comparisons between different samples, the primer concentration used must allow high amplification efficiency (Fraga *et al.*, 2008). Three primer concentrations (100 nM, 300 nM or 400 nM) were used to determine amplification efficiency. RT-qPCR was conducted using 64000

pg of cDNA and amplification conditions as per section 4.2.1.4. Amplification efficiency was evaluated using melt curve cycle analysis, fluorescence and  $C_T$  values for each gene. The products were melted, at the end of the cycling reactions, by slowly increasing the temperature (0.05 °C/sec) and continually monitoring the fluorescence at the same time. Melt curve analysis at the end of a run provides a check that specific amplification has occurred; distinguishes products from non-specific primer-dimers; and can highlight any contamination (Bates *et al.*, 2001). Lower  $C_T$  and higher fluorescence values correspond to more expression of the gene of the interest, multiple peaks represent unspecificity of the primers and a flat curve corresponds to low amplification. Four technical replicates were used (Bustin *et al.*, 2009; Fraga *et al.*, 2008).

#### **6.2.1.3.3.2 Standard curve optimisation**

The standard curve was optimised in two experiments with varying concentrations of cDNA and both using cDNA from total RNA of 32/98 isolate grown *in vitro*: 1) 0.5, 3.5, 24.5, 171.5 or 1200.5 pg cDNA; 2) 100, 500, 2500, 12500 or 62500 pg cDNA. The second series was used as the first one only gave low amplification and flat melt curves. Amplification conditions were used and fluorescence,  $C_T$  values, correlation coefficient ( $R^2$ ) and melt curves were analysed for each gene considering the criteria mentioned in section 6.2.1.3.3.1 (Henry *et al.*, 2006; Iotti *et al.*, 2012). Four technical replicates were used for evaluation.

#### **6.2.1.3.3.3 Optimisation of final cDNA and primer concentration for *in planta* analysis**

Two final concentrations of *in planta* cDNA (35000 pg or 64000 pg) were used to perform RT-qPCR. An initial RT-qPCR was run using 35000 pg cDNA from 40, 64 and 120 hpi samples and a primer concentration of 400 nM for six isolates of *Ptt*. However, the amplification and melt curves were low (Appendix, Figure A4.9A). A second RT-qPCR therefore used 64000 pg, a primer concentration of 400 nM and cDNA from the 120 and 144 hpi samples but the amplification was also low (Appendix, Figure A4.9B) and melt curves were relatively flat. A third RT-qPCR then successfully used 4000 nM final concentration of primers with 64000 pg cDNA (Appendix, Figure A4.9C). Fluorescence signal,  $C_T$  values and melt curves were analysed for each gene considering the criteria mentioned in section 6.2.1.3.3.1. Four technical replicates were used for evaluation.

#### **6.2.1.3.4 Absolute quantification of VRCGs expression using the optimal cDNA and primer concentrations**

The optimal final concentration of cDNA (64000 pg) and primers (4000 nM) was used to quantify the expression of *PttSP1*, *PttXyn11A*, *PttCHFPI*, *PttGPI-CFEM* and *PttGAPDH* in six isolates of *Ptt* at seven timepoints (as per section 6.2.1.2). RNA extraction and DNase treatment were performed as per section 4.2.1.3 and cDNA synthesised as per section 4.2.1.4. Negative controls; no-template control and no-reverse-transcriptase control, and positive control; plasmid containing the gene were used as per section 6.2.1.3. Amplification conditions were used as per section 4.2.1.4 and  $C_T$

values and melt curves were analysed for each gene considering the criteria mentioned in section 6.2.1.3.3.1. The absolute amount of VRCG transcripts was estimated in each sample using the standard curve generated in section 6.2.1.3.3.2. Three technical replicates for each of three biological replicates of each experiment were used.

### **6.2.2 Statistical analysis and photography**

GenStat was used to analyse three biological replicates as per section 2.2.7.

Photos were taken for representative leaves and gels as per section 2.2.3.

## **6.3 Results**

### **6.3.1 Virulence of *Ptt* isolates**

Virulence of the six isolates was also recorded so that it might be correlated with the expression of VRCGs. Symptoms appeared after 64 hpi as small pin-point lesions in leaves infected with more virulent isolates (32/98 and 152/09), but after 98 hpi in leaves infected with 08/08f, 122/09, 55/07 and 123/09 (Figure 6.1). By 98 hpi, necrotic lesions were well developed in leaves infected by 32/98 or 152/09 and disease scores were significantly different ( $P < 0.001$ ,  $LSD = 0.73$ ) from the disease scores for leaves infected by other isolates (Figure 6.2). Necrosis symptoms on leaves, induced by these two isolates, developed very quickly such that the Tekauz score was at the maximum of 10 by 144 hpi and all leaves were dead by 192 hpi. The appearance of necrosis in the leaves infected with 08/08f, 122/09 and 123/09 was delayed until 144 hpi (score= 7, 5.6 and 7.7 respectively), and 120 hpi in 55/07 (score=8.3). By 192 hpi, scores of the disease scale were above 8 in all leaves that were infected with isolates except leaves infected with 122/09 which was 7.2.

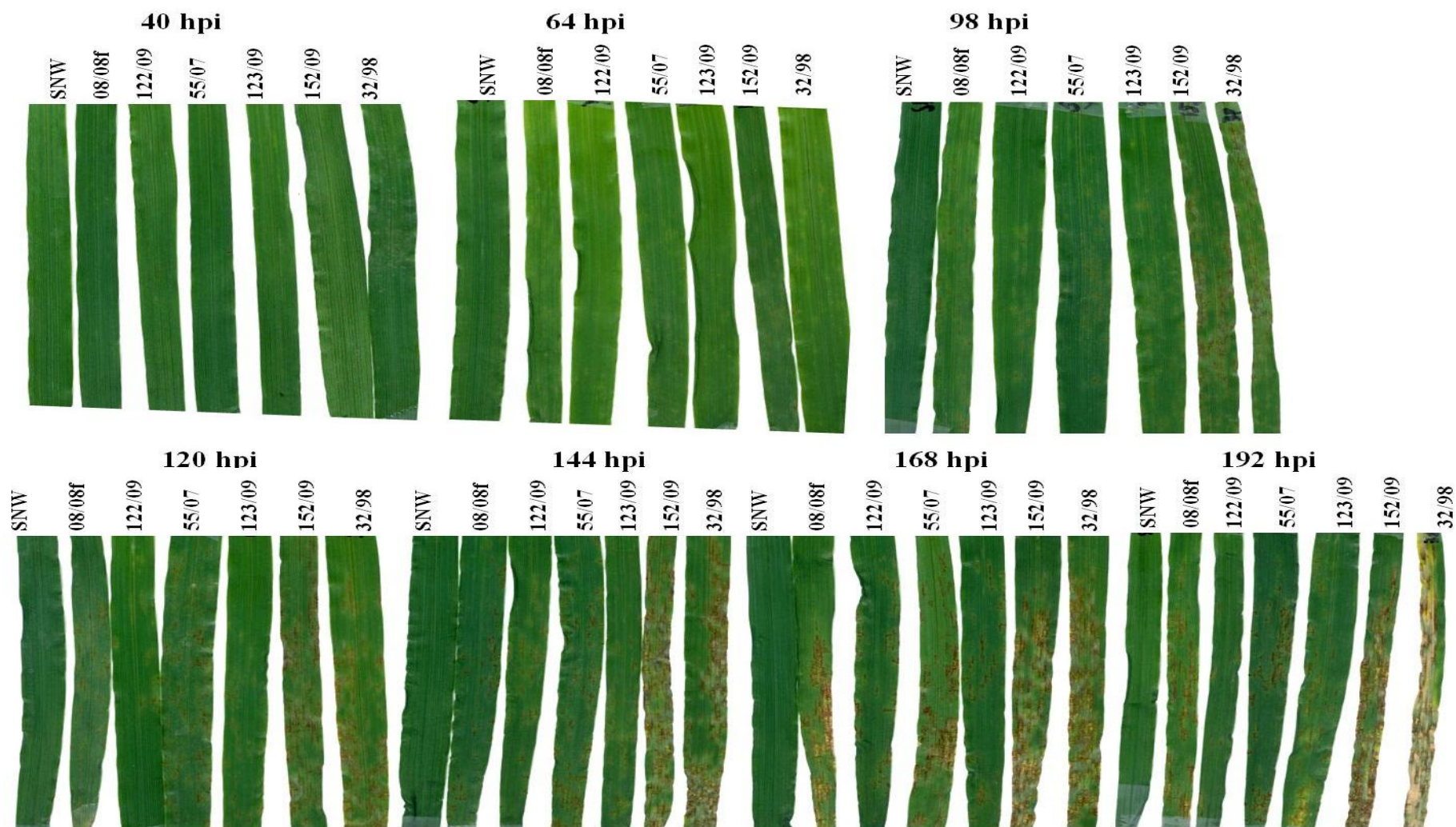


**Figure 6.1. Virulence of six isolates at different time on barley cv. Sloop, starting from 40 hours post inoculation (hpi) until 192 hpi.** Differences in the virulence of the six *Ptt* isolates, plants were treated at Zadok Stage 14. SNW; sterilised nanopure water (SNW), six isolates from low (left) to more (right) virulence, Tekauz's scale was used (0-10).

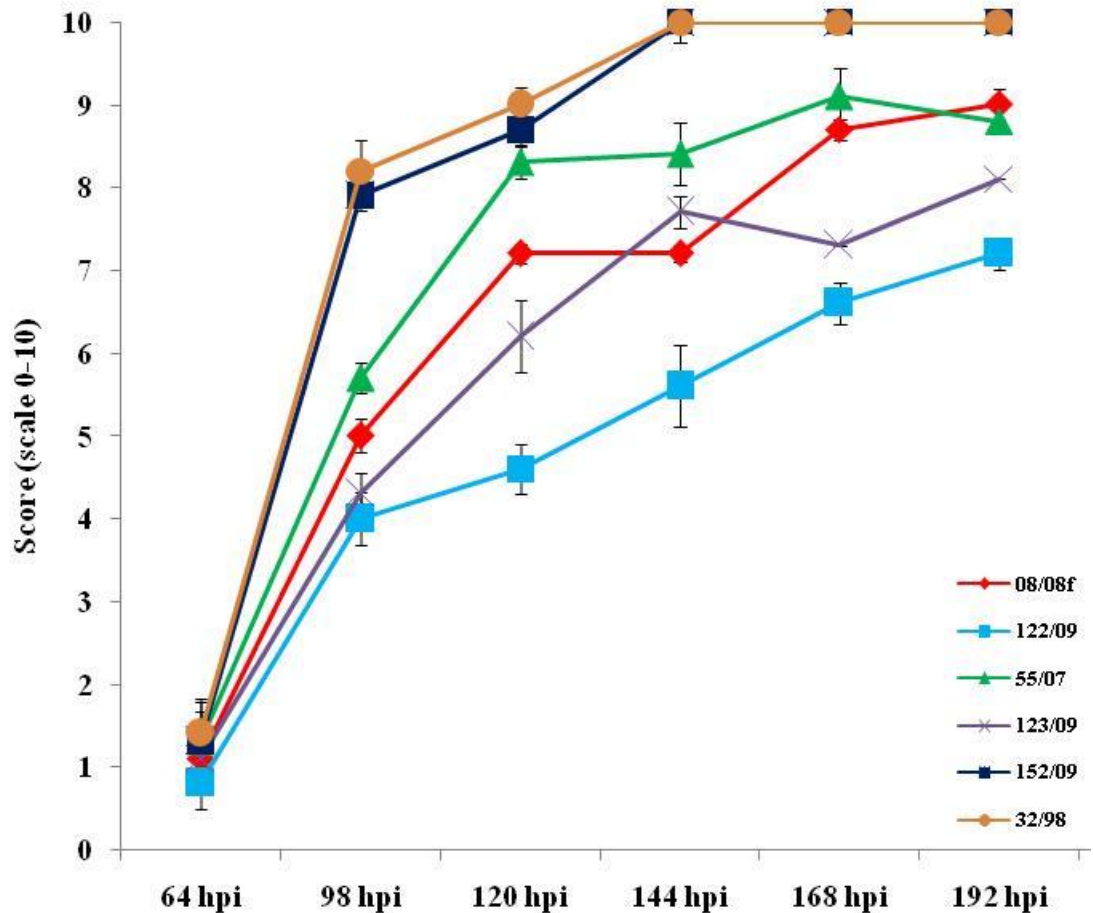


**Figure 6.2. Virulence score of six isolates at different time on barley cv. Sloop, from 64 hours post inoculation (hpi) until 192 hpi.** Twelve plants were used for each time point and isolate, Tekauz's scale was used (0-10). Three biological replicates, the least significant difference (LSD=0.73) at  $P < 0.001$ . Error bars represent the standard error of the mean of three replicates each replicate contained 4 plants.

### 6.3.2 Optimisation of quantitative RT-PCR for VRCGs

Comparative CT ( $\Delta\Delta CT$ ) and absolute quantification were used to evaluate

the appropriate gene expression analysis method *in planta*.

#### 6.3.2.1 VRCGs expression using Comparative $C_T$ ( $\Delta\Delta C_T$ )

The expression of *PttSP1*, *PttXyn11A*, *PttCHFP1* and *PttGPI-CFEM* in the susceptible barley cv. Sloop was measured using the  $C_T$  ( $\Delta\Delta C_T$ ) method at 40 hpi and 192 hpi. 08/08f and *PttGAPDH* were used as the reference sample and reference gene respectively and then the data normalised against

these references. RQ values for the isolate 08/08f for all VRCGs at the both time courses were the same (Appendix, Figure A4.3), the RQ values have been calculated using the software default assuming that 08/08f was the lowest virulent isolate (as reference sample) and *PttGAPDH* was expressed at consistent level during the interaction (as reference gene). However, 08/08f had much lower levels of *PttGAPDH* expression due to the lower amount of fungus, therefore absolute quantification was considered more suitable than the Comparative C<sub>T</sub> ( $\Delta\Delta C_T$ ) method.

#### **6.3.2.2 qPCR for genomic DNA for six isolates at 192 hpi**

Genomic DNA extracted from leaves infected with six isolates at 192 hpi was used to confirm that the variable levels of *PttGAPDH* expression across isolates could be related to the different amounts of fungus during the interaction. gDNA of *PttGAPDH* at 192 hpi, was greatest in leaves infected by the more virulent isolates (32/98 and 152/09) as evidenced by the value of fluorescence (Figure 6.3), compared with other isolates.



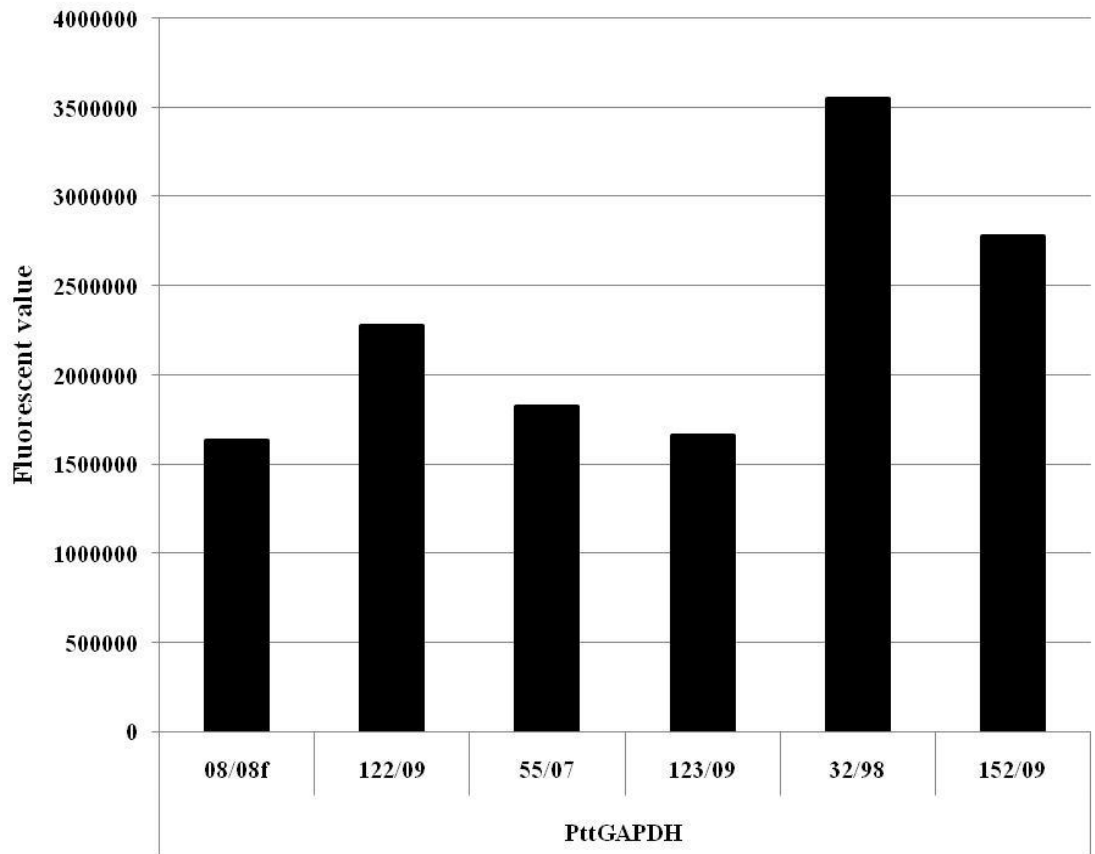


**Figure 6.3. Fluorescent value of qPCR of *PttGAPDH* for six isolates at 192 hours post inoculation (hpi).** Each number represents the value of fluorescent dye at 40 cycles for *PttGAPDH*. High value of *PttGAPDH* in leaves infected with 32/98 and 152/09 represent the amount of the fungus present in the plant tissue compared with low virulence isolates (08/08f and 122/09).

### 6.3.2.3 VRCGs expression using absolute quantification

#### 6.3.2.3.1 Primer efficiency and standard curves

Absolute quantification was used as an alternative analysis method in which the absolute amount of each gene at each timepoint was estimated. Primer efficiency was determined for each set of primers using three concentrations (400 nM, 300 nM or 100 nM). When *in vitro* cDNA of *Ptt* was used, a final concentration of 400 nM provided the greatest amplification regardless of primer sets (Appendix, Figure A4.4).

Two standard curves were performed: one at lower cDNA concentration (0.5 pg to 1200.5 pg) (Appendix, Figure A4.5) and the second at higher cDNA concentration (100 pg to 62500 pg) (Appendix, Figure A4.7). Although a final concentration of 1200.5 pg (in the first curve) (Appendix, Figure A4.5) provided best amplification for *PttXyn11A*, *PttCHFPI*, *PttGPI-CFEM* and *PttGAPDH*; no amplification was detected for *PttSPI* (Figure A4.6). In addition, fluorescence was only detected at a relatively high cycle number (~30 cycles) for most genes,  $R^2$  was too low (Appendix, Figure A4.5) and melt curves were relatively flat suggesting amplification was too low for results to be reliable. However, at the higher concentration of cDNA used in the second curve (Appendix, Figure A4.7), standard curves were linear for all genes (Appendix, Figure A4.8). Using 62500 pg cDNA, fluorescence was detected after 20 to 24 cycles for *PttXyn11A* (Appendix, Figure A4.7), *PttCHFPI*, *PttGPI-CFEM* and *PttGAPDH* compared with *PttSPI* which was detected after 30 cycles. The  $R^2$  of *PttSPI*, *PttXyn11A*, *PttCHFPI*, *PttGPI-CFEM* and *PttGAPDH* were 0.98, 0.96, 0.99, 0.98 and 0.99 respectively (Appendix, Figure A4.7) indicating high PCR efficiency and melt curve analysis showed a single product for each set of primers.

#### **6.3.2.3.2 Optimisation of cDNA concentration *in planta***

Two experiments were performed to optimise the concentration of cDNA *in planta* for six isolates of *Ptt* before running RT-qPCR. The higher concentration of *in vitro* cDNA standard curves (Appendix, Figure A4.7 and Figure A4.8) were used as a reference. RT-qPCR results at 40, 64 and 120

hpi using 35000 pg of *in planta* cDNA and 400 nM primer concentration showed that *PttSP1*, *PttXyn11A*, *PttCHFPI*, *PttGPI-CFEM* and *PttGAPDH* were amplified at low level (Appendix, Figure A4.9A) and their melt curves were flat and consequently unreliable quantification. The same results were observed when 64000 pg cDNA and 400 nM primer concentration were used to amplify VRCGs from plant tissue infected with six isolates at 120 hpi and 144 hpi (Appendix, Figure A4.9B). Therefore, primer concentration was increased up to 4000 nM with the optimal concentration of *in planta* cDNA (64000 pg). Melt curves and  $C_T$  analysis showed successful amplification (Appendix, Figure A4.9C) and single peaks in the melt curves indicated a single product for all VRCGs, therefore 4000 nM primers concentration and 64000 pg *in planta* cDNA were used for absolute quantification.

#### **6.3.2.3.2.1 Absolute quantification of VRCGs during the interaction**

The expression of *PttGPI-CFEM*, *PttSP1*, *PttXyn11A* and *PttCHFPI* transcripts encoding the four corresponding candidate proteins and *PttGAPDH* was measured during the interaction between cv. Sloop and six isolates of *Ptt* with different virulence; 08/08f, 122/09, 55/07, 123/09, 152/09 and 32/98; at 40 hpi, 64 hpi, 98 hpi, 120 hpi, 144 hpi, 168 hpi and 192 hpi using RT-qPCR with 64000 pg of cDNA and 4000 nM of primers. RT-qPCR showed reliable quantification estimated by almost identical standard curves (Appendix, Figure A4.7). *Ptt* isolates showed differences in the amount of *PttGAPDH* transcript being expressed especially by more virulent isolates (152/09 and 32/98) with the amount of *PttGAPDH* cDNA being significantly greater than that observed for other isolates at 120 hpi

( $P < 0.001$ ,  $LSD = 3130$ ) but for 152/09 alone at 192 hpi (Figure 6.4A). However, this gene was almost expressed in a similar amount at infected tissues at 40 hpi to 98 hpi for all isolates.

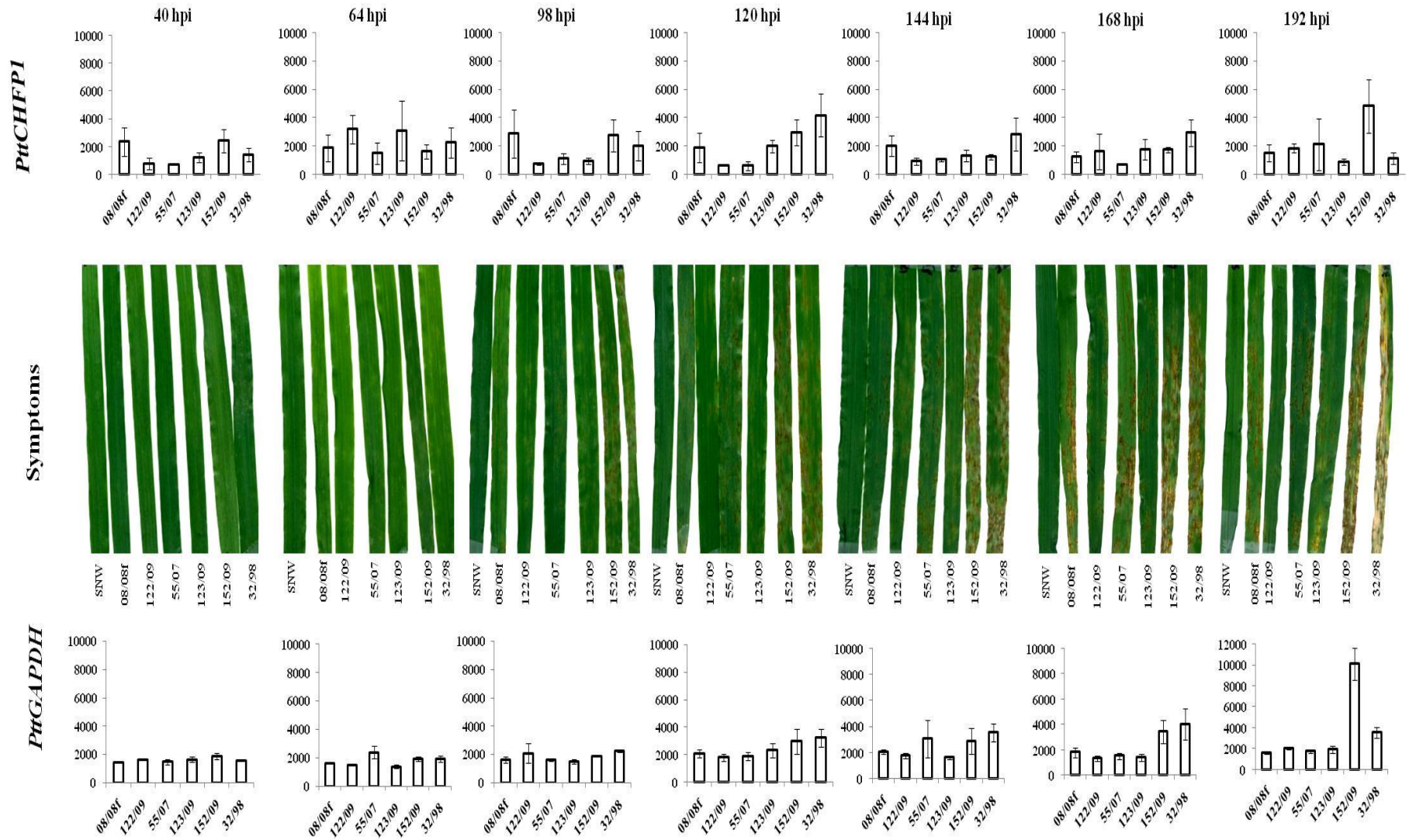
Quantification of *PttXyn11A* showed that more virulent isolates (152/09 and 32/98) produced larger quantities of this transcript in the infected tissues (Figure 6.4A) compared with other isolates. The amount of *PttXyn11A* transcript produced by the six isolates *in planta* during the interaction was similar at 40 hpi and 98 hpi within each time. However, even though the expression of *PttXyn11A* by the more virulent isolates (152/09 and 32/98) appears to be greater at 64, 120 and 144 h it was not significantly different compared with other isolates. The isolate 152/09 expressed *PttXyn11A* at significant levels ( $P < 0.001$ ,  $LSD = 9361$ ) at 168 and 192 hpi, while 32/98 produced significantly more *PttXyn11A* at 168 hpi, before being decreased at 192 hpi.

The expression profile of *PttCHFPI* in six isolates was not significant. However, the more virulent isolates (152/09 and 32/98) appeared to express *PttCHFPI* in larger quantities in the infected leaves at 120 hpi in both isolates and at 192 hpi in 152/09 (Figure 6.4B). The other isolates (08/08f, 122/09, 55/07 and 123/09) showed almost consistent expression profiles.

Absolute quantification results showed that the amount of cDNA (pg) of candidate genes transcripts *PttGPI-CFEM* and *PttSPI* did not significantly differ between all isolates and timepoints, even though they appeared to be differentiated in the cDNA amount (Figure 6.4C and D).



B





D

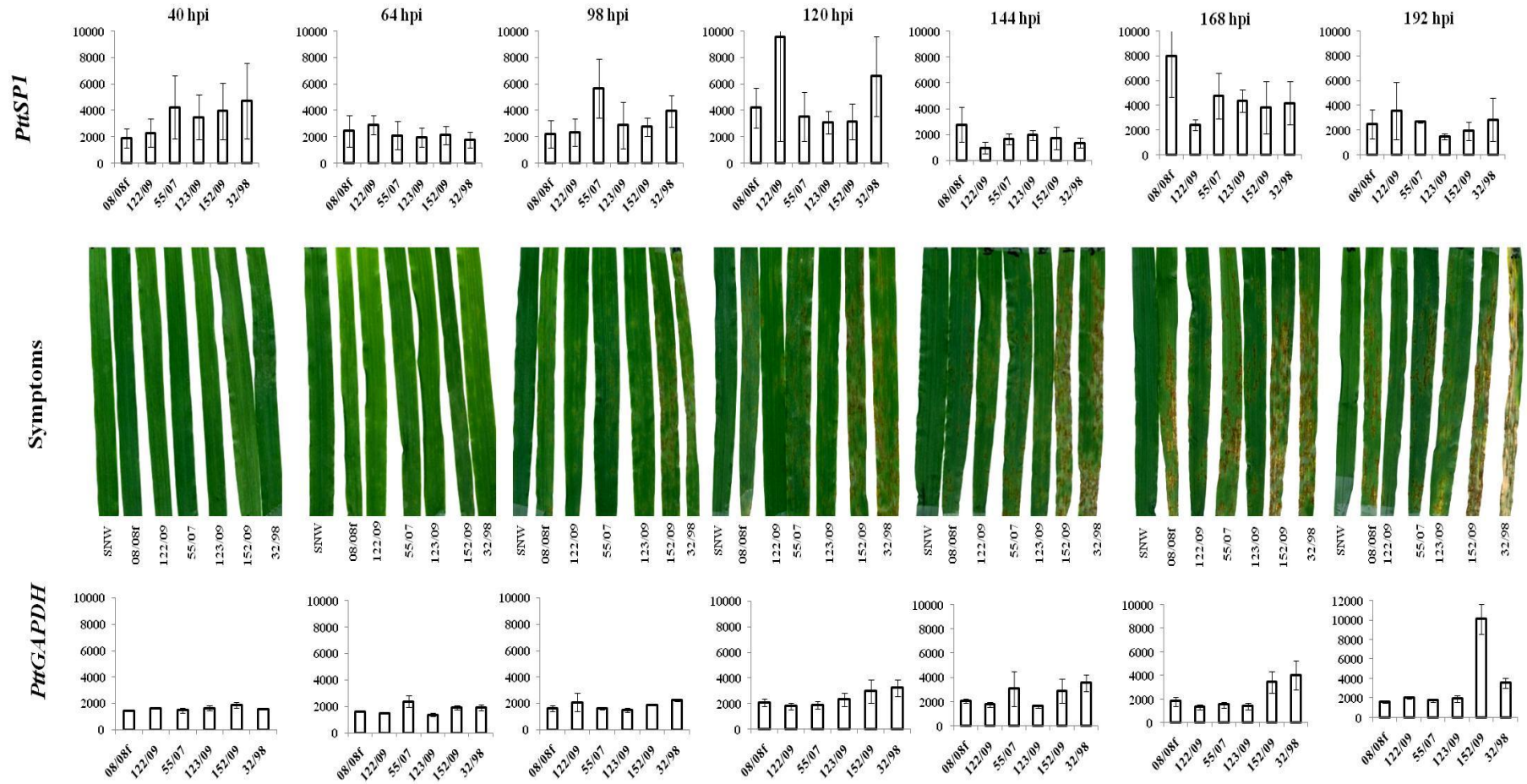


**Figure 6.4. The expression of VRCGs during the interaction of *Ptt* isolates and barley.** The absolute amount of gene transcript measured using RT-qPCR is presented as pg; *PttXyn11A* (A), *PttCHFP1* (B), *PttGPI-CFEM* (C) and *PttSPI* (D). *PttGAPDH* and VRCGs were quantified at 7 timepoints (40 hpi, 64 hpi, 98 hpi, 120 hpi, 144 hpi, 168 hpi and 192 hpi) in three technical replicates of three biological replicates. Representative image for three biological replicates of symptoms of *Ptt* isolates at 7 timepoints is shown. The least significant difference at  $P < 0.01$  (LSD, *PttXyn11A* = 9361, *PttCHFP1* = 2501, *PttGPI-CFEM* = 1606, *PttSPI* = 5421 and *PttGAPDH* = 3130).



#### 6.4 Discussion

The expression profiles of VRCGs indicated that the expression of *PttXyn11A* was upregulated in the most virulent isolates during the *Ptt*-barley interaction compared with the less virulent isolates. In addition, the more virulent isolates have greater fungal growth as evidenced by the high level of expression of *PttGAPDH*. Although there appeared to be different levels of expression of *PttCHFPI*, *PttGPI-CFEM* and *PttSPI* (as represented by the quantity of cDNA), there were no significant differences between isolates and timepoints suggesting that these genes might be expressed at an essential level probably required for pathogenesis, or they might be expressed at a relatively higher level in proportion to the quantity of the fungus.

Several optimisations of RT-qPCR were conducted to determine the most reliable analysis to quantify the expression of VRCGs in six isolates of *Ptt*. These optimisations included changing primer concentration and cDNA concentration relative to each other and generating linear standard curves. Primer concentration can have a great impact on reliability of generated data (Fraga *et al.*, 2008), as highly concentrated primers can lead to the production of non-specific products such as primer-dimers while low concentrations can decrease amplified target (Fraga *et al.*, 2008). The optimal concentration for all primers when using *in vitro* fungal cDNA was 400 nM which falls in the typical range (Fraga *et al.*, 2008). Amplifying the target fungal genes from *in planta* cDNA (cDNA synthesised from mRNA extracted from infected leaves) required a higher concentration of primers (4000 nM) and larger quantity of cDNA compared with when amplifying

cDNA from fungus alone. This was not unexpected given that the plant cDNA is likely to be more abundant than the fungal cDNA. cDNA was synthesised using an oligo (dT) primer that can hybridize to the endogenous poly (A)+, thus indicating that cDNA can be made for any transcribed gene sequence (Fraga *et al.*, 2008). Therefore, the likelihood of amplifying cDNA from mRNA from the plant is also higher.

Due to the inconsistency of the expression of *PttGAPDH* (used as a reference gene) *in planta*, absolute quantification was used in this chapter to quantify the VRCGs expression. Both qPCR and RT-qPCR for genomic DNA and *PttGAPDH* transcript (cDNA) for six isolates indicated that the more virulent isolates (152/09 and 32/98) had grown more abundantly in barley tissue. The high level of *PttGAPDH* gene expression also indicated more fungal growth in the tissue. In addition, there was an association between severe symptoms starting at 120 hpi and the amount of *PttGAPDH* transcript being expressed. These results confirmed our previous findings that the more virulent isolates have greater fungal growth compared with low virulent isolates (Figures 2.6, 2.7, 2.8 A, B and C) and complied with other research results for other fungi such as *P. tritici repentis* and *B. cinerea* (Dushnicky *et al.*, 1996; Kokkelink *et al.*, 2011). Even though relative gene expression analysis using a reference gene like *PttGAPDH* is considered most reliable (Bustin *et al.*, 2009; VanGuilder *et al.*, 2008), in this case, because  $C_T$  changed in a manner proportional to quantity of the fungus, absolute quantification of individual cDNAs was conducted.

RT-qPCR analysis revealed that the expression of *PttXyn11A* was upregulated in the more virulent isolates (152/09 and 32/98), by 168 and 192 hpi there was greater extent of expression level of *PttXyn11A* in both virulent isolates as well as greater symptom development suggesting that the *PttXyn11A* might have a role in the virulence. The observation that *PttXyn11A* were expressed to a greater extent by more virulent *Ptt* isolates *in planta* during the interaction suggested that xylanase may act as a virulence factor as has been observed for *B. cinerea* (Brito *et al.*, 2006; Noda *et al.*, 2010). The symptoms appeared in the plant inoculated with more virulent isolates at 64 hpi and disease scores were significantly different at 98 hpi (Figure 6.1). However, the isolates started to significantly express *PttXyn11A* in the infected tissues at 168 hpi (Figure 6.4A), suggesting that the more virulent isolates (152/09 and 32/98) had grown extensively in the plant tissues and had produced large amounts of  $\beta$ -1, 4 endoxylanase to degrade the cell wall and contribute to the greater symptoms. In addition, the more virulent isolates (152/09 and 32/98) showed a correlation between the fungal growth represented by the expression of *PttGAPDH* and the abundance of *PttXyn11A* transcript especially after 168 hpi. The expression of *PttXyn11A* might encourage the fungus to grow more (represented by *PttGAPDH*) or the growth of the fungus might increase the chance of producing *PttXyn11A*.

As previously discussed (chapter 4 and 5) endo-1, 4- $\beta$ -xylanase A plays an important role in virulence (Brito *et al.*, 2006; Noda *et al.*, 2010) by providing access to nutrients for the fungus through degradation of the plant

cell wall components such as xylans (Beg *et al.*, 2001; Beliën *et al.*, 2006; He *et al.*, 2009; Jaroszuk-Scisel and Kurek, 2012; Torronen *et al.*, 1992). In addition, this enzyme might assist the growth of the hyphae by softening the plant tissues and converting complex plant material into readily assimilated nutrients allowing *Ptt* to grow faster (Noda *et al.*, 2010; Staples and Mayer, 1995). *B. cinerea xyn11A* mutants had decreased growth compared with wildtype when both grew on minimal solid medium with 1% beechwood xylan as the only carbon source (Brito *et al.*, 2006), suggesting that this enzyme not only degrades host cell wall but also promotes growth. Nguyen *et al* (2011) reported that xylanases play a significant role in both vertical penetration and horizontal expansion of *M. oryzae* in infected plants and mutations in this gene reduced the number of lesions, rate of penetration and extent of infected cells. Similarly, Brito *et al.* (2006) showed that disruption mutants of the xylanase gene, *Xyn11A*, in *B. cinerea* delayed the expansion of lesions on tomato infected leaves. The observation in this study that *PttXyn11A* is expressed early in the interaction might suggest that it is enabling greater growth in the more virulent isolates.

Alternatively, it may contribute directly to necrosis via the necrosis-inducing region of the protein, considered to be independent of its catalytic activity (Noda *et al.*, 2010). This necrosis-inducing region function has been proven in *Trichoderma viride* (Furman-Matarasso *et al.*, 1999), *B. cinerea* (Noda *et al.*, 2010) and *T. reesei* (Enkerli *et al.*, 1999). The observation that *PttXyn11A* is expressed more in the more virulent isolates (where necrosis is greater) supports a similar function in *Ptt*. *PttXyn11A* could act by killing

the plant tissue surrounding the infected area allowing *Ptt* to grow on dead tissue. Necrotrophic fungi often promote programmed cell death by signalling to the hosts to kill themselves, as a defence mechanism, prior to their invasion (Hofius *et al.*, 2007; Noda *et al.*, 2010). A similar mechanism has been proposed for *P. teres* on susceptible barley (Able, 2003). Whether Xyn11A has a role in virulence by inducing necrosis directly or degrading the cell wall (or both) remains to be confirmed through mutant analysis of *PttXyn11A*. However, a reliable transformation system has not been established in Australian isolates yet. Although there have been attempts to knock out some genes in *Ptt*, results to date have not been successful (Simon Ellwood, personal communication). Alternatively, the necrosis inducing region could be confirmed by expressing this region heterologously and performing the bioassay test with it.

Although the expression of *PttCHFP1* and *PttSPI* were not significant between all isolates, transcripts of these genes might be enough to be translated to a sufficient protein to be effective in the pathogenesis process. Previous research found that trace amounts of Ptr-ToxB from *P. tritici repentis* (Kim and Strelkov, 2007) and proteinaceous toxins from *Ptt* (Sarpeleh *et al.*, 2007) were required to induce symptoms in wheat and barley respectively. PttCHFP1 shares similarity to an isochorismate hydrolase, as previously discussed (chapter 4). This enzyme has been identified as being produced by plant pathogenic Ascomycetes (Soanes *et al.*, 2008) and has been shown to possibly repress plant defence systems by inhibiting the production of salicylic acid. However, the involvement of

cysteine hydrolase enzymes and the role of salicylic acid needs to be confirmed in the interaction between *Ptt* and barley. *PttSPI* might also have a role in fungal development (as has been discussed in chapter 4). However, the role of *PttCHFP1* and *PttSPI* in virulence needs to be clarified via gene mutations.

RT-qPCR results also showed similarity in the expression profile of *PttGPI-CFEM* in six isolates of *Ptt in planta* at all time courses. This result was expected as fungal proteins containing the CFEM domain appears to be required for hyphae adhesion (DeZwaan *et al.*, 1999; Kulkarni *et al.*, 2003), which is essential pathogenesis processes as has been shown and discussed in chapter 4 (Figure 4.16 and Figure 4.17).

In conclusion, the likely infection scenario is that the more virulent isolates, after attachment to the plant tissue, produce PttXyn11A to either degrade the plant cell wall providing entry to the host cell and the nutrients necessary for fungal development, or by inducing programmed cell death. In addition, if PttCHFP1 is an isochorismate hydrolase then the plant defence response is also suppressed (Keates *et al.*, 2003; Rohe *et al.*, 1995; Soanes *et al.*, 2008) and the fungus is able to grow rapidly in the plant.

## **Chapter 7    General discussion**

Given the importance of net form of net blotch disease of barley, an understanding of the infection process by *Pyrenophora teres* f. *teres* (*Ptt*) is essential to support the development of control strategies for this disease. The research presented in this thesis aimed to provide information about the infection process of barley by isolates of *Ptt* with different virulence by studying conidial germination, hyphal development, toxin production and analysis of virulence-related candidate proteins (VRCPs). This study has shown that *Ptt* isolates had different abilities to grow on barley tissue, and their virulence was usually correlated with their ability to establish quickly. In addition, toxin production appears to have an important role in symptom development with all isolates able to produce toxins that can cause symptoms. However, specific toxins from the same fractions and sub-fractions of the culture filtrates caused symptoms regardless of the virulence of the isolate. Therefore, the observation of symptoms during the interaction suggests that both fungal growth and proteinaceous toxins are required to complete the infection process. PAGE and 2DGE analysis showed that these active fractions contained proteins between 37 and 150 kDa in size. LC-ESI-IT MS analysis of these proteins identified homologs to several groups of proteins previously associated with virulence. Four VRCPs were chosen for further analysis: PttXyn11A, PttCHFP1, PttGPI-CFEM and PttSP1 because of their potential roles in plant cell wall degradation, plant defence inhibition, hyphal adhesion and a potential role in symptom induction (as an effector) respectively. RT-PCR and RT-qPCR analysis of the transcripts of

the VRCs genes, have shown that the expression of *PttXyn11A* was upregulated in the most virulent isolates during the interaction. However, the expression of *PttCHFPI*, *PttGPI-CFEM* and *PttSPI* was constitutive and not different between all isolates during the interaction, suggesting that all isolates have regulated the expression of these genes to an essential level, possibly required for pathogenesis. Therefore, the difference in the virulence (especially the most virulent isolates) might be attributed to the expression level of *PttXyn11A*.

### **7.1 Virulence needs both toxin production and fungal growth**

The virulence of plant pathogens is based upon their ability to colonise plant tissue in a relatively short time and cause extensive tissue damage. The colonisation of the leaves by the *Ptt* fungus is a complicated process requiring hyphal growth and secretion of pathogenic proteins (Berestetskiy, 2008; Solomon and Rathjen, 2010; Stergiopoulos *et al.*, 2013; Tan *et al.*, 2010). Results showed that, in general, the more virulent isolates had greater growth represented by a higher rate of conidial germination (both *in vitro* and *in planta*, Figure 2.5), longer hyphae and more appressoria compared with less virulent isolates (Figure 2.6, Figure 2.7 and Figure 2.8). Additionally, fungal growth was greater in the more virulent isolates as evidenced by the presence of more *PttGAPDH* and its transcript during the interaction (Figure 4.17, Figure 6.3 and Figure 6.4). Some research has reported that conidial germination (germination time and rate) was an essential infection factor which might determine the virulence of fungus (Dantigny *et al.*, 2011; Judet *et al.*, 2008; Vandenberg and Rosnagel,



1990). Fungal growth and toxin production might assist each other in the infection of barley by *Ptt*, as has been shown in similar fungi (Berestetskiy, 2008; Solomon and Rathjen, 2010; Stergiopoulos *et al.*, 2013; Tan *et al.*, 2010). More virulent *Ptt* isolates might have grown more abundantly *in planta* because there was an increase in toxin production and therefore more symptoms and/or vice versa. In addition, the germination process probably required the secretion of proteins which might be involved in pathogenesis. This has been reported for Ptr ToxB of *P. tritici-repentis* which was present in spore germination and culture fluids of a virulent isolate but not in an avirulent isolate (Cao *et al.*, 2009). Furthermore, in the virulent isolate of *P. tritici-repentis* (which also produced a higher amount of Ptr ToxB) the number of appressoria and its formation speed were significantly higher compared with the avirulent isolate (which produced lower amounts of active Ptr ToxB) (Amaike *et al.*, 2008). The most virulent isolates of *Ptt*, therefore, might use a similar mechanism but that requires confirmation in further research. In addition, the lack of an avirulent isolate of *Ptt* on barley varieties grown in Australia prevented a comparison with virulent isolates. This comparison might allow identification of the differences in the protein profile. However, comparisons of *Ptt* isolates with different virulence, which have been made in this study, provided an insight to the contribution of individual proteinaceous toxins to virulence.

#### **7.1.1 Xylanase contributes to *Ptt* virulence**

Hyphal penetration also requires toxins to facilitate host tissue colonisation and consequently fungal nutrition and growth (Berestetskiy, 2008; Wolpert

*et al.*, 2002). These toxins are generally cell wall degradation enzymes (Beliën *et al.*, 2006; Yang *et al.*, 2011). Using LC-ESI-IT MS analyses, an endoxylanase (PttXyn11A, Figure 4.3 and Figure 4.4) was identified in the culture filtrates of *Ptt* isolates (Table 3.8), with the most virulent isolates producing the greatest quantities and greatest xylanase activity *in vitro* (Figure 3.7, Figure 5.21). Bioinformatics analyses characterised PttXyn11A as being homologous with and having similar characteristics to endoxylanase from other fungi (Brito *et al.*, 2006; Ellouze *et al.*, 2011; Noda *et al.*, 2010). Furthermore, *PttXyn11A* expression was upregulated *in vitro* and *in planta* (Figure 4.16, Figure 4.17 and Figure 6.4A), indicating that the *Ptt* fungus might use this toxin to breach the plant cell wall and provide access and nutrients for fungal growth. However, there were no significant differences in the *PttXyn11A* expression profile at the early stages of infection, probably due to the limited fungal material available in the plant tissue. Alternatively, the amount of endoxylanase was possibly small but still enough to break down the cell wall of the plant cells around the first hyphae. In similar research, trace amount of toxins was required to induce symptoms (Kim and Strelkov, 2007; Sarpeleh *et al.*, 2007). This trace amount of PttXyn11A might require low level of gene expression and consequently this expression was not detected by RT-qPCR. Similarly, other researchers have demonstrated the importance of endoxylanase as a virulence factor (Beliën *et al.*, 2006; Ellouze *et al.*, 2011; Enkerli *et al.*, 1999; Gomez-Gomez *et al.*, 2002; Nguyen *et al.*, 2011; Wu *et al.*, 1997). The quantity and persistence of endoxylanase (PttXyn11A) secretion in the

more virulent isolates (32/98 and 152/09) (Figure 6.4A) further supports the proposed function of PttXyn11A as a virulence factor in *Ptt*.

Endoxylanase also has been shown to have necrosis activity by acting as a necrosis-inducing agent (Hofius *et al.*, 2007; Noda *et al.*, 2010). This activity is independent from enzymatic activity (Enkerli *et al.*, 1999; Furman-Matarasso *et al.*, 1999; Nguyen *et al.*, 2011; Rotblat *et al.*, 2002). This research has identified similarity in the necrosis-inducing region in PttXyn11A with other well characterised endoxylanases (TrXyn11A and BcXyn11A of *Trichoderma reesei*, and *Botrytis cinerea* respectively) (Brito *et al.*, 2006; Ellouze *et al.*, 2011), suggesting that PttXyn11A might have the ability to induce necrosis in plants. Bioassay tests of commercial endoxylanase has shown necrosis activity (Figure 5.20), suggesting that the necrosis-inducing region might also exist in the commercial endoxylanase. However, no comparison has been made with this enzyme as the sequence is not publicly available. Therefore, the role of PttXyn11A as a virulence factor and the role of its necrosis-inducing region needs to be confirmed by gene deletion mutants of *Ptt*. However, if gene disruption occurs, the other endoxylanases may take over the role of PttXyn11A. This has been suggested in the interaction between *Magnaporthe oryzae* and rice with other endoxylanase members expressed at higher levels during infection to complement the decrease of endoxylanase activity resulting from the gene disruption (Nguyen *et al.*, 2011). Hence, it would be interesting to look at all the endoxylanases and their role in the *Ptt*-barley interaction.

### 7.1.2 PttCHFP1 might contribute to *Ptt* virulence

LC-ESI-IT MS analysis also revealed that the more virulent isolate of *Ptt* fungus produced peptides that matched to hypothetical protein in *Ptt* database (named PttCHFP1). This protein has shown homology to isochorismatase in *P. tritici-repentis* database (Figure 4.7). Isochorismatase has been proposed to have a role in the inhibition of the plant defence system and more specifically salicylic acid production (El-Bebany *et al.*, 2010; Kunkel and Brooks, 2002; Soanes *et al.*, 2008; Wildermuth *et al.*, 2001). Additionally, chlorosis activity was recorded during the bioassay of recombinant PttCHFP1 (Figure 5.16), however RT-PCR (Figure 4.16 and Figure 4.17) and RT-qPCR (Figure 6.4B) results showed that all isolates upregulated the expression of *PttCHFP1* to the same level.

Interestingly, pathogenesis-related (PR) proteins were identified in the intercellular washing fluids (ICWFs) of susceptible cultivar (Sloop) infected with the virulent isolate of *Ptt* (Table 3.6). Generally, PR proteins are induced in resistant plants as a response to pathogen invasion and their induction is controlled by salicylic acid (Kristensen *et al.*, 1999; Muthukrishnan *et al.*, 2001; Santén *et al.*, 2005; ScottCraig *et al.*, 1995). However, the observation that PR proteins were induced in the susceptible plant during the interaction with *Ptt* might suggested that salicylic acid was still produced and therefore that PttCHFP1 might not act as an isochorismatase as has been previously suggested for similar proteins (El-Bebany *et al.*, 2010; Wildermuth *et al.*, 2001), or that other virulence proteins produced by *Ptt* during the interaction might elicit salicylic acid production. The involvement of cysteine hydrolase enzyme (PttCHFP1) and

the role of salicylic acid, therefore, needs to be confirmed in the interaction between *Ptt* and barley by comparing virulent and avirulent isolates of *Ptt* and investigating whether PttCHFP1 acts as virulence factor.

### **7.1.3 Contribution of other proteinaceous toxins to *Ptt* virulence**

Although PttGPI-CFEM was identified in the active fraction and sub-fraction of the culture filtrates of the most virulent isolate (Table 3.4), RT-PCR (Figure 4.16 and Figure 4.17) and RT-qPCR (Figure 6.4C) analysis has not shown differences in the expression profile of *PttGPI-CFEM* during the interaction between six isolates of *Ptt* and barley. Kulkarni *et al.* (2003) reported that fungal proteins with the CFEM domain are necessary for fungal networking and attachment, therefore these results were not surprising as these isolates have the ability to grow and develop networks *in vitro* (Figure 2.10) and *in planta* (Figure 2.6). In addition, bioinformatics analysis showed that PttGPI-CFEM and PttSP1 were richer in cysteine. Cysteine-rich proteins with no known enzymatic activity have been suggested to be important in some host-pathogen interactions because of their eliciting activity (Keates *et al.*, 2003; Rohe *et al.*, 1995).

Other proteins have been also identified in LC-ESI-IT MS analysis which might assist fungal growth and development such as glucan 1, 3- $\beta$ -glucosidase, GPI-anchored cell wall  $\beta$ -1,3-endoglucanase and 6-phosphogluconolactonase (Table 3.8) (Baladrón *et al.*, 2002; Beg *et al.*, 2001; Beliën *et al.*, 2006; Boonvitthya *et al.*, 2012; Gowda *et al.*, 2006; Hartl *et al.*, 2011; Tamano *et al.*, 2007; Walton, 1994). However, several proteins were identified in the active fraction of the culture filtrates of the

most virulent isolate, the function of these proteins were unknown and annotated as conserved hypothetical protein. These proteins required further characterisation.

#### **7.1.4 Proposed infection process of barley by *Ptt***

Based upon the results obtained from this research the sequence of infection events probably followed during the interaction between *Ptt* and barley has been suggested (Figure 7.1). Conidial germination has occurred by 24 h, then toxins might assist the establishment of the pathogen during infection by promoting the adhesion of the germ tube to the surface of the leaf potentially using PttGPI-CFEM (Kulkarni *et al.*, 2003; Perez *et al.*, 2011). Appressoria formation occurs before the hyphae have penetrated the cell wall (Lightfoot and Able, 2010) using cell wall degradation enzymes (Adams, 2004; Brito *et al.*, 2006; Ellouze *et al.*, 2011; Jorge *et al.*, 2005; Lehtinen, 1993; Nguyen *et al.*, 2011; Noda *et al.*, 2010; Reuveni *et al.*, 2007; Wu *et al.*, 1997) such as PttXyn11A. Additionally, at the early stage of interaction, cross talk might occur between the fungus and plant which may lead to cell death. Several potential pathways have been suggested which might lead to necrosis, including the necrosis-inducing region in the PttXyn11A protein. This region might mediate binding to plant cells (Noda *et al.*, 2010), especially as it is located on the surface of the enzyme and therefore has a direct effect in the necrosis induction. Elicitors released from the plant cell wall during their degradation might also induce necrosis (Ellouze *et al.*, 2011; Nguyen *et al.*, 2011; Noda *et al.*, 2010). In addition, necrosis might occur through elicitor-active carbohydrates released from

fungal cell walls by fungal cell wall degradation enzymes produced by the plant such as endoglucanase and chitinase (Okinaka *et al.*, 1995; Yoshikawa *et al.*, 1990). These enzymes have been identified in the ICWFs of barley plants infected by the most virulent isolate. However, whether chemical degradation of plant and fungal cell wall by cell wall degradation enzymes contributes to plant cell death is still not known. Furthermore, cell death might be induced through potential effectors such as PttSP1, considering that effectors have a role in necrosis (Ciuffetti *et al.*, 2010; Godfrey *et al.*, 2010; Oliver and Solomon, 2010; Solomon and Rathjen, 2010; Stergiopoulos and de Wit, 2009; Tan *et al.*, 2010). Alternatively, proteins with unknown function possibly have roles in the infection process. These molecules might induce programmed cell death in the plant tissue providing optimal conditions for *Ptt* to grow as necrotrophic fungus (Able, 2003; Hofius *et al.*, 2007; Jonathan and Jacques, 2001; Stergiopoulos *et al.*, 2013). In addition, the fungus might repress the plant defence system by inhibiting the production of salicylic acid (Dempsey *et al.*, 1999; El-Bebany *et al.*, 2010; Wildermuth *et al.*, 2001) potentially via secreting PttCHFP1 which appeared as a homolog to isochorismatase. The combination of the actions of these VRCs and other proteinaceous toxins possibly helped *Ptt* to achieve infection.

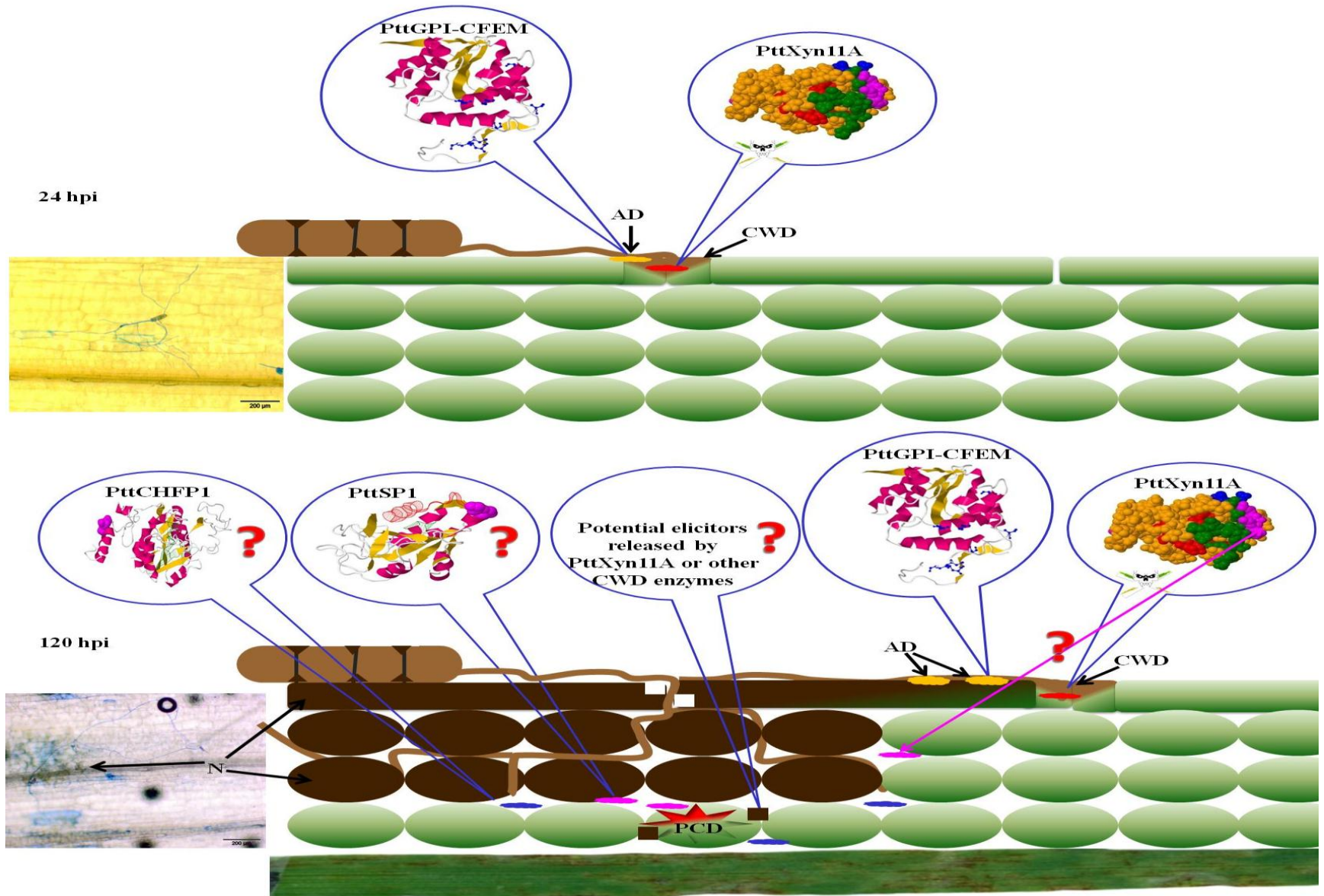


**Figure 7.1. Simplified schematic showing the proposed scenario for *Ptt* infection process.** Two timepoints were used in this diagram (24 hpi and 120 hpi); AD, adhesion; CWD, cell wall degradation; N, necrosis; PCD, programmed cell death. Four virulence-related candidate proteins (VRCPs) were assigned to potential functions in the interaction, question marks indicate uncertain function.



## 7.2 Conclusion and future directions

*Ptt* isolates differed in their virulence from low to extreme and produced a mixture of proteins which was toxic to the barley cv. Sloop. LC-eSI-IT MS analysis identified several groups of proteins including cell wall degradation enzymes, proteins involved in fungal development and several proteins with unknown function. Four VRCPs were detected as more abundant in the culture filtrates of a more virulent isolate (*PttXyn11A*, *PttCHF1*, *PttGPI-CFEM* and *PttSP1*). RT-PCR and RT-qPCR also demonstrated that *PttXyn11A* and *PttGAPDH* were expressed more abundantly by more virulent isolates compared with the other isolates during the plant-pathogen interaction. The expression profile of *PttCHF1*, *PttGPI-CFEM* and *PttSP1* during the interaction of *Ptt* and barley was not significantly different, regardless of isolate. This study is the first to identify individual proteinaceous toxins in *Ptt* culture filtrates and during the *Ptt*-barley interaction. It also provides a model to investigate other proteinaceous toxins that might be involved in the interaction. However, to fully understand the mechanism of *Ptt* infection, more research is required including:

1. Comparative study of virulent and avirulent isolate (possibly through the application of gene mutation) by investigating the differences in fungal growth *in planta* and protein profiles *in vitro* and bioassay of culture filtrate fractions from both isolates.
2. Using the bioassay of the active fractions and sub-fractions to investigate any source of resistance to these toxins in the barley lines through QTL mapping. In addition, QTL mapping might be used to

the identification of the toxin-susceptible/sensitive region in barley cultivars which might lead to identify the toxin targets in the plant.

3. The characterisation of other proteinaceous toxins identified in this study is required including the hypothetical proteins with unknown functions.
4. Using gene deletion as a tool for investigating the pathogenesis role of all proteins but in particular the endoxylanase (*PttXyn11A*) role in the virulence of *Ptt* isolates and necrosis-inducing region.
5. Heterologous expression of necrosis-inducing region in endoxylanase (*PttXyn11A*) and bioassay of the recombinant protein.
6. The role of PttGPI-CFEM in hyphal adhesion also needs to be confirmed through gene mutation.

## References

- Able, A. J.** (2003) Role of reactive oxygen species in the response of barley to necrotrophic pathogens. *Protoplasma* **221**, 137-143.
- Able, A. J., Guest, D. I. and Sutherland, M. W.** (1998) Use of a new tetrazolium-based assay to study the production of superoxide radicals by tobacco cell cultures challenged with avirulent zoospores of *Phytophthora parasitica* var *nicotianae*. *Plant Physiol.* **117**, 491-499.
- Able, A. J., Guest, D. I. and Sutherland, M. W.** (2000) Hydrogen peroxide yields during the incompatible interaction of tobacco suspension cells inoculated with *Phytophthora nicotianae*. *Plant Physiol.* **124**, 899-910.
- Adams, D. J.** (2004) Fungal cell wall chitinases and glucanases. *Microbiology-Sgm* **150**, 2029-2035.
- Adhikari, T. B., Bai, J. F., Meinhardt, S. W., Gurung, S., Myrfield, M., Patel, J., et al.** (2009) Tsn1-mediated host responses to ToxA from *Pyrenophora tritici-repentis*. *Mol. Plant-Microbe Interact.* **22**, 1056-1068.
- Afanasenko, O., Mironenko, N., Filatova, O., Kopahnke, D., Kramer, I. and Ordon, F.** (2007a) Genetics of host-pathogen interactions in the *Pyrenophora teres* f. *teres* (net form) - barley (*Hordeum vulgare*) pathosystem. *Eur. J. Plant Pathol.* **117**, 267-280.
- Afanasenko, O. S., Jalli, M., Pinnschmidt, H. O., Filatova, O. and Platz, G. J.** (2009) Development of an international standard set of barley differential genotypes for *Pyrenophora teres* f. *teres*. *Plant Pathol.* **58**, 665-676.
- Afanasenko, O. S., Mironenko, N. V., Filatova, O. A. and Serenius, M.** (2007b) Structure of *Pyrenophora teres* f. *teres* populations from Leningrad Region and Finland by virulence. *Mikol. Fitopatol.* **41**, 261-268.
- Ahmad, M. F., Yadav, B., Kumar, P., Puri, A., Mazumder, M., Ali, A., et al.** (2012) The GPI anchor signal sequence dictates the folding and functionality of the Als5 adhesin from *Candida albicans*. *PLoS ONE* **7**, e35305.
- Alconada, T. M. and Martinez, M. J.** (1994) Purification and characterization of an extracellular endo-1,4-beta-xylanase from *Fusarium oxysporum* f. sp. *melonis*. *FEMS Microbiol. Lett.* **118**, 305-310.
- Amaike, S., Ozga, J. A., Basu, U. and Strelkov, S. E.** (2008) Quantification of ToxB gene expression and formation of appressoria by isolates of *Pyrenophora tritici repentis* differing in pathogenicity. *Plant Pathol.* **57**, 623-633.
- Amnuaykanjanasin, A. and Daub, M. E.** (2009) The ABC transporter ATR1 is necessary for efflux of the toxin cercosporin in the fungus *Cercospora nicotianae*. *Fungal Genet. Biol.* **46**, 146-158.
- Anderson, J. A., Effertz, R. J., Faris, J. D., Francl, L. J., Meinhardt, S. W. and Gill, B. S.** (1999) Genetic analysis of sensitivity to a

- Pyrenophora tritici-repentis* necrosis-inducing toxin in durum and common wheat. *Phytopathology* **89**, 293-297.
- Angelova, Z., S., G. and W., R.** (2006) Elicitation of plants. *Biotechnol. Biotec. Eq.* **20**, 84-88.
- Angelova-Merhar, V. S., Van Der Westhuizen, A. J. and Pretorius, Z. A.** (2001) beta-1,3-glucanase and chitinase activities and the resistance response of wheat to leaf rust. *J. Phytopathol.* **149**, 381-384.
- Angelova, V. S., van der Westhuizen, A. J. and Pretorius, Z. A.** (1999) Intercellular proteins and beta-1,3-glucanase activity associated with leaf rust resistance in wheat. *Physiol. Plant.* **106**, 393-401.
- Apel, P. C., Panaccione, D. G., Holden, F. R. and Walton, J. D.** (1993) Cloning and targeted gene disruption of *xyl1*, a beta-1,4-xylanase gene from the maize pathogen *Cochliobolus carbonum*. *Mol. Plant-Microbe Interact.* **6**, 467-473.
- ApelBirkhold, P. C. and Walton, J. D.** (1996) Cloning, disruption, and expression of two endo-beta 1,4-xylanase genes, XYL2 and XYL3, from *Cochliobolus carbonum*. *Appl. Environ. Microbiol.* **62**, 4129-4135.
- Avni, A., Anderson, J. D., Holland, N., Rochaix, J. D., Grometelhanan, Z. and Edelman, M.** (1992) Tentoxin sensitivity of chloroplasts determined by Codon-83 of Beta-Subunit of Proton-ATPase. *Science* **257**, 1245-1247.
- Bailey, M. J., Biely, P. and Poutanen, K.** (1992) Interlaboratory testing of methods for assay of xylanase activity. *J. Biotechnol.* **23**, 257-270.
- Baladrón, V., Ufano, S., Dueñas, E., Martín-Cuadrado, A. B., del Rey, F. and Vázquez de Aldana, C. R.** (2002) Eng1p, an endo-1,3-beta-glucanase localized at the daughter side of the septum, is involved in cell separation in *Saccharomyces cerevisiae*. *Eukaryot. Cell* **1**, 774-786.
- Ballance, G. M., Lamari, L. and Bernier, C. C.** (1989) Purification and characterization of a host-selective necrosis toxin from *Pyrenophora-tritici-repentis*. *Physiol. Mol. Plant Pathol.* **35**, 203-213.
- Ballio, A.** (1991) Non-host-selective fungal phytotoxins: Biochemical aspects of their mode of action. *Experientia* **47**, 783-790.
- Barrault, G., Alali, B., Petitprez, M. and Albertini, L.** (1982) Contribution to the study of the toxic activity of *Helminthosporium teres*, a parasite on barley (*Hordeum vulgare*). *Can. J. Bot.* **60**, 330-339.
- Bartnick, S.** (1968) Cell wall chemistry morphogenesis and taxonomy of fungi. *Annu. Rev. Microbiol.* **22**, 87-108.
- Bates, J. A., Taylor, E. J. A., Kenyon, D. M. and Thomas, J. E.** (2001) The application of real-time PCR to the identification, detection and quantification of *Pyrenophora* species in barley seed. *Mol. Plant Pathol.* **2**, 49-57.
- Bayry, J., Aïmanianda, V., Guijarro, J. I., Sunde, M. and Latgé, J.-P.** (2012) Hydrophobins-Unique fungal proteins. *PLoS Pathog* **8**, e1002700.

- Beattie, A. D., Scoles, G. J. and Rossnagel, B. G.** (2007) Identification of molecular markers linked to a *Pyrenophora teres* avirulence gene. *Phytopathology* **97**, 842-849.
- Beg, Q. K., Kapoor, M., Mahajan, L. and Hoondal, G. S.** (2001) Microbial xylanases and their industrial applications: a review. *Appl. Microbiol. Biotechnol.* **56**, 326-338.
- Beliën, T., Van Campenhout, S., Robben, J. and Volckaert, G.** (2006) Microbial endoxylanases: Effective weapons to breach the plant cell-wall barrier or, rather, triggers of plant defense systems? *Mol. Plant-Microbe Interact.* **19**, 1072-1081.
- Bendtsen, J. D., Jensen, L. J., Blom, N., von Heijne, G. and Brunak, S.** (2004) Feature-based prediction of non-classical and leaderless protein secretion. *Protein Eng. Des. Sel.* **17**, 349-356.
- Benhamou, N., Grenier, J. and Asselin, A.** (1991) Immunogold localization of pathogenesis-related protein p14 in tomato root-cells infected by *Fusarium-oxysporum* f sp *radicis-lycopersici*. *Physiol. Mol. Plant Pathol.* **38**, 237-253.
- Bent, A. F. and Mackey, D.** (2007) Elicitors, effectors, and R genes: The new paradigm and a lifetime supply of questions. *Annu. Rev. Phytopathol.* **45**, 399-436.
- Berestetskiy, A. O.** (2008) A review of fungal phytotoxins: from basic studies to practical use. *Appl. Biochem. Microbiol.* **44**, 453-465.
- Betts, M. F., Manning, V. A., Cardwell, K. B., Pandelova, I. and Ciuffetti, L. M.** (2011) The importance of the N-terminus for activity of Ptr ToxB, a chlorosis-inducing host-selective toxin produced by *Pyrenophora tritici repentis*. *Physiol. Mol. Plant Pathol.* **75**, 138-145.
- Bhadauria, V., Zhao, W.-S., Wang, L.-X., Zhang, Y., Liu, J.-H., Yang, J., et al.** (2007) Advances in fungal proteomics. *Microbiol. Res.* **162**, 193-200.
- Boddi, S., Comparini, C., Calamassi, R., Pazzagli, L., Cappugi, G. and Scala, A.** (2004) Cerato-platanin protein is located in the cell walls of ascospores, conidia and hyphae of *Ceratocystis fimbriata* f. sp *platani*. *FEMS Microbiol. Lett.* **233**, 341-346.
- Bogacki, P., Keiper, F. J. and Oldach, K. H.** (2010) Genetic structure of South Australian *Pyrenophora teres* populations as revealed by microsatellite analyses. *Fungal Biol.* **114**, 834-841.
- Bolanos-Garcia, V. M. and Davies, O. R.** (2006) Structural analysis and classification of native proteins from *E. coli* commonly co-purified by immobilised metal affinity chromatography. *Biochimica Et Biophysica Acta-General Subjects* **1760**, 1304-1313.
- Boonvitthya, N., Tanapong, P., Kanngan, P., Burapatana, V. and Chulalaksananukul, W.** (2012) Cloning and expression of the *Aspergillus oryzae* glucan 1,3-beta-glucosidase A (*exgA*) in *Pichia pastoris*. *Biotechnol. Lett.* **34**, 1937-1943.
- Bouajila, A., Zoghلامي, N., Al Ahmed, M., Baum, M., Ghorbel, A. and Nazari, K.** (2011) Comparative virulence of *Pyrenophora teres* f. *teres* from Syria and Tunisia and screening for resistance sources in barley: implications for breeding. *Lett. Appl. Microbiol.* **53**, 489-502.

- Bouajila, A., Zoghalmi, N., Al Ahmed, M., Baum, M., Ghorbel, A. and Nazari, K.** (2012) Pathogenicity spectra and screening for resistance in barley against Tunisian *Pyrenophora teres f. teres*. *Plant Dis.* **96**, 1569-1575.
- Bradford, M. M.** (1976) A rapid and sensitive method for the quantitation of microgram quantities of protein utilizing the principle of protein-dye binding. *Anal. Biochem.* **72**, 248-254.
- Brankatschk, R., Bodenhausen, N., Zeyer, J. and Burgmann, H.** (2012) Simple absolute quantification method correcting for quantitative PCR efficiency variations for microbial community samples. *Appl. Environ. Microbiol.* **78**, 4481-4489.
- Brito, N., Espino, J. J. and Gonzalez, C.** (2006) The endo-beta-1,4-xylanase Xyn11A is required for virulence in *Botrytis cinerea*. *Mol. Plant-Microbe Interact.* **19**, 25-32.
- Brown, M. P., Steffenson, B. J. and Webster, R. K.** (1993) Host-range of *Pyrenophora teres f. teres* isolates from California. *Plant Dis.* **77**, 942-947.
- Brown, N. A., Antoniw, J. and Hammond-Kosack, K. E.** (2012) The predicted secretome of the plant pathogenic fungus *Fusarium graminearum*: A refined comparative analysis. *Plos One* **7**, e33731.
- Bustin, S. A., Benes, V., Garson, J. A., Hellems, J., Huggett, J., Kubista, M., et al.** (2009) The MIQE Guidelines: Minimum Information for Publication of Quantitative Real-Time PCR Experiments. *Clin. Chem.* **55**, 611-622.
- Bustin, S. A. and Nolan, T.** (2004) Analysis of mRNA expression by real-time PCR In: *Real-Time PCR: An Essential Guide*. (Edwards, K., Logan, J. and Saunders, N.), pp. 125-184. Norfolk, U.K: Horizon Bioscience.
- Byther, R. S. and Steiner, G. W.** (1975) Heat-induced resistance of sugarcane to *Helminthosporium sacchari* and Helminthosporoside. *Plant Physiol.* **56**, 415-419.
- Cabib, E., Blanco, N., Grau, C., Rodríguez-Peña, J. M. and Arroyo, J.** (2007) Crh1p and Crh2p are required for the cross-linking of chitin to  $\beta(1-6)$ glucan in the *Saccharomyces cerevisiae* cell wall. *Mol. Microbiol.* **63**, 921-935.
- Campbell, M. A., Medd, R. W. and Brown, J. F.** (2003) Phytotoxicity of metabolites produced by *Pyrenophora semeniperda* in liquid culture. *Aust. J. Exp. Agric.* **43**, 1237-1244.
- Cao, T., Kim, Y. M., Kav, N. N. V. and Strelkov, S. E.** (2009) A proteomic evaluation of *Pyrenophora tritici-repentis*, causal agent of tan spot of wheat, reveals major differences between virulent and avirulent isolates. *Proteomics* **9**, 1177-1196.
- Cao, T., Srivastava, S., Rahman, M. H., Kav, N. N. V., Hotte, N., Deyholos, M. K., et al.** (2008) Proteome-level changes in the roots of *Brassica napus* as a result of *Plasmodiophora brassicae* infection. *Plant Sci.* **174**, 97-115.
- Carresi, L., Pantera, B., Zoppi, C., Cappugi, G., Oliveira, A. L., Pertinhez, T. A., et al.** (2006) Cerato-platanin, a phytotoxic protein from *Ceratocystis fimbriata*: Expression in *Pichia pastoris*,

- purification and characterization. *Protein Expression Purif.* **49**, 159-167.
- Castro, K. P. I., Castro, N. S. I., Maia, Z. A. I., Felipe, M. S. S. I., Pereira, M. I. and Soares, C. M. A. I.** (2005) Fungal molecular biology. *Rev. Inst. Med. trop. S. Paulo* **47**, 48-61.
- Chambers, R. S., Broughton, M. J., Cannon, R. D., Carne, A., Emerson, G. W. and Sullivan, P. A.** (1993) An exo-beta-(1,3)-glucanase of *Candida albicans* - purification of the enzyme and molecular-cloning of the gene. *J. Gen. Microbiol.* **139**, 325-334.
- Choi, Y.-W., Hyde, K. D. and Ho, W. W. H.** (1999) Single spore isolation of fungi. *Fungal Divers.* **3**, 29-38.
- Chu, C. G., Xu, S. S., Faris, J. D., Nevo, E. and Friesen, T. L.** (2008) Seedling resistance to tan spot and *Stagonospora nodorum* leaf blotch in wild emmer wheat (*Triticum dicoccoides*). *Plant Dis.* **92**, 1229-1236.
- Ciuffetti, L. M., Manning, V. A., Pandelova, I., Betts, M. F. and Martinez, J. P.** (2010) Host-selective toxins, Ptr ToxA and Ptr ToxB, as necrotrophic effectors in the *Pyrenophora tritici-repentis*-wheat interaction. *New Phytol.* **187**, 911-919.
- Ciuffetti, L. M. and Tuori, R. P.** (1999) Advances in the characterization of the *Pyrenophora tritici-repentis*-wheat interaction. *Phytopathology* **89**, 444-449.
- Ciuffetti, L. M., Tuori, R. P. and Gaventa, J. M.** (1997) A single gene encodes a selective toxin causal to the development of tan spot of wheat. *Plant Cell* **9**, 135-144.
- Colmenares, A. J., Aleu, J., Duran-Patron, R., Collado, I. G. and Hernandez-Galan, R.** (2002) The putative role of botrydial and related metabolites in the infection mechanism of *Botrytis cinerea*. *J. Chem. Ecol.* **28**, 997-1005.
- Comparini, C., Carresi, L., Pagni, E., Sbrana, F., Sebastiani, F., Luchi, N., et al.** (2009) New proteins orthologous to cerato-platanin in various *Ceratocystis* species and the purification and characterization of cerato-populin from *Ceratocystis populicola*. *Appl. Microbiol. Biotechnol.* **84**, 309-322.
- Crowe, J., Masone, B. S. and Ribbe, J.** (1995) One-step purification of recombinant proteins with the 6xHis tag and Ni-NTA resin. *Mol. Biotechnol.* **4**, 247-258.
- Damerval, C., De Vienne, D., Zivy, M. and Thiellement, H.** (1986) Technical improvements in two-dimensional electrophoresis increase the level of genetic variation detected in wheat-seedling proteins. *Electrophoresis* **7**, 52-54.
- Dantigny, P., Nanguy, S. P.-M., Judet-Correia, D. and Bensoussan, M.** (2011) A new model for germination of fungi. *Int. J. Food Microbiol.* **146**, 176-181.
- Datta, S. K. and Muthukrishnan, S.** (1999) *Plant pathogenesis-related proteins in plants*. USA: CRC Press LLC.
- Daub, M. E. and Ehrenshaft, M.** (2000) The photoactivated *Cercospora* toxin cercosporin: Contributions to plant disease and fundamental biology. *Annu. Rev. Phytopathol.* **38**, 461-490.

- Davies, G. and Henrissat, B.** (1995) Structures and mechanisms of glycosyl hydrolases. *Structure* **3**, 853-859.
- Day, D., Neuburger, M. and Douce, R.** (1985) Biochemical characterization of chlorophyll-free mitochondria from pea leaves. *Funct. Plant Biol.* **12**, 219-228.
- Dayan, F. E., Ferreira, D., Wang, Y.-H., Khan, I. A., McInroy, J. A. and Pan, Z.** (2008) A pathogenic fungi Diphenyl Ether Phytotoxin targets plant Enoyl (Acyl Carrier Protein) Reductase. *Plant Physiol.* **147**, 1062-1071.
- Dayan, F. E., Romagni, J. G. and Duke, S. O.** (2000) Investigating the mode of action of natural phytotoxins. *J. Chem. Ecol.* **26**, 2079-2094.
- de Groot, P. W. J., Brandt, B. W., Horiuchi, H., Ram, A. F. J., de Koster, C. G. and Klis, F. M.** (2009) Comprehensive genomic analysis of cell wall genes in *Aspergillus nidulans*. *Fungal Genet. Biol.* **46**, S72-S81.
- De Groot, P. W. J., Ram, A. F. and Klis, F. M.** (2005) Features and functions of covalently linked proteins in fungal cell walls. *Fungal Genet. Biol.* **42**, 657-675.
- Deadman, M. L. and Cooke, B. M.** (1985) A method of spore production for *Drechslera teres* using detached barley leaves. *Trans. Br. Mycol. Soc.* **85**, 489-493.
- Dempsey, D. A., Shah, J. and Klessig, D. F.** (1999) Salicylic acid and disease resistance in plants. *Crit. Rev. Plant Sci.* **18**, 547-575.
- DeZwaan, T. M., Carroll, A. M., Valent, B. and Sweigard, J. A.** (1999) *Magnaporthe grisea* Pth11p is a novel plasma membrane protein that mediates appressorium differentiation in response to inductive substrate cues. *Plant Cell* **11**, 2013-2030.
- Dilger, M., Felsenstein, F. G. and Schwarz, G.** (2003) Identification and quantitative expression analysis of genes that are differentially expressed during conidial germination in *Pyrenophora teres*. *Mol. Genet. Genomics* **270**, 147-155.
- Dushnicky, L. G., Ballance, G. M., Sumner, M. J. and MacGregor, A. W.** (1996) Penetration and infection of susceptible and resistant wheat cultivars by a necrosis toxin-producing isolate of *Pyrenophora tritici repentis*. *Can. J. Plant Pathol.* **18**, 392-402.
- Dushnicky, L. G., Ballance, G. M., Sumner, M. J. and MacGregor, A. W.** (1998) The role of lignification as a resistance mechanism in wheat to a toxin-producing isolate of *Pyrenophora tritici repentis*. *Can. J. Plant Pathol.* **20**, 35-47.
- Eisenhaber, B., Schneider, G., Wildpaner, M. and Eisenhaber, F.** (2004) A sensitive predictor for potential GPI lipid modification sites in fungal protein sequences and its application to genome-wide studies for *Aspergillus nidulans*, *Candida albicans*, *Neurospora crassa*, *Saccharomyces cerevisiae* and *Schizosaccharomyces pombe*. *J. Mol. Biol.* **337**, 243-253.
- El-Bebany, A. F., Rampitsch, C. and Daayf, F.** (2010) Proteomic analysis of the phytopathogenic soilborne fungus *Verticillium dahliae* reveals



differential protein expression in isolates that differ in aggressiveness. *Proteomics* **10**, 289-303.

- Ellouze, O. E., Loukil, S. and Marzouki, M. N.** (2011) Cloning and molecular characterization of a new fungal xylanase gene from *Sclerotinia sclerotiorum* S2. *BMB Rep.* **44**, 653-658.
- Ellwood, S. R., Liu, Z. H., Syme, R. A., Lai, Z. B., Hane, J. K., Keiper, F., et al.** (2010) A first genome assembly of the barley fungal pathogen *Pyrenophora teres f. teres*. *Genome Biology* **11**.
- Enkerli, J., Felix, G. and Boller, T.** (1999) The enzymatic activity of fungal xylanase is not necessary for its elicitor activity. *Plant Physiol.* **121**, 391-397.
- Eshraghi, L., Aryamanesh, N., Anderson, J. P., Shearer, B., McComb, J. A., Hardy, G., et al.** (2011) A quantitative PCR assay for accurate *in planta* quantification of the necrotrophic pathogen *Phytophthora cinnamomi*. *Eur. J. Plant Pathol.* **131**, 419-430.
- Eubel, H., Heazlewood, J. L. and Millar, A. H.** (2007) Isolation and Subfractionation of Plant Mitochondria for Proteomic Analysis. In: *Plant Proteomics, Methods in Molecular Biology*. (Thiellement, H., Zivy, M., Damerval, C. and Méchin, V.), pp. 49-62. NJ, USA: Humana Press.
- Falquet, L., Pagni, M., Bucher, P., Hulo, N., Sigrist, C. J. A., Hofmann, K., et al.** (2002) The PROSITE database, its status in 2002. *Nucleic Acids Res.* **30**, 235-238.
- Faris, J. D., Anderson, J. A., Francl, L. J. and Jordahl, J. G.** (1996) Chromosomal location of a gene conditioning insensitivity in wheat to a necrosis-inducing culture filtrate from *Pyrenophora tritici-repentis*. *Phytopathology* **86**, 459-463.
- Fernando, T. H. P. S., Jayasinghe, C. K. and Wijesundera, R. L. C.** (2000) Factors affecting spore production, germination and viability of *Colletotrichum acutatum* isolates from *Hevea brasiliensis*. *Mycol. Res.* **104**, 681-685.
- Fiegen, M. and Knogge, W.** (2002) Amino acid alterations in isoforms of the effector protein NIP1 from *Rhynchosporium secalis* have similar effects on its avirulence- and virulence-associated activities on barley. *Physiol. Mol. Plant Pathol.* **61**, 299-302.
- Fraaije, B. A., Butters, J. A., Coelho, J. M., Jones, D. R. and Hollomon, D. W.** (2002) Following the dynamics of strobilurin resistance in *Blumeria graminis f.sp. tritici* using quantitative allele-specific real-time PCR measurements with the fluorescent dye SYBR Green I. *Plant Pathol.* **51**, 45-54.
- Fraga, D., Meulia, T. and Fenster, S.** (2008) Real-Time PCR. In: *Current Protocols Essential Laboratory Techniques*. (pp. 10.13.11-10.13.34. John Wiley & Sons, Inc.
- Francki, R. I. B., Boardman, N. K. and Wildman, S. G.** (1965) Protein synthesis by cell-free extracts from tobacco leaves. I. Amino acid incorporating activity of chloroplasts in relation to their structure. *Biochemistry* **4**, 865-872.
- Friesen, T. L. and Faris, J. D.** (2010) Characterization of the wheat-*Stagonospora nodorum* disease system: what is the molecular basis

- of this quantitative necrotrophic disease interaction? *Can. J. Plant Pathol.* **32**, 20 - 28.
- Friesen, T. L., Faris, J. D., Solomon, P. S. and Oliver, R. P.** (2008a) Host-specific toxins: effectors of necrotrophic pathogenicity. *Cell. Microbiol.* **10**, 1421-1428.
- Friesen, T. L., Meinhardt, S. W. and Faris, J. D.** (2007) The *Stagonospora nodorum*-wheat pathosystem involves multiple proteinaceous host-selective toxins and corresponding host sensitivity genes that interact in an inverse gene-for-gene manner. *Plant J.* **51**, 681-692.
- Friesen, T. L., Stukenbrock, E. H., Liu, Z. H., Meinhardt, S., Ling, H., Faris, J. D., et al.** (2006) Emergence of a new disease as a result of interspecific virulence gene transfer. *Nat. Genet.* **38**, 953-956.
- Friesen, T. L., Zhang, Z. C., Solomon, P. S., Oliver, R. P. and Faris, J. D.** (2008b) Characterization of the interaction of a novel *Stagonospora nodorum* host-selective toxin with a wheat susceptibility gene. *Plant Physiol.* **146**, 682-693.
- Friis, P., Olsen, C. E. and Moller, B. L.** (1991) Toxin production in *Pyrenophora teres*, the Ascomycete causing the Net Spot Blotch disease of barley (*Hordeum vulgare* L.). *J. Biol. Chem.* **266**, 13329-13335.
- Frommer, W. B. and Ninnemann, O.** (1995) Heterologous expression of genes in bacterial, fungal, animal, and plant-cells. *Annu. Rev. Plant Physiol. Plant Mol. Biol.* **46**, 419-444.
- Furman-Matarasso, N., Cohen, E., Du, Q., Chejanovsky, N., Hanania, U. and Avni, A.** (1999) A point mutation in the ethylene-inducing xylanase elicitor Inhibits the  $\beta$ -1-4-endoxylanase activity but not the elicitation activity. *Plant Physiol.* **121**, 345-352.
- Gan, P. H. P., Rafiqi, M., Hardham, A. R. and Dodds, P. N.** (2010) Effectors of biotrophic fungal plant pathogens. *Funct. Plant Biol.* **37**, 913-918.
- Gardiner, D. M., McDonald, M. C., Covarelli, L., Solomon, P. S., Rusu, A. G., Marshall, M., et al.** (2012) Comparative pathogenomics reveals horizontally acquired novel virulence genes in fungi infecting cereal hosts. *PLoS Pathog.* **8**, 1-22.
- Gäumann, E. and Jaag, O.** (1946) Wilt diseases problem in plants. *Cell. Mol. Life Sci.* **2**, 215-220.
- Godfrey, D., Bohlenius, H., Pedersen, C., Zhang, Z. G., Emmersen, J. and Thordal-Christensen, H.** (2010) Powdery mildew fungal effector candidates share N-terminal Y/F/WxC-motif. *BMC Genomics* **11**.
- Goh, T.-K.** (1999) Single-spore isolation using a hand-made glass needle. *Fungal Divers.* **2**, 47-63.
- Gomez-Gomez, E., Roncero, M. I. G., Di Pietro, A. and Hera, C.** (2001) Molecular characterization of a novel endo-beta-1,4-xylanase gene from the vascular wilt fungus *Fusarium oxysporum*. *Curr. Genet.* **40**, 268-275.
- Gomez-Gomez, E., Ruiz-Roldan, M. C., Di Pietro, A., Roncero, M. I. G. and Hera, C.** (2002) Role in pathogenesis of two endo-beta-1,4-

xylanase genes from the vascular wilt fungus *Fusarium oxysporum*. *Fungal Genet. Biol.* **35**, 213-222.

- Görg, A., Postel, W., Günther, S. and Friedrich, C.** (1988) Horizontal two-dimensional electrophoresis with immobilized pH gradients using PhastSystem. *Electrophoresis* **9**, 57-59.
- Gowda, M., Venu, R. C., Raghupathy, M. B., Nobuta, K., Li, H. M., Wing, R., et al.** (2006) Deep and comparative analysis of the mycelium and appressorium transcriptomes of *Magnaporthe grisea* using MPSS, RL-SAGE, and oligoarray methods. *BMC Genomics* **7**, 1-15.
- Gupta, S., Loughman, R., Platz, G. J. and Lance, R. C. M.** (2003) Resistance in cultivated barleys to *Pyrenophora teres f. teres* and prospects of its utilisation in marker identification and breeding. *Aust. J. Agric. Res.* **54**, 1379-1386.
- Haddad, C. R. B. and Mazzafera, P.** (1999) Sodium chloride-induced leaf senescence in *Hydrocotyle bonariensis* Lam. and *Foeniculum vulgare* L. *Braz. Arch. Biol. Techn.* **42**, 0-0.
- Hagborg, W. A. F.** (1970) A device for injecting solutions and suspension into thin leaves of plants. *Can. J. Bot.* **48**, 1135-1136.
- Hahlbrock, K. and Scheel, D.** (1989) Physiology and molecular-biology of phenylpropanoid metabolism. *Annu. Rev. Plant Physiol. Plant Mol. Biol.* **40**, 347-369.
- Hajek, T., Honys, D. and Capkova, W.** (2004) New method of plant mitochondria isolation and sub-fractionation for proteomic analyses. *Plant Sci.* **167**, 389-395.
- Hakulinen, N., Turunen, O., Janis, J., Leisola, M. and Rouvinen, J.** (2003) Three-dimensional structures of thermophilic beta-1,4-xylanases from *Chaetomium thermophilum* and *Nonomuraea flexuosa* - Comparison of twelve xylanases in relation to their thermal stability. *Eur. J. Biochem.* **270**, 1399-1412.
- Hamada, K., Terashima, H., Arisawa, M., Yabuki, N. and Kitada, K.** (1999) Amino acid residues in the omega-minus region participate in cellular localization of yeast glycosylphosphatidylinositol-attached proteins. *J. Bacteriol.* **181**, 3886-3889.
- Hammond-Kosack, K. E. and Rudd, J. J.** (2008) Plant resistance signalling hijacked by a necrotrophic fungal pathogen. *Plant Signal. Behav.* **3**, 993-995.
- Hartl, L., Gastebois, A., Amanianda, V. and Latgé, J. P.** (2011) Characterization of the GPI-anchored endo  $\beta$ -1,3-glucanase Eng2 of *Aspergillus fumigatus*. *Fungal Genet. Biol.* **48**, 185-191.
- Hatvani, L., Szekeres, A., Kredics, L., Antal, Z. and Manczinger, L.** (2004) Isolation of fungicide-resistant mutants from cold-tolerant *Trichoderma* strains and their *in vitro* antagonistic properties. *IOBC WPRS Bulletin* **27**, 369-372.
- Havukainen, R., Torronen, A., Laitinen, T. and Rouvinen, J.** (1996) Covalent binding of three epoxyalkyl xylosides to the active site of endo-1,4-xylanase II from *Trichoderma reesei*. *Biochemistry* **35**, 9617-9624.

- Hayashi, S. and Wu, H. C.** (1990) Lipoproteins in bacteria. *J. Bioenerg. Biomembr.* **22**, 451-471.
- He, J., Yu, B., Zhang, K. Y., Ding, X. M. and Chen, D. W.** (2009) Expression of endo-1, 4-beta-xylanase from *Trichoderma reesei* in *Pichia pastoris* and functional characterization of the produced enzyme. *BMC Biotechnol.* **9**, 56.
- He, P., Shan, L. and Sheen, J.** (2007) Elicitation and suppression of microbe-associated molecular pattern-triggered immunity in plant-microbe interactions. *Cell. Microbiol.* **9**, 1385-1396.
- Henry, S., Bru, D., Stres, B., Hallet, S. and Philippot, L.** (2006) Quantitative detection of the nosZ gene, encoding nitrous oxide reductase, and comparison of the abundances of 16S rRNA, narG, nirK, and nosZ genes in soils. *Appl. Environ. Microbiol.* **72**, 5181-5189.
- Hofius, D., Tsitsigiannis, D. I., Jones, J. D. G. and Mundy, J.** (2007) Inducible cell death in plant immunity. *Semin. Cancer Biol.* **17**, 166-187.
- Horbach, R., Navarro-Quesada, A. R., Knogge, W. and Deising, H. B.** (2011) When and how to kill a plant cell: Infection strategies of plant pathogenic fungi. *J. Plant Physiol.* **168**, 51-62.
- Howlett, B. J.** (2006) Secondary metabolite toxins and nutrition of plant pathogenic fungi. *Curr. Opin. Plant Biol.* **9**, 371-375.
- Hu, X., Nazar, R. N. and Robb, J.** (1993) Quantification of *Verticillium biomass* in wilt disease development. *Physiol. Mol. Plant Pathol.* **42**, 23-36.
- Huang, Y. J., Toscano-Underwood, C., Fitt, B. D., Todd, A. D., West, J. S., Koopmann, B., et al.** (2001) Effects of temperature on germination and hyphal growth from ascospores of A-group and B-group *Leptosphaeria maculans* (phoma stem canker of oilseed rape). *Ann. Appl. Biol.* **139**, 193-207.
- Iotti, M., Leonardi, M., Oddis, M., Salerni, E., Baraldi, E. and Zambonelli, A.** (2012) Development and validation of a real-time PCR assay for detection and quantification of *Tuber magnatum* in soil. *BMC Microbiol.* **12**.
- Jalli, M.** (2011) Sexual reproduction and soil tillage effects on virulence of *Pyrenophora teres* in Finland. *Ann. Appl. Biol.* **158**, 95-105.
- Jarozuk-Scisel, J. and Kurek, E.** (2012) Hydrolysis of fungal and plant cell walls by enzymatic complexes from cultures of *Fusarium* isolates with different aggressiveness to rye (*Secale cereale*). *Arch. Microbiol.* **194**, 653-665.
- Jayasena, K. W., Loughman, R. and Majewski, J.** (2002) Evaluation of fungicides in control of spot-type net blotch on barley. *Crop Protect.* **21**, 63-69.
- Jayasena, K. W., Van Burgel, A., Tanaka, K., Majewski, J. and Loughman, R.** (2007) Yield reduction in barley in relation to spot-type net blotch. *Australas. Plant Pathol.* **36**, 429-433.
- Jin, L. T., Hwang, S. Y., Yoo, G. S. and Choi, J. K.** (2006) A mass spectrometry compatible silver staining method for protein

incorporating a new silver sensitizer in sodium dodecyl sulfate-polyacrylamide electrophoresis gels. *Proteomics* **6**, 2334-2337.

- Jonathan, E. M. and Jacques, H.** (2001) Host-selective toxins as agents of cell death in plant-fungus interactions. *Mol. Plant Pathol.* **2**, 229-239.
- Jorge, I., de la Rosa, O., Navas-Cortes, J. A., Jimenez-Diaz, R. and Tena, M.** (2005) Extracellular xylanases from two pathogenic races of *Fusarium oxysporum* f. sp. *ciceris*: enzyme production in culture and purification and characterization of a major isoform as an alkaline endo-beta-(1,4)-xylanase of low molecular weight. *Anton. Leeuw. Int. J. G.* **88**, 49-59.
- Judet, D., Bensoussan, M., Perrier-Cornet, J. M. and Dantigny, P.** (2008) Distributions of the growth rate of the germ tubes and germination time of *Penicillium chrysogenum* conidia depend on water activity. *Food Microbiol.* **25**, 902-907.
- Jun, H., Bing, Y., Keying, Z., Xuemei, D. and Daiwen, C.** (2009) Sequencing and expression of the xylanase gene 2 from *Trichoderma reesei* Rut C-30 and characterization of the recombinant enzyme and its activity on xylan. *J. Mol. Microbiol. Biotechnol.* **17**, 101-109.
- Kamoun, S.** (2007) Groovy times: filamentous pathogen effectors revealed. *Curr. Opin. Plant Biol.* **10**, 358-365.
- Karlovsky, P.** (1999) Biological detoxification of fungal toxins and its use in plant breeding, feed and food production. *Nat. Toxins* **7**, 1-23.
- Kars, I., Krooshof, G. H., Wagemakers, L., Joosten, R., Benen, J. A. E. and Van Kan, J. A. L.** (2005) Necrotizing activity of five *Botrytis cinerea* endopolygalacturonases produced in *Pichia pastoris*. *Plant J.* **43**, 213-225.
- Kauffmann, S., Legrand, M., Geoffroy, P. and Fritig, B.** (1987) Biological function of pathogenesis-related proteins - 4 PR proteins of tobacco have 1,3-beta-glucanase activity. *EMBO J.* **6**, 3209-3212.
- Keates, S. E., Kostman, T. A., Anderson, J. D. and Bailey, B. A.** (2003) Altered gene expression in three plant species in response to treatment with Nep1, a fungal protein that causes necrosis. *Plant Physiol.* **132**, 1610-1622.
- Kennedy, E. J., Pillus, L. and Ghosh, G.** (2005) Pho5p and newly identified nucleotide pyrophosphatases/ phosphodiesterases regulate extracellular nucleotide phosphate metabolism in *Saccharomyces cerevisiae*. *Eukaryot. Cell* **4**, 1892-1901.
- Keon, J. P. R. and Hargreaves, J. A.** (1983) A cytological study of the net blotch disease of barley caused by *Pyrenophora teres*. *Physiol. Plant Pathol.* **22**, 321-329.
- Kershaw, M. J. and Talbot, N. J.** (1998) Hydrophobins and repellents: Proteins with fundamental roles in fungal morphogenesis. *Fungal Genet. Biol.* **23**, 18-33.
- Khan, S. N., Akter, M. Z. and Sims, P. F. G.** (2002) Cloning and expression analysis of two endo-1,4- $\beta$ -Xylanase genes from *Phanerochaete chrysosporium*. *Plant Tissue Cult.* **12**, 57-68.

- Khoo, K. H., Able, A. J., Chataway, T. K. and Able, J. A.** (2012) Preliminary characterisation of two early meiotic wheat proteins after identification through 2DGE proteomics. *Funct. Plant Biol.* **39**, 222-235.
- Kikot, G. E., Hours, R. A. and Alconada, T. M.** (2009) Contribution of cell wall degrading enzymes to pathogenesis of *Fusarium graminearum*: a review. *J. Basic Microbiol.* **49**, 231-241.
- Kim, K.-H., Willger, S. D., Park, S.-W., Puttikamonkul, S., Grahl, N., Cho, Y., et al.** (2009) TmpL, a transmembrane protein required for intracellular redox homeostasis and virulence in a plant and an animal fungal pathogen. *PLoS Pathog* **5**, e1000653.
- Kim, Y. M. and Strelkov, S. E.** (2007) Heterologous expression and activity of Ptr ToxB from virulent and avirulent isolates of *Pyrenophora tritici repentis*. *Can. J. Plant Pathol.* **29**, 232-242.
- Kiraly, L., Barnaz, B. and Kiralyz, Z.** (2007) Plant resistance to pathogen infection: Forms and mechanisms of innate and acquired resistance. *J. Phytopathol.* **155**, 385-396.
- Knogge, W.** (1996) Fungal infection of plants. *Plant Cell* **8**, 1711-1722.
- Koeck, M., Hardham, A. R. and Dodds, P. N.** (2011) The role of effectors of biotrophic and hemibiotrophic fungi in infection. *Cell. Microbiol.* **13**, 1849-1857.
- Kokkelink, L., Minz, A., Al-Masri, M., Giesbert, S., Barakat, R., Sharon, A., et al.** (2011) The small GTPase BcCdc42 affects nuclear division, germination and virulence of the gray mold fungus *Botrytis cinerea*. *Fungal Genet. Biol.* **48**, 1012-1019.
- Kopetz, V. A., Penno, M. A. S., Hoffmann, P., Wilson, D. P. and Beltrame, J. F.** (2012) Potential mechanisms of the acute coronary syndrome presentation in patients with the coronary slow flow phenomenon - Insight from a plasma proteomic approach. *Int. J. Acarol.* **156**, 84-91.
- Kristensen, B. K., Bloch, H. and Rasmussen, S. K.** (1999) Barley coleoptile peroxidases. Purification, molecular cloning, and induction by pathogens. *Plant Physiol.* **120**, 501-512.
- Kulkarni, R. D., Kelkar, H. S. and Dean, R. A.** (2003) An eight-cysteine-containing CFEM domain unique to a group of fungal membrane proteins. *Trends Biochem. Sci.* **28**, 118-121.
- Kunkel, B. N. and Brooks, D. M.** (2002) Cross talk between signaling pathways in pathogen defense. *Curr. Opin. Plant Biol.* **5**, 325-331.
- Kwon, C. Y., Rasmussen, J. B. and Meinhardt, S. W.** (1998) Activity of Ptr ToxA from *Pyrenophora tritici repentis* requires host metabolism. *Physiol. Mol. Plant Pathol.* **52**, 201-212.
- Lamari, L. and Bernier, C. C.** (1989) Toxin of *Pyrenophora tritici repentis* host-specificity, significance in disease, and inheritance of host-reaction. *Phytopathology* **79**, 740-744.
- Legrand, M., Kauffmann, S., Geoffroy, P. and Fritig, B.** (1987) Biological function of pathogenesis-related proteins - Four tobacco pathogenesis-related proteins are chitinases. *Proc. Natl. Acad. Sci. USA* **84**, 6750-6754.

- Lehmensiek, A., Bester-van der Merwe, A. E., Sutherland, M. W., Platz, G., Kriel, W. M., Potgieter, G. F., et al.** (2010) Population structure of South African and Australian *Pyrenophora teres* isolates. *Plant Pathol.* **59**, 504-515.
- Lehtinen, U.** (1993) Plant cell wall degrading enzymes of *Septoria nodorum*. *Physiol. Mol. Plant Pathol.* **43**, 121-134.
- Leisova, L., Minarikova, V., Kucera, L. and Ovesna, J.** (2006) Quantification of *Pyrenophora teres* in infected barley leaves using real-time PCR. *J. Microbiol. Methods* **67**, 446-455.
- Levine, A., Tenhaken, R., Dixon, R. and Lamb, C.** (1994) H<sub>2</sub>O<sub>2</sub> from the oxidative burst orchestrates the plant hypersensitive disease resistance response. *Cell* **79**, 583-593.
- Lightfoot, D. J. and Able, A. J.** (2010) Growth of *Pyrenophora teres* in planta during barley net blotch disease. *Australas. Plant Pathol.* **39**, 499-507.
- Liu, Z., Ellwood, S. R., Oliver, R. P. and Friesen, T. L.** (2011) *Pyrenophora teres*: profile of an increasingly damaging barley pathogen. *Mol. Plant Pathol.* **12**, 1-19.
- Liu, Z., Faris, J. D., Oliver, R. P., Tan, K.-C., Solomon, P. S., McDonald, M. C., et al.** (2009) SnTox3 acts in effector triggered susceptibility to induce disease on wheat carrying the Snn3 gene. *PLoS Pathog.* **5**, e1000581.
- Liu, Z. H., Faris, J. D., Meinhardt, S. W., Ali, S., Rasmussen, J. B. and Friesen, T. L.** (2004a) Genetic and physical mapping of a gene conditioning sensitivity in wheat to a partially purified host-selective toxin produced by *Stagonospora nodorum*. *Phytopathology* **94**, 1056-1060.
- Liu, Z. H., Friesen, T. L., Ling, H., Meinhardt, S. W., Oliver, R. P., Rasmussen, J. B., et al.** (2006) The Tsn1-ToxA interaction in the wheat-*Stagonospora nodorum* pathosystem parallels that of the wheat-tan spot system. *Genome* **49**, 1265-1273.
- Liu, Z. H., Friesen, T. L., Rasmussen, J. B., Ali, S., Meinhardt, S. W. and Faris, J. D.** (2004b) Quantitative trait loci analysis and mapping of seedling resistance to *Stagonospora nodorum* leaf blotch in wheat. *Phytopathology* **94**, 1061-1067.
- Liu, Z. H., Zhong, S., Stasko, A. K., Edwards, M. C. and Friesen, T. L.** (2012) Virulence profile and genetic structure of a North Dakota population of *Pyrenophora teres* f. *teres*, the causal agent of net form net blotch of barley. *Phytopathology* **102**, 539-546.
- Livak, K. J. and Schmittgen, T. D.** (2001) Analysis of relative gene expression data using real-time quantitative PCR and the 2(T)(-Delta Delta C) method. *Methods* **25**, 402-408.
- Lu, H. J., Fellers, J. P., Friesen, T. L., Meinhardt, S. W. and Faris, J. D.** (2006) Genomic analysis and marker development for the Tsn1 locus in wheat using bin-mapped ESTs and flanking BAC contigs. *Theor. Appl. Genet.* **112**, 1132-1142.
- Luke, H. H. and Wheeler, H. E.** (1955) Toxin production by *Helminthosporium victoriae*. *Phytopathology* **45**, 453-458.

- Lyngs Jørgensen, H. J., Lübeck, P. S., Thordal-Christensen, H., de Neergaard, E. and Smedegaard-Petersen, V.** (1998) Mechanisms of induced resistance in barley against *Drechslera teres*. *Phytopathology* **88**, 698-707.
- Manning, V. A., Chu, A. L., Steeves, J. E., Wolpert, T. J. and Ciuffetti, L. M.** (2009) A host-selective toxin of *Pyrenophora tritici repentis*, Ptr ToxA, induces photosystem changes and reactive oxygen species accumulation in sensitive wheat. *Mol. Plant-Microbe Interact.* **22**, 665-676.
- Manning, V. A. and Ciuffetti, L. M.** (2005) Localization of Ptr ToxA produced by *Pyrenophora tritici-repentis* reveals protein import into wheat mesophyll cells. *Plant Cell* **17**, 3203-3212.
- Manning, V. A., Hamilton, S. M., Karplus, P. A. and Ciuffetti, L. M.** (2008) The Arg-Gly-Asp-containing, solvent-exposed loop of Ptr ToxA is required for internalization. *Mol. Plant-Microbe Interact.* **21**, 315-325.
- Manning, V. A., Hardison, L. K. and Ciuffetti, L. M.** (2007) Ptr ToxA interacts with a chloroplast-localized protein. *Mol. Plant-Microbe Interact.* **20**, 168-177.
- Markham, J. E. and Hille, J.** (2001) Host-selective toxins as agents of cell death in plant-fungus interactions. *Mol. Plant Pathol.* **2**, 229-239.
- Martin-Cuadrado, A. B., Duenas, E., Sipiczki, M., de Aldana, C. R. V. and del Rey, F.** (2003) The endo-beta-1,3-glucanase eng1p is required for dissolution of the primary septum during cell separation in *Schizosaccharomyces pombe*. *J. Cell Sci.* **116**, 1689-1698.
- Maruyama, C. and Hamano, Y.** (2009) The biological function of the bacterial isochorismatase-Like Hydrolase SttH. *Biosci. Biotech. Bioch.* **73**, 2494-2500.
- Mathre, D. E.** (1997) *Compendium of Barley Diseases, 2nd ed.* St. Paul, Minn: American Phytopathological Society.
- Mavrodi, D. V., Ksenzenko, V. N., Bonsall, R. F., Cook, R. J., Boronin, A. M. and Thomashow, L. S.** (1998) A seven-gene locus for synthesis of phenazine-1-carboxylic acid by *Pseudomonas fluorescens* 2-79. *J. Bacteriol.* **180**, 2541-2548.
- McLean, M. S., Howlett, B. J. and Hollaway, G. J.** (2009) Epidemiology and control of spot form of net blotch (*Pyrenophora teres f. maculata*) of barley: a review. *Crop Pasture Sci.* **60**, 303-315.
- Méchin, V., Damerval, C. and Zivy, M.** (2007) Total protein extraction with TCA-Acetone. In: *Plant Proteomics: Methods and Protocols.* (Thiellement, H., Méchin, V., Damerval, C. and Zivy, M.), pp. 1-8. Totowa, NJ, USA: Humana Press Inc.
- Meeley, R. B., Johal, G. S., Briggs, S. P. and Walton, J. D.** (1992) A biochemical phenotype for a disease resistance gene of maize. *Plant Cell* **4**, 71-77.
- Meeley, R. B. and Walton, J. D.** (1991) Enzymatic detoxification of Hc-Toxin, the host-selective cyclic peptide from *Cochliobolus carbonum*. *Plant Physiol.* **97**, 1080-1086.
- Ment, D., Gindin, G., Rot, A., Soroker, V., Glazer, I., Barel, S., et al.** (2010) Novel technique for quantifying adhesion of *Metarhizium*



- anisopliae* conidia to the tick cuticle. *Appl. Environ. Microbiol.* **76**, 3521-3528.
- Miethbauer, S., Heiser, I. and Liebermann, B.** (2003) The phytopathogenic fungus *Ramularia collo-cygni* produces biologically active rubellins on infected barley leaves. *J. Phytopathol.* **151**, 665-668.
- Miller, J. D. and Arnison, P. G.** (1986) Degradation of deoxynivalenol by suspension-cultures of the Fusarium head blight resistant wheat cultivar Frontana. *Can. J. Plant Pathol.* **8**, 147-150.
- Mittelheuser, C. J. and Van Steveninck, R. F. M.** (1972) Light-induced effects of tris on ultrastructure of leaf tissue. *Aust. J. Biol. Sci.* **25**, 517.
- Möbius, N. and Hertweck, C.** (2009) Fungal phytotoxins as mediators of virulence. *Curr. Opin. Plant Biol.* **12**, 390-398.
- Morais do Amaral, A., Antoniw, J., Rudd, J. J. and Hammond-Kosack, K. E.** (2012) Defining the predicted protein secretome of the fungal wheat leaf pathogen *Mycosphaerella graminicola*. *Plos One* **7**, e49904.
- Mouyna, I., Fontaine, T., Vai, M., Monod, M., Fonzi, W. A., Diaquin, M., et al.** (2000) Glycosylphosphatidylinositol-anchored Glucanoyltransferases play an active role in the biosynthesis of the fungal cell wall. *J. Biol. Chem.* **275**, 14882-14889.
- Murray, G. M. and Brennan, J. P.** (2010) Estimating disease losses to the Australian barley industry. *Australas. Plant Pathol.* **39**, 85-96.
- Muthukrishnan, S., Liang, G. H., Trick, H. N. and Gill, B. S.** (2001) Pathogenesis-related proteins and their genes in cereals. *Plant Cell Tiss. Org.* **64**, 93-114.
- Navarre, D. A. and Wolpert, T. J.** (1999) Victorin induction of an apoptotic/senescence-like response in oats. *Plant Cell* **11**, 237-249.
- Nguyen, Q. B., Itoh, K., Van Vu, B., Tosa, Y. and Nakayashiki, H.** (2011) Simultaneous silencing of endo- $\beta$ -1,4 xylanase genes reveals their roles in the virulence of *Magnaporthe oryzae*. *Mol. Microbiol.* **81**, 1008-1019.
- Nimchuk, Z., Eulgem, T., Holt Iii, B. F. and Dangl, J. L.** (2003) Recognition and response in the plant immune system. *Annu. Rev. Genet.* **37**, 579-609.
- Noda, J., Brito, N. and Gonzalez, C.** (2010) The *Botrytis cinerea* xylanase Xyn11A contributes to virulence with its necrotizing activity, not with its catalytic activity. *BMC Plant Biol.* **10**.
- Okinaka, Y., Mimori, K., Takeo, K., Kitamura, S., Takeuchi, Y., Yamaoka, N., et al.** (1995) A structural model for the mechanisms of elicitor release from fungal cell-walls by plant beta-1,3-endoglucanase. *Plant Physiol.* **109**, 839-845.
- Oliver, R. P. and Solomon, P. S.** (2010) New developments in pathogenicity and virulence of necrotrophs. *Curr. Opin. Plant Biol.* **13**, 415-419.
- Osbourn, A. E.** (2001) Tox-boxes, fungal secondary metabolites, and plant disease. *Proc. Natl. Acad. Sci. USA* **98**, 14187-14188.

- Parada, R. Y., Sakuno, E., Mori, N., Oka, K., Egusa, M., Kodama, M., et al.** (2008) *Alternaria brassicae* produces a Host-Specific Protein Toxin from germinating spores on host leaves. *Phytopathology* **98**, 458-463.
- Parsons, J. F., Calabrese, K., Eisenstein, E. and Ladner, J. E.** (2003) Structure and mechanism of *Pseudomonas aeruginosa* PhzD, an isochorismatase from the phenazine biosynthetic pathway. *Biochemistry* **42**, 5684-5693.
- Pazzagli, L., Cappugi, G., Manao, G., Camici, G., Santini, A. and Scala, A.** (1999) Purification, characterization, and amino acid sequence of cerato-platanin, a new phytotoxic protein from *Ceratocystis fimbriata* f. sp. *platani*. *J. Biol. Chem.* **274**, 24959-24964.
- Peever, T. L. and Milgroom, M. G.** (1994) Genetic structure of *Pyrenophora teres* populations determined with random amplified polymorphic DNA markers. *Can. J. Bot.* **72**, 915-923.
- Perez, A., Ramage, G., Blanes, R., Murgui, A., Casanova, M. and Martinez, J. P.** (2011) Some biological features of *Candida albicans* mutants for genes coding fungal proteins containing the CFEM domain. *FEMS Yeast Res.* **11**, 273-284.
- Petrosino, J. F. and Palzkill, T.** (1996) Systematic mutagenesis of the active site omega loop of TEM-1 beta-lactamase. *J. Bacteriol.* **178**, 1821-1828.
- Plaine, A., Walker, L., Da Costa, G., Mora-Montes, H. M., McKinnon, A., Gow, N. A. R., et al.** (2008) Functional analysis of *Candida albicans* GPI-anchored proteins: Roles in cell wall integrity and caspofungin sensitivity. *Fungal Genet. Biol.* **45**, 1404-1414.
- Rasmussen, J. B., Kwon, C. Y. and Meinhardt, S. W.** (2004) Requirement of host signaling mechanisms for the action of Ptr ToxA in wheat. *Eur. J. Plant Pathol.* **110**, 333-335.
- Rau, D., Attene, G., Brown, A. H. D., Nanni, L., Maier, F. J., Baftnas, V., et al.** (2007) Phylogeny and evolution of mating-type genes from *Pyrenophora teres*, the causal agent of barley "net blotch" disease. *Curr. Genet.* **51**, 377-392.
- Rau, D., Brown, A. H. D., Brubaker, C. L., Attene, G., Balmas, V., Saba, E., et al.** (2003) Population genetic structure of *Pyrenophora teres* Drechs. the causal agent of net blotch in Sardinian landraces of barley (*Hordeum vulgare* L.). *Theor. Appl. Genet.* **106**, 947-959.
- Reiss, E. and Bryngelsson, T.** (1996) Pathogenesis-related proteins in barley leaves, induced by infection with *Drechslera teres* (Sacc) Shoem and by treatment with other biotic agents. *Physiol. Mol. Plant Pathol.* **49**, 331-341.
- Reuveni, M., Sheglov, N., Eshel, D., Prusky, D. and Ben-Arie, R.** (2007) Virulence and the production of endo-1,4-beta-glucanase by isolates of *Alternaria alternata* involved in the moldy-core disease of apples. *J. Phytopathol.* **155**, 50-55.
- Ririe, K. M., Rasmussen, R. P. and Wittwer, C. T.** (1997) Product differentiation by analysis of DNA melting curves during the polymerase chain reaction. *Anal. Biochem.* **245**, 154-160.

- Robinson, J. and Jalli, M.** (1996) Diversity among Finnish net blotch isolates and resistance in barley. *Euphytica* **92**, 81-87.
- Rohe, M., Gierlich, A., Hermann, H., Hahn, M., Schmidt, B., Rosahl, S., et al.** (1995) The race-specific elicitor, NIP1, from the barley pathogen, *Rhynchosporium secalis*, determines avirulence on host plants of the RRS1 resistance genotype. *EMBO J.* **14**, 4168-4177.
- Rohringer, R., Ebrahimnesbat, F. and Wolf, G.** (1983) Proteins in intercellular washing fluids from leaves of barley (*Hordeum vulgare* L). *J. Exp. Bot.* **34**, 1589-1605.
- Rotblat, B., Enshell-Seijffers, D., Gershoni, J. M., Schuster, S. and Avni, A.** (2002) Identification of an essential component of the elicitation active site of the EIX protein elicitor. *Plant J.* **32**, 1049-1055.
- Roy, A., Kucukural, A. and Zhang, Y.** (2010) I-TASSER: a unified platform for automated protein structure and function prediction. *Nature Protocols* **5**, 725-738.
- Ruiz-Roldan, M. C., Di Pietro, A., Huertas-Gonzalez, M. D. and Roncero, M. I. G.** (1999) Two xylanase genes of the vascular wilt pathogen *Fusarium oxysporum* are differentially expressed during infection of tomato plants. *Mol. Gen. Genet.* **261**, 530-536.
- Ruiz-Roldán, M. C., Maier, F. J. and Schäfer, W.** (2001) PTK1, a Mitogen-activated-protein kinase gene, is required for conidiation, appressorium formation, and pathogenicity of *Pyrenophora teres* on barley. *Mol. Plant-Microbe Interact.* **14**, 116-125.
- Ruiz, M. C., DiPietro, A. and Roncero, M. I. G.** (1997) Purification and characterization of an acidic endo-beta-1,4-xylanase from the tomato vascular pathogen *Fusarium oxysporum* f sp. *lycopersici*. *FEMS Microbiol. Lett.* **148**, 75-82.
- Saarelainen, R., Paloheimo, M., Fagerström, R., Suominen, P. and Nevalainen, K. M. H.** (1993) Cloning, sequencing and enhanced expression of the *Trichoderma reesei* endoxylanase II (pI 9) gene xln2. *Molec. Gen. Genet.* **241**, 497-503.
- Sacristan, S. and Garcia-Arenal, F.** (2008) The evolution of virulence and pathogenicity in plant pathogen populations. *Mol. Plant Pathol.* **9**, 369-384.
- Sáida, F.** (2001) Overview on the expression of toxic gene products in *Escherichia coli*. *Curr. Protoc. Protein Sci.*
- Saitou, N. and Nei, M.** (1987) The neighbor-joining method - a new method for reconstructing phylogenetic trees. *Mol. Biol. Evol.* **4**, 406-425.
- Santén, K., Marttila, S., Liljeroth, E. and Bryngelsson, T.** (2005) Immunocytochemical localization of the pathogenesis-related PR-1 protein in barley leaves after infection by *Bipolaris sorokiniana*. *Physiol. Mol. Plant Pathol.* **66**, 45-54.
- Sarma, G. N., Manning, V. A., Ciuffetti, L. M. and Karplus, P. A.** (2005) Structure of Ptr ToxA: An RGD-containing host-selective toxin from *Pyrenophora tritici-repentis*. *Plant Cell* **17**, 3190-3202.

- Sarpeleh, A.** (2007) Role of *Pyrenophora teres* toxins in net blotch of barley. In: *School of Agriculture, Food and Wine : Plant and Food Science*. (ed.^eds.), pp. 219. Adelaide: University of Adelaide.
- Sarpeleh, A., Tate, M. E., Wallwork, H., Catcheside, D. and Able, A. J.** (2009) Characterisation of low molecular weight phytotoxins isolated from *Pyrenophora teres*. *Physiol. Mol. Plant Pathol.* **73**, 154-162.
- Sarpeleh, A., Wallwork, H., Catcheside, D. E. A., Tate, M. E. and Able, A. J.** (2007) Proteinaceous metabolites from *Pyrenophora teres* contribute to symptom development of barley net blotch. *Phytopathology* **97**, 907-915.
- Sarpeleh, A., Wallwork, H., Tate, M. E., Catcheside, D. E. A. and Able, A. J.** (2008) Initial characterisation of phytotoxic proteins isolated from *Pyrenophora teres*. *Physiol. Mol. Plant Pathol.* **72**, 73-79.
- Schena, L., Nigro, F., Ippolito, A. and Gallitelli, D.** (2004) Real-time quantitative PCR: a new technology to detect and study phytopathogenic and antagonistic fungi. *Eur. J. Plant Pathol.* **110**, 893-908.
- Schertler, G. F. X.** (1992) Overproduction of membrane proteins. *Curr. Opin. Struct. Biol.* **2**, 534-544.
- Schoffemeer, E. A. M., Klis, F. M., Sietsma, J. H. and Cornelissen, B. J. C.** (1999) The cell wall of *Fusarium oxysporum*. *Fungal Genet. Biol.* **27**, 275-282.
- Schoffemeer, E. A. M., Vossen, J. H., van Doorn, A. A., Cornelissen, B. J. C. and Haring, M. A.** (2001) FEM1, a *Fusarium oxysporum* glycoprotein that is covalently linked to the cell wall matrix and is conserved in filamentous fungi. *Mol. Genet. Genomics* **265**, 143-152.
- Schumacher, M. C., Resenberger, U., Seidel, R. P., Becker, C. F. W., Winklhofer, K. F., Oesterhelt, D., et al.** (2010) Synthesis of a GPI anchor module suitable for protein post-translational modification. *Peptide Science* **94**, 457-464.
- Schurch, S., Linde, C. C., Knogge, W., Jackson, L. F. and McDonald, B. A.** (2004) Molecular population genetic analysis differentiates two virulence mechanisms of the fungal avirulence gene NIP1. *Mol. Plant-Microbe Interact.* **17**, 1114-1125.
- ScottCraig, J. S., Kerby, K. B., Stein, B. D. and Somerville, S. C.** (1995) Expression of an extracellular peroxidase that is induced in barley (*Hordeum vulgare*) by the powdery mildew pathogen (*Erysiphe graminis* f sp *hordei*). *Physiol. Mol. Plant Pathol.* **47**, 407-418.
- Serenius, M., Manninen, O., Wallwork, H. and Williams, K.** (2007) Genetic differentiation in *Pyrenophora teres* populations measured with AFLP markers. *Mycol. Res.* **111**, 213-223.
- Serenius, M., Mironenko, N. and Manninen, O.** (2005) Genetic variation, occurrence of mating types and different forms of *Pyrenophora teres* causing net blotch of barley in Finland. *Mycol. Res.* **109**, 809-817.
- Smedegård, V.** (1977) Isolation of two toxins produced by *Pyrenophora teres* and their significance in disease development of net-spot blotch of barley. *Physiol. Plant Pathol.* **10**, 203-208, IN201, 209-211.

- Soanes, D. M., Alam, I., Cornell, M., Wong, H. M., Hedeler, C., Paton, N. W., et al.** (2008) Comparative genome analysis of filamentous fungi reveals gene family expansions associated with fungal pathogenesis. *Plos One* **3**, e2300
- Solomon, P. S. and Rathjen, J. P.** (2010) Pathogen effectors shed light on plant diseases. *Funct. Plant Biol.* **37**, III-IV.
- Sonoda, H., Suzuki, K. and Yoshida, K.** (2002) Gene cluster for ferric iron uptake in *Agrobacterium tumefaciens* MAFF301001. *Genes Genet. Syst.* **77**, 137-146.
- Stanford, D. R., Whitney, M. L., Hurto, R. L., Eisaman, D. M., Shen, W. C. and Hopper, A. K.** (2004) Division of labor among the yeast sol proteins implicated in tRNA nuclear export and carbohydrate metabolism. *Genetics* **168**, 117-127.
- Staples, R. C. and Mayer, A. M.** (1995) Putative virulence factors of *Botrytis cinerea* acting as a wound pathogen. *FEMS Microbiol. Lett.* **134**, 1-7.
- Stergiopoulos, I., Collemare, J., Mehrabi, R. and De Wit, P.** (2013) Phytotoxic secondary metabolites and peptides produced by plant pathogenic Dothideomycete fungi. *FEMS Microbiol. Rev.* **37**, 67-93.
- Stergiopoulos, I. and de Wit, P. J. G. M.** (2009) Fungal effector proteins. *Annu. Rev. Phytopathol.* **47**, 233-263.
- Stleger, R. J., Bidochka, M. J. and Roberts, D. W.** (1994) Characterization of a novel carboxypeptidase produced by the entomopathogenic fungus *Metarhizium anisopliae*. *Arch. Biochem. Biophys.* **314**, 392-398.
- Strange, R. N.** (2007) Phytotoxins produced by microbial plant pathogens. *Nat. Prod. Rep.* **24**, 127-144.
- Strelkov, S. E., Lamari, L. and Ballance, G. M.** (1999) Characterization of a host-specific protein toxin (Ptr ToxB) from *Pyrenophora tritici repentis*. *Mol. Plant-Microbe Interact.* **12**, 728-732.
- Takken, F. L. W. and Joosten, M. H. A. J.** (2000) Plant resistance genes: their structure, function and evolution. *Eur. J. Plant Pathol.* **106**, 699-713.
- Tamano, K., Satoh, Y., Ishii, T., Terabayashi, Y., Ohtaki, S., Sano, M., et al.** (2007) The  $\beta$ -1,3-exoglucanase gene *exgA* (*exg1*) of *Aspergillus oryzae* is required to catabolize extracellular glucan, and is induced in growth on a solid surface. *Biosci., Biotechnol., Biochem.* **71**, 926-934.
- Tan, K., Oliver, R. P., Solomon, P. S. and Moffat, C. S.** (2010) Proteinaceous necrotrophic effectors in fungal virulence. *Funct. Plant Biol.* **37**, 907-912.
- Tanaka, H., Okuno, T., Moriyama, S., Muguruma, M. and Ohta, K.** (2004) Acidophilic xylanase from *Aureobasidium pullulans*: efficient expression and secretion in *Pichia pastoris* and mutational analysis. *J. Biosci. Bioeng.* **98**, 338-343.
- Tekauz, A.** (1985) A numerical scale to classify reactions of barley to *Pyrenophora teres*. *Can. J. Plant Pathol.* **7**, 181-183.

- Templeton, M. D., Rikkerink, E. H. A. and Beever, R. E.** (1994) Small, cysteine-rich proteins and recognition in fungal-plant interactions. *Mol. Plant-Microbe Interact.* **7**, 320-325.
- Thordal-Christensen, H.** (2003) Fresh insights into processes of nonhost resistance. *Curr. Opin. Plant Biol.* **6**, 351-357.
- Tiede, A., Bastisch, I., Schubert, J., Orlean, P. and Schmidt, R. E.** (1999) Biosynthesis of glycosylphosphatidylinositols in mammals and unicellular microbes. *Biol. Chem.* **380**, 503-523.
- Tomas, A. and Bockus, W. W.** (1987) Cultivar-specific toxicity of culture filtrates of *Pyrenophora-tritici-repentis*. *Phytopathology* **77**, 1337-1340.
- Tomas, A., Feng, G. H., Reeck, G. R., Bockus, W. W. and Leach, J. E.** (1990) Purification of a cultivar-specific toxin from *Pyrenophora-tritici-repentis*, causal agent of tan spot of wheat. *Mol. Plant-Microbe Interact.* **3**, 221-224.
- Toone, W. M., Rudd, K. E. and Friesen, J. D.** (1991) *deaD*, a new *Escherichia coli* gene encoding a presumed ATP-dependent RNA helicase, can suppress a mutation in *rpsB*, the gene encoding ribosomal protein-s2. *J. Bacteriol.* **173**, 3291-3302.
- Torronen, A., Mach, R. L., Messner, R., Gonzalez, R., Kalkkinen, N., Harkki, A., et al.** (1992) The two major xylanases from *Trichoderma reesei*: Characterization of both enzymes and genes. *Nat. Biotechnol.* **10**, 1461-1465.
- Tuori, R. P., Wolpert, T. J. and Ciuffetti, L. M.** (1995) Purification and immunological characterization of toxic components from cultures of *Pyrenophora tritici-repentis*. *Mol. Plant-Microbe Interact.* **8**, 41-48.
- Tuori, R. P., Wolpert, T. J. and Ciuffetti, L. M.** (2000) Heterologous expression of functional Ptr ToxA. *Mol. Plant-Microbe Interact.* **13**, 456-464.
- Turkkan, M. and Dolar, F. S.** (2008) Role of phytotoxins in plant diseases. *Tarim Bilm. Derg.* **14**, 87-94.
- Turkyilmaz, B., Aktas, L. Y. and Guven, A.** (2011) Salinity induced differences in growth and nutrient accumulation in five barley cultivars. *Turk. J. Field Crops* **16**, 84-92.
- Valueva, T. A. and Mosolov, V. V.** (2004) Role of inhibitors of proteolytic enzymes in plant defense against phytopathogenic microorganisms. *Biochemistry (Moscow)* **69**, 1305-1309.
- Van Loon, L., Pierpoint, W., Boller, T. and Conejero, V.** (1994) Recommendations for naming plant pathogenesis-related proteins. *Plant Mol. Biol. Rep.* **12**, 245-264.
- Van Loon, L. C.** (1997) Induced resistance in plants and the role of pathogenesis-related proteins. *Eur. J. Plant Pathol.* **103**, 753-765.
- van Tegelen, L. J. P., Moreno, P. R. H., Croes, A. F., Verpoorte, R. and Wullems, G. J.** (1999) Purification and cDNA cloning of isochorismate synthase from elicited cell cultures of *Catharanthus roseus*. *Plant Physiol.* **119**, 705-712.

- Vancaesele, L. and Grumbles, J.** (1979) Ultrastructure of the interaction between *Pyrenophora teres* and a susceptible barley host. *Can. J. Bot.* **57**, 40-47.
- Vandenberg, C. G. J. and Rossnagel, B. G.** (1990) Effects of temperature and leaf wetness period on conidium germination and infection of barley by *Pyrenophora teres*. *Can. J. Plant Pathol.* **12**, 263-266.
- VanGuilder, H. D., Vrana, K. E. and Freeman, W. M.** (2008) Twenty-five years of quantitative PCR for gene expression analysis. *BioTechniques* **44**, 619-626.
- Varki, A., Cummings, R. and Esko, J.** (1999) Glycophospholipid Anchors. In: *Essentials of Glycobiology*. (pp. 653. NY, USA: Cold Spring Harbor Laboratory Press.
- Vincent, D., Balesdent, M. H., Gibon, J., Claverol, S., Lapaillerie, D., Lomenech, A. M., et al.** (2009) Hunting down fungal secretomes using liquid-phase IEF prior to high resolution 2-DE. *Electrophoresis* **30**, 4118-4136.
- Wakarchuk, W. W., Campbell, R. L., Sung, W. L., Davoodi, J. and Yaguchi, M.** (1994) Mutational and crystallographic analyses of the active site residues of the *Bacillus circulans* xylanase. *Protein Sci.* **3**, 467-475.
- Wallwork, H.** (2000) *Cereal leaf and stem diseases*. Canberra: Grains Research and Development Corporation.
- Walters, D., Newton, A. and Lyon, G.** (2007) *Induced Resistance for Plant Defence: A Sustainable Approach to Crop Protection*. UK: Blackwell Publishing.
- Walton, J. D.** (1994) Deconstructing the cell wall. *Plant Physiol.* **104**, 1113-1118.
- Walton, J. D.** (1996) Host-selective toxins: Agents of compatibility. *Plant Cell* **8**, 1723-1733.
- Walton, J. D.** (2006) HC-toxin. *Phytochemistry* **67**, 1406-1413.
- Wang, X., Li, X. and Li, Y.** (2007) A modified Coomassie Brilliant Blue staining method at nanogram sensitivity compatible with proteomic analysis. *Biotechnol. Lett.* **29**, 1599-1603.
- Weiergang, I., Jorgensen, H. J. L., Moller, I. M., Friis, P. and Smedegård-Petersen, V.** (2002) Correlation between sensitivity of barley to *Pyrenophora teres* toxins and susceptibility to the fungus. *Physiol. Mol. Plant Pathol.* **60**, 121-129.
- Weiland, J. J., Steffenson, B. J., Cartwright, R. D. and Webster, R. K.** (1999) Identification of molecular genetic markers in *Pyrenophora teres f. teres* associated with low virulence on 'Harbin' barley. *Phytopathology* **89**, 176-181.
- Wevelsiep, L., Kogel, K. H. and Knogge, W.** (1991) Purification and characterization of peptides from *Rhynchosporium secalis* inducing necrosis in barley. *Physiol. Mol. Plant Pathol.* **39**, 471-482.
- Wevelsiep, L., Ruppig, E. and Knogge, W.** (1993) Stimulation of barley plasmalemma H<sup>+</sup>-ATPase by phytotoxic peptides from the fungal pathogen *Rhynchosporium secalis*. *Plant Physiol.* **101**, 297-301.
- Wijk, K. J., Peltier, J.-B. and Giacomelli, L.** (2007) Isolation of chloroplast proteins from *Arabidopsis thaliana* for proteome

- analysis. In: *Plant Proteomics, Methods in Molecular Biology*. (Thiellement, H., Zivy, M., Damerval, C. and Méchin, V.), pp. 43-48. NY, USA: Humana Press Inc.
- Wildermuth, M. C., Dewdney, J., Wu, G. and Ausubel, F. M.** (2001) Isochorismate synthase is required to synthesize salicylic acid for plant defence. *Nature* **414**, 562-565.
- Wittwer, C. T., Herrmann, M. G., Moss, A. A. and Rasmussen, R. P.** (1997) Continuous fluorescence monitoring of rapid cycle DNA amplification. *BioTechniques* **22**, 130-138.
- Wolpert, T. J., Dunkle, L. D. and Ciuffetti, L. M.** (2002) Host-selective toxins and avirulence determinants: What's in a name? *Annu. Rev. Phytopathol.* **40**, 251-285.
- Wong, D.** (2010) Using proteomics to identify phytotoxins unique to the spot or net form of *Pyrenophora teres*. In: *School of Agriculture, Food and Wine: Plant and Food Science*. pp. 102: The University of Adelaide, Honours thesis.
- Wong, D. C., Ismail, I. A., Godfrey, D. and Able, A. J.** (2012) Death by toxin net blotch disease of barley. *Microbiology Australia* **33**, 34-35.
- Wu, S. C., Ham, K. S., Darvill, A. G. and Albersheim, P.** (1997) Deletion of two endo-beta-1,4-xylanase genes reveals additional isozymes secreted by the rice blast fungus. *Mol. Plant-Microbe Interact.* **10**, 700-708.
- Xi, K., Bos, C., Turkington, T. K., Xue, A. G., Burnett, P. A. and Juskiw, P. E.** (2008) Interaction of net blotch and scald on barley. *Can. J. Plant Pathol.* **30**, 329-334.
- Xiong, J.** (2006) *Essential bioinformatics*. NY, USA: Cambridge University Press
- Yang, F. E. N., Jensen, J. D., Svensson, B., Jorgensen, H. J. L., Collinge, D. B. and Finnie, C.** (2011) Secretomics identifies *Fusarium graminearum* proteins involved in the interaction with barley and wheat. *Mol. Plant Pathol.* **13**, 445-453.
- Yoder, O. C.** (1980) Toxins in pathogenesis. *Annu. Rev. Phytopathol.* **18**, 103-129.
- Yoshikawa, M., Takeuchi, Y. and Horino, O.** (1990) A mechanism for ethylene-induced disease resistance in soybean - enhanced synthesis of an elicitor-releasing factor, beta-1,3-endoglucanase. *Physiol. Mol. Plant Pathol.* **37**, 367-376.
- You, B. J., Lee, M. H. and Chung, K. R.** (2008) Production of cercosporin toxin by the phytopathogenic *Cercospora* fungi is affected by diverse environmental signals. *Can. J. Microbiol.* **54**, 259-269.
- Zadoks, J., Chang, C. T. T. and Konzak, C. F.** (1974) A decimal code for the growth stages of cereal. *Weed Res.* **14**, 415-421.
- Zajc, A., Romao, M. J., Turk, B. and Huber, R.** (1996) Crystallographic and fluorescence studies of ligand binding to N-carbamoylsarcosine amidohydrolase from *Arthrobacter* sp. *J. Mol. Biol.* **263**, 269-283.
- Zdobnov, E. M. and Apweiler, R.** (2001) InterProScan – an integration platform for the signature-recognition methods in InterPro. *Bioinformatics* **17**, 847-848.



- Zhang, H. F., Francl, L. J., Jordahl, J. G. and Meinhardt, S. W.** (1997) Structural and physical properties of a necrosis-inducing toxin from *Pyrenophora tritici-repentis*. *Phytopathology* **87**, 154-160.
- Zhang, Y.** (2008) I-TASSER server for protein 3D structure prediction. *BMC Bioinformatics* **9**.
- Zhang, Y. and Skolnick, J.** (2004) Scoring function for automated assessment of protein structure template quality. *Proteins: Struct. Funct. Bioinform.* **57**, 702-710.

## Appendix 1

### A numerical scale to classify reactions of barley to *Ptt*

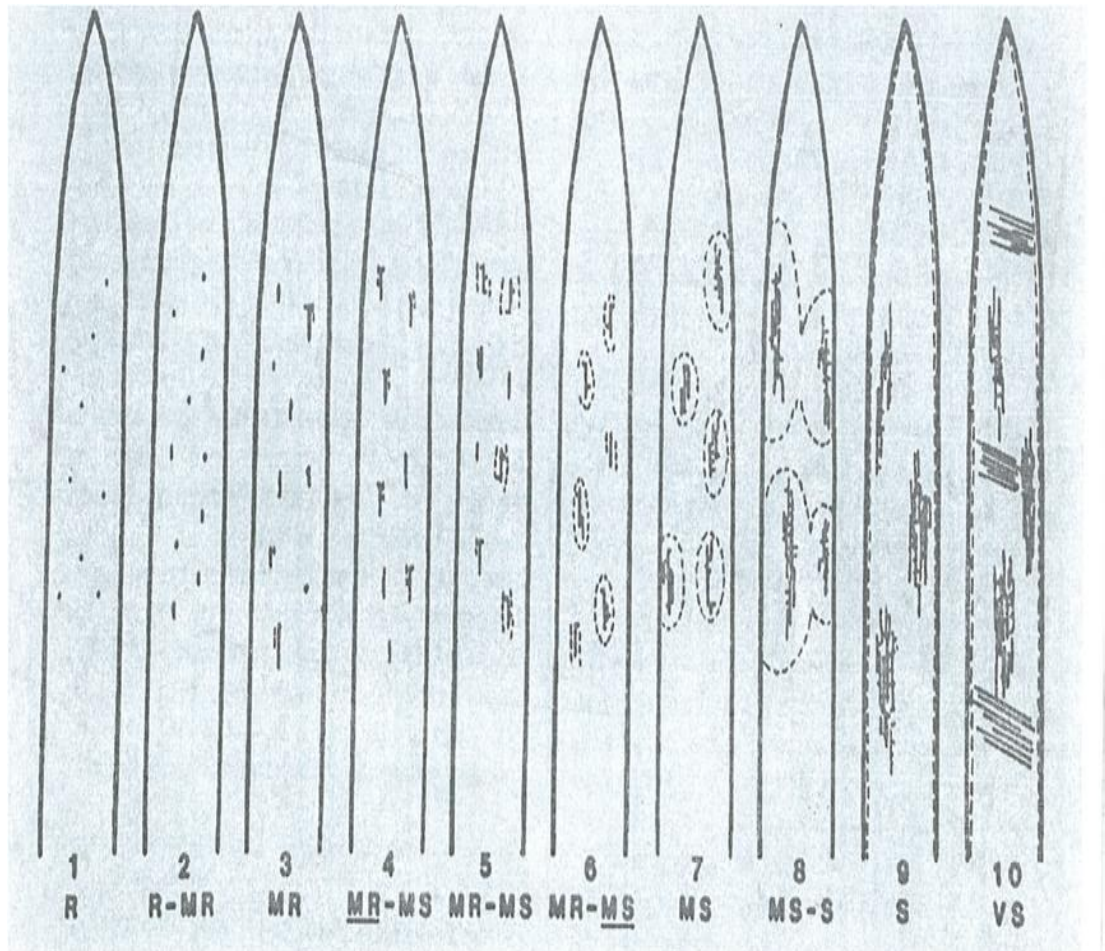


**Figure A1.1.** Tekauz's scale (Tekauz, 1985); the scale describes the reaction of barley to *P. teres f. teres* and illustrates these reaction using numbers from 1 to 10. Ten types of lesions classify the reactions of barley: R, resistant; MR, moderately resistant; MS, moderately susceptible; S, susceptible; VS, very susceptible. Underlined reactions indicate predominant reaction and dotted lines indicate extent of chlorosis and shaded lines indicate necrosis. Reproduced by permission (Appendix 5).

## Fungal development scale

**Table A1.1. A numerical scale to assess development of *P. teres* during its growth upon barley using light microscopy (Lightfoot and Able, 2010).**

<b>Score</b>	<b>Parameters (definition)</b>
<b>0</b>	Conidia are visible but have not germinated.
<b>1</b>	The majority of conidia have germinated with short, fine emerging hyphae less than one epidermal cell in length (up to 250 $\mu$ m long).
<b>2</b>	Hyphae are still quite fine but are the length of between one and three epidermal cells (up to 750 $\mu$ m long).
<b>3</b>	Hyphae starting to branch and may extend beyond three epidermal cells. Some appressoria may have formed
<b>4</b>	Hyphae have extensive branching and starting to thicken. Branches from original hyphae may now extend beyond one epidermal cell.
<b>5</b>	Hyphae have thickened and some penetration pegs are evident.
<b>6</b>	Hyphae have thickened further; penetration pegs are evident, growth of mycelia starting to become evident below epidermal cell layer and in the mesophyll
<b>7</b>	First leaf symptoms appear (necrotic spots), multiple penetrations, hyphae thickening and mycelia more evident in mesophyll. Browning of individual cells close to the pathogen evident.
<b>8</b>	Hyphae starting to branch further and becoming dendritic (tree-like branching). Finer hyphae growing between the original thicker hyphae on the surface of the leaf. Cells browning in a wider area.
<b>9</b>	Early signs of stomata developing in epidermal cell layer: thickened mycelia in clumps evident. Host cells appear to be collapsing.
<b>10</b>	Stomata appear mature with conidiophores emerging through the cuticle. Host cells have undergone advanced senescence and appear collapsed. Both chlorosis and necrosis clearly evident.

## Appendix 2 Optimisation of RT-PCR cycles

Saturation point of RT-PCR products varied between candidate genes (Figure A2.1), the optimal cycles for *PttSPI*, *PttGPI-CEFM* and *PttGAPDH* was 39 compared with the saturation point of *PttXyn11A* and *PttCHFPI* which was 33. Optimal cycle number was used in downstream PCR amplifications.



**Figure A2.1. RT-PCR cycle number optimisation for VRCGs *PttSPI*, *PttXyn11A*, *PttCHFPI*, *PttGPI-CFEM* and *PttGAPDH*.** Ten day colony mycelium of 32/98 isolate (the more virulent) grown on FCM, representative image for three biological replicates.

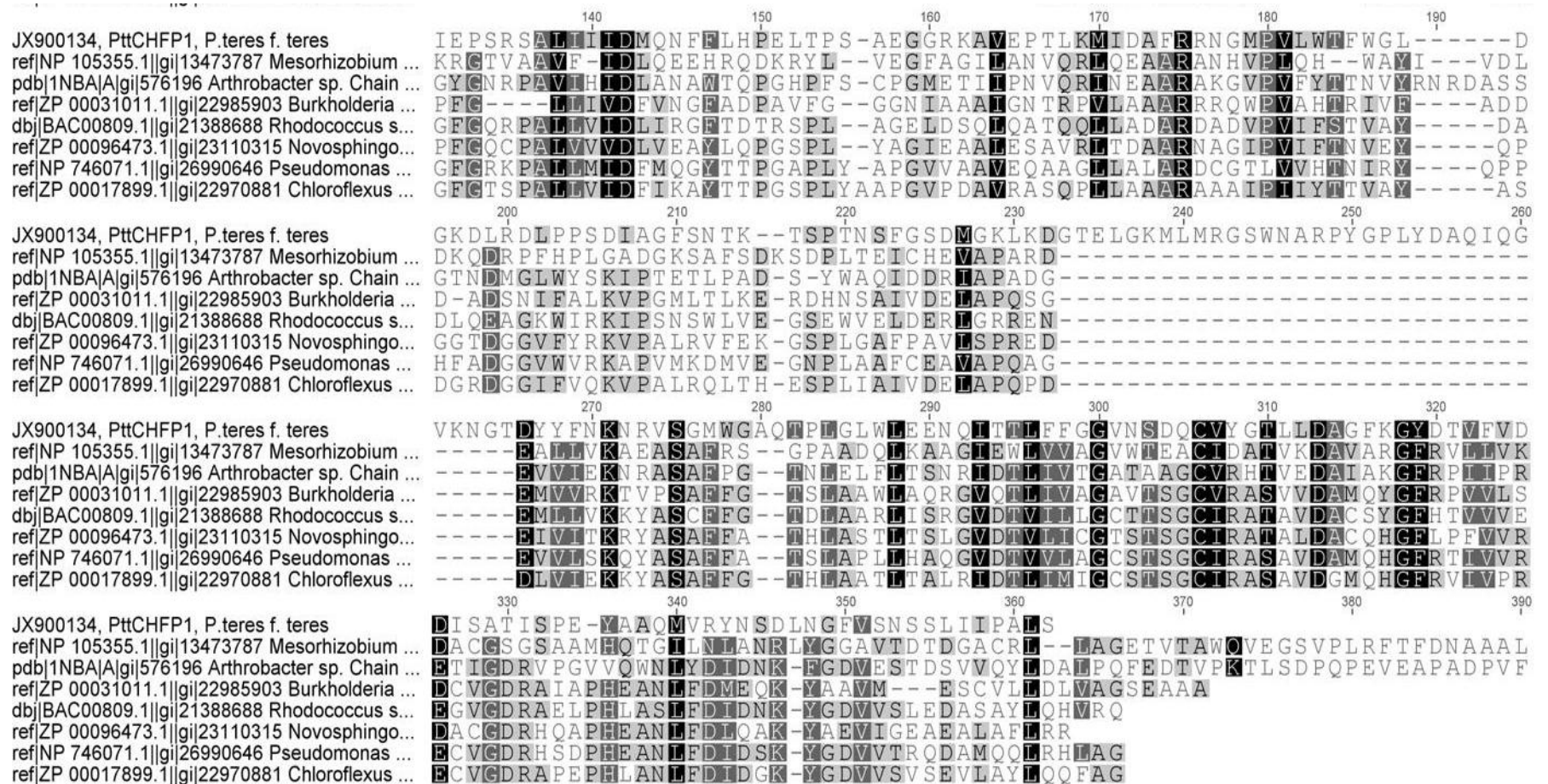


**Figure A2.2. Multiple alignment of PtCHFP1 and CSHase family proteins.** The sequences were obtained from NCBI databases. Regions of the proteins identified in the blast searches were aligned using Geneious. The accession numbers and species names of the sequences are indicated on the left side and the range of the residues from the original sequence is indicated at the top of the sequences. Sequence identity shown in black bold and conserved in gray, 8 sequences from different species were aligned using Geneious using MUSCLE.

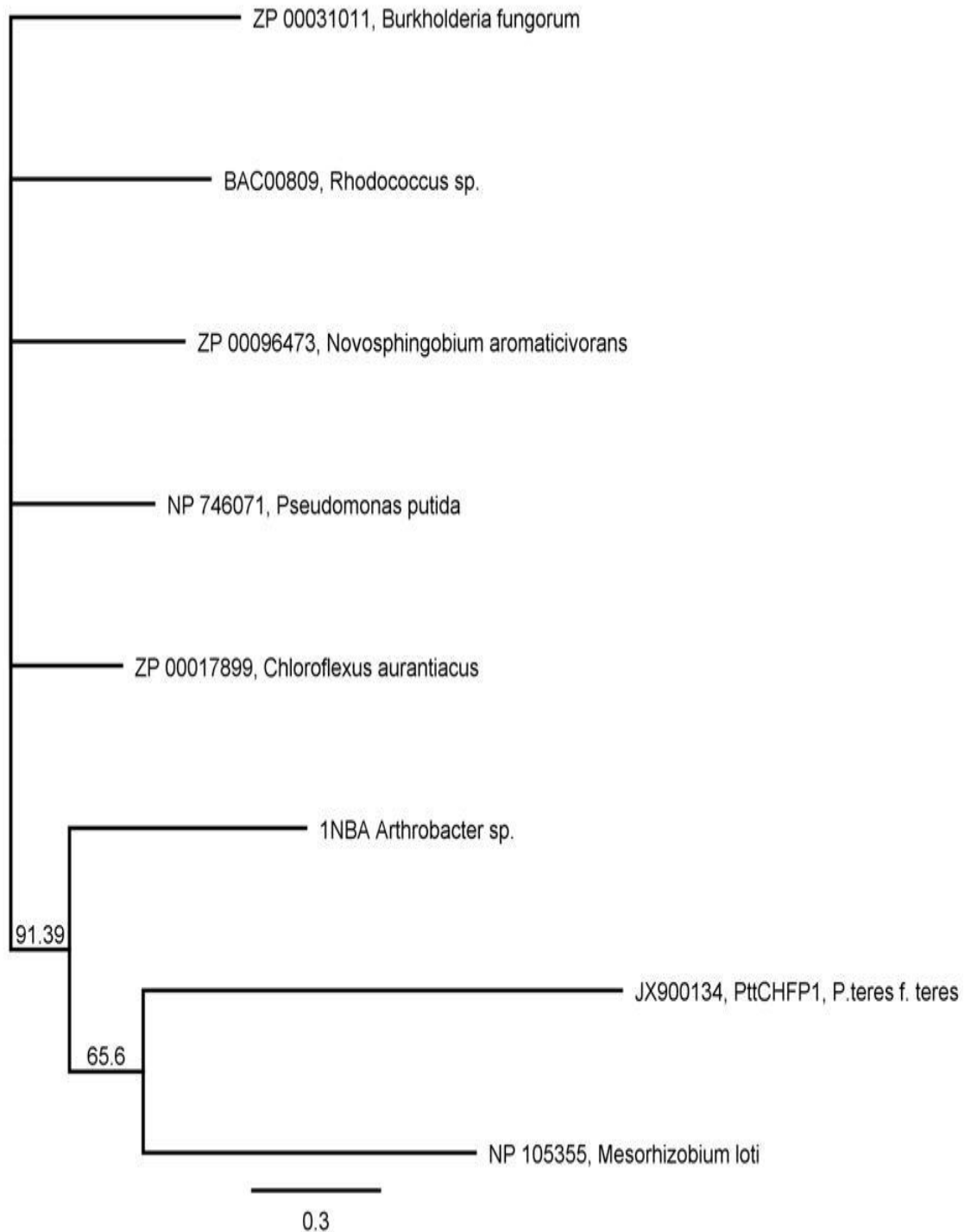


**Figure A2.3. The evolutionary history of PttCHFP1 and its homologues from CSHase family.** Phylogenetic analysis was inferred using the Neighbor joining method. The bootstrap consensus tree from 10000 replicates is taken to represent the evolutionary history of 9 taxa. The percentage of replicate trees in which the associated taxa clustered together in the bootstrap test (10000 replicates) are shown next to the branches. The tree is drawn to scale, with branch lengths in the same units as those of the evolutionary distances used to infer the phylogenetic tree. Geneious was used to conduct phylogenetic analysis, 8 sequences from different species were aligned using Geneious with MUSCLE used to construct the tree.

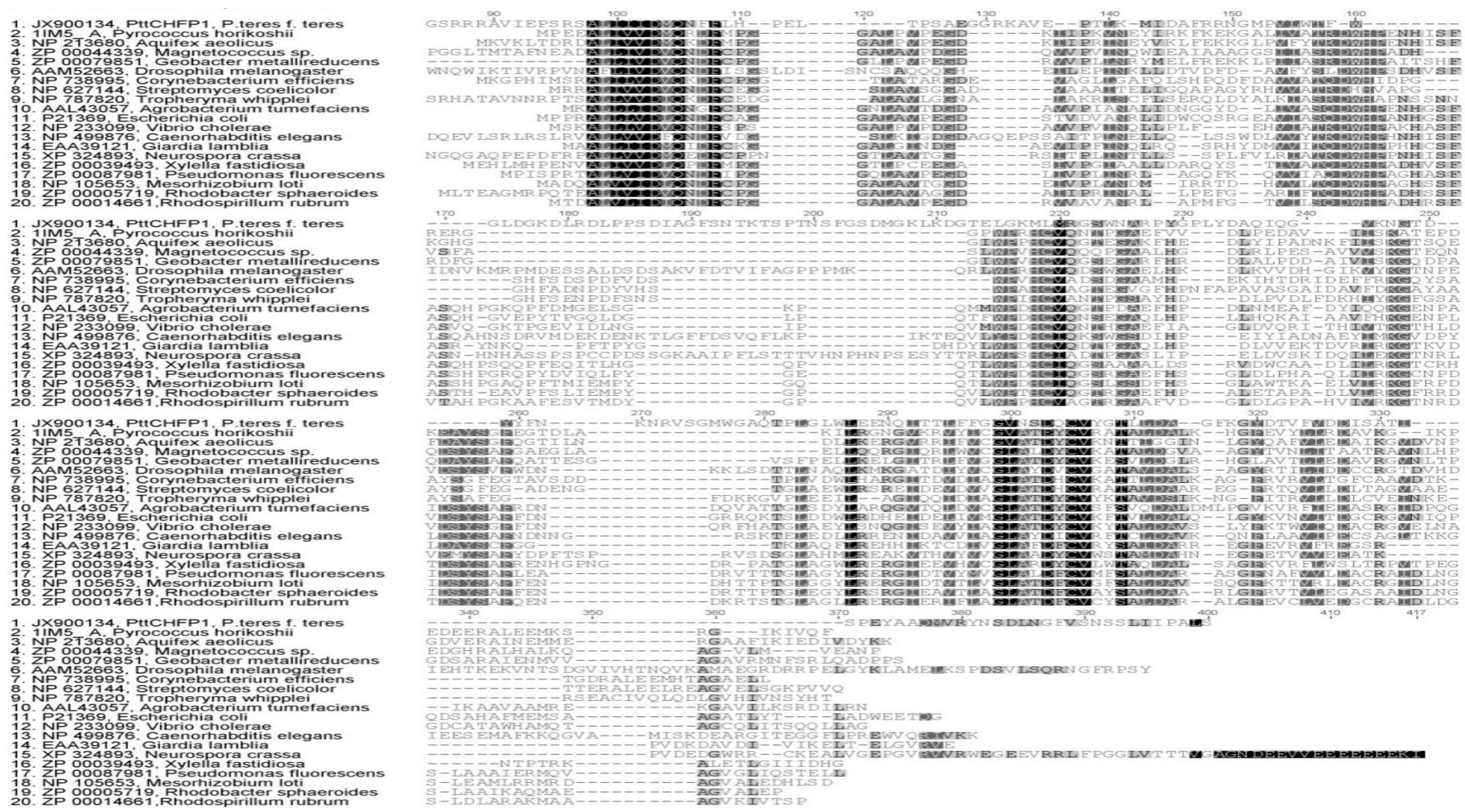
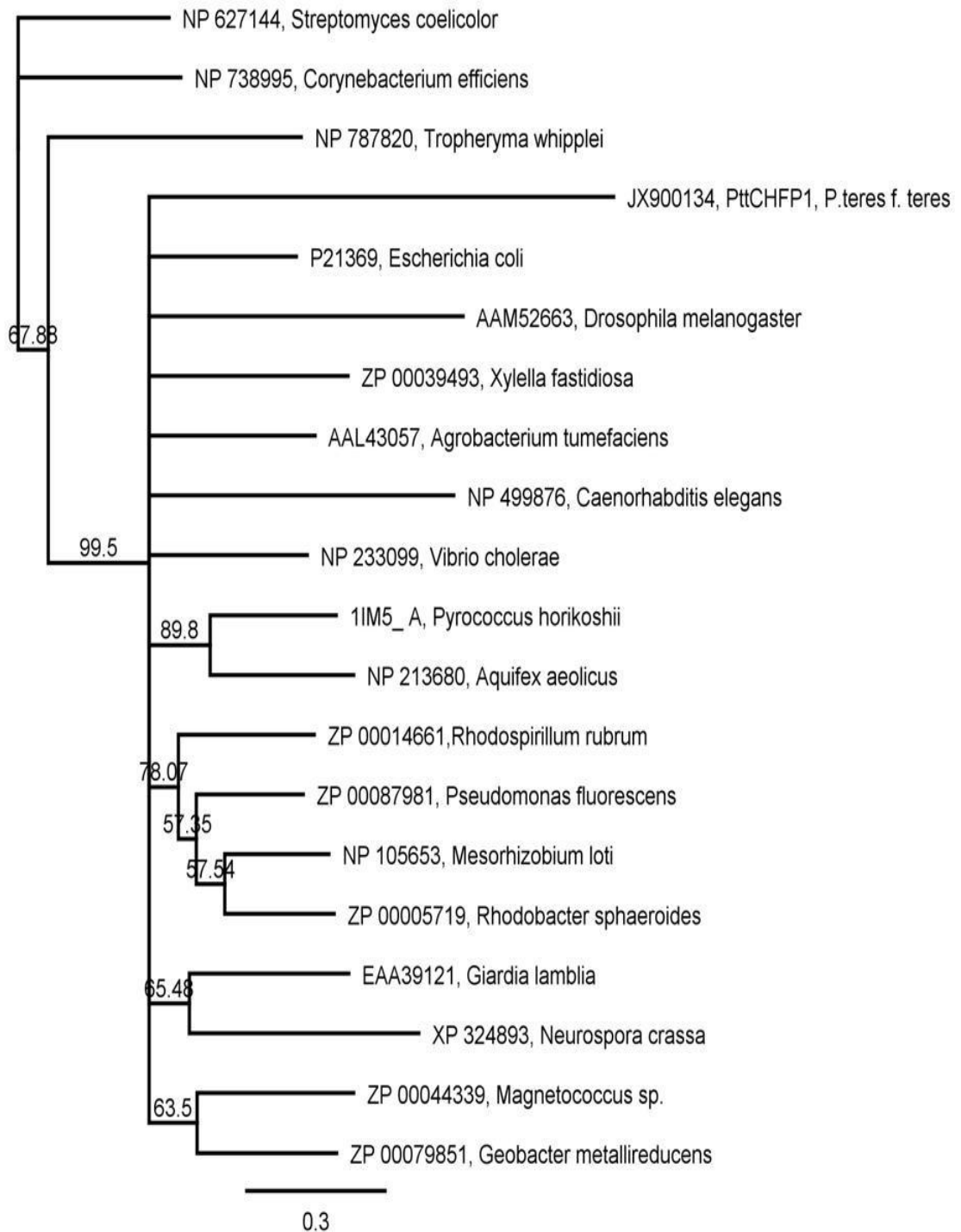
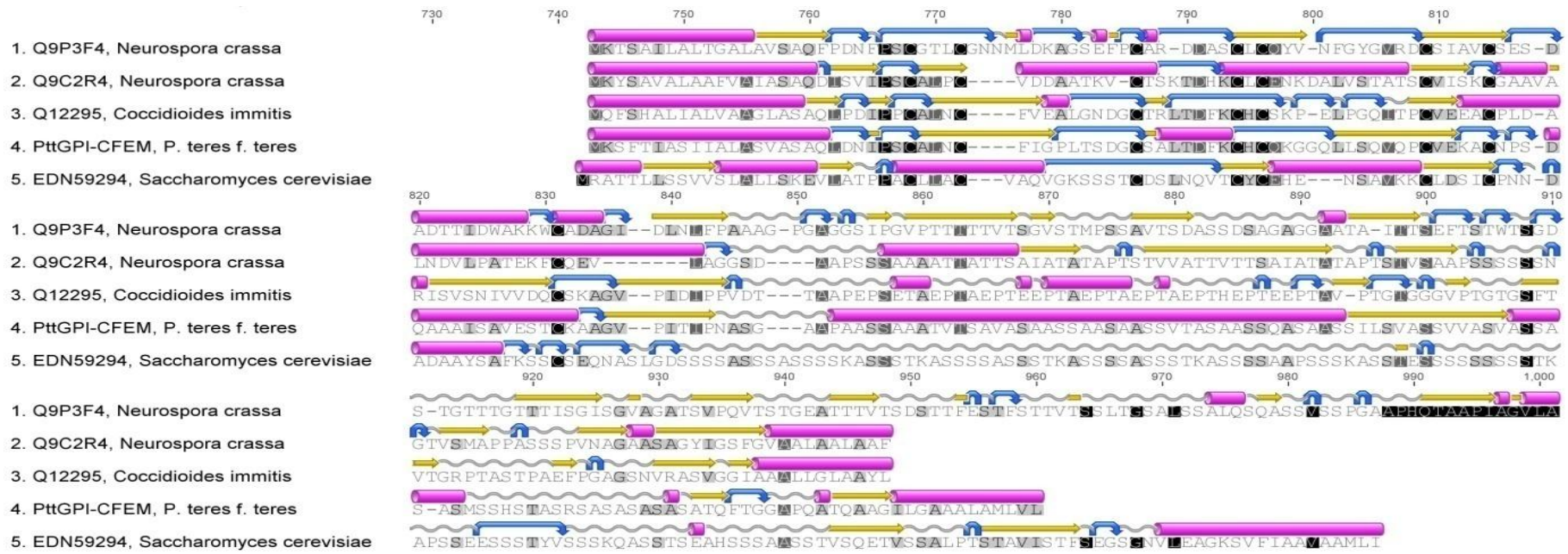


Figure A2.4. Multiple alignment of PttCHFP1 and Nicotinamidase family proteins. The sequences were obtained from NCBI databases. Regions of the proteins identified in the blast searches were aligned using Geneious. The accession numbers and species names of the sequences are indicated on the left side and the range of the residues from the original sequence is indicated at the top of the sequences. Sequence identity shown in bold black and conserved in gray, 20 sequences from different species were aligned using Geneious using MUSCLE.



**Figure A2.5. The evolutionary history of PttCHFP1 and its homologues from Nicotinamidase family.** Phylogenetic analysis was inferred using the Neighbor joining method. The bootstrap consensus tree from 10000 replicates is taken to represent the evolutionary history of 9 taxa. The percentage of replicate trees in which the associated taxa clustered together in the bootstrap test (10000 replicates) are shown next to the branches. The tree is drawn to scale, with branch lengths in the same units as those of the evolutionary distances used to infer the phylogenetic tree. Geneious was used to conduct phylogenetic analysis, 8 sequences from different species.





**Figure A2.6. Secondary structure of PttGPI-CFEM and 4 selected members of CFEM family.** Alpha helices (purple cylinders), coil (gray curve shapes), Beta strand (yellow arrows) and turn (blue curves) are shown for the secondary structure.

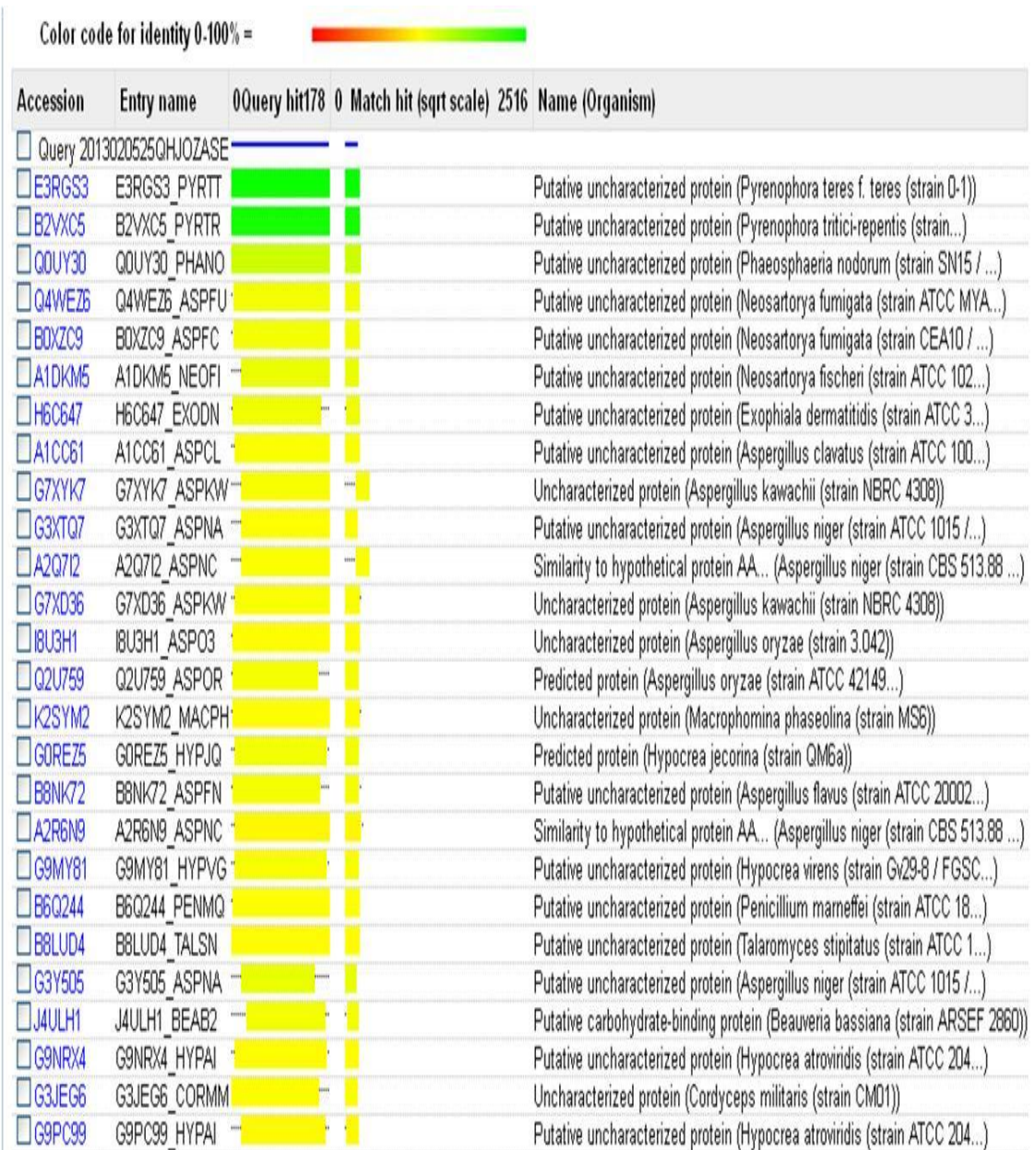
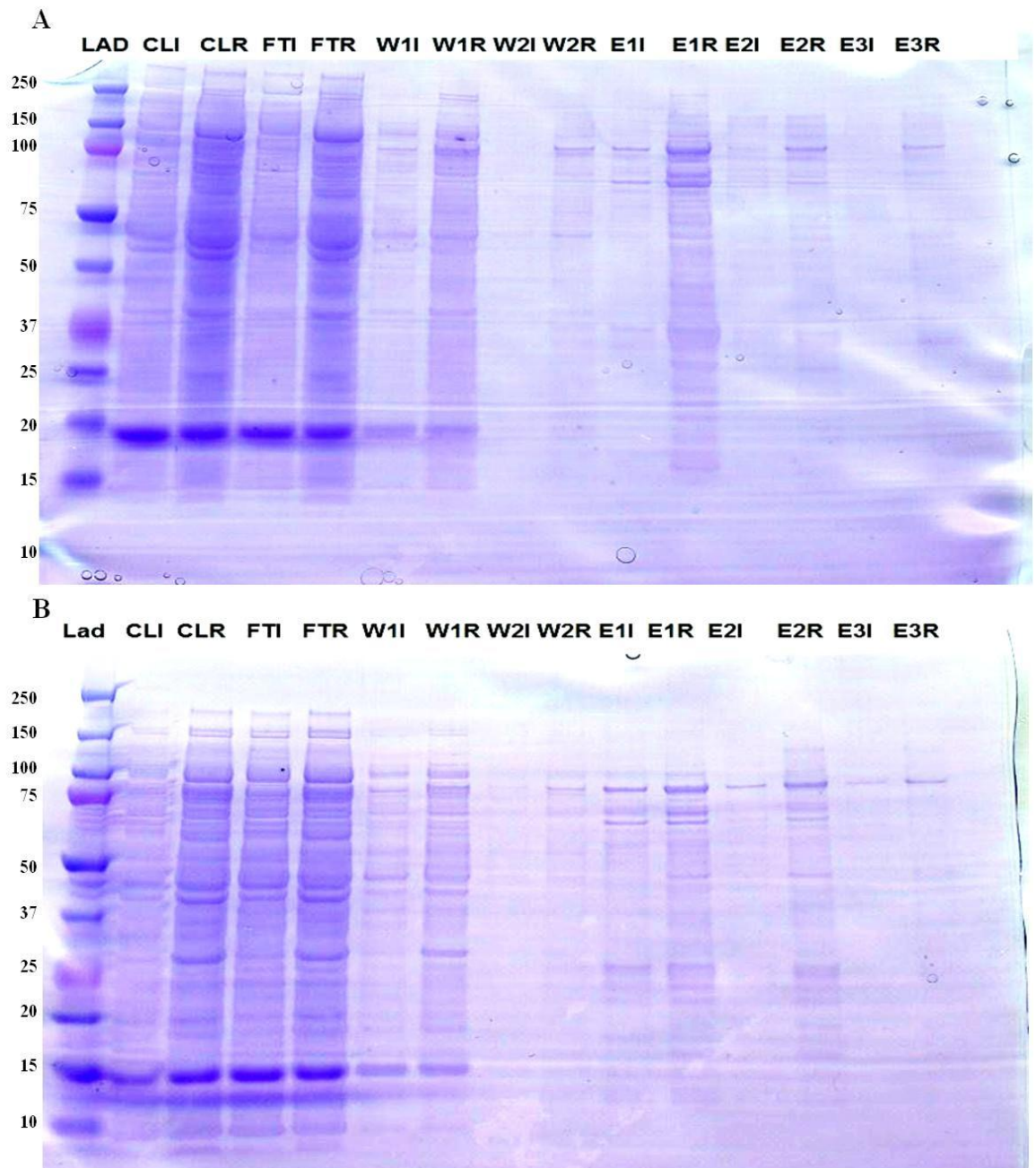
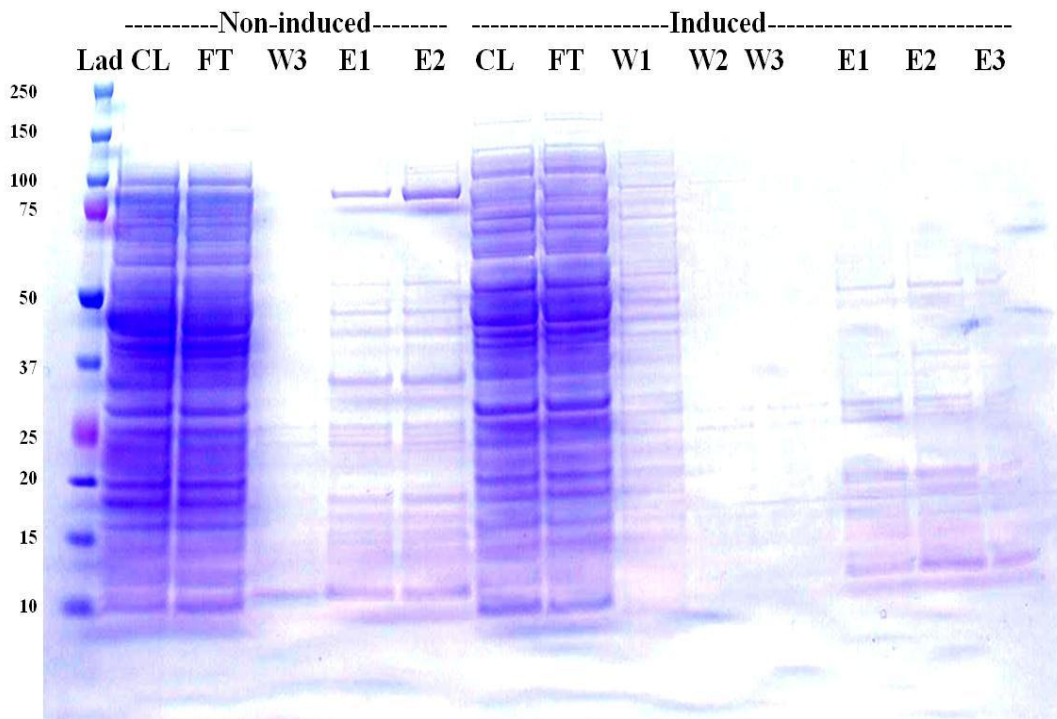


Figure A2.7. Graphical summary of PttSP1 BLAST in UniProtKB databases.

### Appendix 3



**Figure A3.1. Native extraction of heterologous expression of PttXyn11A from *E. coli* with different temperatures.** Two incubation temperature 16°C (A) and 23°C (B) were used, L-arabinose (0.4%) was added to LB media for induction and D(+)-glucose for repression of recombinant protein, cells incubated for 6 h. Native conditions was used for protein purification. CLI, clear lysate fractions for induced cells; and CLR, non-induced; FTI, flow through fraction for induced cells; FTR, flow through non-induced; WI, two washing fraction for induced; WR, two washing for non-induced; EI, three elutions fractions for induced cells; and ER, two elutions non-induced.



**Figure A3.2. Denaturing extraction of heterologous expression of PttXyn11A in new transformant of *E. coli*.** L-arabinose (0.4%) was added to LB media for induction and D(+)-glucose for repression of recombinant protein, cells incubated for 6 h. CL, clear lysate fractions; FT, flow through; W, washing fractions; E, elutions fractions.

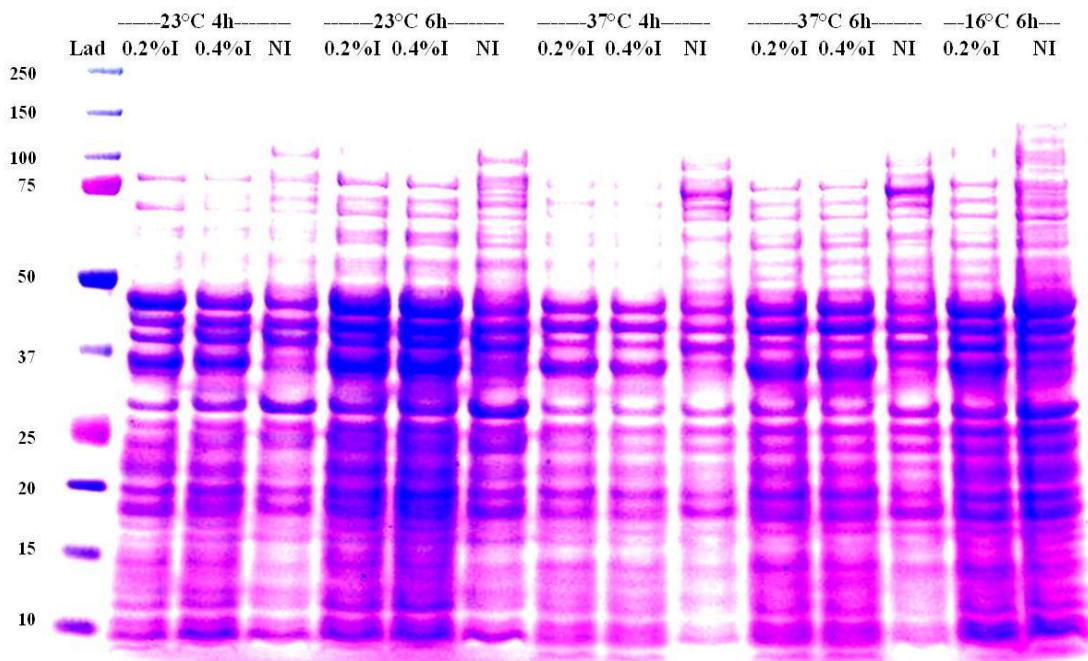


**Figure A3.3. Optimisation of heterologous expression of PttCHFP1 in *E. coli* with different incubation conditions and L-arabinose concentration.** Two incubation time (4 h and 6 h) and two concentrations of L-arabinose (0.2% and 0.4%) at three incubation temperatures (23°C, 37°C and 16°C) were used, D(+)-glucose was used to repress the expression of recombinant protein. Denatured conditions was used for protein purification. I, clear lysate fractions for induced cells; and NI, non-induced were loaded in PAGE.

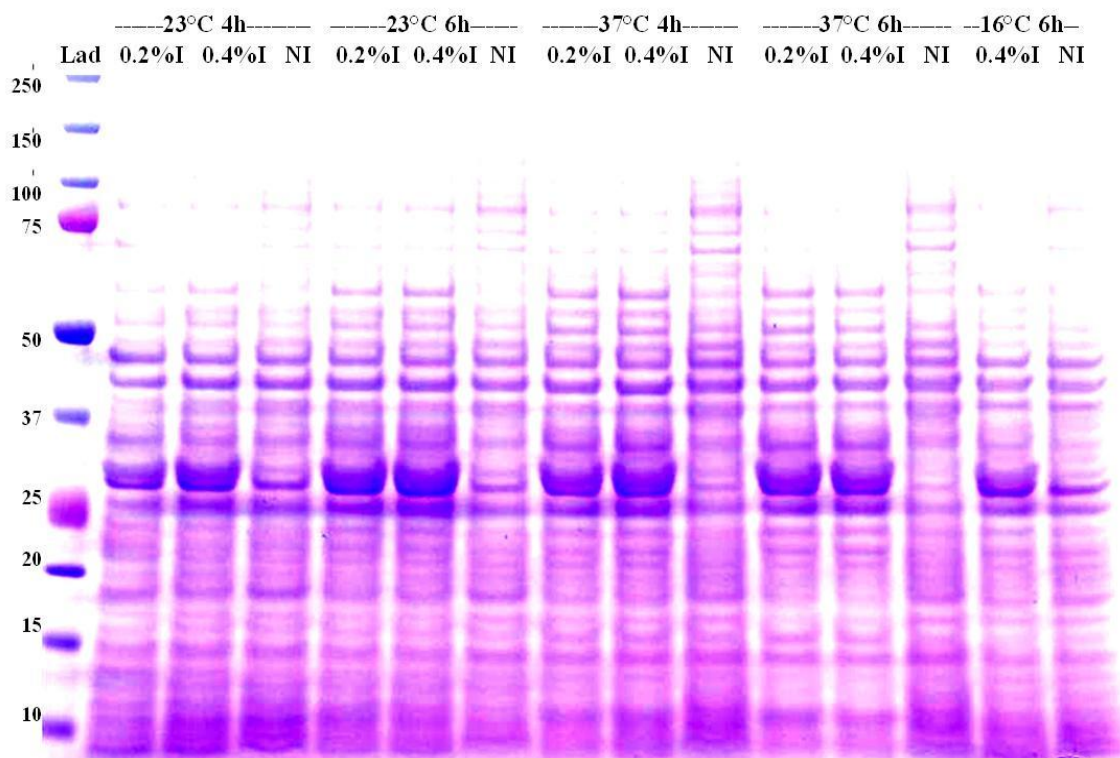


**Figure A3.4. Optimisation of heterologous expression of PttSP1 in *E. coli* with different incubation conditions and L-arabinose concentration.** Two incubation time (4 h and 6 h) and two concentrations of L-arabinose (0.2% and 0.4%) at three incubation temperatures (23°C, 37°C and 16°C) were used, D(+)-glucose was used to repress the expression of recombinant protein. Denatured conditions was used for protein purification. I, clear lysate fractions for induced cells; and NI, non-induced were loaded in PAGE.

**Appendix 4**  
**Partial product of VRCGs**

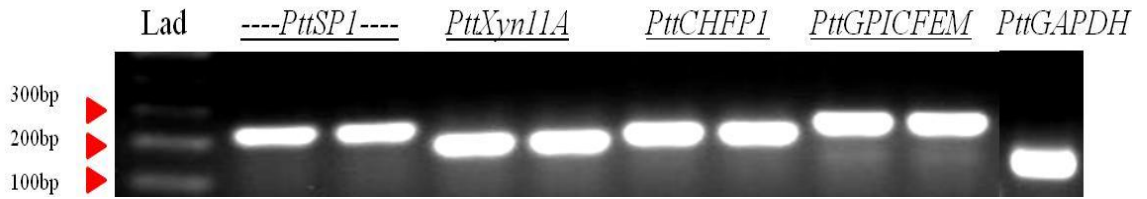


**Figure A4.1. RT-PCR products (partial product) for four VRCGs isolated from 32/98 mycelium grown for 10 day on FCM. *PttSP1* 225 pb, *PttXyn11A* 184 bp, *PttCHF1* 202 bp, *PttGPICFEM* 156 bp. Using qRT-PCR primers and conventional RT-PCR, five VRCGs were successfully isolated from 32/98 mycelium grown for 10 days at FCM as evidenced by a single band for each product at appropriate size.**

**A**

	1	10	20	30	40	50	60	70	80	90	100	110	120	130
ORF	----- ----- ----- ----- ----- ----- ----- ----- ----- ----- ----- ----- ----- -----													
PP	ATGGTTGCCTTCTACTATCCTCCTCGCTTTGGGCAGTGCCACCAGCGGCTCTCGCCTCACTCTCGGTCTTATCCTCGATGCTGAAGCCAGGGGCGAATCTGCCAATTGACTTCCCGCTCCACCCCG													
Consensus	.....													
	131	140	150	160	170	180	190	200	210	220	230	240	250	260
ORF	----- ----- ----- ----- ----- ----- ----- ----- ----- ----- ----- ----- -----													
PP	CCGGCACTGGCATGAAACATGGCTTCTTACTCTTTCTGGACCGATGGCCAGGGTCAGGTGACTTACAACAACGGCAACGCTGGCTCCTACAGTGCCAGTGAGCAACGTCGGTAACTTCGTTGCCGG													
Consensus	.....cCAGGcTcaaGTGACT.ACAa..ACGGCAACGCTGGCTCCTACAGTGCCAGTGAGCAACGTCGGTAACTTCGTTGCCGG													
	261	270	280	290	300	310	320	330	340	350	360	370	380	390
ORF	----- ----- ----- ----- ----- ----- ----- ----- ----- ----- ----- ----- -----													
PP	CAAGGATGGAAACCTGGATCCACCCGTGTAGTCACCTACAGCGGTACCTGGAAACGCTCAGATGTCAACTCTTACATCTCTTTATGGATGGACTCGCAACCCCTGATCGAATACTACATCGTTGAG													
Consensus	CAAGGATGGAAACCTGGATCCACCCGTGTAGTCACCTACAGCGGTACCTGGAAACGCTCAGATGTCAACTCCA.....													
	391	400	410	420	430	440	450	460	470	480	490	500	510	520
ORF	----- ----- ----- ----- ----- ----- ----- ----- ----- ----- ----- ----- -----													
PP	GCCTACGGCTCCTACRACCTGCTTCTGCTGCTCAGAGAGGGTCAAGTCCAGTCTGACGGGGCACATACGACATTCTCCAGACTACCCGCTACRACAGCCTTCCATCGACGGTACCCAGACATTCC													
Consensus	.....													
	521	530	540	550	560	570	580	590	600	610	620	630	640	650
ORF	----- ----- ----- ----- ----- ----- ----- ----- ----- ----- ----- ----- -----													
PP	AGCAATTCTGGTCTGTCCGCACCAGCAAGAGGGTCGGTGGTACCATCACTGTCAAGAACCACTTCGATGCCTGGGCCAAGTACGGACAAAGCTTGGACACACACTATCAATTCTTGCTACCGAGGG													
Consensus	.....													
	651	660	670	680	690	696								
ORF	----- ----- ----- ----- -----													
PP	ATACCAGAGCTCTGGTTCGGCTCCATCACTGTCAAGCAGCTTTAA													
Consensus	.....													

# B

	1	10	20	30	40	50	60	70	80	90	100	110	120	130
ORF	----- ----- ----- ----- ----- ----- ----- ----- ----- ----- ----- ----- ----- -----													
PP	ATGAAGCTCGCTGCGCCCTTCGTAGCCGCCACGGCAGCTCTGCCCTCGCGTCGTCCACCATCACACAGCGTACCAGAACATCACGCTCCCAACAGCCACACCACCTCCTCGGCAACATTTACACC													
Consensus	.....													
	131	140	150	160	170	180	190	200	210	220	230	240	250	260
ORF	----- ----- ----- ----- ----- ----- ----- ----- ----- ----- ----- ----- -----													
PP	ACTGGATCTACCTCGGAARTGATACCTATGACCTAACGCGGTCCATGGTGGCACCCACGACTAAGCCCGTCACCATCCCCATGACCGGATCCCGGGACGCGCCGTCATCGAACCTCACGTTCCGCACT													
Consensus	.....GTAGT--ATGCTGGA--CCACGACTAAGCCCGTCACCATCCCCATGACCGGATCCCGGGACGCGCCGTCATCGAACCTCACGTTCCGCACT GcaGT..ATGcTGGa..CCACGACTAAGCCCGTCACCATCCCCATGACCGGATCCCGGGACGCGCCGTCATCGAACCTCACGTTCCGCACT													
	261	270	280	290	300	310	320	330	340	350	360	370	380	390
ORF	----- ----- ----- ----- ----- ----- ----- ----- ----- ----- ----- ----- -----													
PP	CATCATAATCGACATGCAGAACTTTTTCTGCACCCGGAGCTCACGCCAGCGCCGAAAGCGGGCGAAGCAGTGGAGCCGACTCTGAAGATGATTGACGCGTTTCGTAGAACGGCATGCCCGTGCTC													
Consensus	CATCATAATCGACATGCAGAACTTTTTCTGCACCCGGAGCTCACGCCAGCGCCGAAAGCGGGCGAAGCAGTGGAGCCGACT CATCATAATCGACATGCAGAACTTTTTcTGCACCCGGAGCTCACGCCAGCGCCGAAAGCGGGCGAAGCAGTGGAGCCGACT.....													
	391	400	410	420	430	440	450	460	470	480	490	500	510	520
ORF	----- ----- ----- ----- ----- ----- ----- ----- ----- ----- ----- ----- -----													
PP	TGGACCTTCGCGGCTCGACGGAAAGGATCTCCGAGATCTACCTCCTTCGGACATTGCGGGCTTCTCAACACAAGACCAGTCCGACAATTCGTTTGGCAGCGACATGGGCAAACTGAAGACGGCA													
Consensus	.....													
	521	530	540	550	560	570	580	590	600	610	620	630	640	650
ORF	----- ----- ----- ----- ----- ----- ----- ----- ----- ----- ----- ----- -----													
PP	CCGAGCTGGGCAAAATGCTGATGCGCGCTCGTGGAACGCGAGACCATATGGGCCATTGTACGATGCGCAGATCCAGGTGTCAGAACGGGACGGACTATTACTTCAACAAAACCGTGTGAGCGGCAT													
Consensus	.....													
	651	660	670	680	690	700	710	720	730	740	750	760	770	780
ORF	----- ----- ----- ----- ----- ----- ----- ----- ----- ----- ----- ----- -----													
PP	GTGGGGTGCAGACACCGCTTGGTCTCTGGCTGGAAAGAGAACCAATCACCACTCTCTTCTTCGGAGGCGTAACTCGGATCAATGCGTGTACGGTACGCTCCTAGATGCCGGTTTCAGGGCATGAC													
Consensus	.....													
	781	790	800	810	820	830	840	850	860	870	880	890	900	906
ORF	----- ----- ----- ----- ----- ----- ----- ----- ----- ----- ----- ----- -----													
PP	ACCGCTTCGTTGATGACATTTCCGCCACAATCAGTCCGGAATATGCCGCTCAARTGGTCAGGTACARTTCAGACCTCAACGGTTTTGTATCCAATTCCTCTTTGATCATACCCGCACTCTCCTAG													
Consensus	.....													



# C

```
1      10      20      30      40      50      60      70      80      90      100     110     120     130
|-----|-----|-----|-----|-----|-----|-----|-----|-----|-----|-----|-----|
ORF    ATG AAG AGC TTC ACC ATC GCC CTC CAT CAT CGC TCT GGC CTT GTT GCT CAG CCC AGC TTG ACA TAT CCC GTC ATG CGC TCT TAA CTT GCT TCAT CGG TCC CCG ACC AGC GAC GGC TGT CTT GCT CTA
PP
Consensus .....

131     140     150     160     170     180     190     200     210     220     230     240     250     260
|-----|-----|-----|-----|-----|-----|-----|-----|-----|-----|-----|-----|
ORF    CCG ACT TCA AGT GCC AC TGC CAA A GGG CGG CAG C TCC TTT CTC AGG TCC AG C C C TGC GTC GAG AAG GCT TGC AAC CTT CTG ACC AGG CCG CCG CCA TCT CCG CTG TCG AGT C TACT TGC AAG GCC GC
PP      GAG AGC G--TGCC A G- GGG CGG CAG C TCC TTT CTC AGG TCC AG C C C TGC GTC GAG AAG GCT TGC AAC CTT CTG ACC AGG CCG CCG CCA TCT CCG CTG TCG AGT C TACT TGC AAG GCC GC
Consensus ..... aAG aGC .. TGCC aA , GGG CGG CAG C TCC TTT CTC AGG TCC AG C C C TGC GTC GAG AAG GCT TGC AAC CTT CTG ACC AGG CCG CCG CCA TCT CCG CTG TCG AGT C TACT TGC AAG GCC GC

261     270     280     290     300     310     320     330     340     350     360     370     380     390
|-----|-----|-----|-----|-----|-----|-----|-----|-----|-----|-----|-----|
ORF    TGG TGT GCC ATC ACC ATC C C C A A C G C C A G T G G T G T G C C C C T G C T G C C A G C T C A G C T G C T G C C A C C G T G A C C T C C G C T G T C G C C T C T G C T G C A T C T T C T G C C G C C T C T G C T G C C T C C C T C C G T A C T G C A
PP      TGG TGT GCC ATC ACC ATC C C C A A C G C C A G T G G T G T G C C C C T G C T G C C A G C T C A G C T G C T G C C A C C G T G A C C T C C G C T G T C G A A C
Consensus TGG TGT GCC ATC ACC ATC C C C A A C G C C A G T G G T G T G C C C C T G C T G C C A G C T C A G C T G C T G C C A C C G T G A C C T C C G C T G T C G aac .....

391     400     410     420     430     440     450     460     470     480     490     500     510     520
|-----|-----|-----|-----|-----|-----|-----|-----|-----|-----|-----|-----|
ORF    TCAG CTGC CTTCTCC AAG CCTCC GCG CTTCTTCG ATCCTATCC GTCGCC TCTTCGG TCGTTGC C TCCG TCG ATCCTCTGC C TCCG ATCC ATGTC ATCTCA CTCC ACTG CTTCC GCTCTGCC AGTG
PP
Consensus .....

521     530     540     550     560     570     580     590     600     610     620 624
|-----|-----|-----|-----|-----|-----|-----|-----|-----|-----|-----|
ORF    CCAG CGC TTTG CCTCG GCC ACTCAG TTCA CCG GTGG TGT CCTCAG GCC ACTCAG GCTGCC GGTAT CCTCG GTGCTG C C C T TGC CATG C TCG TCTTGTAA
PP
Consensus .....
```



**Figure A4.2. Sequence confirmation and alignment of qRT-PCR primers products with the full length of corresponding genes.** ORF, open reading frame aligned with PP, partial product of VRCGs sequences; (A) *PttSPI*, (B) *PttXyn11A*, (C) *PttCHFP1*, (D) *PttGPI-CFEM* and *PttGAPDH* (E). Partial sequences for VRCGs were match the targeted genes confirming the specificity of qRT-PCR primers, few base pairs were mismatched the targeted genes (*PttSPI* 225 pb, *PttXyn11A* 184 bp, *PttCHFP1* 202 bp, *PttGPICFEM* 156 bp).

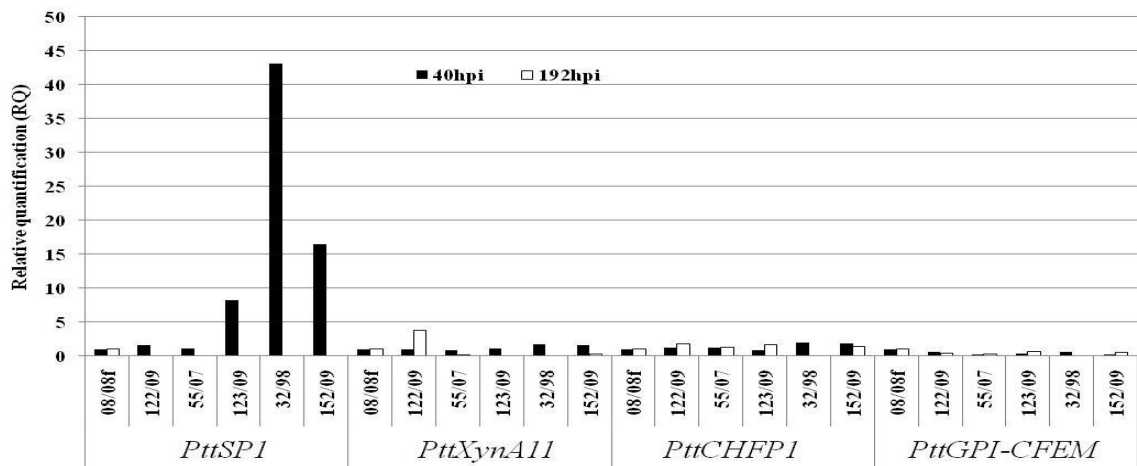


**Figure A4.3. Expression of VRCGs at 40 and 192 hours post inoculation (hpi) using comparative CT ( $\Delta\Delta C_T$ ) method.** RQ = Relative quantification of *PttSP1*, *PttXyn11A*, *PttCHFP1* and *PttGPI-CFEM*. Comparative  $C_T$  ( $\Delta\Delta C_T$ ) method uses 08/08f and *PttGAPDH* as a reference sample and reference gene respectively and then normalised the data against these references.

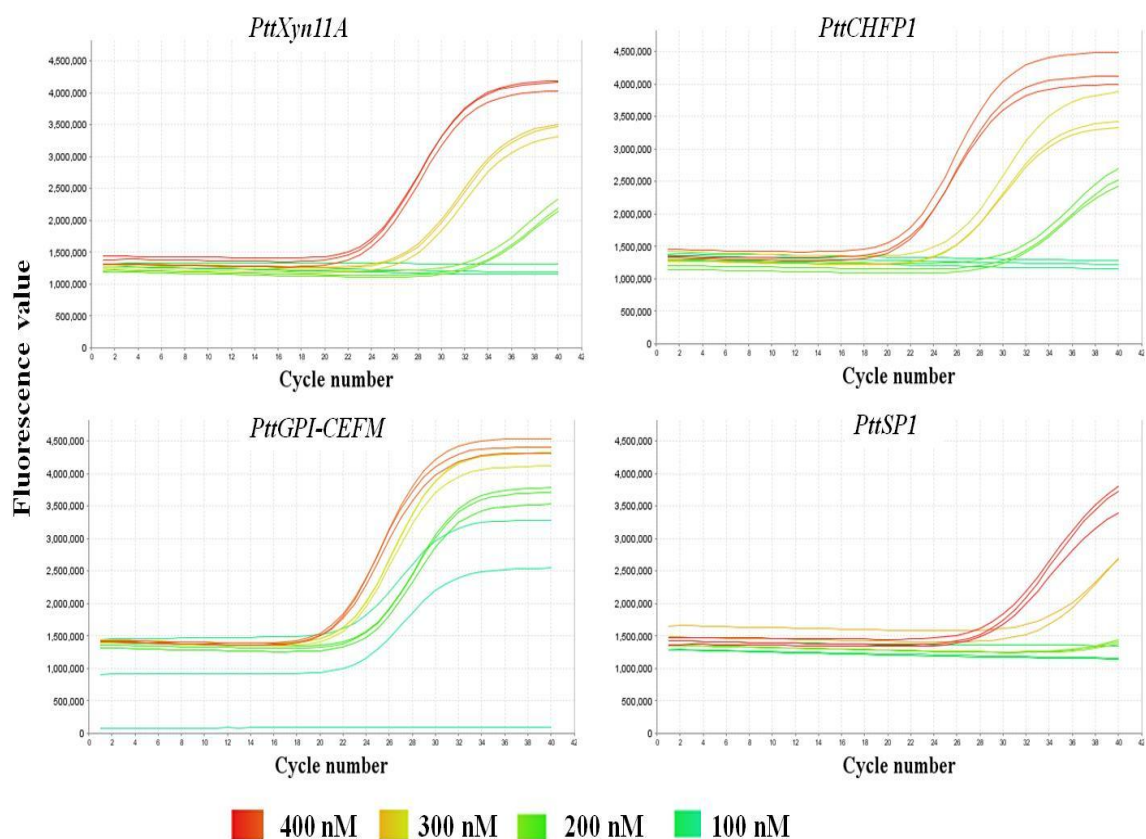


**Figure A4.4. Amplification efficiency for VRCGs at different primer concentrations.** Three primer concentrations were used; 400 nM, 300 nM, 100 nM final concentration, three technical replicates were used.

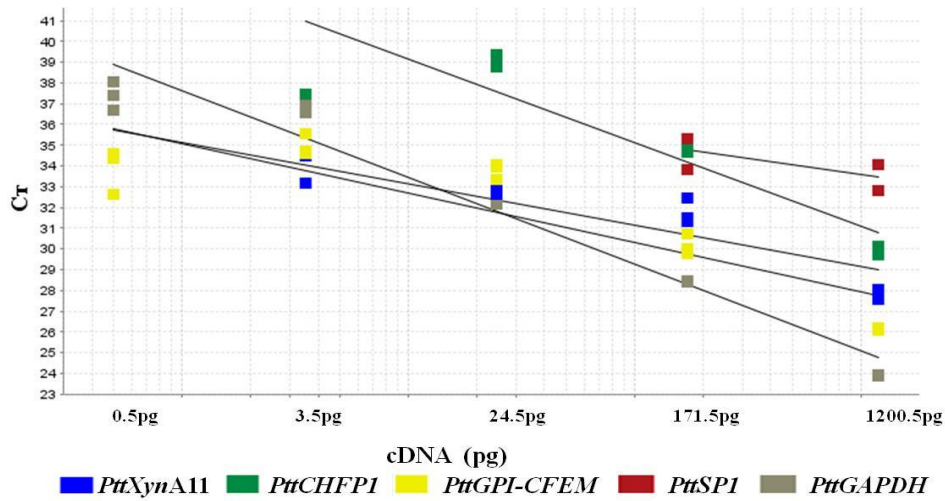


**Figure A4.5. Standard curves for VRCGs with low concentration of cDNA.** Five concentrations (0.5 pg, 3.5 pg, 24.5 pg, 171.5 pg and 1200.5 pg) of cDNA were used for each VRCG, standard curves were generated using ViiA™ 7 software using four technical replicates.  $C_T$  values are shown in Y axis.  $R^2$  for *PttSP1* 0.48, *PttXyn11A* 0.79, *PttCHFPI* 0.38, *PttGPI-CFEM* 0.75 and *PttGAPDH* 0.95.

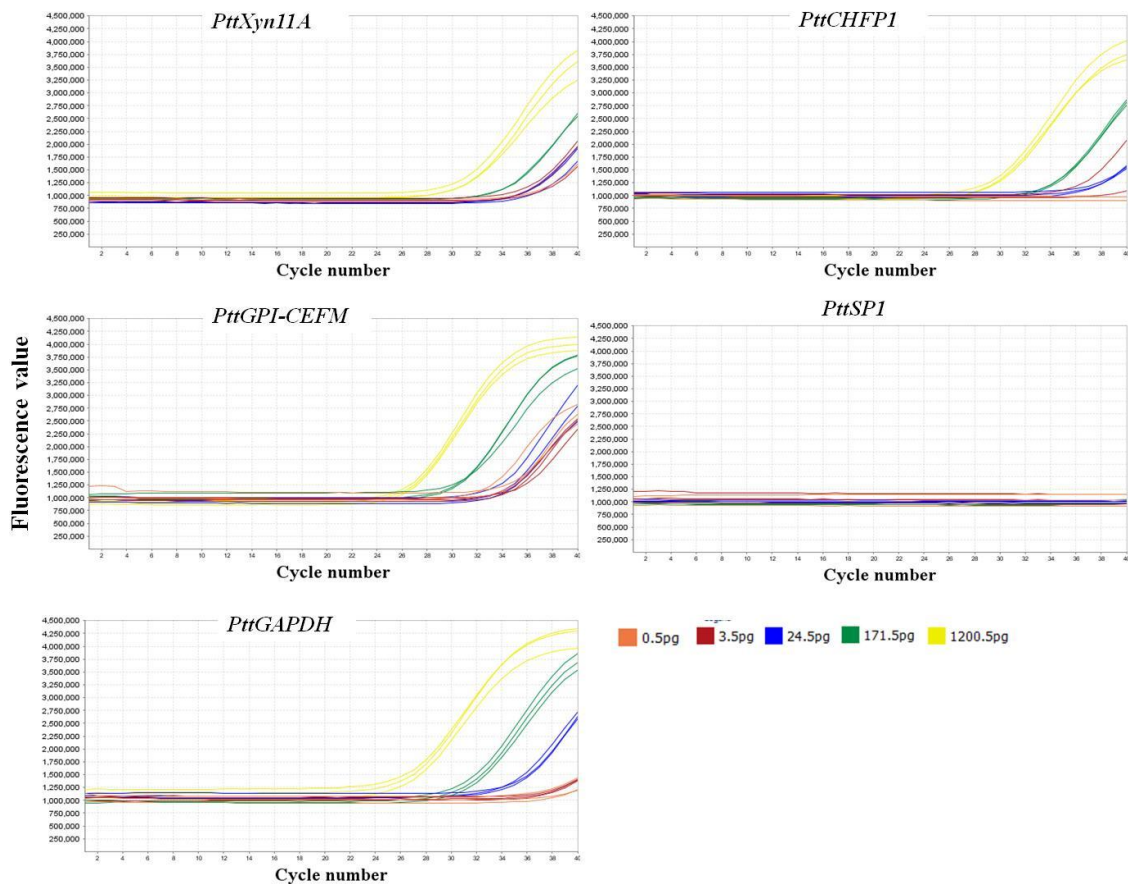


**Figure A4.6. Optimising of standard curve for VRCGs at lower cDNA concentration.** Seven folds of concentrations were used (0.5-1200.5 pg). cDNA at 1200.5 pg perform high efficiency for all genes. *PttSP1*, *PttXyn11A*, *PttCHFPI*, *PttGPI-CFEM* and *PttGAPDH*. However,  $C_T$  value was high and  $R^2$  was low.

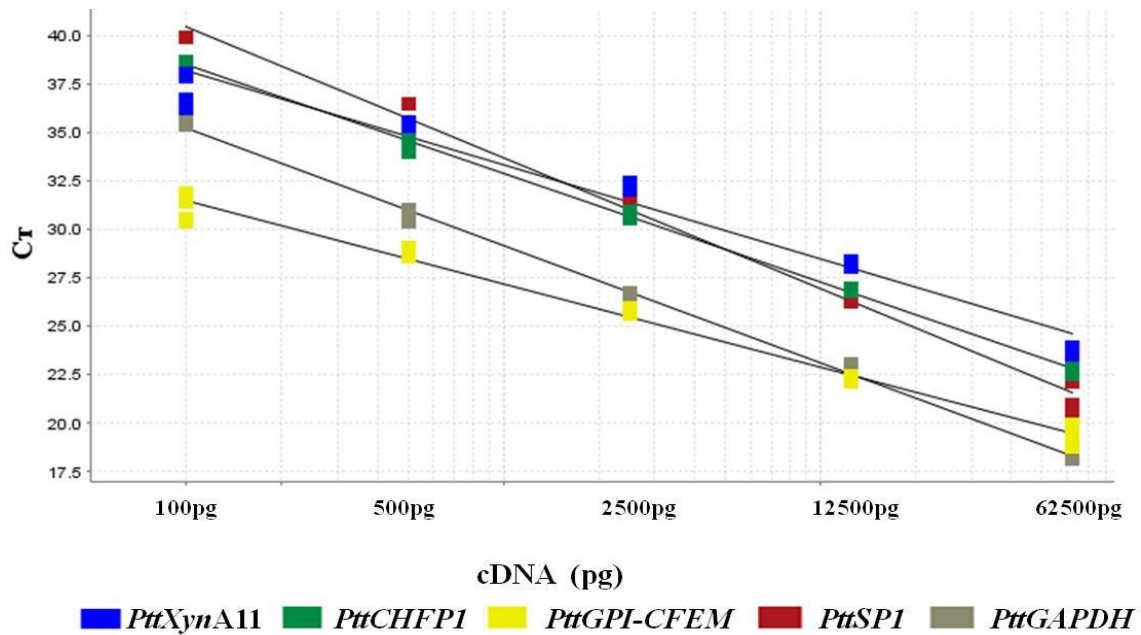


**Figure A4.7. Standard curve for VRCGs with high concentration of cDNA.** Five concentrations (100 pg, 500 pg, 2500 pg, 12500 pg and 62500 pg) of cDNA were used for each VRCG, standard curves were generated using ViiA™ 7 software using four technical replicates.  $C_T$  values are shown in Y axis.  $R^2$  for *PttSP1* 0.98, *PttXyn11A* 0.96, *PttCHFPI* 0.99, *PttGPI-CFEM* 0.98 and *PttGAPDH* 0.99.

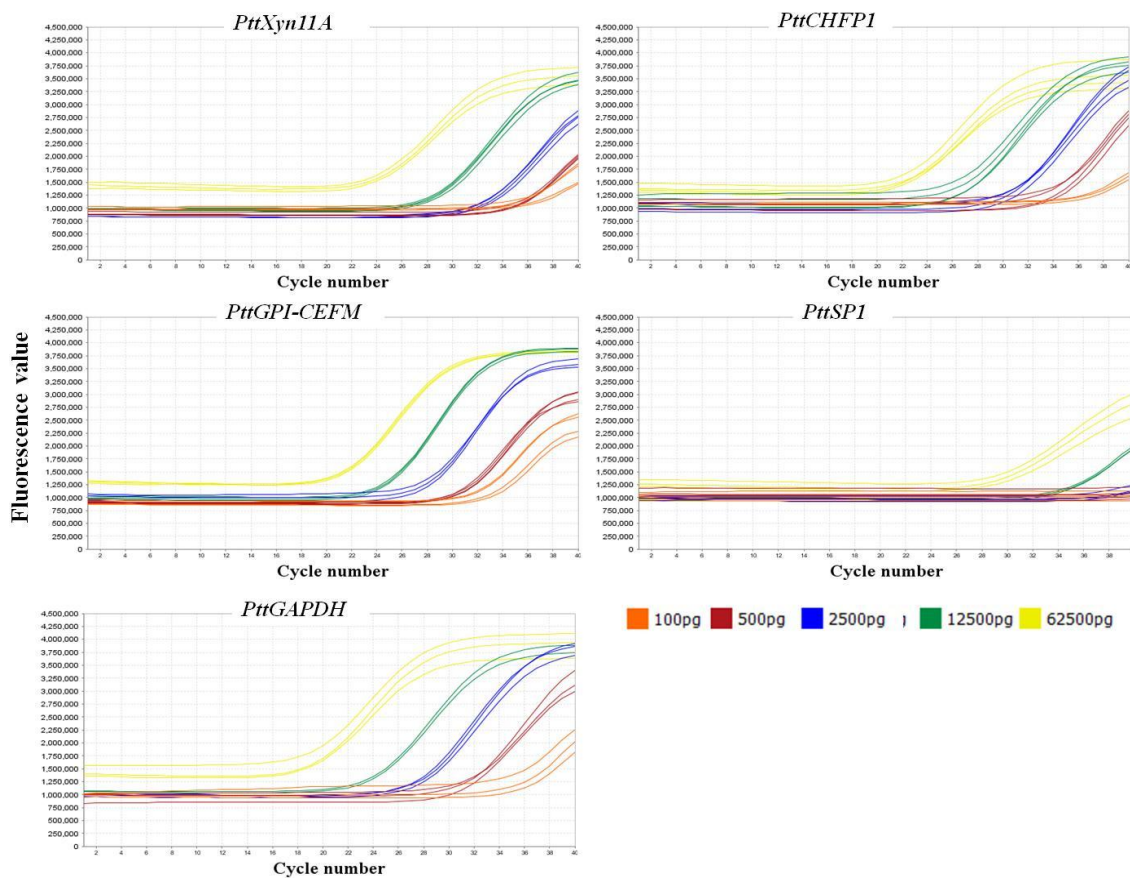


**Figure A4.8. Optimising standard curve for VRCGs at higher cDNA concentration.** Five folds of concentrations were used (100-62500 pg). cDNA at 62500 pg perform high amplification for all genes.

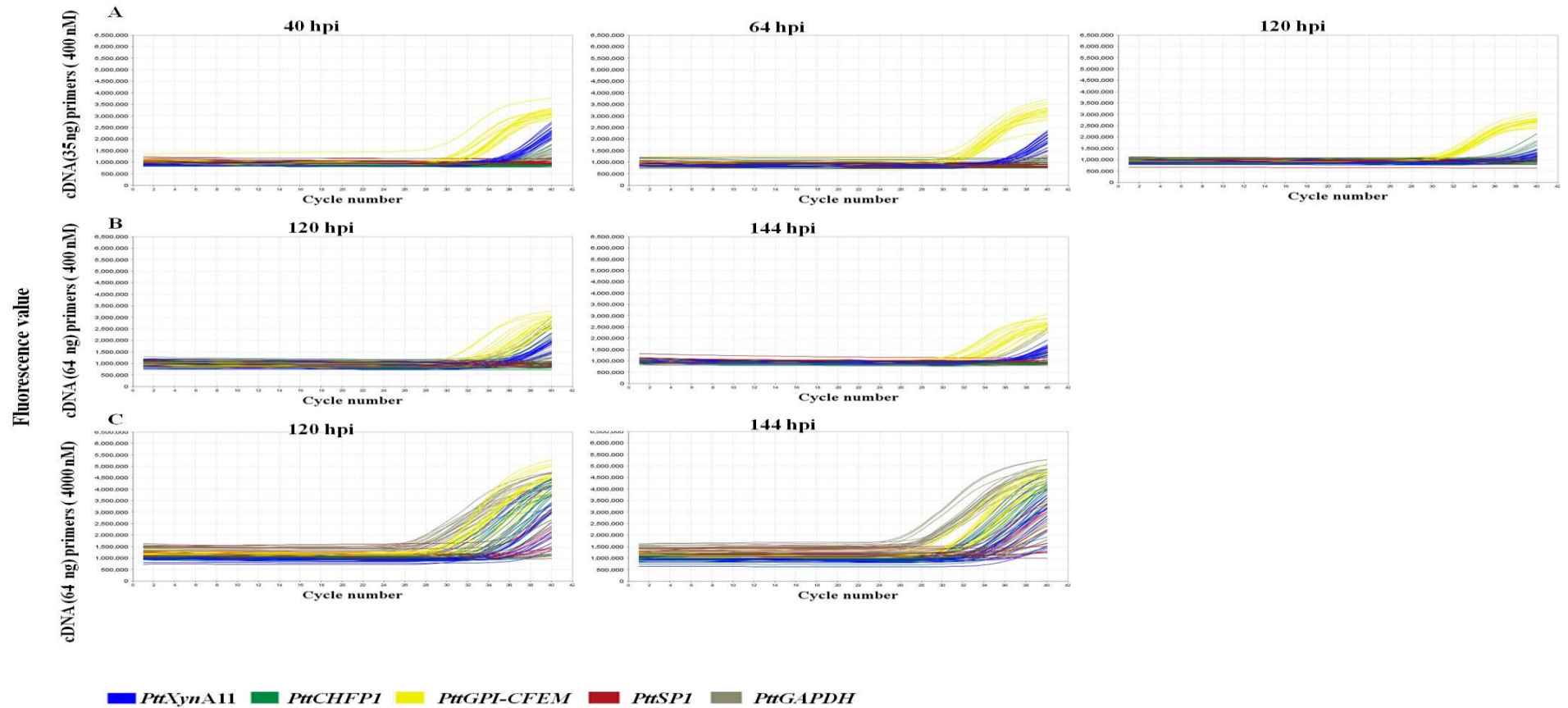


**Figure A4.9.** The expression of VRCGs (*PttSPI*, *PttXyn11A*, *PttCHFPI*, *PttGPI-CFEM* and *PttGAPDH*) in (pg) at 40, 64, 120 and 144 hours post inoculation (hpi) in six isolates of *Ptt* in three experiments. Absolute quantification using standard curve (Figure 4.7), final concentration for cDNA (3500 pg or 64000 pg) and primers (400 nM or 4000 nM). Low concentration of cDNA resulted low amplification and flat melt curve and consequently unreliable quantification.

## Appendix 5 Copyright permission for Figure A.1.1

Dr. Tekauz, Andy  
Senior Research Scientist  
195 Dafoe Rd  
Winnipeg, Manitoba R3T 2M9  
Telephone: 204-983-0944  
Fax: 204-983-4604  
Email: andy.tekauz@agr.gc.ca  
5/3/2013

Dear Dr Tekauz, Andy,

### Request for Permission

My name is Ismail A. Ismail. I am a postgraduate student at the University of Adelaide, Australia and as a requirement of my PhD degree, will be submitting a thesis entitled "Characterisation of the proteinaceous toxins isolated from *Pyrenophora teres f. teres*".

It is a requirement of the University of Adelaide that a digital version of the final accepted thesis be submitted to the Australasian Digital Theses (ADT) Program. This digital version is stored on the University's server but is accessible at no cost by members of the public on the World Wide Web via the ADT database. The ADT database (<http://adt.caul.edu.au>) is the national repository of theses in Australia and is not-for-profit.

My thesis includes the material described below ("Figure 1 a") in which you hold copyright or in relation to which you may be authorised to grant a licence. I wish to seek from you a limited, royalty-free, non-exclusive licence, for an indefinite period of time, to reproduce, communicate and publish the Material as part of my Thesis in the method set out above. The Material will of course be fully and correctly referenced.

### Description of the Material

Title: A numerical scale to classify reactions of barley to *Pyrenophora teres*.  
Volume and issue number: 7  
Year of publication: 1984  
Author / Editor: Tekauz, A.  
Publisher: Can. J. Plant Pathol.  
Page number/s: 181-183  
Description of Material: Figure 1 a

If you agree to grant the licence, please sign below and return this whole document to me by fax, e-mail or post. If you do not agree, please notify me in writing.

Yours sincerely,

Ismail A. Ismail  
PhD candidate, School of Agriculture, Food and Wine  
The University of Adelaide  
Waite Research Institute  
PMB1, Glen Osmond SA 5064, South Australia, Australia  
Phone: +61 8 83136547  
Fax: +61 8 8303 7109  
Email: ismail.ismail@adelaide.edu.au

I / WE HAVE THE RIGHT TO GRANT A LICENCE FOR THE USE OF THE MATERIAL AS DESCRIBED ABOVE AND HEREBY GRANT YOU SUCH LICENCE.

Signed for and on behalf of Canadian Journal of Plant Pathology/Tekauz, A: \_\_

Position: Research Scientist (Retiree)

Date: March 7, 2013